AFIT/DS/ENY/95-02

Optimal Mixed-Norm Control Synthesis for Discrete-Time Linear Systems

DISSERTATION
David R. Jacques
Captain, USAF

AFIT/DS/ENY/95-02

The views expressed in this dissertation are those of the author and do not reflect the official policy or position of the Department of Defense or the U. S. Government.

AFIT/DS/ENY/95-02

Optimal Mixed-Norm Control Synthesis for Discrete-Time Linear Systems

DISSERTATION

Presented to the Faculty of the Graduate School of Engineering

of the Air Force Institute of Technology

Air University

In Partial Fulfillment of the

Requirements for the Degree of

Doctor of Philosophy

David R. Jacques, B.S., M.S.

Captain, USAF

June, 1995

AFIT/DS/ENY/95-02

Optimal Mixed-Norm Control Synthesis for Discrete-Time Linear Systems

David R. Jacques, B.S., M.S.

Captain, USAF

Approved:

D Brett Ridgely 15 May 95

Dr. D. Brett Ridgely, Research Advisor

Peter S. Maybeck 15 May 95

Dr. Peter S. Maybeck

R. A. Canfield 16 May 95

Maj. Robert A. Canfield, PhD

Alan V. Lair 15 May 95

Dr. Alan V. Lair

Robert A. Calico, Jr

Dean

Acknowledgements

This research, and the resulting dissertation, would not have been possible without the moral and technical support of my instructors, friends and family. Although it is not possible to thank everyone who has influenced my work, I would like to take this opportunity to thank those who have been the most influential in my life in recent years.

Dr Brett Ridgely, my research advisor, provided the challenge and the motivation for taking on this research. Through Dr Ridgely, I became part of a research group which approached the mixed-norm control problem from several different angles. This team concept allowed any one of us to accomplish far more then we would have if we had worked alone on our projects. Throughout my research, Dr Ridgely provided valuable insight into the optimal control problem, and his editorial assistance for reports, conference papers, and this dissertation were indispensable. Above all, I consider Dr Ridgely a friend, and his moral support was every bit as valuable as his technical support.

Several former members of Dr Ridgely's research group deserve special thanks. LtCol Dave Walker endured countless hours of discussions on this topic, and he provided the basis for much of the numerical work presented in this dissertation. More importantly, LtCol Walker showed me how to complete a dissertation, and for this I am eternally grateful. Capt Mark Spillman deserves thanks for troubleshooting and improving many of my algorithms, and his contribution towards the creation of MXTOOLS can not be overstated.

I would like to thank the members of my research committee who provided both the breadth and depth of knowledge I needed to complete this dissertation. Dr Peter Maybeck is responsible for most of what I learned on system modelling. Further, his enthusiasm for the topic provided more incentive than he will ever realize, and his comments on the dissertation resulted in a final document far better than the earlier versions. Maj Bob Canfield provided me with the technical knowledge I needed to develop the numerical algorithms discussed in this dissertation. He was part of the team responsible for the creation of MXTOOLS, and remains an invaluable part of the overall research group.

Dr Alan Lair acted as the Dean's representative on my committee, and he provided the mathematical insight necessary for much of the analytical work in the dissertation. I am forever grateful for his assistance. I would also like to thank Dr Mark Oxley for his assistance in formulating this topic and reviewing my prospectus.

The most important support I have received throughout this effort has undoubtedly come from my wife, Lynette, and daughter, Nicole. Lynette gave me the incentive to not only attempt the program, but to continue the research when the results did not come as quickly as I would have liked. For all the days she was greeted with blank stares because my mind was on my research, I apologize to her and I am grateful she put up with it. Nicole sacrificed "play time with Dad" in order for me to finish this dissertation. Since this lost time can never be made up, I can only hope that she will somehow benefit from my having completed this program. To Lynette and Nicole, I love you both, and I can't thank you enough for your understanding over the past three years.

Finally, I would never have been in a position to even start this research if not for the guidance I received from my parents. For this, I am grateful to them. I have been blessed with educational opportunities my father only dreamed of, and he taught me to never take them for granted. My father was not able to see the completion of this work, but his influence and support remain with me. For this reason, I dedicate this work to the memory of my father, Joseph L. Jacques.

David R. Jacques

Table of Contents

List of Figures

List of Tables

Abstract

The general mixed-norm optimal control problem for discrete-time linear systems is considered. The approach taken is to minimize the H_2 norm of a transfer function, while constraining the ℓ_1 and/or H_∞ norms of dissimilar transfer functions associated with the same underlying system. Analytical results for the optimal (free-order) problem are presented for both the H_2/ℓ_1 and H_2/H_∞ problems. Two numerical methods are presented for solving the free-order H_2/ℓ_1 control problem, and the second method is extended to accommodate an H_∞ constraint. The free-order methods yield convex optimization problems with unique optimal solutions, but the high controller order makes them impractical for anything but a limits-of-performance type analysis. In order to obtain implementable controllers, a fixed-order method is developed for solving the $H_2/\ell_1/H_\infty$ problem with an arbitrary number and variety of constraints. The controller order is fixed to that of an initial stabilizing controller. The resulting optimization problem is non-convex, but can be solved efficiently using gradient-based nonlinear programming methods. The fixed-order numerical method is demonstrated using several SISO and MIMO examples. The discrete-time, fixed-order method is then combined with existing continuous-time algorithms to provide a single MATLAB toolbox for synthesis of mixed-norm controllers.

Optimal Mixed-Norm Control Synthesis for

Discrete-Time Linear Systems

I. Introduction

1.1 Overview

The primary requirement for almost every control system is that it must stabilize the plant for which it is designed. This objective is referred to as *nominal stability*, and it is guaranteed by virtually all modern control synthesis techniques. Further, the Youla parametrization [1] provides a convenient representation of all compensators which achieve nominal stability. Besides stability concerns, we typically have performance specifications which must be met. Whereas nominal stability is a clear-cut characteristic, *nominal performance* specifications are often in a form which cannot be applied directly to a given synthesis technique. For example, time domain specifications are often difficult to incorporate into frequency domain synthesis techniques. Often the performance specifications are not representable as hard constraints; instead, they are expressed in terms such as "get as much of this characteristic as you can". This latter type of requirement often lends itself to *optimal* control methods whereby a performance measure is expressed as a functional, and the functional is minimized over all compensators providing nominal stability.

Consider the linear system shown in Figure 1.1, where w is an exogenous input, and z is an output we wish to control. The requirements on the compensator, K, are that it stabilizes the closed loop system and provides for some measure of performance as defined by the control engineer. Linear Quadratic Gaussian (LQG) methods [2, 3], for example, take a stochastic approach by assuming all disturbances can be modeled as the outputs of shaping filters driven by zero-mean, white, Gaussian noise. They then combine a minimum error covariance state estimator (Kalman filter) with a regulator designed to minimize a weighted sum of the squares of control usage and output signals. H_2 optimization [4], which can be seen as a generalization of steady-state LQG, minimizes the energy of the

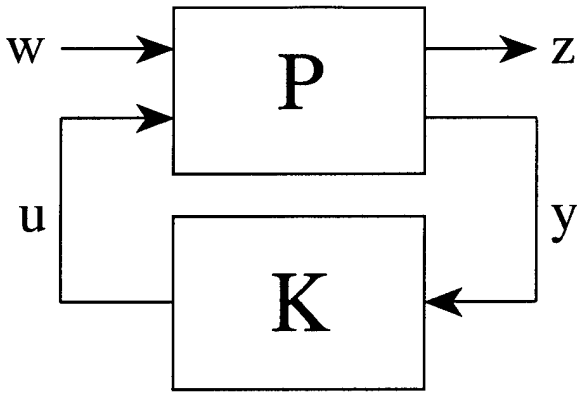

Figure 1.1 Feedback System

output signals while still assuming white noise inputs. For cases where the inputs to the system are not modeled accurately as white noise, other techniques are required. The H_∞ methodology [4] allows us to minimize the energy of the output response to a worst case set of unknown but bounded energy inputs. H_∞ methods are often used for model matching and/or minimization of a weighted sensitivity function. The minimization of the maximum magnitude of the response to a worst case set of bounded magnitude inputs is termed ℓ_1 optimization [5]. While LQG and H_2 design methods date back to the 1960's, H_∞ methods were developed in the 1980's, and ℓ_1 theory and methodology (1986-present) is considered by most to be not yet fully mature. H_2 and H_∞ are primarily frequency domain methods. The ℓ_1 method, however, is inherently a time domain technique, and it is a natural setting for problems where tight tracking (terrain following) or hard control surface limits (positions and/or rates) are important performance measures.

The nominal performance problem admits unknown disturbances, but it assumes the plant is precisely known. Realistically, this is never possible. Usually the plant model is a greatly simplified representation of a system which is generally nonlinear and/or of significantly higher dimension than our design model. Once plant uncertainties (or variations with time) are admitted to the problem, our first concern must be whether or not closed-loop stability is preserved in the presence of admissible plant variations. This now becomes a *robust stability* problem. LQG/LTR was an attempt to provide stability margins without leaving the realm of H_2 optimization. Generally, however, H_2 has been shown to be ill equipped to handle robustness problems [6]. One way to consider the robust stability

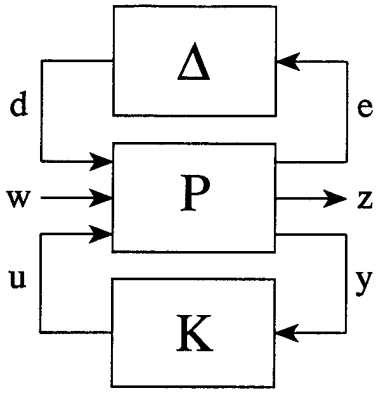

Figure 1.2 Feedback System with Plant Uncertainty

problem is to combine all allowable perturbations to the plant into a single unstructured perturbation, Δ, which interacts with the plant as shown in Figure 1.2. We will refer to the compensated plant (closed P-K loop) from d to e as T_{ed}. Robust stability requires that K stabilize the plant for all allowable Δ. Under this concept, the Small Gain Theorem can be used to quantify robust stability.

Theorem 1.1.1 (Small Gain Theorem) *Let $T_{ed} \in H_\infty$. Assume $\Delta \in H_\infty$ is connected from e to d as shown in Figure 1.2. Then the closed-loop system is internally stable if*

$$\|T_{ed}\Delta\|_\infty \leq \|T_{ed}\|_\infty \|\Delta\|_\infty < 1 \tag{1.1}$$

Proof: See [7]. ∎

A second version of the Small Gain Theorem which uses the ℓ_1 norm instead of the H_∞ norm can be defined [5]. Clearly, progressively minimizing either the ∞-norm or 1-norm of T_{ed} will make the system robustly stable to increasingly larger plant perturbations as quantified by the ∞-norm or 1-norm of Δ, respectively. This implies that either H_∞ or ℓ_1 methods are applicable to the robust stability problem. Which of these methods is more applicable depends on whether the plant uncertainty is best modeled as having bounded energy or bounded magnitude.

While the three methods mentioned above are by no means an exhaustive list of the design methods available to the controls engineer, among the three of them, a wide

variety of problems can be addressed. A realistic application, however, may require combined results from each of these methodologies. For instance, using an aircraft example, we are concerned with rejecting disturbances due to wind gusts which often are modeled as white noise inputs (via shaping filters). We are also interested in limiting the energy of certain outputs in response to inputs which are best described as having bounded energy, and tracking concerns dictate that we limit or minimize the maximum magnitude of certain responses. Control surfaces have finite limits which must be taken into account, and guaranteed stability margins are typically required to meet handling quality specifications. Finally, the detrimental effects of plant uncertainty (from modeling approximations and time variations) must be minimized. The combination of all these different and often competing requirements suggests that a synthesis technique capable of combining the H_2, H_∞ and ℓ_1 methodologies might be desirable. This is the motivation behind this dissertation.

In general, the mixed-norm control problem can be viewed in terms of finding a desired point (or compensator) on a Pareto-optimal surface (or hypersurface), whereby the respective norms of the individual transfer functions define the axes of the space. Viewed in this context, any one of the norms could be used as an objective, with all others applied as constraints. By varying the constraints, you change your operating location on the surface. This dissertation will use the H_2 norm as the objective function for several reasons. First, previous results by other researchers [8, 9] make this an attractive choice. Second, it is often easier to view robust stability, acceptable tracking error or actuator limits as constraints on the system, and these concerns will usually be addressed using H_∞ or ℓ_1 constraints. Along this line, noise effects (which are best handled by H_2) are typically something you wish to minimize, rather than constrain the value of. Finally, the free-order H_2/ℓ_1 problem addressed in this dissertation is well suited to quadratic or sequential quadratic programming methods [10] if the H_2 subproblem is used for the objective function. Thus, the problem to be addressed in this dissertation is: Find an internally stabilizing compensator K that achieves

$$\inf_{K\,stabilizing} \{\|T_{zw}\|_2 \ : \ \|T_{ed}\|_x \leq \gamma\} \tag{1.2}$$

where $x = \{1 \text{ or } \infty\}$ and γ is fixed *a priori* based on the desired level of robustness and/or nominal performance. There are a wide variety of methods available for solving this mathematical programming problem numerically.

In addition to choosing an overall design method, a controls engineer often faces a decision on whether to work with continuous-time or discrete-time systems. While most physical systems to be controlled are continuous-time in nature, the majority of the controllers are implemented digitally. Historically, most engineers design in continuous-time and then discretize the resulting controller. The primary drawback with this approach is that the effects of sampling rate on performance cannot be investigated until the design is discretized. Also, while the transfer function ∞-norm is invariant under the bilinear transformation used to discretize a controller [11], the same cannot be said about the 2-norm or 1-norm. Lastly, there is no direct continuous-time analog to the present ℓ_1 synthesis method. An alternative approach to design allows the engineer to develop a discrete-time controller directly using a discretized version of the plant model. Although final simulations must still be run with the continuous-time plant, most of the stability concerns due to sampling rate are directly incorporated into the controller design. For these reasons, the approach used in this research is entirely discrete-time. Where appropriate, important differences between the continuous-time and discrete-time results will be highlighted, but the existing theory and results for continuous-time methods will not be presented.

1.2 Review of Related Work

While as yet there are no published results combining all three norms (H_2 , H_∞ and ℓ_1) into a single synthesis technique, several researchers have combined them in pairs (once again we primarily will be discussing results for discrete-time systems). The mixed H_2/H_∞ problem has been very active since about 1989, and much of the work which was originally developed for continuous-time systems has been re-derived for discrete-time. Haddad, Bernstein and Mustafa [12] present a method whereby an upper bound to the transfer function 2-norm is minimized subject to a constraint on the ∞-norm. Limitations of their results are that they only allow for one distinct set of outputs, and do not allow for dynamic measurement feedback. Also, there is no measure of how conservative the upper

bound is. Kaminer, Khargonekar and Rotea [13] address an H_2/H_∞ problem with two sets of outputs but only one set of inputs, and they transform the problem into one of convex optimization. The objective function they use is still only an upper bound to the 2-norm; in fact, it is the same auxiliary functional used by [12]. The approach in [13] does allow for dynamic measurement feedback. Iglesias, Mustafa, and Glover [14, 15] solve the minimum entropy control problem, which also minimizes an upper bound to the 2-norm. In both of these papers, the authors assume one set of inputs and one set of outputs, which means that the ∞-norm constraint is on the same transfer function on which they to minimize the 2-norm. For the case where entropy is evaluated at the origin, this corresponds to the central H_∞ controller [14, 15].

All of the methods mentioned above result in a fixed order controller (order equal to that of the weighted plant) which minimizes an upper bound to the 2-norm. For continuous-time systems, Ridgely and Walker [8, 9] have developed a method which also results in a fixed-order controller, but the resulting controller order can be increased or decreased as a design option. The Ridgely/Walker approach also allows for two or more distinct sets of outputs and two or more distinct sets of inputs. Further, Walker extended the problem to include singular and multiple H_∞ constraints. Ly and Schomig[16] also addressed a very general H_2/H_∞ problem by casting the H_∞ constraints as a scalar function of symmetric matrix inequalities. As in Walker's method, Ly and Schomig's method is capable of finding reduced and/or increased order compensators with both singular and multiple H_∞ constraints.

A significant finding of Walker's work is that the optimal mixed H_2/H_∞ solution over all compensators is non-rational or infinite order in at least one class of problems. Megretski [17] found a similar result for a more general H_2/H_∞ problem, and his work covers both the continuous-time and discrete-time cases. Sznaier [18, 19] presented a method for solving the discrete-time mixed H_2/H_∞ control problem over arbitrary order compensators. While his method does not solve the problem exactly, a compensator (generally of very high order) can be found which meets the H_∞ constraint and minimizes the 2-norm to within arbitrary accuracy using a finite horizon approach.

Helton and Sideris [20] developed algorithms for the inclusion of time domain constraints (response to a fixed input) in an H_∞ problem, and these algorithms are further developed and applied by Sideris and Rotstein [21, 22]. The time-domain constraints are imposed over a finite time, and a controller is found which minimizes the H_∞ cost over arbitrary order compensators. A problem which is somewhat equivalent to this is addressed by Sznaier [23]. Sznaier's problem is to minimize the magnitude of a specific response to a fixed input while constraining the infinity norm of some transfer function (ℓ_∞ /H_∞). The approach taken by Sznaier is similar to that of his mixed H_2/H_∞ problem mentioned above.

Relatively few results have been published which combine the ℓ_1 norm in a mixed-norm problem. Dahleh and Diaz-Bobillo [5] present a method whereby a linear approximation to an H_∞ constraint is appended to an ℓ_1 optimization problem, but it requires the H_∞ constraint to be on the same transfer function as is used for the ℓ_1 problem. They also present ways in which time domain constraints such as overshoot, rise time and settling time can be added to the ℓ_1 problem. Voulgaris [24] considered a limited H_2/ℓ_1 problem whereby the objective and constraint transfer functions are the same. He was able to show that the true optimal solution to this problem could be found using a truncated problem and quadratic programming methods.

1.3 Research Contributions

The purpose of this research is first to explore the nature of the optimal solution to the H_2/ℓ_1, H_2/H_∞, and $H_2/\ell_1/H_\infty$ control problems for discrete-time linear systems. Next, numerical methods will be developed for solving the optimal H_2/ℓ_1 and $H_2/\ell_1/H_\infty$ problems, and a general numerical approach will be developed for finding fixed-order solutions to a constrained H_2 problem with an arbitrary combination of transfer function constraints. Finally, the fixed-order discrete-time method will be combined with existing continuous-time algorithms to produce a single, comprehensive and cohesive toolbox for solving mixed-norm control problems. The specific contributions of this research are as follows:

i. The research will characterize the optimal solution to the H_2/ℓ_1 control problem. It will be conjectured that the optimal solution to the SISO and one-block MIMO H_2/ℓ_1 control problem will consist of a Finite Impulse Response (FIR) constraint transfer function, but non-FIR objective transfer function. This will stand in contrast to Voulgaris' results, which show that, if the objective and constraint transfer functions are the same, they will be FIR. It will be shown that Voulgaris' results do not extend to the more general case where the objective and constraint transfer functions are different, and supporting evidence for the conjecture regarding the nature of the more general solution will be provided.

ii. Two numerical methods for solving the optimal H_2/ℓ_1 control problem will be developed. Based on the conjecture regarding the nature of the optimal solution, the first method will be capable of solving exactly the SISO and one-block MIMO H_2/ℓ_1 problem. This method will also be capable of approximating the optimal solution to the general multi-block MIMO problem. A second numerical method will be developed which will guarantee convergence within an arbitrary epsilon for a finite truncation level. Further, this second method will be extended to include an H_∞ constraint in the problem.

iii. The nature and existence of the optimal and full-order solutions to the discrete-time H_2/H_∞ problem will be characterized. Most of these results are well established for continuous-time systems, but a complete investigation has not been published for discrete-time.

iv. A completely general method for solving the fixed-order mixed-norm control problem for discrete linear systems will be developed. The method will accommodate an arbitrary collection of transfer function constraints, and will allow easy problem setup and modification. Examples shown using this method will comprise the first published results combining the 1-norm, 2-norm, and ∞-norm of dissimilar transfer functions into a single constrained optimization problem.

v. The fixed-order discrete-time methods will be combined with existing continuous-time algorithms to produce a single toolbox for solving mixed-norm control problems. A

common interface for both continuous-time and discrete-time systems will be provided.

vi. An extension to the fixed-order method will make it possible to address the multi-plant problem whereby the underlying dynamics associated with objective and constraint transfer function no longer must be the same. This will allow the incorporation of robust stability concerns at off-design conditions.

1.4 Dissertation Outline

This dissertation consists of 8 chapters including this introduction. Chapter 2 will present a review of preliminary mathematics, including a discussion of vector spaces, operators, linear systems, Lyapunov and Riccati equations, system norms, convex programming and minimum norm duality theory. Chapter 3 will review H_2 and ℓ_1 control theory.

Chapter 4 will begin to explore the mixed-norm problem by considering the optimal H_2/ℓ_1 control problem. The uniqueness of the optimal compensator will be shown, and an important conjecture regarding the nature of the optimal solution will be developed. Following this, two numerical methods will be developed for solving the optimal H_2/ℓ_1 control problem, and the second method will be extended to include an H_∞ constraint. The first numerical method will be demonstrated using a SISO F-16 longitudinal flight controller.

Chapter 5 will explore the optimal and full-order H_2/H_∞ control problem. The results in this chapter will parallel those found by Ridgely [8] and Walker [9] for continuous-time systems. The optimal solution to a special case will be shown to be a non-rational H_2 function. A Lagrange multiplier approach to the full-order problem will be taken by appending a Lyapunov equation associated with the H_2 problem and a Riccati equation associated with the H_∞ constraint. Conclusions regarding the existence of the solution vs. controller order will be made.

Chapter 6 will develop the numerical method for the fixed-order solution of the general $H_2/\ell_1/H_\infty$ problem. It will be demonstrated that the problem is non-convex, and the issue of convexity vs. controller order will be explored. The SISO F-16 problem will

be used to demonstrate a fixed-order H_2/ℓ_1 solution, and it will be compared to the free-order solution of Chapter 4. The example will also be extended to an $H_2/\ell_1/H_\infty$ problem by appending an additional H_∞ constraint. Chapter 7 will consist of two examples of fixed-order mixed-norm control. The first example will be a MIMO model of an A-4 aircraft. A longitudinal controller will be designed for terrain following applications. The second example will demonstrate a SISO multi-plant example using the American Control Conference benchmark robust stability problem [25].

Chapter 8 will present some recommendations and conclusions from this research. Finally, a description and brief user's manual for the Mixed-Norm Toolbox for MATLAB will be provided as an Appendix to this dissertation.

II. Preliminary Mathematics

This chapter provides a review of the mathematics and terminology involved in this dissertation. Much of the presentation for the first half of this chapter is taken from the recent book by Dahleh and Diaz-Bobillo[5].

2.1 Signals, Sequences, and Linear Spaces

We will denote by $\ell_p^n(Z)$, sometimes dropping both the argument and superscript, the space of all n-vector valued sequences with integer index k such that

$$x(k) \in l_p \Rightarrow \|x\|_p := \left(\sum_{k=-\infty}^{\infty} \sum_{i=1}^{n} |x_i(k)|^p \right)^{1/p} < \infty \tag{2.1}$$

The cases which we are interested in are $p = 1, 2, \infty$. The norms for $p = 1, 2$ are obvious from the definition above, while the signal ∞-norm is defined as

$$\|x\|_\infty := \sup_k \max_i |x_i(k)| \tag{2.2}$$

The signal ∞-norm represents the maximum magnitude over all time, while the 2-norm represents the energy of the signal, and the 1-norm is simply a summation of the absolute value. With these definitions for the signal norms, the spaces associated with them can be viewed as nested sets; $\ell_1 \subset \ell_2 \subset \ell_\infty$. In the case of real bounded energy signals (ℓ_2) we can define an inner product on the space as

$$\langle x, y \rangle := \sum_{k=-\infty}^{\infty} y^T(k) x(k) \tag{2.3}$$

With this definition, the signal space ℓ_2 can be shown to be a Hilbert space. There is no inner product for the spaces ℓ_1 and ℓ_∞; these spaces come under the more general definition of Banach spaces.

The Fourier Transform of a sequence can be defined as

$$X(e^{j\theta}) := \sum_{k=-\infty}^{\infty} x(k)e^{jk\theta} \tag{2.4}$$

The space of Fourier Transforms of elements of ℓ_2 is also a Hilbert space (denoted by $\mathcal{L}_2$) with the inner product defined as

$$\langle X, Y \rangle := \frac{1}{2\pi} \int_0^{2\pi} Y^*(e^{j\theta}) X(e^{j\theta}) d\theta \tag{2.5}$$

A useful property of the Fourier Transform is that it preserves the norm, and in general $\langle x, y \rangle = \langle X, Y \rangle$. The following example is taken from Dahleh and Diaz-Bobillo[5].

Example *It is quite common in the case of bounded energy signals to define complex-valued spaces. Consider the space ℓ_2 of complex valued sequences, with the inner product defined as*

$$\langle x, y \rangle := \sum_{k=-\infty}^{\infty} y^*(k)x(k) \tag{2.6}$$

If x is in $\ell_2(Z)$, then X is in $\mathcal{L}_2[0, 2\pi]$. The converse of this statement is also true, since the inverse Fourier Transform is defined for every element in $\mathcal{L}_2$. The space $\ell_2(Z)$ can be written as a direct sum of two spaces of one-sided sequences, namely $\ell_2(Z_+)$ and $\ell_2(Z_-)$, where 0 is in Z_+, i.e.,

$$\ell_2(Z) = \ell_2(Z_+) \oplus \ell_2(Z_-) \tag{2.7}$$

Fourier Transforms of the elements of $\ell_2(Z_+)$ have the property that they admit analytic continuation in the open unit disc. The space of all such functions is denoted by H_2 , i.e., if $G(\lambda)$ is in H_2 , then $G(e^{-j\theta})$ is in $\mathcal{L}_2[0, 2\pi]$, and $G(\lambda)$ is analytic in the open unit disc. Similarly, $\ell_2(Z_-)$ is transformed to functions that are analytic in the complement of the open unit disc. Such a space is denoted by $H_2^\perp$. It follows that

$$\mathcal{L}_2[0, 2\pi] = H_2 \oplus H_2^\perp \tag{2.8}$$

A signal is said to be white (and of unit intensity) if

$$\lim_{N\to\infty} \frac{1}{N} \sum_{k=0}^{N-1} x(k)x^T(k+\tau) = \begin{cases} I & \tau = 0 \\ 0 & \tau \neq 0 \end{cases} \tag{2.9}$$

2.2 Operators

Mathematically, systems can be viewed as operators between input and output signal spaces. The system may be described as an input-output map, or as a state space realization of this map. More will be said about state space realizations in the next section.

Denote by P_k, the standard truncation operator on ℓ_p. An operator T is *causal* (proper) if $P_kT = P_kTP_k$ for all k. Further, it is *strictly causal* if $P_kT = P_kTP_{k-1}$ for all k. Denote by S, the standard unit shift operator on ℓ_p. An operator T is *time-invariant* if it commutes with the unit shift operator, i.e., $ST = TS$.

Example *(Taken from [5]) A sequence h in ℓ_1 defines an operator on ℓ_p as follows:*

$$hx(k) = h * x(k) = \sum_{j=0}^{\infty} h(j)x(k-j) \tag{2.10}$$

This is easily recognized as the convolution operator, and it is linear, time-invariant, and causal. Now consider a more general function f defined on $Z_+ \times Z_+$ which subsequently defines a linear operator on ℓ_p.

$$y(k) = (fx)(k) = \sum_{j=0}^{\infty} f(k,j)x(j) \tag{2.11}$$

This operator can be represented as an infinite matrix

$$f := \begin{bmatrix} f(0,0) & f(0,1) & f(0,2) & \cdots \\ f(1,0) & f(1,1) & f(1,2) & \cdots \\ f(2,0) & f(2,1) & f(2,2) & \cdots \\ \vdots & \vdots & \vdots & \ddots \end{bmatrix} \tag{2.12}$$

The operator f is time invariant if and only if $f(k,j) = f(k+\tau, j+\tau)$ for all $\tau > 0$. Further, f is causal if and only if $f(k,j) = 0$ for all $j > k$, and strictly causal if and

only if $f(k,j) = 0$ *for all* $j \geq k$.

Let T be a linear operator from X to Y, both normed linear spaces. T is a *bounded* operator (and *continuous*) if and only if its induced norm is finite, i.e.,

$$\|T\| := \sup_{x \neq 0} \frac{\|Tx\|}{\|x\|} < \infty \tag{2.13}$$

We will usually deal with the case in which the input/output spaces are the same (but of possibly different dimension). We say a linear system is *stable* with respect to the input/output space X if it is bounded as a linear operator on X. Bounded linear operators share a sub-multiplicative property which states that if T_1 and T_2 are both bounded linear operators on X into X, then

$$\|T_1 T_2\| \leq \|T_1\| \, \|T_2\| \tag{2.14}$$

For the particular case in which R is a bounded, linear, causal, time-invariant operator from ℓ_∞^n to ℓ_∞^m, we have

$$\|R\| := \max_{1 \leq i \leq m} \sum_{j=1}^{n} \sum_{k=0}^{\infty} |r_{ij}(k)| = \max_{1 \leq i \leq m} \sum_{j=1}^{n} \|r_{ij}\|_1 \tag{2.15}$$

where r denotes the time domain representation of the operator R, and r_{ij} is the ij^{th} element of a multiblock r. This norm will be referred to as the system 1-norm, and transfer functions with bounded 1-norms are said to be in ℓ_1, with the norm denoted as $\|.\|_1$.

For an element r in ℓ_1, we define the λ-*transform* as

$$R(\lambda) := \sum_{k=0}^{\infty} r(k) \lambda^k \tag{2.16}$$

$R(\lambda)$ is analytic on the open unit disc, and continuous on the boundary. The λ-transform should not be confused with the usual z-transform, which uses a negative exponent in the summation. The space of all λ-transforms of ℓ_1 elements is denoted by $\mathcal{A}$, and in fact $\mathcal{A}$ and ℓ_1 are merely different representations of the same space.

For the particular case in which R is a bounded, linear, causal, time-invariant operator from ℓ_2^n to ℓ_2^m, we typically deal with multiplication operators via Fourier transforms. Denote by $\mathcal{L}_\infty$ the space of all complex-valued matrix functions that are bounded on the unit circle, i.e.,

$$R \in \mathcal{L}_\infty \;\Rightarrow\; \|R\|_\infty \;:=\; \operatorname*{ess\,sup}_\theta [R(e^{j\theta})] \;<\; \infty \tag{2.17}$$

The subspace of elements that are analytic in the unit disc and bounded on the unit circle is denoted by H_∞. We can strengthen this development with the following theorem.

Theorem 2.2.1 *Every bounded linear time-invariant operator on $\mathcal{L}_2[0, 2\pi]$ is a multiplication operator by an element R in $\mathcal{L}_\infty$. The induced norm of this operator is $\|R\|_\infty$. Further, every bounded, linear, time-invariant, causal operator on H_2 is a multiplication operator by an element R in H_∞. The induced norm of this operator is also given by $\|R\|_\infty$.*

Proof: See Dahleh and Diaz-Bobillo [5], Theorem 2.3.2. ∎

In order to clarify the relation between members of H_∞ and $\mathcal{A}$, we can say

$$\mathcal{A}^{m\times n} \;\subset\; H_\infty^{m\times n} \tag{2.18}$$

$$\|R\|_\infty \;\leq\; \sqrt{m}\,\|R\|_1 \tag{2.19}$$

where m is the dimension of the output space.

It is also important to know when an operator has a stable inverse. For this, we present the following theorem.

Theorem 2.2.2 *Let H be in $\mathcal{A}$. Then H^{-1} is in $\mathcal{A}$ if and only if*

$$\inf_{|\lambda| \leq 1} |H(\lambda)| \;>\; 0 \tag{2.20}$$

Further, the same can be said for H in H_∞.

Proof: See [5]. ∎

The system 2-norm is not an operator norm on any space X into itself, and for this reason it does not have the sub-multiplicative property. The 2-norm is a measure of the

energy contained in the pulse response, and is given by

$$\|R\|_2^2 \;:=\; \frac{1}{2\pi}\int_{-\pi}^{\pi} tr\left[R(e^{j\theta})R^T(e^{-j\theta})\right]d\theta \;=\; \sum_{k=0}^{\infty} tr\left[r(k)r^T(k)\right] \tag{2.21}$$

If the input of the system is assumed to be a white noise signal, then the root mean square (rms) power of the output is equal to $\|R\|_2$. More will be said concerning all the norms in a later section.

2.3 Finite Dimensional, Linear, Time-Invariant Systems

The state space form for finite dimensional, linear, time-invariant (FDLTI) systems is

$$\begin{aligned} x(k+1) &= Ax(k) + Bu(k) \\ y(k) &= Cx(k) + Du(k) \end{aligned} \tag{2.22}$$

where the state vector $x \in \mathbf{R}^n$, the input vector $u \in \mathbf{R}^m$, the output vector $y \in \mathbf{R}^p$, and A, B, C, D are real coefficient matrices with appropriate dimensions. We will often use the shorthand notation to denote a system G;

$$G \;\equiv\; \left[\begin{array}{c|c} A & B \\ \hline C & D \end{array}\right] \tag{2.23}$$

The notation $G = (A, B, C, D)$ will also be used to denote to same state space quadruple. The system is stable if and only if the eigenvalues of A lie in the open unit disc. Denoting by $\mathbf{R}H_\infty$ the space of all stable, finite-dimensional systems, we see that $\mathbf{R}H_\infty$ lies in the intersection of ℓ_1 and H_∞.

We denote the *reachability subspace* as

$$R_t(A,B) = Image\left[B \quad AB \quad A^2B \quad \cdots \quad A^{t-1}B\right] \tag{2.24}$$

$R_t(A,B)$ is a subspace of $\mathbf{R}^n$ which consists of the states x_t that can be reached in t time steps from the origin. (A,B) is said to be *reachable* if

$$\text{rank}\,[\,B \quad AB \quad A^2B \quad \cdots \quad A^{t-1}B\,] \;=\; n \qquad (2.25)$$

The *controllability subspace* is defined as

$$C_t(A,B) = \{x \in R^n : A^t x \in R_t(A,B)\} \qquad (2.26)$$

which consists of the states x_o that can be steered to the origin in t time steps. The pair (A,B) is said to be *controllable* if $C_t(A,B) = \mathbf{R}^n$. We note that reachability implies controllability, and if A is non-singular, controllability and reachability are equivalent. Using duality we can state that (C,A) is *observable* if (A^T,C^T) is reachable, and (C,A) is *constructible* if (A^T,C^T) is controllable. Finally, we note that observability implies constructibility, and the two are equivalent if A is non-singular.

Given any real, rational, proper transfer function there exists a state space realization, but it is not unique. A realization (A,B,C,D) is said to be *minimal* if A is of smallest dimension. It can be shown that a realization is minimal if (A,B) is reachable and (C,A) is observable [26]. The z-domain transfer function of G can be written as

$$G(z) \;=\; C(zI - A)^{-1}B \;+\; D \qquad (2.27)$$

and the unit pulse response for G can be written as

$$G(k) = \begin{cases} D & k \;=\; 0 \\ CA^{k-1}B & k \;>\; 0 \end{cases} \qquad (2.28)$$

The nominal feedback system considered in this dissertation is given in Figure 2.1.

The system can be represented as a 2×2 block transfer function matrix mapping the inputs w and u to the outputs z and y:

$$\begin{Bmatrix} z \\ y \end{Bmatrix} \;=\; \begin{bmatrix} P_{zw} & P_{zu} \\ P_{yw} & P_{yu} \end{bmatrix} \begin{Bmatrix} w \\ u \end{Bmatrix} \qquad (2.29)$$

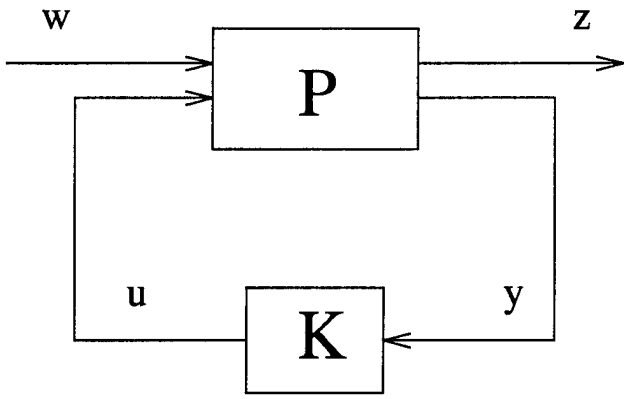

Figure 2.1 Nominal Feedback System

The closed-loop transfer function from w to z can be determined from the *lower fractional transformation* (LFT)

$$F_l(P,K) \;=\; P_{zw} \;+\; P_{zu}K(I - P_{yu}K)^{-1}P_{yw} \tag{2.30}$$

The system is *well posed* if and only if $(I - P_{yu}K)$ is invertible for all z. The system is guaranteed to be well posed if P_{yu} or K is strictly causal. Well-posedness will be assumed in this dissertation.

The system in Figure 2.1 can be written in state space form as

$$P \;=\; \left[\begin{array}{c|cc} A & B_w & B_u \\ \hline C_z & D_{zw} & D_{zu} \\ C_y & D_{yw} & D_{yu} \end{array}\right] \tag{2.31}$$

$$K \;=\; \left[\begin{array}{c|c} A_c & B_c \\ \hline C_c & D_c \end{array}\right] \tag{2.32}$$

Well-posedness can now be seen as $(I - D_cD_{yu})$ being invertible. Further, the closed loop transfer function from w to z can be written as

$$T_{zw} \;=\; \left[\begin{array}{c|c} A_{cl} & B_{cl} \\ \hline C_{cl} & D_{cl} \end{array}\right] \tag{2.33}$$

$$A_{cl} = \begin{bmatrix} A + B_u Z_1 D_c C_y & B_u Z_1 C_c \\ B_c Z_2 C_y & A_c + B_c Z_2 D_{yu} C_c \end{bmatrix} \tag{2.34}$$

$$B_{cl} = \begin{bmatrix} B_w + B_u Z_1 D_c D_{yw} \\ B_c Z_2 D_{yw} \end{bmatrix} \tag{2.35}$$

$$C_{cl} = [C_z + D_{zu} Z_1 D_c C_y \quad D_{zu} Z_1 C_c] \tag{2.36}$$

$$D_{cl} = [D_{zw} + D_{zu} Z_1 D_c D_{yw}] \tag{2.37}$$

$$Z_1 = [I - D_c D_{yu}]^{-1}, \; Z_2 = [I - D_{yu} D_c]^{-1} \tag{2.38}$$

The closed loop system is said to be *internally stable* if A_{cl} is stable. The pair (A,B) is said to be *stabilizable* if and only if there exists a constant matrix K such that $(A-BK)$ is stable. Equivalently, (A, B) is stabilizable if and only if, for some non-singular transformation T_c,

$$T_c^{-1} A T_c = \begin{bmatrix} A_{c_{11}} & A_{c_{12}} \\ 0 & A_{c_{22}} \end{bmatrix}, \; T_c^{-1} B = \begin{bmatrix} B_{c_1} \\ 0 \end{bmatrix} \tag{2.39}$$

where $(A_{c_{11}}, B_{c_1})$ is reachable and $A_{c_{22}}$ is stable. Likewise, (C, A) is said to be *detectable* if and only if there exists a constant matrix L such that $(A - LC)$ is stable. Equivalently, for some non-singular transformation T_o,

$$T_o^{-1} A T_o = \begin{bmatrix} A_{o_{11}} & 0 \\ A_{o_{21}} & A_{o_{22}} \end{bmatrix}, \; C T_o = [C_{o_1} \quad 0] \tag{2.40}$$

and $(C_{o_1}, A_{o_{11}})$ is observable and $A_{o_{11}}$ is stable. Stabilizibility is not in general preserved under output injection (state estimation via output measurements), nor is detectability preserved under state feedback. To address the cases where these properties are preserved, we introduce stronger notions of these two properties. (A, B, C, D) is said to be *strongly stabilizable* if $(A - LC, B - LD)$ is stabilizable for all L. (A, B, C, D) is said to be *strongly detectable* if $(C - DK, A - BK)$ is detectable for all K.

The following theorem gives some basic conditions for internal stability.

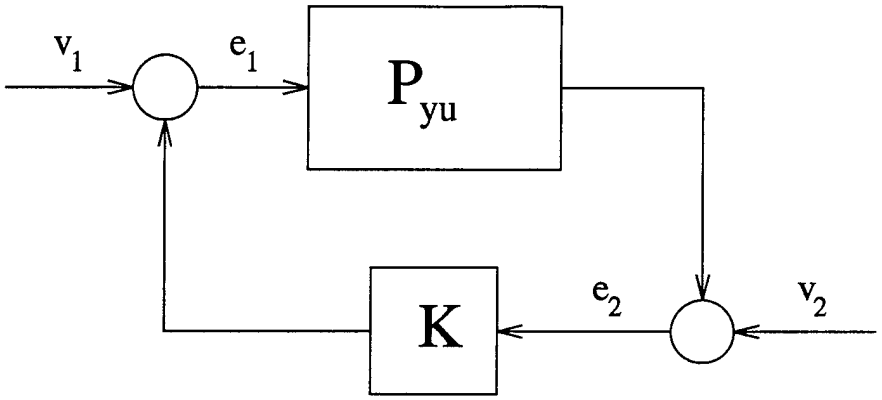

Figure 2.2 Internal Stability System

Theorem 2.3.1 *Assume the realization of P is minimal. Then there exists a causal K achieving internal stability in Figure 2.1 if and only if (A, B_u) is stabilizable and (C_y, A) is detectable.*

Proof: See Kwaakernak and Sivan[2], Theorem 6.4.6. ∎

A controller K which achieves internal stability will be called a *stabilizing*, or *admissible* controller. If such a controller exists then P is said to be stabilizable.

Theorem 2.3.2 *K is a stabilizing controller for P if and only if K is a stabilizing controller for P_{yu}.*

Proof: The proof for continuous-time systems is found in [27], but it applies equally well for discrete-time systems. See also [5]. ∎

Theorem 2.3.2 says that only P_{yu} must be considered for analyzing internal stability for Figure 2.1. Now consider Figure 2.2 for which internal stability implies that, for all bounded inputs (v_1, v_2), the outputs (e_1, e_2) remain bounded. The system in figure 2.1 is internally stable if and only if the system in figure 2.2 is internally stable. Additionally, we can say the system in Figure 2.2 is internally stable if and only if $(I - P_{yu}K)$ is invertible and all four transfer functions in

$$\begin{bmatrix} I & -K \\ -P_{yu} & I \end{bmatrix}^{-1} = \begin{bmatrix} I + K(I - P_{yu}K)^{-1}P_{yu} & K(I - P_{yu}K)^{-1} \\ (I - P_{yu}K)^{-1}P_{yu} & (I - P_{yu}K)^{-1} \end{bmatrix} \tag{2.41}$$

which maps (v_1, v_2) to (e_1, e_2), are causal and stable. See Chapter 4, [27].

2.4 *Lyapunov Equations*

The general form of the discrete-time Lyapunov equation is

$$A^T X A + C^T C = X \tag{2.42}$$

Theorem 2.4.1 *Consider (2.42);*

i. If A is stable, then (2.42) has a unique, positive semi-definite solution X for all C. Further, if (C, A) is observable, then $X > 0$.

ii. Suppose (C, A) is detectable and $X \geq 0$ solves (2.42); then A is stable.

Proof: See Theorems 2.15, 2.16, [28]. ∎

If A is stable, then $A^T X A = X$ implies $X = 0$, which follows from the uniqueness of the solution in Theorem 2.4.1.

2.5 *Algebraic Riccati Equations*

The general algebraic Riccati equation for discrete-time problems is

$$X = A^T X A + Q - \left(S + B^T X A\right)^T \left(R + B^T X B\right)^{-1} \left(S + B^T X A\right) \tag{2.43}$$

where A, B, Q, C and R are real coefficient matrices, Q and R are symmetric, Q is positive semi-definite and R is positive definite. This equation naturally arises from the steady state control problem

$$\min J(u) = \sum_{k=0}^{\infty} \begin{bmatrix} x(k) \\ u(k) \end{bmatrix}^T \begin{bmatrix} Q & S^T \\ S & R \end{bmatrix} \begin{bmatrix} x(k) \\ u(k) \end{bmatrix} \tag{2.44}$$

$$\text{subject to } x(k+1) = Ax(k) + Bu(k)\,, \quad \lim_{k \to \infty} x(k) = 0 \tag{2.45}$$

and hence the term Discrete-time Control Algebraic Riccati Equation (DCARE). We are primarily interested in the Hermitian (and more specifically, symmetric) solutions to (2.43). Note that, for X to be a solution to (2.43), $(R + B^T X B)$ must be invertible. The closest counterpart to this for the continuous-time case is that R must be positive definite, but

this does not involve the solution matrix, X. For state feedback, $u(k) = -Kx(k)$, the feedback gain can be expressed in terms of the solution to (2.43);

$$K = (R + B^T X B)^{-1} (S + B^T X A) \tag{2.46}$$

Theorem 2.5.1 *Assume (A, B) stabilizable, $R > 0$, and define*

$$M = \{X \mid X = X^*,\ R + B^T X B > 0,\ X \text{ solves } (2.43)\} \tag{2.47}$$

Further, assume $M \neq \emptyset$. Then

i. $\exists\ X_+ \in M \ni X_+ > X,\ \forall\ X \in M \ni X \neq X_+$

ii. $|\lambda_i \left(A - B\,(R + B^T X + B)^{-1} (S + B^T X + A)\right)| \leq 1,\ \forall\ i$

where $\lambda(A)$ denotes the set of eigenvalues of A.

Proof: See Theorem 3.1, [29]. The uniqueness of X_+ comes from [30]. ∎

Define the matrix $[H\ J]$ such that

$$[H \quad J]^T [H \quad J] = \begin{bmatrix} Q & S^T \\ S & R \end{bmatrix} \tag{2.48}$$

The following theorem shows equivalence of certain assumptions which will be used later in the development.

Theorem 2.5.2 *$R + B^T X B$ is non-singular if and only if (A, B, H, J) is left invertible.*

Proof: See [28]. ∎

Theorem 2.5.3 *Assume (A, B) stabilizable, and the quadruple (A, B, H, J) is left invertible and strongly detectable. Then there exists a unique $X \geq 0$ which solves (2.43) and*

$$A - B\,(R + B^T X + B)^{-1} (S + B^T X + A) \tag{2.49}$$

is stable. The matrix X is called the stabilizing solution.

Proof: See Lemma 3.6, [28]. ∎

Strong detectability of (A, B, H, J) is not necessary for the existence of a solution, but relaxation of this condition may result in either no solution or a non-unique positive semi-definite solution to (2.43). Further, given a solution X to (2.43), the gain K is unique if and only if (A, B, H, J) is left invertible. If we set $S = 0$, $Q = H^T H \geq 0$, and $R > 0$, then (A, B) stabilizable and (H, A) detectable are necessary and sufficient conditions for the existence of a unique, positive semi-definite solution to (2.43). [31]

A similar theory can be developed for the DARE of the estimation problem which is the dual of (2.43), i.e.,

$$Y = AYA^T + \tilde{Q} - (AYC^T + \tilde{S})^T(\tilde{R} + CYC^T)^{-1}(AYC^T + \tilde{S}) \tag{2.50}$$

where $\tilde{R} = \tilde{R}^T > 0$, and $\tilde{Q} = \tilde{Q}^T \geq 0$. Its stabilizing solution has the property that the injection matrix

$$L = \left(AYC^T + \tilde{S}\right)\left(\tilde{R} + CYC^T\right)^{-1} \tag{2.51}$$

makes $(A - LC)$ stable [28].

There are several ways of solving the DARE. Molinari [30], who has one of the earlier papers written on the DARE, used a factorization approach. For large problems, iterative techniques based on Newton's method have become popular. These methods, however, will not be discussed in this dissertation. The most popular methods for solving DARE's are those based on either Potter's or Laub's method. Potter's method for DARE's is based on finding the invariant subspaces of an associated symplectic matrix M. This symplectic matrix is the discrete-time counterpart of the Hamiltonian matrix used for continuous-time systems. It turns out that M has half its eigenvalues inside the unit circle (stable) and half its eigenvalues outside the unit circle (unstable).

If we define $\hat{A} = A - BR^{-1}S$ and $\hat{Q} = Q - S^T R^{-1} S$, (2.43) can be written as

$$X = \hat{A}^T X \hat{A} + \hat{Q} - \hat{A}^T XB\left(R + B^T XB\right)^{-1} B^T X\hat{A} \tag{2.52}$$

H is said to be *symplectic* if $HJH^T = J$, where J is defined as

$$J = \begin{bmatrix} 0 & I \\ -I & 0 \end{bmatrix} \tag{2.53}$$

and it is assumed that H is partitioned consistently with the identity matrices of J. If A is non-singular, we can define the symplectic matrix

$$M = \begin{bmatrix} \hat{A} + BR^{-1}B^T\hat{A}^{-T}\hat{Q} & -BR^{-1}B^T\hat{A}^{-T} \\ -\hat{A}^{-T}Q & \hat{A}^{-T} \end{bmatrix} \tag{2.54}$$

The matrix M can be used to solve (2.52) in much the same way as the Hamiltonian matrix is used for continuous-time systems. The solution is obtained from a basis for the eigenvectors associated with the stable eigenspace of M. Notice, however, that the formulation of M requires the invertibility of A. Also note that if we set $S = 0$ (no cross-weights), we have $\hat{A} = A$, $\hat{Q} = Q$. This implies that our plant must be invertible to use this approach. This restriction is unique to discrete-time systems, and it can be especially troublesome for discretized plants with pure time delays (see Ch.7, [32]). To remove the restriction of plant invertibility, or improve the numerics if the plant is nearly singular, the generalized eigenvalue approach of Laub can be used [31].

A pair of matrices $S = (S_1, S_2)$, where $S_1,\ S_2 \in C^{2n\times 2n}$, are called *symplectic* (or a *symplectic pair*) if $S_1 J S_1^T = S_2 J S_2^T$, where J is as defined previously. These matrices are important when working with the matrix pencil $S_1 - \lambda S_2$. If S_2 is nonsingular we can define $M = S_2^{-1}S_1$, and solving the resulting equation $M - \lambda I = 0$ is now a familiar eigenvalue problem. The generalized eigenvalue problem is defined via

$$S_1\nu = \lambda S_2\nu \tag{2.55}$$

The generalized eigenvalues are the roots of $\det(S_1 - \lambda S_2) = 0$, and with each generalized eigenvalue, λ_i, the non-zero vector ν_i satisfying (2.55) is called a generalized eigenvector. If λ is a generalized eigenvalue of multiplicity $r > 1$, then the set of vectors $\{\nu_1, \ldots, \nu_l\}$

satisfying

$$\begin{aligned} S_1\nu_1 &= \lambda S_2\nu_1 \\ (S_1 - \lambda S_2)\,\nu_k &= S_2\nu_{k-1}\ ,\ k = 2,3,\ldots,l \ \leq\ r \end{aligned} \tag{2.56}$$

will be called a chain of generalized principal vectors.

Consider (2.52) and define the symplectic pair

$$S_1 = \begin{bmatrix} \hat{A} & 0 \\ -\hat{Q} & I \end{bmatrix}\ ,\ S_2 = \begin{bmatrix} I & BR^{-1}B^T \\ 0 & \hat{A}^T \end{bmatrix} \tag{2.57}$$

Theorem 2.5.4 *Assume $(\hat{A}, B)$ stabilizable and $(H, \hat{A})$ is detectable where $H^TH = \hat{Q}$, rank(H) = rank$(\hat{Q})$. Then none of the eigenvalues of (2.55) lie on the unit circle. Further, λ an eigenvalue of (2.55) implies λ^{-1} is an eigenvalue of (2.55), further implying n eigenvalues inside the unit circle, and n eigenvalues outside the unit circle.*

Proof: See Theorem 3,4 [31]. ∎

[31] also shows that when $\hat{A}$ is non-singular, all of the eigenvalues of (2.55) are non-zero. Further, if $\hat{A}$ is singular, there must be at least one eigenvalue equal to zero.

Theorem 2.5.5 *Assumptions the same as for Theorem 2.5.4. If $\lambda = 0$ is an eigenvalue with multiplicity r, then there are only $2n - r$ finite eigenvalues for (2.55).*

Proof: See Theorem 5, [31]. ∎

If we denote by V the $2n \times n$ matrix of the generalized eigenvectors and principal vectors associated with the n stable eigenvalues, then V is said to be a basis for the stable eigenspace $S_1V = S_2VT$, where T is the $n \times n$ upper left block of the Jordan form corresponding to all $\lambda_i \ni |\lambda| < 1$.

Lemma 2.5.1 *Assumption same as Theorem 2.5.4. All solutions of (2.52) are of the form $X = V_2V_1^{-1}$ where $V = [V_1^T \ \ V_2^T]^T$ is a set of n generalized eigenvectors and principal vectors of (2.55).*

Proof: See Lemma 1, [31]. ∎

Lemma 2.5.2 *Assume* $V = [V_1^T \;\; V_2^T]^T$ *is any set of generalized eigenvectors and principal vectors, and denote by* T *the corresponding* $n \times n$ *block in Jordan canonical form. Further, assume* V_1 *is non-singular. Then*

i. If $(R + B^T X B)$ *is invertible, then* $X = V_2 V_1^{-1}$ *solves (2.52).*

ii. If T *is stable, then* $X = X^T$.

Proof: See Lemma 2, [31]. ∎

Theorem 2.5.6 *Assumptions same as Theorem 2.5.4. Let* $V = [V_1^T \;\; V_2^T]^T$ *be a basis for the stable eigenspace associated with (2.55). Then*

i. V_1^{-1} *exists and* $X = V_2 V_1^{-1}$ *solves (2.52) and* $X = X^T \geq 0$. *If* $(H, \hat{A})$ *is observable, then* $X = X^T > 0$.

ii. The closed loop spectrum, which lies inside the unit circle, is given by

$$\lambda\left(\hat{A} - B\left(R + B^T X B\right)^{-1} B^T X \hat{A}\right) \tag{2.58}$$

Proof: See Theorem 6, [31]. ∎

Several comments are in order. First, if $\hat{A}$ is invertible, then S_2 is invertible, and it can be shown that the matrix $S_2^{-1} S_1$ is symplectic [5]. From here, we can use the method described earlier to solve (2.52), finding a basis for the invariant subspace associated with the standard eigenvalue problem. Second, to avoid possible numerical problems when forming the Jordan canonical form, a similar approach using generalized Schur vectors can be used to solve (2.52). It turns out that the generalized Schur vectors associated with the stable eigenvalues span the same subspace as the generalized eigenvectors and principal vectors. Schur methods are common in ARE solvers for continuous-time systems, and this method will not be described further in this dissertation. The interested reader should consult [32], Chapter 7, and the references therein.

Before moving on to discuss the specific DARE associated with the H_∞ problem, we need to define and discuss the Riccati operator for discrete-time systems. We once again refer to the symplectic pair $S = (S_1, S_2)$, with S_1, S_2 defined as before. Assume no eigenvalues of (2.55) on the unit circle, and let $V = [V_1^T \;\; V_2^T]^T$ be a basis for the stable eigenspace associated with (2.55). If V_1 is invertible (or, equivalently, Image $\left\{[V_1^T \;\; V_2^T]^T\right\}$ and Image $\left\{[0 \;\; I]^T\right\}$ are complementary), we can define $X = V_2 V_1^{-1}$. Since X is uniquely determined by S, we can define an operator $Ric(S)$ such that $X = Ric(S)$. The domain of Ric contains symplectic pairs such that the following conditions hold [11] :

i. *STABILITY*: The eigenvalue problem (2.55) has no solutions on the unit circle.

ii. *COMPLEMENTARITY*: V_1 is invertible.

iii. *INVERTIBILITY*: $(I + BR^{-1}B^T X)$ is invertible. (By the Matrix Inversion Lemma, this is equivalent to $R + B^T X B$ being invertible.)

If the symplectic pair meets these conditions, we say $S \in Dom(Ric)$.

Theorem 2.5.7 *Suppose* $S \in Dom(Ric), X = Ric(S)$. *Then*

i. $X = X^T$

ii. $(R + B^T X B)$ *and* $(I + BR^{-1}B^T X)$ *are non-singular*

iii. X *solves (2.52)*

iv. The matrix $\hat{A} - B\left(R + B^T X B\right)^{-1} B^T X \hat{A} = \left[\left(I + BR^{-1}B^T X\right)^{-1} \hat{A}\right]$ *is stable.*

Proof: See Lemma 2.1, [11], and Lemma 2.3, [33]. ∎

X is called the stabilizing solution of (2.52), and it is unique. For the dual problem associated with the filter, see Remark 2.1, [33].

2.6 Calculating the System Norms

In this dissertation, the 1, 2, and ∞-norms will be considered. We already briefly discussed the interpretation of these norms in a previous section, but we will now discuss how the norms can be calculated. We begin with a method for calculating the 2-norm.

2.6.1 Calculating the 2-norm. Assume $G = (A, B, C, D)$ is stable. The system 2-norm can be calculated as

$$\|G\|_2 = \sqrt{tr\left[DD^T + CPC^T\right]} = \sqrt{tr\left[D^T D + B^T Q B\right]} \tag{2.59}$$

where P and Q are the reachability and observability grammians, which are the positive semi-definite solutions of the discrete-time Lyapunov equations

$$APA^T + BB^T = P \tag{2.60}$$

$$A^T QA + C^T C = Q \tag{2.61}$$

Note that, unlike the case for continuous time, the 2-norm remains finite for $D \neq 0$ in discrete time.

2.6.2 Calculating the ∞-norm. The calculation of the ∞-norm involves computing the maximum singular value of the matrix transfer function over all frequencies. Recall the definition

$$\|G\|_\infty := \operatorname*{ess\,sup}_\theta \left[R\left(e^{j\theta}\right)\right] \tag{2.62}$$

A straightforward method of estimating this value is to evaluate the singular values at several points along the unit circle and take the maximum over all points. The accuracy of this method clearly depends on the number of points, and the value obtained will always be a lower bound for the actual ∞-norm. However, in cases where we are only interested in meeting a (possibly conservative) norm constraint, this may be the most efficient method. A second approach, based on the Discrete Bounded Real Lemma [34], makes use of the generalized eigenvalue problem in (2.55) associated with a particular Riccati equation. It yields a conservative upper bound which can be obtained with any degree of accuracy desired (with obvious limitations based on machine precision). This method will be described subsequently.

Consider the system $G = (A, B, C, D)$, and define the symplectic pair $S = (S_1, S_2)$, where

$$S_1 = \begin{bmatrix} A_s & 0 \\ \gamma^{-2} C^T S^{-1} C & I \end{bmatrix}, \quad S_2 = \begin{bmatrix} I & BR^{-1}B^T \\ 0 & A_s{}^T \end{bmatrix} \tag{2.63}$$

$$R = (I - \gamma^{-2} D^T D) \tag{2.64}$$

$$S = (I - \gamma^{-2} D D^T) \tag{2.65}$$

$$A_s = A + \gamma^{-2} B R^{-1} D^T C \tag{2.66}$$

S is the symplectic pair associated with the Riccati equation

$$X = A^T X A + C^T C - \left(D^T C + B^T X A\right)^T \left(\gamma^2 I - D^T D - B^T X B\right)^{-1} \left(D^T C + B^T X A\right) \tag{2.67}$$

Following are several theorems which are useful for calculating the ∞-norm or checking to see if a constraint has been met. We will need a preliminary definition; $X = X^T \geq 0$ is called a strong solution if $\gamma^2 I - D^T D - B^T X B > 0$, X solves (2.67), and the eigenvalues of

$$A + B\left(\gamma^2 I - D^T D - B^T X B\right)^{-1} \left(D^T C + B^T X A\right) \tag{2.68}$$

are in the closed unit disc.

Theorem 2.6.1 (Discrete Bounded Real Lemma) *The following statements are equivalent.*

i. A *is stable and* $\|G\|_\infty \leq \gamma$

ii. (C, A) *has no unobservable modes on the unit circle and* $\exists$ *a strong solution* $X = X^T \geq 0$ *to (2.67)* $\ni \gamma^2 I - D^T D - B^T X B > 0$

Proof: See Theorem 2.1 [34]. ∎

Theorem 2.6.2 (Discrete Strict Bounded Real Lemma) *The following statements are equivalent.*

i. A *is stable and* $\|G\|_\infty < \gamma$

ii. $\exists$ *a matrix* $\tilde{X} = \tilde{X}^T$ *satisfying*

$$A^T\tilde{X}A - \tilde{X} + C^TC - \left(D^TC + B^T\tilde{X}A\right)^T \left(\gamma^2 I - D^TD - B^T\tilde{X}B\right)^{-1} \left(D^TC + B^T\tilde{X}A\right) < 0 \tag{2.69}$$

such that $\gamma^2 I - D^TD - B^T\tilde{X}B > 0$

iii. $\exists$ *a stabilizing solution* $X = X^T \geq 0$ *to (2.67)* $\ni \gamma^2 I - D^TD - B^TXB > 0$

Further, $X < \tilde{X}$.

Proof: See Theorem 2.2, [34]. ∎

Theorem 2.6.3 *Suppose* $\bar{\sigma}(D) < \gamma$ *and* A *is stable, where* $\bar{\sigma}(D)$ *denotes the maximum singular value of* D. *Then the following statements are equivalent.*

i. $\|G\|_\infty < \gamma$

ii. $S \in Dom(Ric)$, $\gamma^2 I - D^TD - B^TXB > 0$, $X = Ric(S) \geq 0$. *(*$Ric(S) > 0$ *if* (C, A) *is observable)*

Proof: See [11]. ∎

The following theorem is especially helpful for calculating the ∞-norm.

Theorem 2.6.4 *Assume* A *is stable and* $\exists\ \gamma > 0$ *such that the following hold:*

i. $\exists\ \theta_0 \in [0, 2\pi)$ *with* $\bar{\sigma}\left[G\left(e^{j\theta_0}\right)\right] < \gamma$

ii. γ *is not a singular value of* D

Then $\|G\|_\infty < \gamma$ *if and only if* S *has no generalized eigenvalues on the unit circle.*

Proof: See Theorem 4.4.1, [5]. ∎

Theorems 2.6.3 and 2.6.4 can easily be used to define a bisection algorithm for calculating $\|G\|_\infty$, similar to what is done for the continuous-time case. This is done in [5].

2.6.3 Calculating the 1-norm. Like the ∞-norm, the system 1-norm must, in general, be approximated. Also like the ∞-norm, the 1-norm can be approximated to within an arbitrarily small ϵ. Assume G is a stable transfer function with state-space realization (A, B, C, D). The pulse response of the system G is given by

$$G(k) = \begin{cases} D & k = 0 \\ CA^{k-1}B & k > 0 \end{cases} \tag{2.70}$$

If the system is stable, all the eigenvalues of A are inside the unit disc, and for all $\epsilon > 0$ there exists N such that $\|G\|_1 - \|P_N G\|_1 < \epsilon$, where P_N is the truncation operator. The value of N, which will in general be conservative, can be estimated from the spectral radius of A. An alternative method for bounding the truncation error avoids some of the conservatism of the eigenvalue method [5], and this method will be described subsequently.

For any system G, the ℓ_1 norm can be written as

$$\|G\|_1 = \|P_N G\|_1 + \|\tilde{G}\|_1 \tag{2.71}$$

where

$$\tilde{G} \equiv \{0, CA^N B, CA^{N+1}B, \ldots\} \equiv \left[\begin{array}{c|c} A & A^N B \\ \hline C & 0 \end{array}\right] \tag{2.72}$$

Further, it can be shown that

$$\frac{\tilde{\sigma}_1}{\sqrt{p}} \leq \|\tilde{G}\|_1 \leq 2\sqrt{m} \sum_{i=1}^{n} \tilde{\sigma}_i \tag{2.73}$$

where p is the number of outputs, m is the number of inputs,

$$\tilde{\sigma}_i = \sqrt{\lambda_i \left(Q A^N P \left(A^T\right)^N \right)} \tag{2.74}$$

and P and Q are the reachability and observability grammians of G. For stable G, $\tilde{\sigma}_i$ approaches zero as N approaches infinity. Given $\epsilon > 0$, define

$$N_{min} := \min \left\{ N \mid 2\sqrt{m} \sum_{i=1}^{n} \tilde{\sigma}_i - \frac{\tilde{\sigma}_1}{\sqrt{p}} < \epsilon \right\} \tag{2.75}$$

Then

$$\|P_{N_{min}}G\|_1 + \frac{\tilde{\sigma}_1}{\sqrt{p}} \leq \|G\|_1 \leq \|P_{N_{min}}G\|_1 + 2\sqrt{m}\sum_{i=1}^{n}\tilde{\sigma}_i \tag{2.76}$$

where

$$\|P_{N_{min}}G\|_1 = \max_{1\leq i\leq p}\sum_{j=1}^{m}\sum_{k=0}^{N_{min}}|g_{ij}(k)| \tag{2.77}$$

2.7 Convex Optimization

This section is an introduction into some key concepts of convex programming which will be necessary for this work. For a complete discussion of this topic, the reader is referred to [35, 36, 37, 38, 39, 40].

Let X be a vector space, $x_1, x_2 \in X$, and $\alpha \in (0,1)$. Then a *convex combination* of x_1 and x_2 is $\alpha x_1 + (1-\alpha)x_2$. A set $C \subset X$ is said to be a *convex set* if, for every $x_1, x_2 \in C$, all convex combinations of x_1 and x_2 are also contained in C. Defining a functional $f : C \rightarrow \mathbf{R}$, f is said to be a *convex functional* if

$$f[\alpha x_1 + (1-\alpha)x_2] \leq \alpha f(x_1) + (1-\alpha)f(x_2) \tag{2.78}$$

for all $x_1, x_2 \in C$ and all $\alpha \in (0,1)$. Furthermore, f is said to be a *strictly convex functional* if strict inequality holds in (2.78), whenever $x_1 \neq x_2$.

Suppose $f(x)$, $g_1(x), \ldots, g_m(x)$ are functionals defined on some subset C of a vector space X. We are interested in the following *program*:

$$\mathcal{P} \begin{cases} \text{Minimize } f(x) \text{ subject to} \\ g_i(x) \leq 0 \text{ for all } i \\ \text{where } x \in C \subset X \end{cases} \tag{2.79}$$

The functional $f(x)$ is called the *objective*, and the functional inequalities $g_i(x) \leq 0$ are called the *constraints*. A vector $x \in C$ is said to be an *admissible point* for $\mathcal{P}$ if it satisfies all the constraints in $\mathcal{P}$. The set A of all admissible points is called the *admissible region* for $\mathcal{P}$. If A is not empty, the $\mathcal{P}$ is said to be *consistent*, and if there exists an $x \in A$ such that $g_i(x) < 0$ for all i, then $\mathcal{P}$ is said to be *superconsistent*. If $\mathcal{P}$ is a consistent program

and there exists an $x^* \in A$ such that $f(x^*) \leq f(x)$ for all $x \in A$, then x^* is a *solution* for $\mathcal{P}$. Furthermore, if $\mathcal{P}$ is superconsistent, then the admissible region has an interior point. This is a necessary assumption for the main theorem of this section.

If the objective $f(x)$, the constraints $g_i(x)$, and the underlying set C are all convex, then $\mathcal{P}$ is called a *convex program.* In this case the admissible set A will always be convex. The *Lagrangian* $\mathcal{L}$ of the convex program $\mathcal{P}$ is defined as

$$\mathcal{L}(x, \Lambda) := f(x) + \sum_{i=1}^{m} \lambda_i g_i(x) \tag{2.80}$$

where $x \in C$, $\Lambda := [\lambda_1, \ldots, \lambda_m]^T \in \mathbf{R}^m$, and $\lambda_i \geq 0$ for all i.

The following theorem is the central result of convex programming.

Theorem 2.7.1 (Kuhn-Tucker Theorem – Saddle Point Form) *Suppose $\mathcal{P}$ given in (2.79) is a superconsistent convex program. Then $x^* \in C$ is a solution of $\mathcal{P}$ if and only if there exists a $\Lambda^* \in \mathbf{R}^m$ such that:*

i. $\lambda_j^* \geq 0$ *for all* j

ii. $\mathcal{L}(x^*, \Lambda) \leq \mathcal{L}(x^*, \Lambda^*) \leq \mathcal{L}(x, \Lambda^*)$
for all $x \in C$ *and all* $\Lambda \in \mathbf{R}^m$ *such that* $\lambda_j \geq 0$ *for all* j

iii. $\lambda_j g_j(x^*) = 0$ *for all* j

Proof: See [40], Theorem 5.2.13. ∎

The above theorem is just one form of the famous group of related theorems called Kuhn-Tucker (KT) Theorems. For the convex analysis in this work, the saddle point form will be sufficient. For additional forms of the KT Theorem, see, for instance, [37, 39, 40]. The results of Theorem 2.7.1 are referred to as the *Kuhn-Tucker conditions*, or just the KT conditions.

The next theorem deals with the uniqueness of the solution to a convex program.

Theorem 2.7.2 *Suppose $\mathcal{P}$ is the convex program given in (2.79) and $x^* \in C$ satisfies the Kuhn-Tucker conditions. If f(x) is strictly convex, then x^* is unique.*

Proof: See [38], Corollary to Theorem 9.4.1. ∎

2.8 Duality in Minimum Norm Problems

The final section of this chapter will discuss a dual approach for solving minimum norm problems. An excellent source for this subject is [39].

Let X be a normed, linear, vector space. A functional $f : X \rightarrow \mathbf{R}$ is a *linear functional* if

$$f(\alpha x_1 + \beta x_2) = \alpha f(x_1) + \beta f(x_2) \tag{2.81}$$

for all $x_1, x_2 \in X$ and for all $\alpha, \beta \in \mathbf{R}$. Further, f is a *bounded linear functional* if there is some $M \in \mathbf{R}$ such that

$$|f(x)| \leq M\|x\| \tag{2.82}$$

for all $x \in X$. The infimum over all such M is called the norm of f, denoted $\|f\|$. The space of all bounded linear functionals on X is called the *dual* of X and is denoted $X^\star$. Given $x^\star \in X^\star$, then

$$\|x^\star\| := \sup_{\|x\| \leq 1} |x^\star(x)| \tag{2.83}$$

The spaces under consideration in this work will be H_2 and L_2, which are Hilbert spaces, and as such have special properties which will simplify the dual problem. Let X be a Hilbert space. Then the following theorem provides a representation of bounded linear functionals on X.

Theorem 2.8.1 (Riesz-Fréchet) *Assume X is a Hilbert space. If f is a bounded linear functional on X, then there exists a unique vector $y \in X$ such that*

$$f(x) = \langle x, y \rangle \tag{2.84}$$

for all $x \in X$. Furthermore,

$$\|f\| = \|y\| \tag{2.85}$$

and every $y \in X$ determines a unique bounded linear functional in this way.

Proof: See [39], Theorem 5.3.2. ∎

Thus, linear functionals on a Hilbert space can be represented uniquely by a vector in the space. For the remainder of this work it will be assumed that $[\cdot]^\star$ is the vector which represents the actual functional in the dual space; while this is an abuse of notation, it will simplify the discussion.

Another key concept in duality theory is alignment. A vector $x^\star \in X^\star$ is said to be *aligned* with a vector $x \in X$ if

$$\langle x, x^\star \rangle = \|x^\star\| \|x\| \tag{2.86}$$

Finally, let X be a normed vector space. Then the *support functional* of a convex set $K \subset X$ is defined on $X^\star$ as

$$h(x^\star) := \sup_{x \in K} \langle x, x^\star \rangle \tag{2.87}$$

The next theorem provides the main results from duality theory for the minimum norm problem.

Theorem 2.8.2 (Minimum Norm Duality) *Assume X is a real normed vector space. Let $d > 0$ denote the distance from a point $x_1 \in X$ to some convex set $K \subset X$ having support functional h, then*

$$d = \inf_{x \in K} \|x - x_1\| = \max_{\|x^\star\| \leq 1} [\langle x_1, x^\star \rangle - h(x^\star))] \tag{2.88}$$

where the maximum on the right is achieved by some $x_0^\star \in X^\star$. If the infimum on the left is achieved by some $x_0 \in K$, then $-x_0^\star$ is aligned with $x_0 - x_1$.

Proof: See [39], Theorem 5.13.1. ∎

Therefore, the primal problem (an infimization over elements in the primal space) can be transformed into a maximization problem over elements in the dual space. While this may not always provide a complete solution to the problem, when combined with the alignment condition, optimal solutions can often be found.

2.9 Summary

This chapter introduced definitions and notations for signals, sequences and linear spaces. Further, we reviewed some operator theory, and introduced the special type of operators used to represent LTI systems. For LTI systems, we introduced definitions of stability, controllability, observability, and other related concepts. A brief review of Lyapunov equations and discrete algebraic Riccati equations was presented. This was followed by an introduction to the basic concepts of convex programming, including the Kuhn-Tucker Theorem. Finally, duality concepts were used to convert an infimization problem into a maximation problem in the dual space.

III. Review of Related Control Theory

This dissertation explores constrained optimization approaches to combining the H_2, ℓ_1, and H_∞ norms of dissimilar but related transfer functions. This chapter will provide a review of some of the relevant theory associated with each of the individual methods. Although Linear Quadratic Gaussian (LQG) and H_2 synthesis methods are well established, the review in this chapter will serve to clear up some common misconceptions regarding causality and optimality for the discrete-time problem. In contrast to H_2, the ℓ_1 control theory is relatively new, with ℓ_1 synthesis methods only becoming available in the late 1980's. Although the ℓ_1 synthesis methods will not be used in this dissertation, the nature of the solution resulting from ℓ_1 synthesis has some parallels in the mixed-norm problem. For this reason, and to acquaint the reader with this relatively new theory, the ℓ_1 optimal control theory will be reviewed.

H_∞ control theory will not be covered in this chapter. The reason is that standard H_∞ synthesis methods were not used in this research, and these methods are not necessary to understand how the H_∞ constraints were applied in the mixed-norm setting. The most relevant portions of H_∞ theory for this work are the Bounded Real Lemma and the calculation of the ∞-norm, which were covered in Chapter II. For present purposes, it suffices to say that H_∞ control synthesis has the effect of flattening over all frequencies the maximum singular-value of the closed-loop system with weights [4]. It is a minimization of the maximum gain over all frequency. A complete development of the state-space solution to the discrete-time H_∞ problem is contained in [11]. An excellent review of discrete-time H_∞ (as well as H_2 and ℓ_1) control synthesis is also contained in [5].

3.1 Parametrization of All Stabilizing Controllers

Consider the feedback system given in Figure 3.1 where $K \in \mathbf{K}$, the set of all stabilizing controllers. $\mathbf{K}$ is not a convex set; thus, the tools of convex analysis can not be applied directly. However, a parametrization of all stabilizing controllers over a convex set has been developed from the work of Youla, *et al* [1]. A complete discussion of the parametrization can be found in [27, 5]. This will only be an introduction into the key

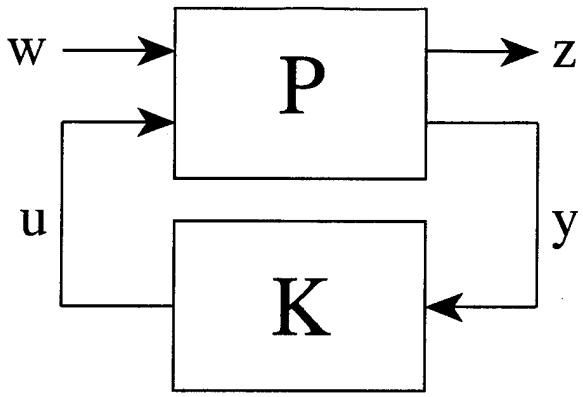

Figure 3.1 Feedback system

ideas needed for this work. First we need to introduce the idea of a coprime factorization of a transfer function.

3.1.1 Coprime Factorizations. Two stable, rational function matrices F, G are *right-coprime* with respect to the space of stable systems if they have an equal number of columns and there exist stable function matrices X, Y such that

$$\begin{bmatrix} X & Y \end{bmatrix} \begin{bmatrix} F \\ G \end{bmatrix} = XF + YG = I \tag{3.1}$$

Further, F and G are *left-coprime* with respect to the space of stable systems if they have an equal number of rows and there exist stable function matrices X, Y such that

$$\begin{bmatrix} F & G \end{bmatrix} \begin{bmatrix} X \\ Y \end{bmatrix} = FX + GY = I \tag{3.2}$$

Let G be a proper transfer function matrix. Then writing $G = NM^{-1}$ where N and M are right-coprime is called a *right-coprime factorization* of G. Similarly, the factorization $G = \tilde{M}^{-1}\tilde{N}$ where $\tilde{N}$ and $\tilde{M}$ are left-coprime is called a *left-coprime factorization* of G. Finally, for each proper matrix G, there exist stable $N, M, \tilde{N}, \tilde{M}, X, Y, \tilde{X}, \tilde{Y}$ such that

$$G = NM^{-1} = \tilde{M}^{-1}\tilde{N} \tag{3.3}$$

and

$$\begin{bmatrix} \tilde{X} & -\tilde{Y} \\ -\tilde{N} & \tilde{M} \end{bmatrix} \begin{bmatrix} M & Y \\ N & X \end{bmatrix} = I \tag{3.4}$$

Equations (3.3) and (3.4) constitute a *doubly-coprime factorization* of G.

3.1.2 Parametrization. The following presents a method of parametrizing all stabilizing controllers.

Theorem 3.1.1 *Assume G is a proper transfer function matrix with a doubly-coprime factorization given by (3.3) and (3.4). Then the set of all controllers K which stabilize G is parametrized by*

$$K = (Y - MQ)(X - NQ)^{-1} \tag{3.5}$$

$$= (\tilde{X} - Q\tilde{N})^{-1}(\tilde{Y} - Q\tilde{M}) \tag{3.6}$$

where Q is stable.

Proof: See [5], Theorem 5.2.2. ∎

Theorem 3.1.1 does not specify a space for Q. In fact, the space in which Q lies depends on the space in which stability is defined [5].

i. If the closed-loop transfer function must be LTI and ℓ_1 stable (bounded 1-norm), then the parametrization is over $Q \in \ell_1$.

ii. If the closed-loop system must be finite-dimensional, LTI and ℓ_1 stable, then the parametrization is over $Q \in \mathbf{R}H_\infty$ (the real rational elements of H_∞).

iii. If the closed-loop system must be LTI and H_∞ stable (bounded ∞-norm), then the parametrization is over $Q \in H_\infty$.

iv. If the closed-loop system must be finite-dimensional, LTI and H_∞ stable, then the parametrization is over $Q \in \mathbf{R}H_\infty$.

Extensions can be made for time-varying and/or non-linear systems, and these extensions are discussed in [5].

Recall that P in Figure 3.1 can be partitioned as

$$P = \begin{bmatrix} P_{zw} & P_{zu} \\ P_{yw} & P_{yu} \end{bmatrix} \tag{3.7}$$

Also, recall from Theorem 2.3.2 that a controller K stabilizes P if and only if it stabilizes P_{yu}. Using this, we can parametrize all internally stable closed-loop transfer functions T_{zw}.

Theorem 3.1.2 *Let the stable factors $N, M, \tilde{N}, \tilde{M}, X, Y, \tilde{X}, \tilde{Y}$ represent a doubly-coprime factorization of P_{yu}, K be defined as in Theorem 3.1.1, and define*

$$T_1 = P_{zw} + P_{zu}M\tilde{Y}P_{yw} \tag{3.8}$$

$$T_2 = P_{zu}M \tag{3.9}$$

$$T_3 = \tilde{M}P_{yw} \tag{3.10}$$

Then T_1, T_2, T_3 are stable and

$$T_{zw} = T_1 - T_2QT_3 \tag{3.11}$$

Furthermore, spanning Q over all elements in its appropriate space generates all stabilizing K from equations 3.5 and 3.6.

Proof: See [27], Theorem 4.5.1, and [5], Chapter 5. ∎

3.2 Steady-State Linear Quadratic Gaussian (LQG) Control Synthesis

Consider the system

$$x(k+1) = Ax(k) + Bu(k) + w(k) \tag{3.12}$$

$$y(k) = Cx(k) + v(k) \tag{3.13}$$

where w, v are zero mean white Gaussian processes with covariance

$$E\left\{\begin{bmatrix} w(j) \\ v(j) \end{bmatrix}\begin{bmatrix} w(k)^T & v(k)^T \end{bmatrix}\right\} = \begin{bmatrix} Q_1 & S_1^T \\ S_1 & R_1 \end{bmatrix}\delta_{jk} \tag{3.14}$$

Note that we are assuming no direct feedforward of the control u in the measurement y ($D_{yu} = 0$). We wish to design a dynamic compensator which stabilizes the closed-loop system and minimizes the quadratic cost functional

$$J(u) = E\left\{\sum_{k=-\infty}^{\infty}\begin{bmatrix} x(k)^T & u(k)^T \end{bmatrix}\begin{bmatrix} Q_2 & S_2 \\ S_2^T & R_2 \end{bmatrix}\begin{bmatrix} x(k) \\ u(k) \end{bmatrix}\right\} \tag{3.15}$$

This is an infinite horizon problem which results in a constant-gain (but dynamic) compensator. Assuming the weighting and covariance matrices are positive semidefinite, we can express them in the form

$$\begin{bmatrix} Q_1 & S_1^T \\ S_1 & R_1 \end{bmatrix} = \begin{bmatrix} B_1 \\ D_1 \end{bmatrix}\begin{bmatrix} B_1^T & D_1^T \end{bmatrix} \tag{3.16}$$

$$\begin{bmatrix} Q_2 & S_2 \\ S_2^T & R_2 \end{bmatrix} = \begin{bmatrix} C_2^T \\ D_2^T \end{bmatrix}\begin{bmatrix} C_2 & D_2 \end{bmatrix} \tag{3.17}$$

If we admit only strictly causal compensators, the optimal steady-state compensator for this system (under assumptions to be specified shortly) is well known to consist of a steady state Kalman filter in cascade with a Linear Quadratic Regulator (LQR). This is referred to as a Linear Quadratic Gaussian (LQG) compensator.

$$x_c(k+1) = Ax_c(k) + Bu(k) - K_f\left(y(k) - Cx_c(k)\right) \tag{3.18}$$

$$u(k) = K_c x_c(k) \tag{3.19}$$

The certainty equivalence principle associated with LQG states that the filter gain (K_f) and regulator gain (K_c) are the same as those resulting from independent estimator and regulator designs [3]. Certainty equivalence, if it is a valid assumption, also holds for non-strictly causal compensators, but the final form is slightly different from that shown above. We now state the theorem describing strictly causal LQG synthesis.

Theorem 3.2.1 *Assume*

i. (A, B) *stabilizable,* (C, A) *detectable.*

ii. (A, B_1, C, D_1) *is strongly stabilizable and right invertible.*

iii. (A, B, C_2, D_2) *is strongly detectable and left invertible.*

Then

i. $\exists!\ X = X^T \geq 0$ *such that*

$$X = A^T X A + Q_2 - \left(A^T X B + S_2\right)\left(R_2 + B^T X B\right)^{-1}\left(B^T X A + S_2^T\right) \tag{3.20}$$

ii. $\exists!\ Y = Y^T \geq 0$ *such that*

$$Y = AYA^T + Q_1 - \left(AYC^T + S_1^T\right)\left(R_1 + CYC^T\right)^{-1}\left(CYA^T + S_1\right) \tag{3.21}$$

iii. The gains which stabilize $A + BK_c$, $A + K_f C$ *and minimize* J *are unique, where*

$$K_c = -\left(R_2 + B^T X B\right)^{-1}\left(B^T X A + S_2^T\right) \tag{3.22}$$

$$K_f = -\left(AYC^T + S_1^T\right)\left(R_1 + CYC^T\right)^{-1} \tag{3.23}$$

iv. The minimum cost realized is

$$J_{opt} = tr\left[YK_c^T(R_2 + B^T X B)K_c\right] + tr[XQ_1] \tag{3.24}$$

$$= tr[YQJ_2] + tr\left[XK_f(CYC^T + R_1)K_f^T\right] \tag{3.25}$$

Proof: See Theorem 5.5, [28]. ∎

If we restrict the problem above to one in which measurement and process driving noise are uncorrelated and there are no state/control cross weights in the performance index, we can significantly reduce the number of assumptions required.

Theorem 3.2.2 *Assume* $S_i = 0$, $Q_i \geq 0$, $R_i > 0$, $i = 1,2$. *Further, assume* (A, B) *stabilizable, and* (C, A) *detectable. Then*

i. $\exists!\ X = X^T \geq 0$ *such that*

$$X = A^T X A + Q_2 - A^T X B \left(R_2 + B^T X B\right)^{-1} B^T X A \tag{3.26}$$

ii. $\exists!\ Y = Y^T \geq 0$ *such that*

$$Y = AYA^T + Q_1 - AYC^T \left(R_1 + CYC^T\right)^{-1} CYA^T \tag{3.27}$$

iii. The gains which stabilize $A + BK_c$, $A + K_f C$ *and minimize* J *are unique, where*

$$K_c = -\left(R_2 + B^T X B\right)^{-1} B^T X A \tag{3.28}$$

$$K_f = -AYC^T \left(R_1 + CYC^T\right)^{-1} \tag{3.29}$$

iv. The minimum cost realized is

$$J_{opt} = tr\left[Y K_c^T (R_2 + B^T X B) K_c\right] + tr[XQ_1] \tag{3.30}$$

$$= tr[YQJ_2] + tr\left[X K_f (CYC^T + R_1) K_f^T\right] \tag{3.31}$$

Proof: See [28]. ∎

Theorem 3.2.1 is not the most general theorem dealing with discrete-time LQG, because it allows only strictly causal ($D_c = 0$) compensators. Note that a feedforward term in the measurement could have been included without change to the assumptions of Theorem 3.2.1; only the final form of the filter and the final cost would change. To see this, we will first consider the simpler problem addressed by Theorem 3.2.2. Define the control and filter gains, respectively, as

$$K_c = -\left(R_2 + B^T X B\right)^{-1} B^T X A \tag{3.32}$$

$$\tilde{K}_f \;=\; -YC^T\left(R_1 + CYC^T\right)^{-1}\;,\;\; K_f = A\tilde{K}_f \tag{3.33}$$

where X solves (3.26) and Y solves (3.27). We need to introduce $\hat{x}(k^-)$ and $\hat{x}(k^+)$ as the estimate of $x(k)$ before and after, respectively, the incorporation of the k^{th} measurement. Within the estimator, we have a propagation equation,

$$\hat{x}(k+1^-) = A\hat{x}(k^+) + B_u(k) \tag{3.34}$$

and an update equation

$$\hat{x}(k^+) = \hat{x}(k^-) - \tilde{K}_f\left(y(k) - C\hat{x}(k^-)\right) \tag{3.35}$$

Substituting (3.35) into (3.34), we obtain

$$\hat{x}(k+1^-) = \left(A + A\tilde{K}_f C\right)\hat{x}(k^-) - A\tilde{K}_f y(k) + Bu(k) \tag{3.36}$$

Basing the control law on all information up to, but not including, the most recent measurement yields a control law

$$u(k) = K_c\hat{x}(k^-) \tag{3.37}$$

This amounts to a strict causality assumption. Substituting (3.37) into (3.36) results in a compensator of the form

$$K_{sc} \;=\; \left[\begin{array}{c|c} A + BK_c + A\tilde{K}_f C & -A\tilde{K}_f \\ \hline K_c & 0 \end{array}\right] \tag{3.38}$$

$$\;=\; \left[\begin{array}{c|c} A + BK_c + K_f C & -K_f \\ \hline K_c & 0 \end{array}\right] \tag{3.39}$$

Note that $D_{sc} = 0$, indicating a strictly causal compensator.

If we now allow our control law to be based on all information up to and including the most recent measurement, our control law will have the form

$$u(k) = K_c \hat{x}(k^+) \tag{3.40}$$

Substituting (3.40) into (3.36) now yields a causal, but not strictly causal, compensator.

$$K_{nsc} = \left[\begin{array}{c|c} A + BK_c + A\tilde{K}_f C + BK_c\tilde{K}_f C & -A\tilde{K}_f - BK_c\tilde{K}_f \\ \hline K_c + K_c\tilde{K}_f C & -K_c\tilde{K}_f \end{array}\right] \tag{3.41}$$

For the case where A is invertible, equation (3.41) can be written as

$$K_{nsc} = \left[\begin{array}{c|c} A + BK_c + K_f C + BK_c A^{-1} K_f C & -K_f - BK_c A^{-1} K_f \\ \hline K_c + K_c A^{-1} K_f C & -K_c A^{-1} K_f \end{array}\right] \tag{3.42}$$

K_{nsc}, if it can be implemented, will result in better 2-norm performance when compared to K_{sc}, because K_{nsc} takes advantage of a more accurate estimate of the states $x(k)$. A requirement for implementation is that the computational delay associated with incorporating the latest measurement into the estimate must be negligible compared to the sample period. Implementation methods for ensuring this requirement is met, as well as a more complete discussion of the causality assumption, can be found in [41].

The previous results can be extended to the case where $S_i \neq 0,\ i = 1, 2$ by redefining the control and filter gains (3.33) as

$$K_c = -\left(R_2 + B^T X B\right)^{-1} \left(B^T X A + S_2^T\right) \tag{3.43}$$

$$\tilde{K}_f = -\left(Y C^T + S_1^T\right) \left(R_1 + C Y C^T + C S_1^T + S_1 C^T\right)^{-1} \tag{3.44}$$

where X solves (3.20) and Y solves (3.21). These gains can now be used directly in either (3.38) or (3.41) to form the desired compensator for this more general problem.

3.3 H_2 Optimal Control Synthesis

Now consider the H_2 optimization problem where the system is given by

$$G = \left[\begin{array}{c|cc} A & B_w & B_u \\ \hline C_z & D_{zw} & D_{zu} \\ C_y & D_{yw} & D_{yu} \end{array}\right] \tag{3.45}$$

Once again, it is not necessary to assume $D_{yu} = 0$, but it eases the notation. We wish to find a strictly causal, stabilizing compensator which minimizes the 2-norm of the closed loop transfer function. Let us also define

$$\begin{bmatrix} B_w \\ D_{yw} \end{bmatrix} \begin{bmatrix} B_w^T & D_{yw}^T \end{bmatrix} = \begin{bmatrix} Q_1 & S_1^T \\ S_1 & R_1 \end{bmatrix} \geq 0 \tag{3.46}$$

$$\begin{bmatrix} C_z^T \\ D_{zu}^T \end{bmatrix} \begin{bmatrix} C_z & D_{zu} \end{bmatrix} = \begin{bmatrix} Q_2 & S_2 \\ S_2^T & R_2 \end{bmatrix} \geq 0 \tag{3.47}$$

With these definitions, Theorem 3.2.1 can be applied directly to solve the H_2 optimization problem. If we make some common orthogonality assumptions, $D_{zu}^T C_z = 0$ and $B_w D_{yw}^T = 0$, and also assume $R_1 > 0, R_2 > 0$, then Theorem 3.2.2 can also be applied. The first two assumptions are equivalent to the LQG assumptions of having no cross weights between states and control, and uncorrelated measurement and plant driving noises, respectively. The third and fourth assumptions insure that the resulting control problem will be non-singular, and they are equivalent to the LQG assumptions of no perfect measurements or free control usage, respectively.

We would now like to state the problem in a form consistent with the use of the Riccati operator. Define the symplectic pairs

$$S = \left(\begin{bmatrix} A_S & 0 \\ -Q_S & I \end{bmatrix}, \begin{bmatrix} I & B_u R_2^{-1} B_u^T \\ 0 & A_S^T \end{bmatrix} \right) \tag{3.48}$$

$$T = \left(\begin{bmatrix} A_T^T & 0 \\ -Q_T & I \end{bmatrix}, \begin{bmatrix} I & C_y^T R_1^{-1} C_y \\ 0 & A_T \end{bmatrix} \right) \tag{3.49}$$

where

$$A_S = A - B_u R_2^{-1} S_2^T \tag{3.50}$$

$$Q_S = Q_2 - S_2 R_2^{-1} S_2^T \tag{3.51}$$

$$A_T = A - S_1^T R_1^{-1} C_y \tag{3.52}$$

$$Q_T = Q_1 - S_1^T R_1^{-1} S_1 \tag{3.53}$$

We can now apply Theorem 2.5.6 to this problem.

Theorem 3.3.1 *Assume (A_S, B_u) stabilizable, (C_z, A_S) detectable, (A_T, B_w) stabilizable, and (C_y, A_T) detectable. Then*

i. $S \in Dom(Ric)$, $X = X^T = Ric(S) \geq 0$.

ii. $T \in Dom(Ric)$, $Y = Y^T = Ric(T) \geq 0$.

iii. The unique minimizing gains are given by

$$K_c = -\left(R_2 + B_u^T X B_u\right)^{-1} \left(B_u^T X A + S_2^T\right) \tag{3.54}$$

$$K_f = -\left(AYC_y^T + S_1^T\right)\left(R_1 + C_y Y C_y^T\right)^{-1} \tag{3.55}$$

Proof: Follows directly from Theorem 2.5.6 and Theorem 3.2.1. ∎

The resulting 2-norm can be calculated using (2.59), where the closed loop transfer function, T_{zw}, can be obtained from a lower fractional transformation of G and K.

$$T_{zw} = F_l(G, K) \tag{3.56}$$

$$K = \left[\begin{array}{c|c} A + B_u K_c + K_f C_y & -K_f \\ \hline K_c & 0 \end{array}\right] \tag{3.57}$$

$$T_{zw} = \left[\begin{array}{cc|c} A & B_u K_c & B_w \\ -K_f C_y & A + B_u K_c + K_f C_y & -K_f D_{yw} \\ \hline C_z & D_{zu} K_c & D_{zw} \end{array}\right] \tag{3.58}$$

Often D_{zw} and D_c are assumed zero for the H_2 development. Indeed, for the continuous-time case,

$$(D_{zw} + D_{zu} D_c D_{yw}) = 0 \tag{3.59}$$

is necessary for the 2-norm to be finite; therefore, if $D_{zw} \neq 0$, then $D_c \neq 0$ and is completely determined by (3.59) [42]. This is not the case for discrete-time. D_{zw} has no effect on the resulting compensator, and although it will affect the final cost, the 2-norm will remain finite for a non-zero feedforward term as defined by (3.59).

If we admit compensators which are not strictly causal, we only need to redefine the filter gain

$$\tilde{K}_f = -\left(Y C_y^T + S_1^T\right)\left(R_1 + C_Y C_y^T + C_y S_1^T + S_1 C_y^T\right)^{-1} \tag{3.60}$$

where $Y = Ric(T)$. The optimal H_2 compensator can now be written as

$$K_c = \left[\begin{array}{c|c} A + B_u K_c + A\tilde{K}_f C_y + B_u K_c \tilde{K}_f C_y & -A\tilde{K}_f - B_u K_c \tilde{K}_f \\ \hline K_c + K_c \tilde{K}_f C_y & -K_c \tilde{K}_f \end{array}\right] \tag{3.61}$$

Before we leave the H_2 optimal control problem, we need to discuss the parametrization of all H_2 sub-optimal controllers. We will again consider the same plant, G, and we are assuming (A, B_u) stabilizable and (C_y, A) detectable as well as all other general assumptions made above. Further, we need to define

$$R_c = D_{zu}^T D_{zu} + B_u^T X B_u \tag{3.62}$$

$$R_f = D_{yw} D_{yw}^T + C_y Y C_y^T \tag{3.63}$$

where X and Y are the symmetric, positive semi-definite solutions to the control and filter DARE's, respectively. For the control and filter gains, we will use the definitions from

(3.54) and (3.55). With these definitions and assumptions, we can now state the following theorem.

Theorem 3.3.2 *Let α_0 denote the minimum obtainable 2-norm of the stable closed loop transfer function, T_{zw}. For $\alpha \geq \alpha_0$, all stabilizing controllers that guarantee $\|T_{zw}\|_2 \leq \alpha$ are given by*

$$K(Q) = F_l(J,Q) \,\forall\, Q \ni \|Q\|_2^2 \leq \alpha^2 - \alpha_0^2 \tag{3.64}$$

and J is given by

$$J = \left[\begin{array}{c|cc} A + B_u K_c + K_f C_y & -K_f & -B_u R_c^{-1/2} \\ \hline K_c & 0 & R_c^{-1/2} \\ R_f^{-1/2} C_y & R_f^{-1/2} & 0 \end{array}\right] \tag{3.65}$$

Proof: See Theorem 13.2.2, [5]. ∎

3.4 ℓ_1 Optimal Control Synthesis

While the H_∞ problem can be viewed as a minimization of the maximum gain over all frequency, the ℓ_1 problem is a minimization of the maximum peak-to-peak gain over all time. Formally stated, we wish to minimize the ∞-norm of the output sequence for an unknown but bounded amplitude input sequence. This problem was first introduced by Vidyasagar [43], but it was Dahleh and Pearson who were responsible for its more general solution [44, 45]. The majority of the work done on ℓ_1 optimization has concentrated on discrete-time systems, where the full power of duality and linear programming can be brought to bear on the problem. Although results for continuous-time systems have appeared in the literature, they consist primarily of methods to convert the problem to an equivalent discrete-time system. The present discussion is drawn from [46, 5].

3.4.1 Problem Formulation. Consider the system

$$\left\{\begin{array}{c} m \\ y \end{array}\right\} = \left[\begin{array}{cc} P_{mr} & P_{mu} \\ P_{yr} & P_{yu} \end{array}\right] \left\{\begin{array}{c} r \\ u \end{array}\right\} \tag{3.66}$$

where $r(k) \in \mathbf{R}^{n_r}$ is an input sequence of unknown but bounded magnitude, $m(k) \in \mathbf{R}^{n_m}$ is the output sequence we wish to regulate, and n_r, n_m are the dimensions of the input vector r and output vector m, respectively. We seek a dynamic measurement feedback controller K, such that $u = Ky$. The closed loop system can be represented as

$$\Phi = F_l(P, K) = T_{mr} = P_{mr} + P_{mu}K(I - P_{yu}K)^{-1}P_{yr} \tag{3.67}$$

The ℓ_1 optimization problem can be stated as follows: Among all internally stabilizing controllers, find the one that minimizes the maximum peak-to-peak gain of Φ operating on the space of disturbances with magnitude bounded by 1, i.e.,

$$\nu_0 = \inf_{K stabilizing} \|\Phi\|_1 \tag{3.68}$$

Using the Youla parametrization from (3.11), we can express the closed loop transfer function as an affine expression over a subset in the ℓ_1 operator space

$$\Phi = H - UQV \tag{3.69}$$

where $H, U, V \in \ell_1$ of dimension $(n_m \times n_r)$, $(n_m \times n_u)$ and $(n_y \times n_r)$, respectively, and Q is a stable ℓ_1 transfer function of dimension $(n_u \times n_y)$. When we refer to the λ-domain representation of a transfer function (obtained via the λ-transform), we will use a $\hat{}$ notation, e.g. $\hat{\Phi}$ is the λ-domain representation of the ℓ_1 transfer function Φ. Further, a lower case letter will be used for the sequence representation of the individual sequence components, e.g. ϕ_{ij} is the ℓ_1 sequence representing the ij^{th} block of Φ.

If we define the set

$$\Sigma = \{R \in \ell_1 \mid R = UQV \text{ for some } Q \in \ell_1\} \tag{3.70}$$

then we can redefine the problem as

$$\nu_0 = \inf_{R \in \Sigma} \|H - R\|_1 \tag{3.71}$$

From duality theory [39] we can pose the problem in the dual space (ℓ_∞) as a maximization problem:

$$\nu_0 \;=\; \max_{G\in\Sigma^\perp,\ \|G\|_\infty\le 1} \langle H, G\rangle \tag{3.72}$$

where the the bounded linear functional G evaluated at H is defined as

$$\langle H, G\rangle \;=\; \sum_{i=1}^{n_m}\sum_{j=1}^{n_r}\sum_{k=0}^{\infty} g_{ij}(k)h_{ij}(k) \tag{3.73}$$

and

$$\Sigma^\perp \;=\; \{G \;\in\; \ell_\infty \,|\, \langle R, G\rangle \;=\; 0,\ \forall\ R \;\in\; \Sigma\ \} \tag{3.74}$$

The duality results can be strengthened by saying that if a solution to the primal problem exists, say Φ_0, then it must be aligned with every solution G to the dual problem, i.e.,

$$\langle \Phi_0, G_0\rangle \;=\; \|\Phi_0\|_1\|G_0\|_\infty \tag{3.75}$$

A more useful form of the alignment conditions is

i. If $|g_{0_{ij}}(k)| < \max_{1\le j\le n_r} \|g_{0_{ij}}\|_\infty$, then $\phi_{0_{ij}}(k) = 0$

ii. $\phi_{0_{ij}}(k)g_{0_{ij}}(k) \ge 0$

iii. $\|\Phi_{0_i}\|_1 = \nu_0,\ \forall\, i = 1,\ldots,n_m \ni\ G_{0_i} \neq 0$

iv. If $G_{0_i} \equiv 0$ then Φ_{0_i} can be anything $\ni\ \|\Phi_{0_i}\|_1 \le \nu_0$

Items iii and iv state that each row sum of norms of Φ will be precisely active (i.e., equal to ν_0) if the corresponding row of the dual variables (G_0) is non-zero. This is supported by the observation that the MIMO one-block problem tends to result in all row sums being active. The first item provides even more insight as to the nature of the solution. It states that, if the dual constraint is not precisely active for given time steps (k), then the primal variables ($\phi_{0_{ij}}(k)$) will be precisely zero for those time steps. The nature of the problem is such that the dual constraints will cease to be active beyond a certain time step, resulting in a finite time (support length) non-zero pulse response. Stated another way, the alignment conditions predict the FIR nature of the solution. These aspects of the solution will be explored further once the full ℓ_1 problem has been formulated.

As mentioned earlier, the most general solution to the ℓ_1 problem uses linear programming to solve the constrained optimization problem. The constraints on the problem come from interpolation conditions, which are in fact conditions on the null space of the operator $\hat{R}$. The complete development of the interpolation conditions goes beyond the scope of this dissertation and will not be discussed in entirety. The interested reader is referred to Chapter 6 of [5]. It suffices to say that $\hat{R}$ must contain both the left unstable zero structure of $\hat{U}$ and the right unstable zero structure of $\hat{V}$ if $\hat{R}$ is to be equivalent to $\hat{U}\hat{Q}\hat{V}$ for some stable $\hat{Q}$. An additional set of conditions imposes the correct rank conditions on $\hat{R}$. These are referred to as the zero and rank interpolation conditions, respectively. These conditions can be specified by Theorem 3.4.1, for which we will require a few definitions and a preliminary result from complex variable theory.

Lemma 3.4.1 *Given $\hat{f} : \mathbf{C} \rightarrow \mathbf{C}$, where $\hat{f}$ is analytic in the open unit disc, then*

$$\hat{f}^{(k)}(\lambda_0) \;=\; 0,\; k = 1, \ldots, (\sigma - 1) \tag{3.76}$$

for λ_0 in the open unit disc if and only if

$$\hat{f}(\lambda) \;=\; (\lambda - \lambda_0)^{\sigma}\hat{g}(\lambda) \tag{3.77}$$

where $\hat{g}(\lambda)$ is analytic in the open unit disc. (Note: $\hat{f}^{(k)}(\lambda_0)$ denotes the k^{th} derivative of $\hat{f}$ at λ_0.)

Proof: This is a well known result from complex variable theory [46]. ∎

We will assume, without loss of generality, that $\hat{U}(\lambda)$ has full column rank and $\hat{V}(\lambda)$ has full row rank. We will define the Smith McMillan decompositions [47] of $\hat{U}$ and $\hat{V}$ as follows:

$$\hat{U} \;=\; \hat{L}_U \hat{M}_U \hat{R}_U \tag{3.78}$$

$$\hat{V} \;=\; \hat{L}_V \hat{M}_V \hat{R}_V \tag{3.79}$$

where $\hat{L}_U$,$\hat{R}_U$,$\hat{L}_V$ and $\hat{R}_V$ are unimodular matrices (their determinant is equal to a nonzero constant), and the first n_u rows of $\hat{M}_U$ and the first n_y columns of $\hat{M}_V$ are diagonal matrices (with the remaining entries being zero). For $i \in \{1, 2, \ldots, n_u\}$, we will denote by $\sigma_{U_i}(\lambda_0)$ the algebraic multiplicity of the zero λ_0 for $\hat{U}(\lambda)$, and similarly define $\sigma_{V_j}(\lambda_0)$ for $\hat{V}(\lambda)$. Denote by Λ_{UV} the set of zeros of $\hat{U}$ and $\hat{V}$ in the unit disc. Note, we are using the λ-transform instead of the z-transform, and for this discussion we are assuming Λ_{UV} is in the open unit disc.

We can now define the following polynomial row and column vectors:

$$\hat{\alpha}_i(\lambda) = \left(\hat{L}_U^{-1}\right)_i(\lambda) \tag{3.80}$$

$$\hat{\beta}_i(\lambda) = \left(\hat{R}_V^{-1}\right)_j(\lambda) \tag{3.81}$$

Theorem 3.4.1 *Given $R \in \ell_1$, $\exists\, Q \in \ell_1 \ni R = UQV$ if and only if for all $\lambda_0 \in \Lambda_{UV}$, the following conditions hold:*

i. Zero Interpolation:

$$\left(\hat{\alpha}_i \hat{R} \hat{\beta}_j\right)^{(k)}(\lambda_0) = 0,\ \forall \begin{cases} i = 1, \ldots, n_u \\ j = 1, \ldots, n_y \\ k = 0, \ldots, \sigma_{U_i}(\lambda_0) + \sigma_{V_j}(\lambda_0) - 1 \end{cases} \tag{3.82}$$

ii. Rank Interpolation:

$$\left(\hat{\alpha}_i \hat{R}\right)(\lambda) \equiv 0, \quad \forall \quad i = n_u, \ldots, n_m \tag{3.83}$$

$$\left(\hat{\beta}_j \hat{R}\right)(\lambda) \equiv 0, \quad \forall \quad j = n_y, \ldots, n_r \tag{3.84}$$

Proof: See Theorem 3.1, [46]. ∎

For the one-block problem ($n_r = n_y$, and $n_m = n_u$), only zero interpolation conditions must be considered; however, for general multi-block problems ($n_r \geq n_y$, and $n_m \geq n_u$) both rank and zero interpolation conditions must be considered. Theorem 3.4.1 completely

defines the set Σ. The remaining step in the problem formulation is to identify the subspace of ℓ_∞ which annihilates Σ.

For all (i,j,k) in the ranges defined by Theorem 3.4.1, for $l = 0,1,\ldots$, and all $\lambda_0 \in \Lambda_{UV}$, define the following sequences of matrices in ℓ_∞ :

$$[RF_{ijk\lambda_0}(l)]_{qp} := \sum_{t=0}^{\infty}\sum_{s=0}^{\infty} \alpha_{iq}(s-l)\beta_{pj}(t-s)\, \Re\left[(\lambda^t)^{(k)}\right]\Big|_{\lambda=\lambda_0} \tag{3.85}$$

$$[IF_{ijk\lambda_0}(l)]_{qp} := \sum_{t=0}^{\infty}\sum_{s=0}^{\infty} \alpha_{iq}(s-l)\beta_{pj}(t-s)\, \Im\left[(\lambda^t)^{(k)}\right]\Big|_{\lambda=\lambda_0} \tag{3.86}$$

It can be shown that $\hat{R}$ satisfies the zero interpolation conditions if and only if $\langle R, RF_{ijk\lambda_0}\rangle = 0$ and $\langle R, IF_{ijk\lambda_0}\rangle = 0$. Further, the subspace spanned by the zero interpolation conditions is finite dimensional. For the rank interpolation conditions, define the following sequences of $n_m \times n_r$ matrices:

$$X_{\alpha_i qt}(l) := \begin{bmatrix} \vdots & & \vdots & \vdots & \vdots & & \vdots \\ 0 & \cdots & 0 & \alpha_i^T(t-l) & 0 & \cdots & 0 \\ \vdots & & \vdots & \vdots & \vdots & & \vdots \end{bmatrix} \tag{3.87}$$

$$X^T_{\beta_j pt}(l) := \begin{bmatrix} \vdots & & \vdots & \vdots & \vdots & & \vdots \\ 0 & \cdots & 0 & \beta_j^T(t-l) & 0 & \cdots & 0 \\ \vdots & & \vdots & \vdots & \vdots & & \vdots \end{bmatrix}^T \tag{3.88}$$

where α_i^T makes up the q^{th} column and β_j^T makes up the p^{th} row of $X_{\alpha_i qt}(l)$ and $X_{\beta_j pt}(l)$, respectively. Then the rank interpolation conditions are satisfied if and only if $\langle R, X_{\alpha_i qt}\rangle = 0$ and $\langle R, X_{\beta_j pt}\rangle = 0$ for t = 0,1, ... In contrast with the zero interpolation sequences, the linear span of the rank interpolation conditions is infinite dimensional.

We now state a theorem which specifies the existence of the optimal solution to the ℓ_1 optimization problem.

Theorem 3.4.2 *If every $\lambda_0 \in \Lambda_{UV}$ is strictly inside the unit disc, then $\exists\ R_0 \in \Sigma$ such that*

$$\nu_0 = \|H - R_0\|_1 = \inf_{R\in\Sigma} \|H - R\|_1 \tag{3.89}$$

Proof: See Theorem 4.1, [46]. ∎

3.4.2 The Linear Programming Problem. In order to solve either the primal or dual problem through linear programming, the nonlinearities associated with the ℓ_1 norm calculation must be removed, and the interpolation conditions defining the feasible set must be specified in a more convenient notation. To express $\|\Phi\|_1$ in linear form, redefine $\Phi = \Phi^+ - \Phi^-$, where Φ^+ and Φ^- are both non-negative sequences. The 1-norm can now be expressed as

$$\|\Phi\|_1 \;=\; \max_i \sum_{j=1}^{n_r} \sum_{k=0}^{\infty} \left(\phi_{ij}^+(k) + \phi_{ij}^-(k) \right) \tag{3.90}$$

This holds as long as, for each k, either $\phi_{ij}^+(k)$ or $\phi_{ij}^-(k)$ is zero. That this condition will always be satisfied can be seen by fixing $\Phi(k)$. The nature of the optimization problem is such that we are now minimizing the sum of non-negative variables ($\phi_{ij}^+(k)$ and $\phi_{ij}^-(k)$) whose difference is a given value $\phi_{ij}(k)$. It is now easily seen that either $\phi_{ij}^+(k)$ or $\phi_{ij}^-(k)$ will always be equal to zero.

Each of the equations defining the zero and rank interpolation conditions can be viewed as a linear equality constraint on the sequence Φ. Define

$$M_{ij} : \ell_1 \to \mathbf{R}^{c_z} \qquad \text{where } c_z \;:=\; \sum_{\lambda_0 \in \Lambda_{UV}} \sum_{i=1}^{n_y} \sum_{j=1}^{n_u} \left(\sigma_{U_i}(\lambda_0) + \sigma_{V_j}(\lambda_0) \right) \tag{3.91}$$

$$\bar{M}_{ij} : \ell_1 \to \ell_1 \tag{3.92}$$

where M_{ij} and $\bar{M}_{ij}$ are formed by taking the coefficients of the zero and rank interpolation conditions, respectively, that act on ϕ_{ij}. The set of feasible closed-loop transfer sequences can now be characterized by the set of equality constraints

$$\sum_{i=1}^{n_m} \sum_{j=1}^{n_r} M_{ij} \phi_{ij} \;=\; \sum_{i=1}^{n_m} \sum_{j=1}^{n_r} M_{ij} h_{ij} \;=\; b_{zero} \;\in\; \mathbf{R}^{c_z} \tag{3.93}$$

$$\sum_{i=1}^{n_m} \sum_{j=1}^{n_r} \bar{M}_{ij} \phi_{ij} \;=\; \sum_{i=1}^{n_m} \sum_{j=1}^{n_r} \bar{M}_{ij} h_{ij} \;=\; b_{rank} \;\in\; \ell_1 \tag{3.94}$$

The *Primal Linear Programming Problem* (PLPP) can now be stated as, find

$$\nu_0 := \min \nu \tag{3.95}$$

subject to

$$\xi(i) + \sum_{j=1}^{n_r} \sum_{k=0}^{\infty} \left(\phi_{ij}^+(k) + \phi_{ij}^-(k) \right) = \nu \ , \ i = 1, \ldots, n_m \tag{3.96}$$

$$\sum_{i=1}^{n_m} \sum_{j=1}^{n_r} M_{ij} \left(\phi_{ij}^+(k) + \phi_{ij}^-(k) \right) = b_{zero} \tag{3.97}$$

$$\sum_{i=1}^{n_m} \sum_{j=1}^{n_r} \bar{M}_{ij} \left(\phi_{ij}^+(k) + \phi_{ij}^-(k) \right) = b_{rank} \tag{3.98}$$

$$\xi(i), \ \phi_{ij}^+(k), \ \phi_{ij}^-(k) \ \geq \ 0 \ \forall \, i, k \tag{3.99}$$

where ξ is a non-negative n_m-vector of slack variables. For the dual problem, we define $\zeta \in \ell_\infty$ as the sequence of dual variables, and we partition ζ accordingly with the set of equality constraints from the primal problem, i.e., $\zeta = (-\zeta_0, \zeta_1, \zeta_2)$ where $\zeta_0 \in \mathbf{R}^{n_m}$, $\zeta_1 \in \mathbf{R}^{c_z}$, and $\zeta_0 \in \ell_\infty$. The *Dual Linear Programming Problem* (DLPP) can now be stated as, find

$$\nu_0 = \max_{\zeta_0, \zeta_1, \zeta_2} \left(\langle b_{zero}, \zeta_1 \rangle + \langle b_{rank}, \zeta_2 \rangle \right) \tag{3.100}$$

subject to

$$\zeta_0 \geq 0 \, , \ \sum_{i=1}^{n_m} \zeta_0(i) \leq 1 \tag{3.101}$$

$$-\zeta_0(i) \leq \left(M_{ij}^T \zeta_1 + \bar{M}_{ij}^T \zeta_2 \right)(k) \leq \zeta_0(i) \tag{3.102}$$

$$\text{for} \quad \begin{cases} i = 1, \ldots, n_m \\ j = 1, \ldots, n_r \\ k = 0, 1, \ldots \end{cases}$$

3.4.3 Solution Methods — SISO and One-Block Problems. As mentioned in the previous section, there are no rank interpolation conditions for the one-block problem. The

resulting primal problem has an infinite number of variables and only a finite number of equality constraints. Equivalently, the dual problem has finitely many variables and an infinite number of constraints. With the assumption that Λ_{UV} is in the open unit disc, however, it is possible to bound the index at which the ∞-norm is achieved.

Lemma 3.4.2 *Let M be a full column rank infinite matrix mapping $\mathbf{R}^n$ to c_0. Then there exists a positive integer N such that*

$$\| (I - P_N) Mx\|_\infty \ < \ \|P_N Mx\|_\infty, \quad \forall \ x \ \in \ \mathbf{R}^n \ , \ x \ \neq \ 0 \tag{3.103}$$

where P_N is the truncation operator.

Proof: See Lemma 6.1, [46]. ∎

Once the index is bounded, the alignment conditions dictate zero values for $\phi_{ij}(k), \ k \ > \ N$. This results in finitely many variables for the PLPP or, equivalently, finitely many equations for the DLPP. Because of the resulting finite dimensional problem, the one-block ℓ_1 optimization problem can be solved exactly for the case where there are no unstable zeros of Λ_{UV} on the unit circle. The method for handling unit circle zeros is covered in [5, 48], and will not be discussed further.

3.4.4 A SISO Example. To demonstrate both the primal and dual problem approaches, consider a SISO example where we wish to minimize a weighted sensitivity function. Define (in the λ-domain)

$$\hat{P}(\lambda) \ = \ \frac{\lambda(\lambda - 0.2)}{(\lambda - 2.0)(\lambda - 0.5)} \tag{3.104}$$

$$\hat{W}(\lambda) \ = \ \frac{1}{(1 - 0.6\lambda)} \tag{3.105}$$

We wish to minimize $\|W(I - PK)^{-1}\|_1$ over all stabilizing K. Rearranging, we have

$$\Phi \ = \ H - UQ \tag{3.106}$$

$$\hat{H} \ = \ \frac{(\lambda - 2.0)(\lambda - 0.5)(4.26\lambda + 1)}{(1 - 0.6\lambda)} \tag{3.107}$$

$$\hat{U} = \frac{(\lambda - 2.0)(\lambda - 0.5)(\lambda - 0.2)\lambda}{(1 - 0.6\lambda)} \tag{3.108}$$

The unstable zeros of $\hat{U}$ are $\Lambda_{UV} = \Lambda_U = 0.5, 0.2, 0$. There are no rank interpolation conditions, and the zero interpolation conditions are given by $\hat{R}(\lambda) = 0$ for all $\lambda \in \Lambda_U$. This implies

$$V_\infty^T(\phi^+ - \phi^-) = b_{zero} \tag{3.109}$$

where

$$V_\infty^T = \begin{bmatrix} (0.5)^0 & (0.5)^1 & (0.5)^2 & \cdots \\ (0.2)^0 & (0.2)^1 & (0.2)^2 & \cdots \\ (0)^0 & (0)^1 & (0)^2 & \cdots \end{bmatrix} \tag{3.110}$$

$$b_{zero} = \begin{Bmatrix} h(0.5) \\ h(0.2) \\ h(0) \end{Bmatrix} = \begin{Bmatrix} 0 \\ 0.8406 \\ 1 \end{Bmatrix} \tag{3.111}$$

Because the zeros of U are purely real, there are no interpolation conditions due to $\langle R, IF_{ijk\lambda_0} \rangle$.

We find that the upper bound on the length of Φ_0 is $N = 2$, so our constraints are now specified as

$$V_2^T(\phi^+ - \phi^-) = b_{zero} \tag{3.112}$$

where

$$V_\infty^T = \begin{bmatrix} 1 & \frac{1}{2} & \frac{1}{4} \\ 1 & \frac{1}{5} & \frac{1}{25} \\ 1 & 0 & 0 \end{bmatrix} \tag{3.113}$$

PLPP can now be written as

$$\nu_0 = \min_{\phi^+, \phi^-} \sum_{k=0}^{2} (\phi^+(k) + \phi^-(k)) \tag{3.114}$$

subject to

$$\begin{bmatrix} 1 & -1 & \frac{1}{2} & -\frac{1}{2} & \frac{1}{4} & -\frac{1}{4} \\ 1 & -1 & \frac{1}{5} & -\frac{1}{5} & \frac{1}{25} & -\frac{1}{25} \\ 1 & -1 & 0 & 0 & 0 & 0 \end{bmatrix} \begin{Bmatrix} \phi^+(0) \\ \phi^-(0) \\ \phi^+(1) \\ \phi^-(1) \\ \phi^+(2) \\ \phi^-(2) \end{Bmatrix} = \begin{bmatrix} 0 \\ 0.8406 \\ 1 \end{bmatrix} \tag{3.115}$$

DLPP is written as

$$\nu_0 = \max_{\alpha \in \mathbf{R}^3} \alpha^T b_{zero} \tag{3.116}$$

subject to

$$|V_2 \alpha| \leq 1 \tag{3.117}$$

where $\alpha^T = [\alpha_1 \ \alpha_2 \ \alpha_3]$ represents the dual variables. The solution to the problem is

$$\nu_0 = 12.41 \ , \ \hat{\Phi}_0 = 1 + 2.47\lambda - 8.94\lambda^2 \tag{3.118}$$

In solving DLPP, we find $\alpha_0^T = [-8.0 \ \ 25.0 \ \ -18.0]$, and the alignment conditions can be used to get Φ_0 from α_0.

As a comparison, Table 3.1 shows the same problem being solved via H_2 and H_∞ methods, and the resulting norm values. As expected, the 1-norm is always an upper bound to the ∞-norm, and the gap between these norms is smallest for the case where the 1-norm is being minimized. As a side note, we also see that the 2-norm maintains a finite value for the H_∞ problem, and in this case does not increase significantly from the optimal 2-norm. Although not the subject of this chapter, this represents a significant difference from the continuous-time case.

3.4.5 Solution Methods — General MIMO Multi-Block Problems. Unlike the one-block problem, the multi-block PLPP (and DLPP) has infinitely many variables and infinitely many constraints. For this reason, approximate methods must be used to solve the problem. The *Finitely Many Variables* (FMV) [5] approach truncates the number of variables (effectively imposing a finite pulse response) in the primal problem. It can be

Table 3.1 Comparison of Norms for ℓ_1, H_2, and H_∞ Synthesis

Objective	$\|WS\|_1$	$\|WS\|_2$	$\|WS\|_\infty$
$\min \|WS\|_1$	12.41	9.33	10.75
$\min \|WS\|_2$	16.22	7.19	10.46
$\min \|WS\|_\infty$	14.42	7.75	8.27

shown that assuming $\phi_{ij}(k) \equiv 0$ for k greater than some specified index N_V makes the product $M_{ij}\phi_{ij}(k)$ vanish for k greater than N_V + constant, where the constant depends on the order of $\hat{\alpha}_i(\lambda)$ and $\hat{\beta}_j(\lambda)$. Note, however, that if the elements of b_{rank} are not zero at this point, then the equality constraints will be violated, indicating no feasible solution.

Theorem 3.4.3 *Given a multi-block problem and a positive integer N_V, there exists a finitely supported feasible solution Φ if and only if $(\alpha_i * H)(k) = 0$ and $(\beta_j * H)(k) = 0$ for k greater than N_V + constant, $i = n_u + 1, \ldots, ns$, and $j = n_y + 1, \ldots, nr$.*

Proof: See Theorem 7.1 and Corollary 7.1, [46]. ∎

The FMV method results in additional constraints on the problem, and this produces a sub-optimal solution, if one exists. For the cases where the FMV method provides a solution, the optimal solution (ν_0) will be approached from above as N_V approaches infinity. By itself, the FMV method has marginal utility because it provides no information on how far away from optimal the approximation is, and the order of the resulting compensator increases with N_V. The first of these drawbacks can be addressed through a dual method which will be described subsequently.

Instead of truncating the number of variables, it is possible to approximate the problem by truncating the number of constraints in PLPP. This method, termed the *Finitely Many Equations* method (FME) [5], simply ignores all but the first N_E constraints, resulting in a less constrained problem and a super-optimal (infeasible) solution. Like the one-block problem, it can be shown that the resulting super-optimal problem is indeed finitely supported and finite dimensional. In addition to having better existence properties than the FMV method, the FME method produces a lower bound to the optimal 1-norm,

and it converges from below as N_E approaches infinity. Assuming existence of FMV solutions, the two methods can be combined in an iterative manner to achieve a sub-optimal solution with any degree of accuracy desired; however, the resulting compensator will usually be exceedingly large. The next method to be described was developed[46] specifically to address the problem of order inflation and existence of feasible solutions.

The *Delay Augmentation* method (DA) approximates the optimal solution by embedding the problem in a larger one-block problem for which there is an exact solution. This is done by augmenting U and V with pure delays. For a general multi-block problem, partition the system as

$$\begin{bmatrix} \Phi_{11} & \Phi_{12} \\ \Phi_{21} & \Phi_{22} \end{bmatrix} = \begin{bmatrix} H_{11} & H_{12} \\ H_{21} & H_{22} \end{bmatrix} - \begin{bmatrix} U_1 \\ U_2 \end{bmatrix} Q \begin{bmatrix} V_1 & V_2 \end{bmatrix} \tag{3.119}$$

We now augment U and V with N^{th} order shifts, and augment Q to the appropriate dimensions.

$$\begin{bmatrix} \Phi_{11} & \Phi_{12} \\ \Phi_{21} & \Phi_{22} \end{bmatrix} = \begin{bmatrix} H_{11} & H_{12} \\ H_{21} & H_{22} \end{bmatrix} - \begin{bmatrix} U_1 & 0 \\ U_2 & S_N \end{bmatrix} \begin{bmatrix} Q_{11} & Q_{12} \\ Q_{21} & Q_{22} \end{bmatrix} \begin{bmatrix} V_1 & V_2 \\ 0 & S_N \end{bmatrix} \tag{3.120}$$

or

$$\Phi_N = H - U_N Q_N R_N = H - R_N \tag{3.121}$$

By expanding the expression for R_N , we can write

$$\Phi_N = H - U Q_{11} V - S_N \tilde{R}_N \tag{3.122}$$

where

$$\tilde{R}_N = \begin{bmatrix} 0 & U_1 Q_{12} \\ Q_{21} V_1 & Q_{21} V_2 + U_2 Q_{12} + S_N Q_{22} \end{bmatrix} \tag{3.123}$$

Essentially what we have done is given the problem extra degrees of freedom (Q_{12},Q_{21},Q_{22}) with which to work, resulting in a super-optimal (infeasible) solution which is a lower bound to the optimal solution. However, if we drop the last term in the expression for the optimal Φ_N, ($S_N \tilde{R}_N$), it can be shown that the resulting optimal closed loop norm for the

augmented problem

$$\|H - UQ_{0_{11}}V\|_1 \tag{3.124}$$

is an upper bound to the optimal solution. This means that by solving a single one-block problem, for which a solution is guaranteed to exist if there are no zeros on the unit circle, we can obtain both an upper and lower bound to the optimal solution.

To understand how the DA algorithm attempts to prevent compensator order inflation, we need to discuss the support structure of the optimal ℓ_1 solution. Most one-block problems have optimal solutions with all row norms equal to ν_0 and are characterized by a finite pulse response [46]. This generality does not hold for the multi-block case, but if the inputs and outputs are reordered such that the dominant block in the optimization occupies the 1-1 (upper left) partition, then the DA algorithm can "capture" the finite pulse response of the dominant block. The remaining rows will have a growing support length, but the compensator order will remain fixed based on the support length of the dominant block. For problems where the optimization problem is dominated by a block of n_u or fewer rows, this can lead to compensator orders significantly less than those found using FMV and or FME approaches. Essentially what is occurring is that the remaining rows are being effectively ignored in the optimization problem. Note that, depending on the locations of the zeros, the DA algorithm can also suffer from order inflation problems; however, even in these cases the DA algorithm avoids the problem of existence in the FMV method, and it provides both an upper and lower bound to the optimal solution. Once again, the reader is referred to [46, 5] for details on the support structure of optimal solutions.

3.5 Summary

This chapter began with the Youla parametrization of all stabilizing controllers. This parametrization allows us to pose the control synthesis problem as a search over a convex set. Next, the LQG and regular H_2 problems were developed, with and without a strict causality assumption being enforced. It was shown that the same Riccati equations can be used to solve both problems, but the final cost and form of the controller differed,

depending on whether the control law was based on all, or only past measurements. A parametrization of H_2 suboptimal controllers was shown to be a an LFT of a particular matrix and a convex set in H_2 . The ℓ_1 control synthesis problem was introduced, and it was shown to be solvable using linear programming techniques. Further, it was shown that SISO and one-block MIMO problems could be solved exactly, and the resulting closed-loop transfer function is FIR. Methods for approximating the solution for multi-block MIMO problems were introduced. The next chapter will begin to explore the optimal mixed-norm problem, beginning with an H_2/ℓ_1 formulation.

IV. The Optimal H_2/ℓ_1 Control Problem

4.1 Introduction

Many researchers have studied the mixed-norm control synthesis problem, but most have been forced to be content with sets of coupled necessary conditions or numerical algorithms for their solution. Of these researchers, very few have been able to find analytic solutions to even the simplest of the mixed-norm problems. Walker [9] used the minimum-norm duality theorem to formulate and solve a special case of the SISO, continuous-time H_2/H_∞ problem. He showed that the optimal solution to the H_2/H_∞ problem can be a non-rational compensator, and Megretsky [17] showed a similar result for a more general H_2/H_∞ problem. The significance of these results is that the true optimal H_2/H_∞ compensator cannot generally be attained using a fixed order or rational approach.

A somewhat different result has been obtained for the H_2/ℓ_1 problem. Voulgaris [24] investigated the SISO H_2/ℓ_1 problem for the case where $T_{zw} = T_{mr}$. He used the Lagrange duality theorem [39] to pose the dual problem, and showed that the optimal solution results in an FIR closed-loop system. Although at first glance these results appear surprising, we should note that the SISO and MIMO one-block ℓ_1 optimal compensators also result in FIR closed-loop systems. Failed attempts to extend Voulgaris' method to the case where $T_{zw} \neq T_{mr}$ have suggested that this more general problem does not necessarily have a FIR solution, and this chapter will demonstrate that this is in fact the case.

This chapter will consider both analytical and numerical solutions to the optimal H_2/ℓ_1 control problem. A complete analytical solution to this problem has not yet been found, but the results presented in this chapter will provide valuable insight as to the nature of the solution. Based on this insight, two numerical methods for solving the optimal H_2/ℓ_1 control problem will be developed. The first method will be based on a conjecture that the constraint transfer function will be FIR for SISO and one-block MIMO problems. Assuming the conjecture holds, we can then solve these problems exactly using finite truncation levels. This method will be demonstrated using a SISO F-16 aircraft example. A second method will be developed which guarantees convergence, regardless of whether or not the constraint transfer function is FIR.

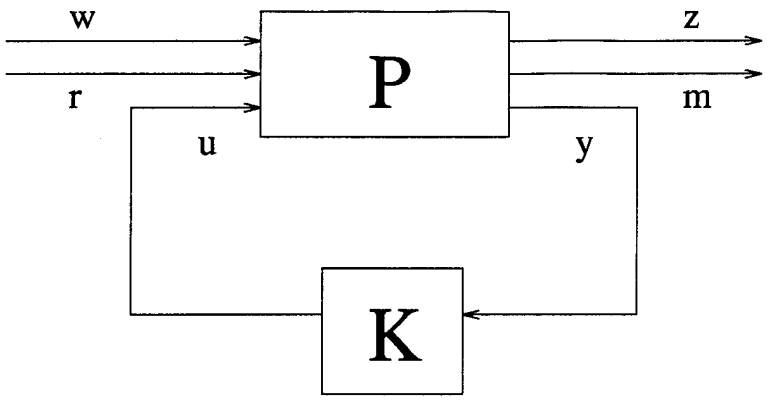

Figure 4.1 General mixed H_2/ℓ_1 optimization problem

4.2 Problem Setup

The system considered for the H_2/ℓ_1 control problem is shown in Figure 4.1. It contains two sets of exogenous inputs and controlled outputs. In general, no relationship is assumed between r and w, or m and z, other than they include the same underlying system dynamics. The input r is assumed to be a signal of unknown but bounded magnitude with $\|r\|_\infty \leq 1$, and the input w is assumed to be the discrete-time equivalent of zero-mean white Gaussian noise (WGN) of unit intensity. Note that, unlike the continuous-time case, the discrete-time equivalent of WGN has finite covariance. The plant $P(z)$ is formed by augmenting the system dynamics with stable weighting functions on the inputs and outputs. These weighting functions are typically chosen according to standard H_2 and/or H_∞ synthesis methods [3, 4]. Since we are interested in the closed-loop transfer functions from w to z and r to m, the system can be broken down into an H_2 problem and an ℓ_1 problem. Using transfer function notation, we write

$$P_2 := \begin{bmatrix} P_{zw} & P_{zu} \\ P_{yw} & P_{yu} \end{bmatrix} \tag{4.1}$$

$$P_1 := \begin{bmatrix} P_{mr} & P_{mu} \\ P_{yr} & P_{yu} \end{bmatrix} \tag{4.2}$$

The objective of mixed H_2/ℓ_1 control is to minimize the 2-norm of the closed loop transfer function T_{zw}, while constraining the 1-norm of the closed loop transfer function

T_{mr} to be less than some specified level. Mathematically, the problem can be stated as follows:

For the system shown in Figure 4.1, find an admissible controller $K(z)$ that achieves

$$\alpha^* = \inf_{K\ stabilizing} \|T_{zw}\|_2 \tag{4.3}$$

subject to the constraint $\|T_{mr}\|_1 \leq \nu$, where

$$T_{zw} = P_{zw} + P_{zu}K\left(I - P_{yu}K\right)^{-1}P_{yw} \tag{4.4}$$

$$T_{mr} = P_{mr} + P_{mu}K\left(I - P_{yu}K\right)^{-1}P_{yr} \tag{4.5}$$

Walker [9] has shown that, if P_{yu} is detectable and stabilizable, and only stable weighting functions are used at the inputs and outputs, then the following are equivalent:

i. K stabilizes P_{yu}

ii. K stabilizes P_2

iii. K stabilizes P_1

iv. K stabilizes P

Throughout this chapter we will be assuming that P_{yu} is detectable and stabilizable. Further, we will assume both P_{yw} and P_{zu} are non-zero, thus ensuring $\|T_{zw}\|_2$ is affected by K. Finally, we will assume that there is at most one compensator such that $\|T_{zw}\|_2 = 0$. This is not a physically restrictive assumption, since it applies to the unrealistic case where the input has no effect on the output of the closed-loop system. This last assumption is there for mathematical purposes only; it will be used to show that the general H_2/ℓ_1 compensator is unique, as will be done in the next section.

To simplify the discussion, we make the following definitions:

$$\underline{\nu} := \inf_{K admissible} \|T_{mr}\|_1 \tag{4.6}$$

$$\underline{\alpha} := \inf_{K admissible} \|T_{zw}\|_2 \tag{4.7}$$

$$K_{2_{opt}} := \text{the unique } K(z) \text{ that makes } \|T_{zw}\|_2 = \underline{\alpha} \tag{4.8}$$

$$\overline{\nu} := \|T_{mr}\|_1 \text{ when } K(z) = K_{2_{opt}} \tag{4.9}$$

$$K_{mix} := \text{a solution to the } H_2/\ell_1 \text{ problem for some } \nu > \underline{\nu} \tag{4.10}$$

$$\nu^* := \|T_{mr}\|_1 \text{ when } K(z) = K_{mix} \tag{4.11}$$

$$\alpha^* := \|T_{zw}\|_2 \text{ when } K(z) = K_{mix} \tag{4.12}$$

We will first make some statements regarding existence and uniqueness of the optimal compensator analogous to that by Walker[9]. Once that is complete, we will then pose the dual problem in order to gain additional insight into the nature of the solution.

4.3 Existence and Uniqueness of the Optimal Compensator

We can pose the H_2/ℓ_1 problem as one of optimizing a functional over a convex set by making use of the Youla parametrization of all stabilizing compensators for P_{yu}. First, define a doubly-coprime factorization of P_{yu}

$$P_{yu} = NM^{-1} = \tilde{M}^{-1}\tilde{N} \tag{4.13}$$

and

$$\begin{bmatrix} \tilde{Y} & -\tilde{X} \\ -\tilde{N} & \tilde{M} \end{bmatrix} \begin{bmatrix} M & X \\ N & Y \end{bmatrix} = I \tag{4.14}$$

The set of all K which stabilize P_{yu} (in the ℓ_1 sense) is parametrized over $Q \in \ell_1$ by

$$K(Q) = (X + MQ)(Y + NQ)^{-1} \tag{4.15}$$

$$= (\tilde{Y} + Q\tilde{N})^{-1}(\tilde{X} + Q\tilde{M}) \tag{4.16}$$

If we define

$$K_0 := K(Q = 0) = XY^{-1} = \tilde{Y}^{-1}\tilde{X} \tag{4.17}$$

$$J = \begin{bmatrix} K_0 & -\tilde{Y}^{-1} \\ Y^{-1} & -Y^{-1}N \end{bmatrix} \tag{4.18}$$

then all stabilizing K can be formed as a lower fractional transformation [5] of J and Q

$$K = F_\ell(J, Q) \tag{4.19}$$

With these definitions we can now rewrite the closed loop transfer functions as

$$T_{zw}(Q) = T_{1_2} + T_{2_2} Q T_{3_2} \tag{4.20}$$

$$T_{mr}(Q) = T_{1_1} + T_{2_1} Q T_{3_1} \tag{4.21}$$

where

$$T_{1_2} = P_{zw} - P_{zu} X \tilde{M} P_{yw} \tag{4.22}$$

$$T_{2_2} = -P_{zu} M \tag{4.23}$$

$$T_{3_2} = \tilde{M} P_{yw} \tag{4.24}$$

and

$$T_{1_1} = P_{mr} - P_{mu} X \tilde{M} P_{yr} \tag{4.25}$$

$$T_{2_1} = -P_{mu} M \tag{4.26}$$

$$T_{3_1} = \tilde{M} P_{yr} \tag{4.27}$$

If we assume, without loss of generality, that the doubly-coprime factorization was chosen such that $K_0 = K_{2_{opt}}$, then

$$T_{zw}(Q = 0) = T_{1_2} \implies \|T_{1_2}\|_2 = \underline{\alpha} \tag{4.28}$$

We are also assuming that the doubly-coprime factorization of P_{yu} is determined from an n_2-order realization of P_{yu}, where n_2 is the minimal order of P_2. Specifically, if we define a minimal order realization of P_2

$$P_2 = \left[\begin{array}{c|cc} A_2 & B_w & B_{u_2} \\ \hline C_z & D_{zw} & D_{zu} \\ C_{y_2} & D_{yw} & D_{yu} \end{array}\right] \tag{4.29}$$

then P_{yu} can be written as

$$P_{yu} = C_{y_2}(zI - A_2)^{-1}B_{u_2} + D_{yu} \tag{4.30}$$

Although it is not necessary, we will assume $D_{yu} = 0$ in order to satisfy the requirement for well-posedness of the problem. This is usually an easy condition to meet in practice, since any dynamic lag associated with either the sensors or actuators will ensure it is satisfied. This assumption will be removed in Chapter VI, and it will be replaced by the more general restriction on well-posedness of the problem. We can now adapt a lemma from Walker's work [9] to our discrete-time problem.

Lemma 4.3.1 *If $Q \in \ell_1$, then $\|T_{zw}(Q)\|_2$ is a strictly convex real functional of Q on ℓ_1.*

Proof: Let $Q_1, Q_2 \in \ell_1$ and let $\alpha \in (0,1)$. By assumption, both Q_1 and Q_2 cannot result in $\|T_{zw}\|_2 = 0$ unless $Q_1 = Q_2$, which is a trivial case. Eliminating this trivial case, we can proceed as follows:

$$\begin{aligned} &\|T_{1_2} + T_{2_2}\left[\alpha Q_1 + (1-\alpha)Q_2\right]T_{3_2}\|_2 \\ &\quad = \|\alpha T_{1_2} + \alpha T_{2_2}Q_1T_{3_2} + (1-\alpha)T_{1_2} + (1-\alpha)T_{2_2}Q_2T_{3_2}\|_2 \qquad (4.31) \\ &\quad = \|\alpha[T_{1_2} + T_{2_2}Q_1T_{3_2}] + (1-\alpha)[T_{1_2} + T_{2_2}Q_2T_{3_2}]\|_2 \qquad (4.32) \\ &\quad \leq \alpha\|T_{1_2} + T_{2_2}Q_1T_{3_2}\|_2 + (1-\alpha)\|T_{1_2} + T_{2_2}Q_2T_{3_2}\|_2 \qquad (4.33) \end{aligned}$$

where equality holds if and only if the vectors in (4.33) are colinear. However, colinearity implies $\exists\ \beta \in \mathbf{R}$ such that

$$T_{1_2} + T_{2_2} Q_1 T_{3_2} = \beta(T_{1_2} + T_{2_2} Q_2 T_{3_2}) \tag{4.34}$$

$$\Rightarrow T_{2_2} Q_1 T_{3_2} = (\beta - 1) T_{1_2} + \beta T_{2_2} Q_2 T_{3_2} \tag{4.35}$$

$$\Rightarrow Q_1 = (\beta - 1) T_{2_2}^{-1} T_{1_2} T_{3_2}^{-1} + \beta Q_2 \tag{4.36}$$

and, since $T_{2_2}^{-1} T_{1_2} T_{3_2}^{-1} \notin \ell_1$ [18], this implies $Q_1 \notin \ell_1$, which contradicts the initial assumption. This implies the two-norm is a strictly convex functional. ∎

Using the same argument, it is easy to show that the 1-norm constraint is convex. We can now state that the optimal H_2/ℓ_1 controller is unique.

Theorem 4.3.1 *Let $\nu > \underline{\nu}$ be given. Then the controller which satisfies the H_2/ℓ_1 optimization problem is unique. Furthermore, the following hold:*

i. If $\nu \geq \overline{\nu}$, then the resulting controller is $K_{2_{opt}}$

ii. If $\underline{\nu} < \nu \leq \overline{\nu}$, then $\nu^* = \nu$ at the optimal (i.e., the solution will satisfy the ℓ_1 constraint with equality).

Proof: This is a trivial extension of Walker[9], Theorem 4.2.1. ∎

The preceding development is based on an operator theoretic approach, which leaves the compensator free to take on any order. This is necessary for several reasons. First, the ℓ_1 optimal compensator must be found with a free-order approach, and in some cases the ℓ_1 optimal compensator may be non-rational and/or infinite-order. Even for SISO or one-block MIMO problems which result in a finite order ℓ_1 optimal controller, the order of the optimal controller is not known *a priori*. Second, even with the H_∞ problem in which the optimal controller order is known *a priori*, it has been shown that the optimal mixed H_2/H_∞ compensator can be non-rational [9]. For these reasons, a non-rational or infinite order optimal compensator is conjectured for the most general H_2/ℓ_1 problem. However, recent results suggest that a finite order optimal solution, as opposed to a fixed-order

solution, may exist for the SISO or one-block MIMO H_2/ℓ_1 problem, and these results will be discussed later in this chapter.

4.4 The H_2/ℓ_1 Dual Problem

The problem we wish to solve can be restated as: Find an admissible controller $K(z)$ that achieves

$$\alpha^* = \inf_{Q \in \ell_1} \|T_{1_2} + T_{2_2} Q T_{3_2}\|_2 \tag{4.37}$$

subject to the constraint

$$\|T_{1_1} + T_{2_1} Q T_{3_1}\|_1 \leq \nu \text{ , where } \nu \in (\underline{\nu}, \overline{\nu}). \tag{4.38}$$

For the case of nonsingular SISO or one block MIMO constraints, we can expand this to $\nu \in [\underline{\nu}, \overline{\nu})$. In order to pose the dual problem, we will consider the SISO case, with all other assumptions the same as those in the previous sections. For the SISO case, we can now define

$$T_{zw} = T_{1_2} + T_{23_2} Q \tag{4.39}$$

$$T_{mr} = T_{1_1} + T_{23_1} Q \tag{4.40}$$

where $T_{23_2} = T_{2_2} T_{3_2}$ and $T_{23_1} = T_{2_1} T_{3_1}$. We will make use of an inner-outer factorization to transform the H_2 objective as follows: Let $T_{23_2} = T_{23_{2_i}} T_{23_{2_o}}$, where $T_{23_{2_i}}$ is a unitary inner function and $T_{23_{2_o}}$ is a stable and minimum phase outer function. Then,

$$\|T_{1_2} + T_{23_2} Q\|_2 = \|T_{23_{2_i}}^{-1} T_{1_2} + T_{23_{2_o}} Q\|_2 \tag{4.41}$$

$$= \|R - X\|_2 \tag{4.42}$$

where $R := T_{23_{2_i}}^{-1} T_{1_2}$, $S = -T_{23_{2_o}}$, and $X := SQ$. Noting that $\ell_1 \subset H_2$, T_{zw} will be stable for all $Q \in \ell_1$. Further, since we demonstrated that both $\|T_{zw}\|_2$ and $\|T_{mr}\|_1$ are convex on $Q \in \ell_1$, this can be seen as a convex parametrization.

The H_2/ℓ_1 problem as stated meets all the necessary assumptions to apply the Minimum Norm Duality Theorem (Theorem 2.8.2), but to date no clean expression for the support functional has been obtained. However, if we consider a more restrictive problem whereby $T_{1_1} = 0$ and $T_{23_1} = I$, we will be able to define the support functional and proceed with posing the dual problem. It must be noted that the resulting optimization problem will now be implicitly dependent on the parametrization used for the objective transfer function, and we will be assuming that this parametrization will *not* result in $K_{2opt} = K(Q = 0)$. Because the parametrization is no longer arbitrary, this results in an artificial problem which may have no physical significance; it will be used only to illustrate the mathematical nature of the optimal solution. (Note: a less restrictive problem whereby $T_{1_1} \neq 0$ can be posed, and the support functional can be found. However, it provides no further insight into the solution of the problem and it is notationally more cumbersome.) Our problem is now to find $Q \in \ell_1$ which achieves

$$\alpha^* = \inf_{X \in K} \|R - X\|_2 \tag{4.43}$$

where the set K is defined as

$$K = \{X = SQ \in H_2 \mid Q \in \ell_1,\ \|Q\|_1 \leq \nu\} \tag{4.44}$$

Applying the Minimum Norm Duality Theorem we get

$$\alpha^* = \max_{\|X^*\|_2 \leq 1} [\langle R, X^* \rangle - h(X^*)] \tag{4.45}$$

where $X^* \in L_2^*$. Since L_2 is a Hilbert Space, we note that $L_2 \cong L_2^*$ and functionals can be defined as inner products.

In order to proceed with the definition of the support functional, we will define an equivalent problem using time-domain sequences. We note that a stable, discrete transfer function can be represented by its causal unit pulse response sequence. Notationally, $T(z)$ will be represented by the sequence $t(k), k = 0, 1, 2, \ldots$. Similarly, an unstable, discrete transfer function will have a sequence representation consisting of both causal and

anticausal parts. Where we have multiplication in the z-domain, we have convolution in the time domain, which will be represented using an infinite matrix notation [18]. For example, considering stable S and Q, $X = SQ$ will have sequence representation

$$\begin{aligned} x &= \tau_s q \\ x(k) &= \sum_{l=0}^{\infty} s(k-l)q(l) \end{aligned} \tag{4.46}$$

where

$$S(z) = \sum_{k=0}^{\infty} s(k)z^{-k}, \quad Q(z) = \sum_{k=0}^{\infty} q(k)z^{-k} \tag{4.47}$$

$$\tau_s = \begin{bmatrix} s(0) & 0 & 0 & 0 & \cdots \\ s(1) & s(0) & 0 & 0 & \cdots \\ s(2) & s(1) & s(0) & 0 & \cdots \\ s(3) & s(2) & s(1) & s(0) & \ddots \\ \vdots & \vdots & \vdots & \ddots & \ddots \end{bmatrix} \tag{4.48}$$

Using this notation we can define an equivalent convex set where our solution sequence must lie

$$k = \{x = \tau_s q \in \ell_2(Z_+) \mid q \in \ell_1(Z_+),\ \|q\|_1 \leq \nu\} \tag{4.49}$$

Our problem is now stated as

$$\alpha^* = \inf_{x \in k} \|r - x\|_2 = \max_{\|x^*\|_2 \leq 1} [\langle r, x^* \rangle - h(x^*)] \tag{4.50}$$

We now need to define the support functional.

$$h(x^*) := \sup_{x \in k} \langle x, x^* \rangle \tag{4.51}$$

$$= \sup_{\|q\|_1 \leq \nu} \langle \tau_s q, x^* \rangle \tag{4.52}$$

$$= \sup_{\|q\|_1 \leq \nu} \langle q, {\tau_s}^T x^* \rangle \tag{4.53}$$

$$\leq \sup_{\|q\|_1 \leq \nu} \|q\|_1 \|{\tau_s}^T x^\star\|_\infty \tag{4.54}$$

We can create a tighter upper bound for $h(x^\star)$ by noting that any negative time elements of the sequence ${\tau_s}^T x^\star$, which is generally non-causal, will be eliminated in the inner product by the associated elements of q, which is restricted to causal sequences. With this, we can state

$$h(x^\star) \leq \sup_{\|q\|_1 \leq \nu} \|q\|_1 \|\overline{P}_c {\tau_s}^T x^\star\|_\infty \tag{4.55}$$

$$\leq \nu \|\overline{P}_c {\tau_s}^T x^\star\|_\infty \tag{4.56}$$

where $\overline{P}_c$ represents an anticausal truncation operator, i.e., for a non-causal sequence m,

$$\overline{P}_c m = \{\ldots, 0, 0, m(0), m(1), m(2), \ldots\} \tag{4.57}$$

Since ${\tau_s}^T x^\star \in \ell_2$, elementwise it must approach 0 as $k \longrightarrow \infty$. This implies that $\|\overline{P}_c {\tau_s}^T x^\star\|_\infty$ will be achieved for some positive finite value of k, say $k = N$. For the case where $q(k) = 0$ for all $k \neq N$, $|q(N)| = \nu$, we see that the upper bound is actually achievable. This implies

$$h(x^\star) = \nu \|\overline{P}_c {\tau_s}^T x^\star\|_\infty \tag{4.58}$$

The dual problem can now be stated as

$$\begin{aligned} \alpha^\star &= \max_{\|x^\star\|_2 \leq 1} \left[\langle r, x^\star \rangle - \nu \|\overline{P}_c {\tau_s}^T x^\star\|_\infty \right] \\ &= \max_{\|x^\star\|_2 \leq 1} \left[\left(\sum_{k=-\infty}^{\infty} r(k) x^\star(k) \right) - \nu \left(\max_{l \in Z^+} \sum_{k=0}^{\infty} s(k) x^\star(k+l) \right) \right] \end{aligned} \tag{4.59}$$

Ideally, we would like to find an algorithm which defines $x^\star(k)$ in terms of $r(k)$, $s(k)$ and preceding elements of r, s and $x^\star$. This would constitute a causal construction algorithm. However, an algorithm such as this has yet to be found, and remains a topic of current research.

For cases where the dual solution can be found and the infimum in (4.50) is achieved for some $q \in \ell_1$, the primal solution, q_o, can be constructed using the alignment condition

$$\langle r - \tau_s q_o, x_o^\star \rangle = \|r - \tau_s q_o\|_2 \|x_o^\star\|_2 \tag{4.60}$$

which can be expressed as

$$r(k) - \sum_{l=0}^{k} s(k-l) q_o(l) = C x^\star(k) \; \forall \; k \tag{4.61}$$

where C is a constant used to satisfy $\|q\|_1 \leq 1$. For the case where $s(0) \neq 0$, an explicit algorithm for constructing q_o is

$$q_o(k) = \begin{cases} \frac{1}{s(0)} \left(r(0) - C x^\star(0) \right) & if \quad k = 0 \\ \frac{1}{s(0)} \left(r(k) - C x^\star(k) - \sum_{l=0}^{k-1} s(k-l) q(l) \right) & if \quad k \geq 1 \end{cases} \tag{4.62}$$

A similar algorithm can be constructed for the case where $s(0) = 0$.

4.5 Insights From a Specific Example

Considerable insight into the nature of the optimal H_2/ℓ_1 problem can be gained by examining the exact solution to a specific example. Specifically, we claim that the general solution to the H_2/ℓ_1 optimization problem is not necessarily FIR in the closed-loop transfer function T_{zw}. We will prove this by showing an example in which the optimal closed loop T_{zw} is not FIR. The significance of this claim is that it shows Voulgaris' [24] results do not extend to the more general case where $T_{zw} \neq T_{mr}$.

Consider the problem where

$$\begin{aligned} r(k) &= \begin{cases} 0 & if \quad k < 0 \\ \frac{1}{k+1} & if \quad k \geq 0 \end{cases} \\ s(k) &= \begin{cases} 0 & if \quad k \neq 0 \\ 1 & if \quad k = 0 \end{cases} \end{aligned} \tag{4.63}$$

The primal problem we are considering is

$$\alpha^* = \inf_{\|q\|_1 \leq 1} \|r - q\|_2 \tag{4.64}$$

which corresponds to $\tau_s = I$ and $x = q$. We note that this particular problem has an unconstrained (H_2 optimal) solution of $q = r$, where we note that $q \in \ell_2$ but $q \notin \ell_1$, i.e. $\|q\|_1 = \infty$. Further, note that the unconstrained q is not FIR. The ℓ_1 optimal solution for this example is easily seen to be $q = 0$ since r is already stable. For the constrained case, the dual problem (4.59) reduces to

$$\alpha^* = \max_{\|x^*\|_2 \leq 1} \alpha(x^*) \tag{4.65}$$

$$\alpha(x^*) = \left[\sum_{k=0}^{\infty} r(k)x^*(k) - \|\overline{P}_c x^*\|_\infty \right] \tag{4.66}$$

We will define a pair of sequences in ℓ_2 as follows:

$$x'(k) = \begin{cases} 0 & if \quad k < 0 \\ \frac{5}{18} & if \quad k \in \{0,1,2\} \\ \frac{1}{k+1} & if \quad k \geq 3 \end{cases} \tag{4.67}$$

$$x''(k) = \frac{x'(k)}{\|x'\|_2} \tag{4.68}$$

where both x' and x'' are in the dual space X^*. We now make the following claim.

Claim $\alpha(x^*) \leq \|x'\|_2$ *for all* $\|x^*\|_2 \leq 1$. *Further,* $\alpha(x'') = \|x'\|_2$ *and thus* x'' *solves (4.65).*

Proof: First we will show that $\alpha(x'') = \|x'\|_2$.

$$\alpha(x'') = \sum_{k=0}^{\infty} \frac{x''(k)}{k+1} - \|\overline{P}_c x''\|_\infty \tag{4.69}$$

$$= x''(0) + \frac{x''(1)}{2} + \frac{x''(2)}{3} + \frac{1}{\|x'\|_2} \sum_{k=3}^{\infty} x'(k)^2 \; - \; x''(0) \tag{4.70}$$

$$= \frac{x''(1)}{2} + \frac{x''(2)}{3} + \frac{1}{\|x'\|_2} \sum_{k=3}^{\infty} x'(k)^2 \tag{4.71}$$

$$= \frac{x'(0)}{\|x'\|_2}\left(\frac{1}{2}+\frac{1}{3}\right)+\frac{1}{\|x'\|_2}\sum_{k=3}^{\infty}x'(k)^2 \tag{4.72}$$

$$= \frac{x'(0)}{\|x'\|_2}\left(x'(0)+x'(1)+x'(2)\right)+\frac{1}{\|x'\|_2}\sum_{k=3}^{\infty}x'(k)^2 \tag{4.73}$$

$$= \frac{1}{\|x'\|_2}\sum_{k=0}^{\infty}x'(k)^2 \tag{4.74}$$

$$= \|x'\|_2 \tag{4.75}$$

Now fix $x^\star \in \ell_2 \ \ni \|x^\star\|_2 \leq 1$. Since $x^\star \in \ell_2$, $|x^\star(k)| < \infty$ for all k, and $|x^\star(k)| \longrightarrow 0$ as $k \longrightarrow \infty$. This implies there exists a finite $N \in Z^+ \ \ni \ |x^\star(N)| = \|\overline{P}_c x^\star\|_\infty$. In order to show $\alpha(x^\star) \leq \|x'\|_2$, we will need to examine separately the case where $N = 0$, $N = 1$, $N = 2$ or $3 \leq N < \infty$. In the interest of continuity, the proof for these cases appears in Appendix A, thus proving $\alpha(x^\star) \leq \|x'\|_2$. ∎

The primal solution q_o for the constrained case can be constructed as follows:

$$q_o(k) = r(k) - Cx^\star(k) \tag{4.76}$$

and $C = \|x'\|_2$ is the required constant in order to insure $\|q\|_1 \leq 1$. With this, we can write

$$q_o = \left\{\frac{13}{18},\ \frac{4}{18},\ \frac{1}{18},\ 0,\ 0,\ \ldots\right\} \tag{4.77}$$

which is FIR. However, the sequence representation of the resulting closed-loop T_{zw} is given by

$$t_{zw} = r - q_o = \left\{\frac{5}{18},\ \frac{5}{18},\ \frac{5}{18},\ \frac{1}{4},\ \frac{1}{5},\ \frac{1}{6},\ \cdots\right\} \tag{4.78}$$

which is <u>not</u> FIR! Although this is the only problem to date that has been solved exactly, numerical results for several other restricted problems have also resulted in FIR q's but non-FIR T_{zw}'s. This seems to support the observation that SISO synthesis problems, in which $\|T_{mr}\|_1$ is constrained or minimized, tend to result in FIR solutions for T_{mr}. This is true for the ℓ_1 synthesis problem and the special case H_2/ℓ_1 problem considered by Voulgaris[24]. When combined with the present results, this observation leads to the

following (unproven) conjecture.

Conjecture *The solution to the SISO constraint H_2/ℓ_1 optimal control problem for the case where $T_{zw} \neq T_{mr}$ will result in a FIR sequence representation for T_{mr}, and, in general, a non-FIR sequence representation for T_{zw}. Further, if this holds for the SISO constraint case, it will also hold for one-block MIMO constraints.*

That T_{zw} can be non-FIR for the SISO constraint case has been proven by example. The conjecture is not that T_{zw} must always be non-FIR, rather it has been shown that the FIR solutions to the SISO ℓ_1 optimal and $T_{zw} = T_{mr}$ mixed cases do not extend to the more general mixed case where $T_{zw} \neq T_{mr}$. Recent results (as yet unpublished) by other researchers support this conjecture based on a related problem [49], and they have also shown that the mixed H_2/ℓ_1 problem considered in this chapter can be approximated to within arbitrary accuracy using what they call a "combination" problem. Assuming that this conjecture holds for the mixed H_2/ℓ_1 problem, straightforward numerical techniques can be defined to solve exactly the SISO and one-block MIMO constraint H_2/ℓ_1 problem. These techniques are the topic of discussion in the next section.

4.6 A Numerical Approach to the Optimal H_2/ℓ_1 Problem

Only the SISO constraint case is developed in this section; however, it will be shown that the results extend to one-block MIMO constraints. We will allow general MIMO transfer functions for the H_2 objective. Using sequence representation for the transfer functions, the H_2/ℓ_1 problem is as follows:

$$\alpha^* = \inf_{q \in \ell_1} \| t_{1_2} + \tau_{2_2} \tau_q t_{3_2} \|_2 \tag{4.79}$$

such that

$$\| t_{1_1} + \tau_1 q \|_1 \leq \nu \tag{4.80}$$

where τ_1, τ_{2_2} and τ_q are the matrix representations of the convolution operators resulting from t_{23_1}, t_{2_2} and q, respectively. For finite truncation levels, this problem can be solved as a quadratic programming (QP) problem. However, this requires the definition of a new set of variables in order to obtain linear expressions for the constraint. This is the

same transformation used by Voulgaris [24] and earlier by Dahleh [5] for the ℓ_1 problem. Although this allows a QP formulation, it triples the number of design variables for the numerical optimization. Further, the quadratic term in the objective function will only be positive semidefinite, with at least two thirds of the eigenvalues being identically zero.

A more straightforward formulation is to use $q(k), k = 0, 1, 2, ..., N$ as the design variables and accept the fact that the constraints will no longer be linear. Mathematically, we can express a problem equivalent to the truncated (4.79) as

$$\underset{q \in R^{N_q}}{\text{minimize}} \left(\frac{1}{2} t_{3_2}{}^T \tau_q{}^T \tau_{2_2}{}^T \tau_{2_2} \tau_q t_{3_2} + t_{3_2}{}^T \tau_q{}^T \tau_{2_2}{}^T t_{1_2} \right) \tag{4.81}$$

subject to the constraint

$$\sum_{k=0}^{N_\phi} |\phi_1(k)| - \nu \leq 0 \tag{4.82}$$

where

$$\phi_1(k) = t_{1_1}(k) + [\tau_1 q](k) \tag{4.83}$$

Although this can no longer be solved directly as a QP problem, it remains convex. Further, analytic gradient expressions are easily defined, and it can be solved efficiently using Sequential Quadratic Programming (SQP) algorithms.

One problem that still needs to be addressed is how to choose an appropriate truncation level for a problem which is generally infinite dimensional. As a minimum, we need to find a truncation which will result in a suboptimal but feasible solution. The conjecture from the preceding section, if it holds, has important implications for this problem. First, we can expect that only a finite number of terms in the constraint summation, say N of them, will be non-zero. Second, in order for ϕ_1 to be FIR, the elements of q beyond $k = N$ will be defined precisely by the first N elements of q, and the need for $[\tau_1 q](k)$ to cancel $t_{1_1}(k)$ for all $k > N$. For each $q(k)$, $k > N$, a single additional equation can be solved exactly to determine its value. Likewise, for an $n \times n$ one-block MIMO constraint problem, there will be n^2 equations which can be solved for n^2 variables for each $k > N$. This suggests that an identical solution (within numerical precision) to the truncated problem will result for all truncation levels (N_q, N_ϕ) greater than N. Although an FIR ϕ_1 does not

imply an FIR q, all the information required to construct the remaining elements of q will be available from the truncated problem.

As an initial test of the conjecture and the proposed numerical method, a SISO F-16 problem was formulated as a mixed-norm problem. The plant includes a short period approximation of the longitudinal dynamics, the objective transfer function is based on a standard LQG problem, and the constraint transfer function is a weighted sensitivity problem. The complete set of plant equations appear in Appendix B, and a more complete analysis of this example will be presented in Chapter VI. The objective of this section is to characterize the optimal solution; thus the complete design problem will not be presented in this chapter. Figure 4.2 shows the Pareto curve generated using a truncation level of $N_q = N_\phi = 100$, resulting in a controller order of 106. In order to demonstrate the FIR nature of the constraint transfer function, we will examine a single constraint level, arbitrarily chosen at $\nu = 2.5$. Figure 4.3 shows a plot of the vectors ϕ_2 and ϕ_1, which are the discrete pulse responses of T_{zw} and T_{mr}, respectively (although T_{mr} is SISO, T_{zw} for this problem has two exogenous inputs and two exogenous outputs). The FIR nature of T_{mr} is clearly evident from the plots, yet T_{zw} shows more of an asymptotic decay as opposed to an FIR behavior. This is consistent with the conjecture that the optimal H_2/ℓ_1 solution generally will result in an FIR constraint transfer function (T_{mr}), but not necessarily so for the objective transfer function (T_{zw}). We also notice in Figure 4.4 that plots of ϕ_1 and q are virtually identical for truncation levels of $N_q = N_\phi$ =100, 200, and 500 (the three plots are indistinguishable in Figure 4.4).

Although the tendency might be to truncate the problem close to the finite support length of ϕ_1 (N) in order to improve efficiency, higher truncation levels are often necessary in order to capture this finite support length successfully. A prematurely truncated problem will result in a low level but non-zero impulse response beyond where the finite support length should end. At a minimum, this means that the 1-norm constraint level is probably not being met. In order to prevent this, truncation levels significantly higher than the final support length of ϕ_1 are often required for numerical solution of the problem. One way of reducing the problem size, while still allowing for high truncation levels, involves truncating q at a significantly lower level than ϕ_1 is truncated. Although this results in

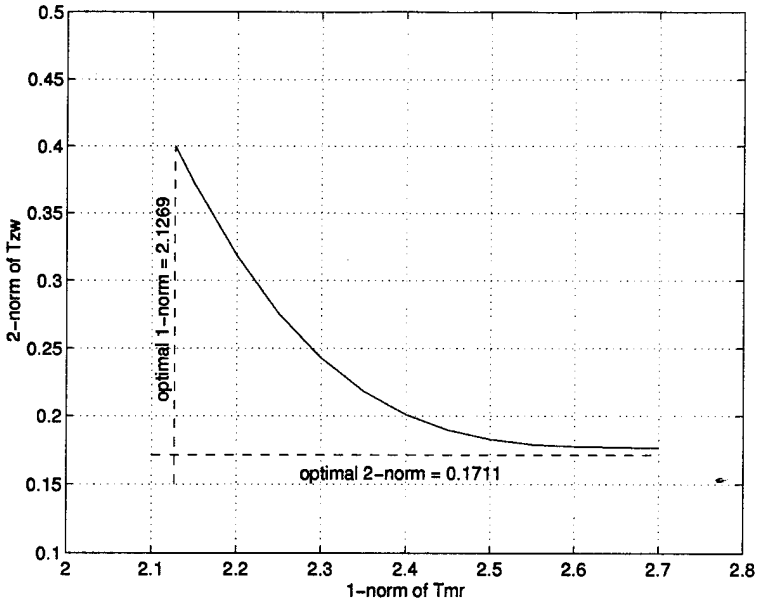

Figure 4.2 Optimal H_2/ℓ_1 Tradeoff Curve for SISO F-16

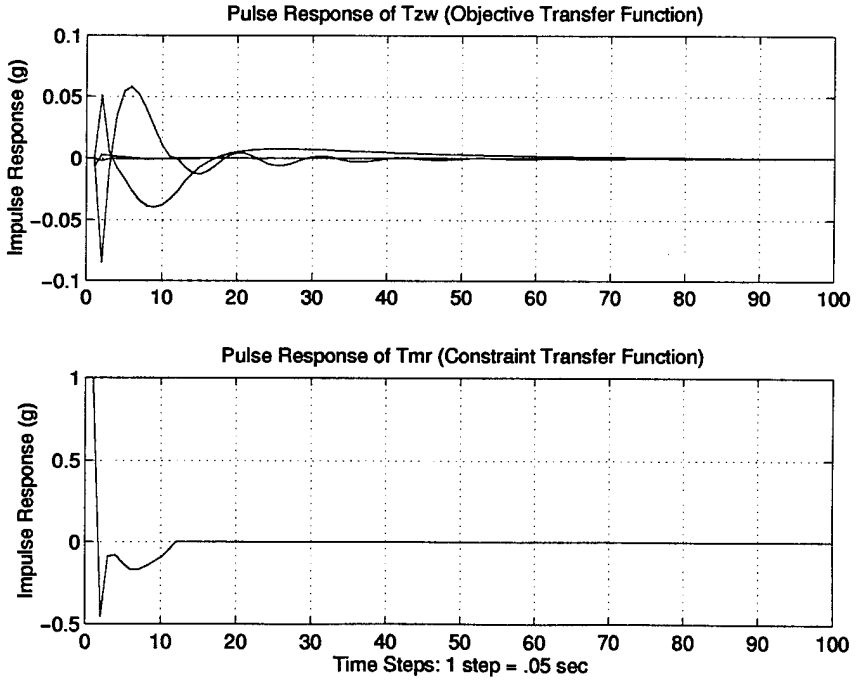

Figure 4.3 Objective and Constraint Pulse Responses, $\nu = 2.5$, $N_q = N_\phi = 100$

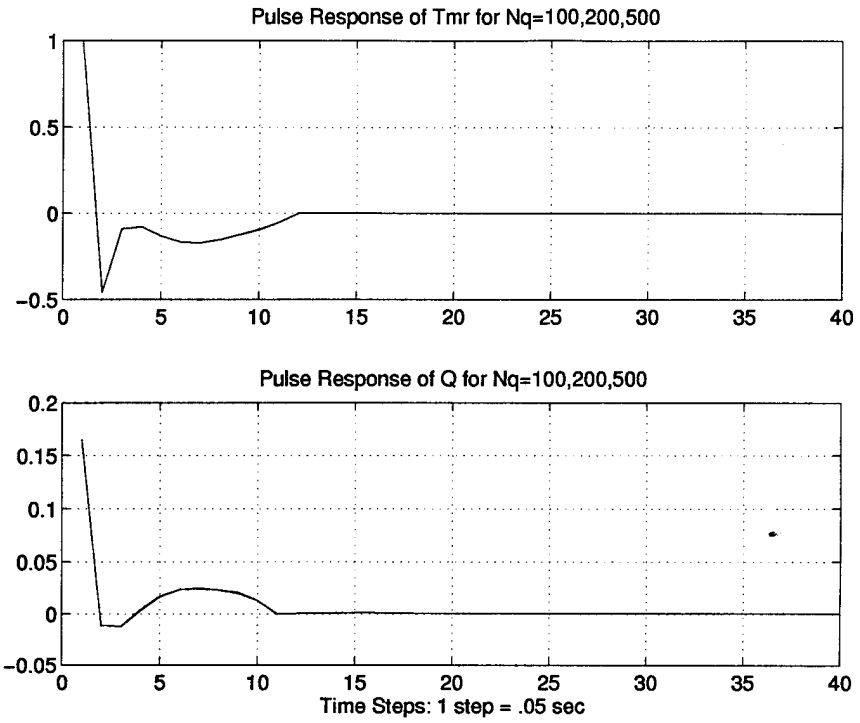

Figure 4.4 Pulse Response of T_{mr} and Q for Varying Truncation Levels

a suboptimal solution to the problem, the distance between this and the optimal solution can be made arbitrarily small simply by increasing the order of q. Figure 4.5 shows the results of different q truncation levels (N_q), while the truncation level of ϕ_1 was held constant at $N_\phi = 500$. For $N_q = 60$ and above, there is almost no difference between the resulting compensators (outside of compensator order), and resulting 2-norms are identical to within numerical error for truncation levels of $N_q = 100$ and above. For many problems, the high truncation levels required for ϕ_1 may make it prohibitive in terms of problem size to truncate q at the same level. This will be especially true for problems with widely separated dynamics, because the sample rate will be driven by the fast dynamics of the system, and the truncation level will be driven by the slow dynamics. Indeed, an example to be shown in Chapter VII will demonstrate that there are many practical problems where truncation levels of 5000-10000 are required.

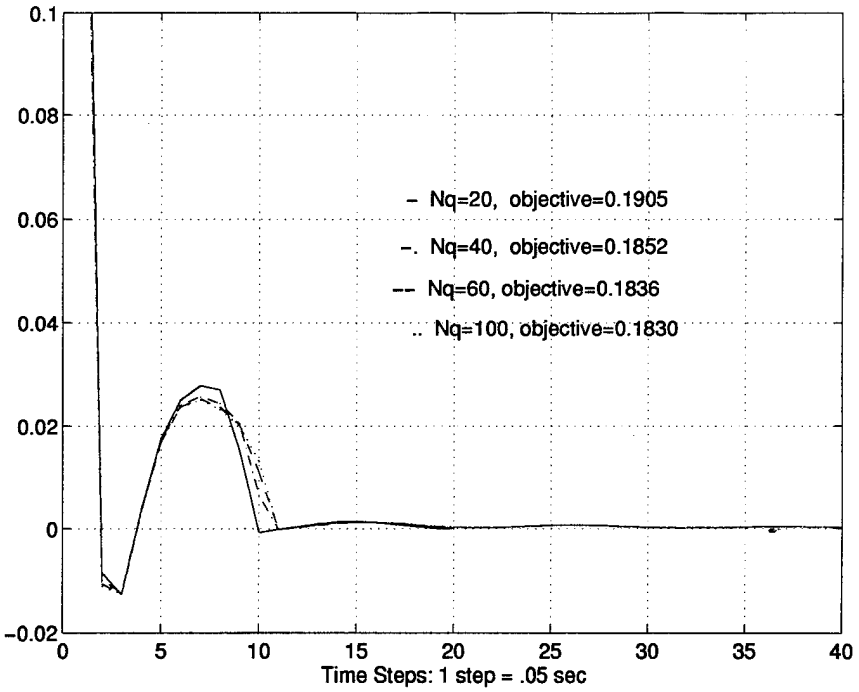

Figure 4.5 Effect of Truncation Level on Optimal Solution, q

4.7 An Alternate Method for Optimal H_2/ℓ_1 Control Synthesis

The numerical method presented in the preceding section is based on the conjecture that the SISO or one-block MIMO problem will result in an FIR constraint transfer function. For multi-block problems, it is anticipated that the constraint transfer function will no longer be FIR in all blocks. Although the numerical method can be used to approximate the solution to multi-block problems, there are no guarantees of accuracy for a given truncation level. In order to address this problem, a second numerical method was developed which approximates the optimal solution to within a specifiable ϵ. Although the development in this section will be for SISO systems, the development is based on an existing method which has been extended to multi-block problems [18, 19]. This method also allows for the addition of an H_∞ constraint to the problem, as will be shown later in this section.

For a SISO problem, the Youla-parametrizations for the closed-loop transfer functions are expressed in Equations (4.39) and (4.40). For this development, we will need to assume the ℓ_1 constraint is nonsingular. Without further loss of generality, the Youla

parametrizations can be selected such that T_{23_1} is an inner function [18], i.e. $T_{23_1}^{\sim} T_{23_1} = I$, where $T_{23_1}^{\sim}(z) = (T_{23_1}(z^{-1}))^T$. The reason for this form of the parametrization will become clear later in the development. The SISO problem (SP) can be stated as, find

$$\alpha^* = \inf_{Q \in RH_\infty} \|T_{1_2} + T_{23_2} Q\|_2 \tag{4.84}$$

subject to

$$\|T_{1_1} + T_{23_1} Q\|_1 \leq \nu \tag{4.85}$$

The restriction of $Q \in \mathbf{R}H_\infty$ can be used, since all real rational elements of ℓ_1 have a representation in $\mathbf{R}H_\infty$ [5]. Although the operator theoretic problem does not assume a real rational compensator, we will be attempting to find a finite order approximation; thus, we can restrict the search to $Q \in \mathbf{R}H_\infty$.

Using time domain expressions of the transfer functions, we obtain (4.79), which is an infinite dimensional optimization problem. Because we seek a finite-dimensional approximation to the solution, we need to be able to truncate the problem with a predictable truncation error. The conjecture made earlier in this chapter implies that this can be done with zero error as long as the constraint transfer function is FIR. However, for multi-block problems it is anticipated that the constraint transfer functions will not be FIR, so a different method for choosing a truncation level is necessary. For this, we will consider a radius constraint first suggested by Sideris and Rotstein [22] as a means to deal with finite horizon constraints, and later used by Sznaier [18] to truncate a free-order H_2/H_∞ problem. The remainder of this section will follow the same line of development as in [18] with modifications necessary to apply it to the H_2/ℓ_1 problem.

Consider a modified problem, where the closed loop poles are constrained to lie within a disc of radius $\delta < 1$. Define

$$\mathbf{R}H_\delta = \{Q \in \mathbf{R}H_\infty \mid Q \text{ is analytic in } |z| \geq \delta\} \tag{4.86}$$

$$\|Q\|_\delta = \sup_{|z|=\delta} |Q(z)| \tag{4.87}$$

For a given transfer function $T(z)$, we will use the notation

$$\hat{T} = \hat{T}\left(\hat{z} = \frac{z}{\delta}\right) = T(\delta\hat{z}) \tag{4.88}$$

Using this notation, we can write $\|T\|_\delta = \|\hat{T}\|_\infty$. A modified SISO problem (MSP) can now be stated as

$$\alpha_\delta^* = \inf_{\hat{Q}\in RH_\infty} \|\hat{T}_{1_2} + \hat{T}_{23_2}\hat{Q}\|_2 \tag{4.89}$$

subject to

$$\|\hat{T}_{1_1} + \hat{T}_{23_1}\hat{Q}\|_1 \ \leq \ \nu \tag{4.90}$$

A supporting lemma will demonstrate that the MSP can be used to approximate the SP.

Lemma 4.7.1 *Any solution to MSP is an admissible solution to SP. Further, for an increasing sequence $\delta_i \rightarrow 1$, the sequence $\alpha_{\delta_i}^*$ converges to α^*.*

Proof: Suppose $Q \in \mathbf{R}H_\delta$ is a solution to MSP. Then,

$$\|\hat{T}_{mr}(\hat{z})\|_1 \ \leq \ \nu \tag{4.91}$$

where

$$\hat{T}_{mr}(\hat{z}) = \sum_{k=0}^{\infty} \hat{t}_{mr}(k)\hat{z}^{-k} \tag{4.92}$$

This implies

$$\sum_{k=0}^{\infty} \left|\hat{t}_{mr}(k)\right| \ \leq \ \nu \tag{4.93}$$

Using the transformation $\hat{z} = z/\delta$, $0 < \delta < 1$, we have

$$T_{mr}(z) = \sum_{k=0}^{\infty} \hat{t}_{mr}(k)\delta^k z^{-k} \tag{4.94}$$

Thus

$$\|T_{mr}(z)\|_1 \ = \ \sum_{k=0}^{\infty} \left|\hat{t}_{mr}(k)\delta^k\right| \tag{4.95}$$

$$= \sum_{k=0}^{\infty} \delta^k \left|\hat{t}_{mr}(k)\right| \tag{4.96}$$

$$\leq \sum_{k=0}^{\infty} \left|\hat{t}_{mr}(k)\right| \tag{4.97}$$

$$= \|\hat{T}_{mr}(\hat{z})\|_1 \leq \nu \tag{4.98}$$

and since the closed loop poles were constrained to lie within the circle of radius $\delta < 1$, T_{zw} and T_{mr} will be stable. This implies that Q is an admissible solution to SP and α^*_δ is an upper bound to α^*. Now consider an increasing sequence $\delta_i \to 1$. Any solution Q_i to MSP with $\delta_i < 1$ will be admissible for MSP with $\delta_{i+1} > \delta_i$. This implies that $\alpha^*_{\delta_i}$ is a non-increasing sequence, and it is bounded below by $\underline{\alpha}$, the minimum value of $\|T_{zw}\|_2$. Following the procedure of Lemma 1 [18], we can complete the proof to show that $\alpha^*_{\delta_i} \to \alpha^*$. ∎

A parametrization of all achievable closed loop transfer functions such that T_{zw} and T_{mr} satisfy the radius constraint can be obtained from (4.39) and (4.40) by performing the transformation $z = \delta\hat{z}$ prior to the factorizations. Furthermore, by combining the transformation with the inner-outer factorization, the resulting $T_{23_1}(z)$ satisfies

$$T_{23_1}\left(\frac{1}{\delta\hat{z}}\right) T_{23_1}(\delta\hat{z}) = I \tag{4.99}$$

The next theorem will show how MSP can be approximated with arbitrary accuracy.

Theorem 4.7.1 *Given $\epsilon > 0$, there exists $N(\epsilon, \delta)$ such that if $Q \in \mathbf{R}H_\delta$ ($\hat{Q} \in \mathbf{R}H_\infty$) satisfies (4.90), then it satifies the following expression:*

$$\sum_{k=N}^{\infty} \left|\left[t_{1_2} + \tau_2 q\right](k)\right|^2 \leq \epsilon^2 \tag{4.100}$$

Proof: Let t_{zw} denote the time domain representation of T_{zw}. Using Cauchy's formula, we can write

$$t_{zw}(k) = \frac{1}{2\pi j} \oint_{|z|=\delta} T_{zw}(z) z^{k-1} dz \ , \ \ j = \sqrt{-1} \tag{4.101}$$

Therefore,

$$t_{zw}(k) \leq \|T_{zw}\|_\delta \delta^k \tag{4.102}$$

Using an equivalent expression for an infinite series, we can write

$$\sum_{k=0}^{\infty} |\delta^k|^2 = \sum_{k=0}^{\infty} (\delta^2)^k = \frac{1}{1-\delta^2}\ , \quad 0 \leq \delta < 1 \tag{4.103}$$

Further,

$$\sum_{k=N}^{\infty} (\delta^k)^2 \ = \ \frac{\delta^{2N}}{1-\delta^2} \tag{4.104}$$

$$\text{implies} \quad \sum_{k=N}^{\infty} |t_{zw}(k)|^2 \ \leq \ \frac{\|T_{zw}\|_\delta^2 \delta^{2N}}{1-\delta^2} \tag{4.105}$$

We need to bound the term $\|T_{zw}\|_\delta^2$

$$\|T_{zw}\|_\delta \leq \|T_{1_2}\|_\delta + \|T_{23_2}\|_\delta \|Q\|_\delta \tag{4.106}$$

All terms on the right side of (4.106) are known except Q, but $\|Q\|_\delta$ can be bounded using the 1-norm constraint

$$\|T_{mr}\|_\delta = \|T_{1_1} + T_{23_1} Q\|_\delta \leq \|T_{mr}\|_1 \leq \nu \tag{4.107}$$

Using the invariance of the ∞-norm under multiplication by an inner function

$$\|T_{mr}\|_\delta = \|T_{23_1}^{\sim} T_{1_1} + Q\|_\delta \leq \|T_{23_1}^{\sim} T_{1_1}\|_\delta + \|Q\|_\delta \tag{4.108}$$

which implies

$$\|Q\|_\delta \leq \nu + \|T_{23_1}^{\sim} T_{1_1}\|_\delta \tag{4.109}$$

Substituting (4.109) into (4.106), we can now define

$$g \ := \ \|T_{1_2}\|_\delta + \|T_{23_2}\|_\delta \left(\nu + \|T_{23_1}^{\sim} T_{1_1}\|_\delta\right) \ \geq \|T_{zw}\|_\delta \tag{4.110}$$

If we choose

$$N \geq \frac{1}{2} \frac{\log\left(\epsilon^2\left(1-\delta^2\right)\right) - \log(g^2)}{\log(\delta)} \tag{4.111}$$

then (4.100) is satisfied. ∎

We now state the SISO finite-dimensional problem (SFDP).

$$\text{For} \qquad \epsilon > 0, 0 < \delta < 1, N = N(\epsilon, \delta)$$

$$\underset{q \in R^N}{\text{minimize}} \left(\sum_{k=0}^{N-1} \left| \left[t_{1_2} + \tau_2 q \right](k) \right|^2 \right)^{\frac{1}{2}} \tag{4.112}$$

$$\text{subject to} \sum_{k=0}^{N-1} \left| \left[t_{1_1} + \tau_1 q \right](k) \right| \leq \nu \tag{4.113}$$

The following theorem and lemma complete the H_2/ℓ_1 development for this section.

Theorem 4.7.2 *Let $Q_{\delta,\epsilon}$ be a solution to SFDP, as defined by equations (4.112) and (4.113). Then $Q_{\delta,\epsilon}$ is an admissible solution to SP and*

$$\alpha_\delta^* \leq \| T_{1_2} + T_{23_2} Q_{\delta,\epsilon} \|_2 \leq \alpha_\delta^* + \epsilon \tag{4.114}$$

where α_δ^* is the optimal value of MSP for the given δ.

Proof: Let $Q_{\delta,\epsilon}$ be a solution to SFDP. Then $Q_{\delta,\epsilon} \in \mathbf{R}H_\delta \subset \mathbf{R}H_\infty$ and

$$\| T_{mr} \|_1 \leq \| \hat{T}_{mr} \|_1 \leq \nu \tag{4.115}$$

which simply restates that $Q_{\delta,\epsilon}$ is admissible for SP.

$$\begin{aligned} \left(\alpha_\delta^*\right)^2 &\leq \| T_{1_2} + T_{23_2} Q_{\delta,\epsilon} \|_2^2 && (4.116) \\ &= \sum_{k=0}^{\infty} \left| \left[t_{1_2} + \tau_2 q_{\delta,\epsilon} \right](k) \right|^2 && (4.117) \\ &= \sum_{k=0}^{N-1} \left| \left[t_{1_2} + \tau_2 q_{\delta,\epsilon} \right](k) \right|^2 + \sum_{k=N}^{\infty} \left| \left[t_{1_2} + \tau_2 q_{\delta,\epsilon} \right](k) \right|^2 && (4.118) \end{aligned}$$

$$\leq \sum_{k=0}^{N-1} \left| \left[t_{1_2} + \tau_2 q_\delta \right](k) \right|^2 + \epsilon^2 \tag{4.119}$$

$$\leq \sum_{k=0}^{\infty} \left| \left[t_{1_2} + \tau_2 q_\delta \right](k) \right|^2 + \epsilon^2 \tag{4.120}$$

$$= \left(\alpha_\delta^*\right)^2 + \epsilon^2 \tag{4.121}$$

$$\leq \left(\alpha_\delta^* + \epsilon\right)^2 \tag{4.122}$$

and this implies

$$\alpha_\delta^* \leq \| T_{1_2} + T_{23_2} Q_{\delta,\epsilon} \|_2 \leq \alpha_\delta^* + \epsilon \tag{4.123}$$

■

Lemma 4.7.2 *Consider an increasing sequence $\delta_i \to 1$, and let α^* and $\alpha^*_{\delta_i,\epsilon}$ denote solutions to SP and SFDP, respectively. Then the sequence $\alpha^*_{\delta_i,\epsilon}$ has an accumulation point α^*_ϵ such that $\alpha^* \leq \alpha^*_\epsilon \leq \alpha^* + \epsilon$.*

Proof: This follows from Lemma 4.7.1, Theorem 4.7.1 and Theorem 4.7.2. ■

For a SISO problem, SFDP will have N variables, and it is anticipated that required values of N will be on the order of 100-500. This should be sufficient to ensure that the finite support structure of the ℓ_1 response is captured for systems with closely spaced poles and sampling frequencies approximately 5-10 times the fastest pole. Despite this high number of variables, the problem should be well behaved numerically due to convexity. Two comments are in order before we leave this topic. First, in order to ensure that the constraint is met, the summation for the constraint will require an index limit higher than the number of variables. In practice, the constraint level can be set at $\nu - \epsilon_1$, $\epsilon_1 > 0$, a separate summation limit can be used for the constraint, and the tolerance of the constraint (for the given truncation level) can be checked using the Hankel singular value method of [5]. Second, there is a considerable amount of conservatism built into the calculation of N for a desired level of accuracy as specified by ϵ (i.e., the truncation level is significantly higher than it needs to be for a given ϵ). Further, a different method of finding N may

allow the removal of the regularity assumption on the ℓ_1 constraint. Methods for reducing this conservatism, thus reducing the value of N, are a topic for future research.

4.7.1 Adding an Approximate H_∞ Constraint. In [5], the authors present a method whereby an approximate (SISO) H_∞ constraint can be appended to a free-order ℓ_1 problem. The development will be repeated here, and applied to the free-order H_2/ℓ_1 problem.

Let $T(z) = \sum_{k=0}^{\infty} t(k) z^{-k}$ be a SISO transfer function with impulse response $\{t(k)\}$. Define

$$T_R(\omega_n) := \Re\left(T\left(e^{j\omega_n}\right)\right) \tag{4.124}$$

$$T_I(\omega_n) := \Im\left(T\left(e^{j\omega_n}\right)\right) \tag{4.125}$$

where $\omega_n \in [0, 2\pi)$ are samples on the unit circle. A set of linear constraints that approximate an H_∞ constraint are

$$T_R(\omega_n)\cos(\theta_m) + T_I(\omega_n)\sin(\theta_m) \leq \gamma \tag{4.126}$$

where

$$\omega_n \in [0, 2\pi), \quad n = 1, \ldots, N_\infty \tag{4.127}$$

$$\theta_m \in [0, 2\pi), \quad m = 1, \ldots, M_\infty \tag{4.128}$$

For given values of ω_n and θ_m, this is a linear operation on T. Further, since T is affine in Q, it will be a linear operation on Q. Specifically

$$T_R(\omega_n) = \sum_{k=0}^{\infty} t(k)\cos(k\omega_n) \tag{4.129}$$

$$T_I(\omega_n) = \sum_{k=0}^{\infty} t(k)\sin(k\omega_n) \tag{4.130}$$

where

$$t(k) = \frac{1}{2\pi j} \oint_{|z|=1} T(z) z^{k-1} dz \tag{4.131}$$

and, using the Youla parametrization,

$$T(z) = T_{1_\infty}(z) + T_{23_\infty}(z) Q(z) \tag{4.132}$$

The full set of constraints can be written as

$$\sum_{k=0}^{\infty} t(k) \cos(k\omega_n - \theta_m) \leq \gamma \tag{4.133}$$

$$\omega_n \in [0, 2\pi) \qquad n = 1, \ldots, N_\infty \tag{4.134}$$

$$\theta_m \in [0, 2\pi) \qquad m = 1, \ldots, M_\infty \tag{4.135}$$

Naturally, the infinite summations would be approximated using the same finite truncations discussed above. This adds a total of $N_\infty M_\infty$ linear constraints to the problem, but it maintains convexity.

This method requires a finite number of frequencies and phase angles to be specified prior to the numerical optimization. A practical method of implementing this technique would be to perform the H_2/ℓ_1 optimization first, and then check where the dominant singular value peaks occur. Initially, a relatively small number of constraints should be sufficient to reduce the dominant peaks, gradually decrementing γ. The further γ is decremented, the more likely it will be that additional peaks will require constraints, thus increasing the overall number of constraints required to constrain the ∞-norm effectively. However, if γ is decremented gradually using this method, it should be possible to keep the total number of required constraints down to a minimum in order to achieve the desired level of robustness or performance as specified by γ. Note that, because the constraint is being approximated, this method offers no guarantees that the exact constraint will be met.

4.7.2 Adding an Exact H_∞ Constraint. Sznaier [18, 19] addressed the H_2/H_∞ problem where the H_2 and H_∞ subproblems share common states. Adapting Sznaier's approach to the $H_2/\ell_1/H_\infty$ problem, the system now being considered has a state space representation

$$P_2 = \left[\begin{array}{c|cccc} A_2 & B_w & B_r & B_d & B_u \\ \hline C_z & D_{zw} & 0 & 0 & D_{zu} \\ C_m & 0 & D_{mr} & 0 & D_{mu} \\ C_e & 0 & 0 & D_{ed} & D_{eu} \\ C_y & D_{yw} & D_{yr} & D_{yd} & D_{yu} \end{array}\right] \tag{4.136}$$

Once again we will restrict ourselves to the SISO problem. Using the Youla parametrization we can express the individual transfer functions as

$$T_{zw} = T_{1_2} + T_{23_2} Q \tag{4.137}$$

$$T_{mr} = T_{1_1} + T_{23_1} Q \tag{4.138}$$

$$T_{ed} = T_{1_\infty} + T_{23_\infty} Q \tag{4.139}$$

Without loss of generality, the parametrization can be done such that T_{23_∞} is inner, which allows us to write

$$\|T_{ed}\|_\infty = \|R + Q\|_\infty \tag{4.140}$$

where

$$R = \tilde{T_{23_\infty}} T_{1_\infty} \tag{4.141}$$

The SISO problem can now be written as

$$\alpha^* = \inf_{Q \in RH_\infty} \|T_{1_2} + T_{23_2} Q\|_2 \tag{4.142}$$

subject to

$$\|T_{1_1} + T_{23_1} Q\|_1 \leq \nu \tag{4.143}$$

$$\|R+Q\|_\infty \leq \gamma \tag{4.144}$$

This represents a convex, infinite dimensional optimization problem. We will again consider a modified SISO problem using the same radius constraint as considered previously in Section 4.7.

$$\alpha_\delta^* = \inf_{Q \in RH_\delta} \|\hat{T}_{1_2} + \hat{T}_{23_2}\hat{Q}\|_2 \tag{4.145}$$

subject to

$$\|\hat{T}_{1_1} + \hat{T}_{23_1}\hat{Q}\|_1 \leq \nu \tag{4.146}$$

$$\|\hat{R}+\hat{Q}\|_\infty \leq \gamma \tag{4.147}$$

Lemma 4.7.1 holds as before, and Theorem 4.7.1 can be replaced with the following:

Theorem 4.7.3 *Let positive numbers ϵ_1 and ϵ_2 be given. There exists $N(\epsilon_1, \epsilon_2, \delta)$ such that, if $Q \in \mathbf{R}H_\infty$ satisfies the constraint $\|R+Q\|_\delta \leq \gamma$, then the following conditions are satisfied:*

$$\sum_{k=N}^{\infty} |[t_{1_2} + \tau_2 q](k)|^2 \leq \epsilon_2^2 \tag{4.148}$$

$$\sum_{k=N}^{\infty} |[t_{1_1} + \tau_1 q](k)| \leq \epsilon_1 \tag{4.149}$$

Proof: Using some of the results from Theorem 4.7.1,

$$\|T_{zw}\|_\delta \leq \|T_{1_2}\|_\delta + \|T_{23_2}\|_\delta \|Q\|_\delta \tag{4.150}$$

$$\leq \|T_{1_2}\|_\delta + \|T_{23_2}\|_\delta (\gamma + \|R\|_\delta) := g_2 \tag{4.151}$$

$$\|T_{mr}\|_\delta \leq \|T_{1_1}\|_\delta + \|T_{23_1}\|_\delta \|Q\|_\delta \tag{4.152}$$

$$\leq \|T_{1_1}\|_\delta + \|T_{23_1}\|_\delta (\gamma + \|R\|_\delta) := g_1 \tag{4.153}$$

Choose

$$N_2 \geq \frac{1}{2}\frac{\log\left(\epsilon_2^2(1-\delta^2)\right) - \log(g_2^2)}{\log(\delta)} \tag{4.154}$$

$$N_1 \geq \frac{1}{2}\frac{\log\left(\epsilon_1(1-\delta)\right) - \log(g_1)}{\log(\delta)} \tag{4.155}$$

$$N \geq \max(N_1, N_2) \tag{4.156}$$

For this value of N, constraints (4.148) and (4.149) will be met. ∎

The SISO finite dimensional problem can now be defined as

For positive numbers $\epsilon_1, \epsilon_2, \gamma, \nu$, with $\delta < 1, \nu > \epsilon_1$ and $N = N(\epsilon_1, \epsilon_2, \delta)$

$$\underset{q \in \mathbf{R}^N}{\text{minimize}} \left(\sum_{k=0}^{N-1} \left| [t_{1_2} + \tau_2 q](k) \right|^2 \right)^{\frac{1}{2}} \tag{4.157}$$

subject to

$$\sum_{k=0}^{N-1} \left| [t_{1_1} + \tau_1 q](k) \right| \leq \nu - \epsilon_1 \tag{4.158}$$

$$\|R + Q\|_\delta \leq \gamma \tag{4.159}$$

Theorem 4.7.2 and Lemma 4.7.2 apply to this problem with little or no modification. What remains to be shown for this problem is how the ∞-norm constraint can be handled. This follows without modification from [18], and is repeated here for the sake of completeness.

Theorem 4.7.4 *Let $Q_F := \sum_{k=0}^{N-1} q(k) z^{-k}$ be given. Then the condition that there exist $Q_R \in \mathbf{R}H_\delta$ such that $\|R+Q\|_\delta \leq \gamma$ where $Q = Q_F + z^{-N} Q_R$ and R has all its poles outside the disk of radius δ, is equivalent to a convex constraint of the form $\|\tilde{Q}\|_2 \leq \gamma$ where $\tilde{Q}$ is a symmetric matrix that is a linear function of the coefficients of Q_F.*

Proof: The proof, as well as the expression for $\tilde{Q}$, can be found in [18]. ∎

Theorem 4.7.5 *A solution to the SISO finite dimensional approximation to the mixed $H_2/\ell_1/H_\infty$ control problem, with cost*

$$\alpha_\delta^* \leq \|T_{zw,\delta}^*\|_2 \leq \alpha_\delta^* + \epsilon_2 \tag{4.160}$$

is given by

$$Q^* = Q_F^* + z^{-N} Q_R^* \tag{4.161}$$

where $q = [q(0), q(1), \ldots, q(N-1)]^T$ solves the following finite dimensional convex optimization problem:

$$q^* = \arg\left[\min_{q \in R^N} \sum_{k=0}^{N-1} \left|\left[t_{1_2} + \tau_2 q\right](k)\right|^2\right] \tag{4.162}$$

subject to

$$\sum_{k=0}^{N-1} \left|\left[t_{1_1} + \tau_1 q\right](k)\right| \leq \nu - \epsilon_1 \tag{4.163}$$

$$\|\tilde{Q}\|_2 \leq \gamma \tag{4.164}$$

and Q_R^* solves the unconstrained Nehari approximation problem

$$Q_R^* = \arg\left[\min_{Q_R \in RH_\delta} \|R + Q\|_\delta\right] \tag{4.165}$$

Proof: See Theorem 2, [18]. ∎

For this $H_2/\ell_1/H_\infty$ problem, the index limit on the ℓ_1 constraint is the same as is used for the H_2 objective because the H_∞ constraint can be used to truncate the problem. Also, the use of the H_∞ constraint to truncate the problem is less conservative than using the ℓ_1 constraint, because we no longer have to use the 1-norm as an upper bound to the ∞-norm. This removes some, but not all, of the conservatism associated with choosing N, and methods of further reducing the conservatism are a topic for future research.

4.8 Summary

This chapter made an important conjecture regarding the solution to the general H_2/ℓ_1 optimization problem. It is possible that a proof for the special case (minimize $\|T_{zw}\|_2$ subject to a constraint on $\|Q\|_1$) can be constructed, but this would only provide further supporting arguments as opposed to a complete mathematical proof. Based on the conjecture, a straightforward numerical method has been formulated. Assuming the conjecture holds, this method is capable of solving the H_2/ℓ_1 control problem exactly. The numerical method was successfully demonstrated on a longitudinal controller design for an F-16 aircraft, to be discussed more fully in Chapter VI. Although the conjecture applies only to SISO and one-block MIMO problems, there is nothing inherent to the numerical method which prevents it from being applied to multi-block problems. All blocks of T_{mr} will most likely not be FIR in this case, but a suboptimal solution should be attainable using this method. Although the accuracy of the multi-block solution can be improved by increasing the truncation level, the accuracy is not quantifiable for a given truncation level using this method. A second numerical method was developed which solves the optimal H_2/ℓ_1 control problem to within a specifiable ϵ, and this method can be extended to multi-block H_2/ℓ_1 and $H_2/\ell_1/H_\infty$ problems.

V. The Optimal and Full-Order H_2/H_∞ Control Problem

When compared to the H_2/ℓ_1 problem discussed in the previous chapter, the H_2/H_∞ problem development is much more mature. For continuous-time systems, Walker [9] posed the general H_2/H_∞ control problem in an operator-theoretical framework and characterized the optimal controller using convex analysis. While a complete analytical solution was not found using this method, the formulation of the problem in this framework provided considerable insight into the nature of the solution. Megretsky [17] was able to construct an optimizing sequence for the general H_2/H_∞ control problem, and, as in Walker's work, he was able to show that the optimal solution can be a non-rational (or infinite-order) transfer function. As an alternative to the optimal (free-order) problem, Ridgely [8] and Walker [9] also investigated sub-optimal fixed-order solutions to the continuous-time H_2/H_∞ control problem. A portion of their fixed-order investigation centered around what will be referred to as the full-order H_2/H_∞ control problem. The full-order problem is one in which the compensator order is assumed to be the same as the underlying H_2 subproblem. Although this problem has yet to admit an analytical solution, significant insight can be gained into the nature of the H_2/H_∞ control problem by studying this special case.

All of the work by Ridgely and Walker has been for continuous-time systems, and very few analytical results have been published for the discrete-time H_2/H_∞ control problem. This chapter will reformulate the H_2/H_∞ problem for discrete-time systems, and reproduce the analytical results of Ridgely and Walker. While there are no surprising differences between the continuous-time and discrete-time results, this chapter serves to formalize the long-standing assumptions that the continuous-time H_2/H_∞ results would apply equally well to discrete-time systems.

5.1 The Optimal H_2/H_∞ Control Problem

5.1.1 Problem Setup and Uniqueness of the Solution. The system considered for the H_2/H_∞ control problem is shown in Figure 5.1. It contains two sets of exogenous inputs and controlled outputs. In general, no relationship is assumed between d and w, or e and z, other than they include the same underlying system dynamics. The input d is

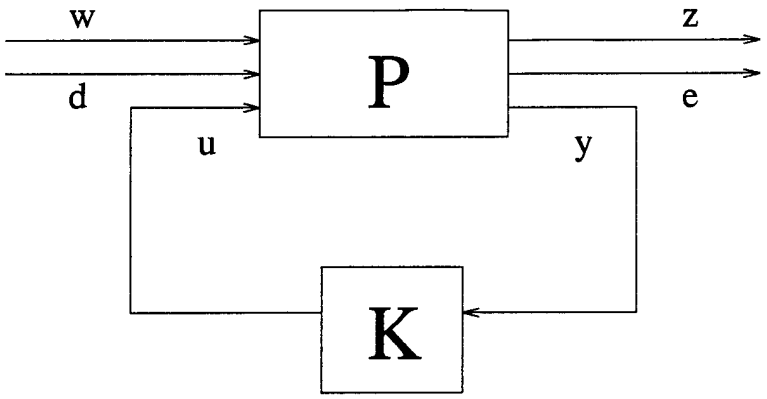

Figure 5.1 General mixed H_2/H_∞ optimization problem

assumed to be a signal of unknown but bounded energy with $\|d\|_2 \leq 1$, and the input w is assumed to be the discrete-time equivalent of zero-mean white Gaussian noise (WGN) of unit intensity. As in the previous chapter, the plant $P(z)$ is formed by augmenting the system dynamics with stable weighting functions on the inputs and outputs. Since we are interested in the closed-loop transfer functions from w to z and d to e, the system can be broken down into an H_2 problem and an H_∞ problem. Using transfer function notation, we write

$$P_2 := \begin{bmatrix} P_{zw} & P_{zu} \\ P_{yw} & P_{yu} \end{bmatrix} \tag{5.1}$$

$$P_\infty := \begin{bmatrix} P_{ed} & P_{eu} \\ P_{yd} & P_{yu} \end{bmatrix} \tag{5.2}$$

The objective of mixed H_2/H_∞ control is to minimize the 2-norm of the closed loop transfer function T_{zw}, while constraining the ∞-norm of the closed loop transfer function T_{ed} to be less than some specified level. Mathematically, the problem can be stated as follows:

For the system shown in Figure 5.1, find an admissible controller $K(z)$ that achieves

$$\alpha^* = \inf_{K \ stabilizing} \|T_{zw}\|_2 \tag{5.3}$$

subject to the constraint $\|T_{ed}\|_\infty \leq \gamma$, where

$$T_{zw} = P_{zw} + P_{zu}K\left(I - P_{yu}K\right)^{-1}P_{yw} \tag{5.4}$$

$$T_{ed} = P_{ed} + P_{eu}K\left(I - P_{yu}K\right)^{-1}P_{yd} \tag{5.5}$$

As in the previous chapter, we will be assuming that P_{yu} is detectable and stabilizable. Further, we will assume both P_{yw} and P_{zu} are non-zero, thus ensuring $\|T_{zw}\|_2$ is affected by K. Finally, we will assume that there is at most one compensator such that $\|T_{zw}\|_2 = 0$.

To simplify the discussion, we make the following definitions:

$$\underline{\gamma} := \inf_{K stabilizing} \|T_{ed}\|_\infty \tag{5.6}$$

$$\underline{\alpha} := \inf_{K stabilizing} \|T_{zw}\|_2 \tag{5.7}$$

$$K_{2_{opt}} := \text{the unique } K(z) \text{ that makes } \|T_{zw}\|_2 = \underline{\alpha} \tag{5.8}$$

$$\overline{\gamma} := \|T_{ed}\|_\infty \text{ when } K(z) = K_{2_{opt}} \tag{5.9}$$

$$K_{mix} := \text{a solution to the } H_2/H_\infty \text{ problem for some } \gamma > \underline{\gamma} \tag{5.10}$$

$$\gamma^* := \|T_{ed}\|_\infty \text{ when } K(z) = K_{mix} \tag{5.11}$$

$$\alpha^* := \|T_{zw}\|_2 \text{ when } K(z) = K_{mix} \tag{5.12}$$

The parametrization from Section 4.3 can be used here by simply replacing P_{mr} with P_{ed}. This results in the convex optimization problem

$$\alpha^* = \inf_{Q \in H_2} \|T_{1_2} + T_{2_2}QT_{3_2}\|_2 \tag{5.13}$$

subject to

$$\|T_{1_\infty} + T_{2_\infty}QT_{3_\infty}\|_\infty \leq \gamma \tag{5.14}$$

Since we have already shown $\|T_{zw}\|_2$ to be strictly convex in Q, we can immediately state the following.

Theorem 5.1.1 *Let $\gamma > \underline{\gamma}$ be given. Then the controller which satisfies the H_2/H_∞ optimization problem is unique. Furthermore, the following hold:*

i. If $\gamma \geq \overline{\gamma}$, then the resulting controller is $K_{2_{opt}}$

ii. If $\underline{\gamma} < \gamma \leq \overline{\gamma}$, then $\gamma^* = \gamma$ at the optimal solution (i.e., the solution will satisfy the H_∞ constraint with equality).

Proof: This is a trivial extension of Walker[9], Theorem 4.2.1. ∎

5.1.2 Dual Approach to the Optimal H_2/H_∞ Control Problem. Walker [9] showed that the solution to the optimal H_2/H_∞ control problem for continuous-time systems can be a non-rational element of H_2. This was shown through the application of the Minimum Norm Duality Theorem to a restricted SISO problem. This section will directly parallel the development in [9], and in so doing will demonstrate that a similar result holds for discrete-time. All of the previous assumptions on the system hold. In addition, for this section only, the system is assumed to be a SISO H_2/H_∞ control problem. The special case to be considered is the same as was examined in Section 4.4, with the exception that the ∞-norm replaces the 1-norm. As in Section 4.4, the optimization problem is implicitly dependent on the Youla parametrization of the objective transfer function, so the parametrization is no longer arbitrary for this special case. The problem is to find a $K(z)$ which satisfies the following:

i. $K(z)$ is internally stabilizing

ii. $\|T_{zw}\|_2$ is minimized

iii. $\|Q\|_\infty \leq \gamma$ where $\gamma \in (\underline{\gamma}, \overline{\gamma})$

This problem will be solved using minimum norm duality. Furthermore, the problem is related to the mixed norm problem and gives some insight into techniques which might be applied to find a solution to the general problem. To date, however, the full mixed problem has not been solved through this approach.

For the SISO case, we can define

$$T_{zw} = T_{1_2} + T_{23_2} Q \tag{5.15}$$

$$T_{ed} = T_{1_\infty} + T_{23_\infty} Q \tag{5.16}$$

where $T_{23_2} = T_{2_2} T_{3_2}$ and $T_{23_\infty} = T_{2_\infty} T_{3_\infty}$. We will again make use of an inner-outer factorization to transform the H_2 objective as follows: Let $T_{23_2} = T_{23_{2_i}} T_{23_{2_o}}$, where $T_{23_{2_i}}$ is a unitary inner function and $T_{23_{2_o}}$ is a stable and minimum phase outer function. Then,

$$\|T_{1_2} + T_{23_2} Q\|_2 = \|T_{23_{2_i}}^{-1} T_{1_2} + T_{23_{2_o}} Q\|_2 \tag{5.17}$$

$$= \|R - X\|_2 \tag{5.18}$$

where $R := T_{23_{2_i}}^{-1} T_{1_2}$, $S = -T_{23_{2_o}}$, and $X := SQ$. Noting that (for discrete-time only) $H_\infty \subset H_2$, T_{zw} will be stable for all $Q \in H_\infty$. Further, since both $\|T_{zw}\|_2$ and $\|T_{ed}\|_\infty$ are convex in Q, this can be seen as a convex parametrization.

Thus, our problem is to find the minimum distance between a point, R, and a convex set in L_2, where the convex set is defined by the continuous mapping $S : H_\infty \to H_2$ of an infinity-norm ball. Our problem is now to find $Q \in H_\infty$ which achieves

$$\alpha^* = \inf_{X \in K} \|R - X\|_2 \tag{5.19}$$

where the set K is defined as

$$K = \{SQ \in H_2 \mid Q \in H_\infty,\ \|Q\|_\infty \leq \gamma\} \tag{5.20}$$

From Theorem 2.8.2 we get

$$\alpha^* = \max_{\|X^*\|_2 \leq 1} [\langle R, X^* \rangle - h(X^*)] \tag{5.21}$$

where $X^\star \in L_2^\star$, which is the dual of L_2, $\langle \cdot, \cdot \rangle$ denotes an inner product, and $h(X^\star)$ is the support functional for the set K defined by

$$h(X^\star) = \sup_{X \in K} \langle X, X^\star \rangle \tag{5.22}$$

The first step in solving the minimum distance problem is to determine the support functional $h(X^\star)$ of the set K. Since L_2 is a Hilbert space, $L_2 \cong L_2^\star$ and functionals can be defined from Theorem 2.8.1 as inner products. With some abuse of notation, the support functional can be written as

$$h(X^\star) := \sup_{X \in K} \langle X, X^\star \rangle = \sup_{X \in K} \frac{1}{2\pi} \int_0^{2\pi} X^*(e^{j\theta}) X^\star(e^{j\theta}) d\theta \tag{5.23}$$

$$\leq \sup_{X \in K} \frac{1}{2\pi} \|Q\|_\infty \int_o^{2\pi} |S^*(e^{j\theta}) X^\star(e^{j\theta})| d\theta \tag{5.24}$$

$$= \frac{\gamma}{2\pi} \int_o^{2\pi} |S^*(e^{j\theta}) X^\star(e^{j\theta})| d\theta \tag{5.25}$$

Thus, (5.25) is an upper bound on the supremum. To determine if it is actually the desired supremum, we will develop a sequence and see if it approaches the upper bound as its index approaches infinity. Let

$$\{\langle X, X^\star \rangle\} = \{\langle X_n, X^\star \rangle\} \tag{5.26}$$

where $X_n = SQ_n$ and

$$Q_n = \begin{cases} \gamma \; sgn(S^* X^\star) & \text{if } \theta \in [\frac{1}{n}, 2\pi - \frac{1}{n}] \\ 0 & \text{otherwise} \end{cases} \tag{5.27}$$

Then

$$\langle X_n, X^\star \rangle = \frac{1}{2\pi} \int_{1/n}^{2\pi - 1/n} Q_n^*(e^{j\theta}) S^*(e^{j\theta}) X^\star(e^{j\theta}) d\theta \tag{5.28}$$

$$= \frac{1}{2\pi} \int_{1/n}^{2\pi - 1/n} \gamma \; sgn[S^*(e^{j\theta}) X^\star(e^{j\theta})] S^*(e^{j\theta}) X^\star(e^{j\theta}) d\theta \tag{5.29}$$

$$= \frac{\gamma}{2\pi}\int_{1/n}^{2\pi-1/n} |S^*(e^{j\theta})X^\star(e^{j\theta})|d\theta \tag{5.30}$$

which approaches (5.25) as n approaches infinity. Thus, $h(X^\star)$ is defined by (5.25). With this definition the problem becomes

$$\alpha^* = \max_{\|X^\star\|_2\leq 1}\left[\langle R, X^\star\rangle - \frac{\gamma}{2\pi}\int_0^{2\pi} |S^*(e^{j\theta})X^\star(e^{j\theta})|d\theta\right] \tag{5.31}$$

$$= \max_{\|X^\star\|_2\leq 1}\left[\frac{1}{2\pi}\int_0^{2\pi} R^*(e^{j\theta})X^\star(e^{j\theta})d\theta - \frac{\gamma}{2\pi}\int_0^{2\pi} |S^*(e^{j\theta})X^\star(e^{j\theta})|d\theta\right] \tag{5.32}$$

$$\leq \max_{\|X^\star\|_2\leq 1}\left[\frac{1}{2\pi}\int_0^{2\pi} \left(|R(e^{-j\theta})| - \gamma|S(e^{-j\theta})|\right)|X^\star(e^{j\theta})|d\theta\right] \tag{5.33}$$

$$= \max_{\|X^\star\|_2\leq 1}\left[\frac{1}{2\pi}\int_{E_\gamma} \left(|R(e^{-j\theta})| - \gamma|S(e^{-j\theta})|\right)|X^\star(e^{j\theta})|\right] \tag{5.34}$$

where E_γ is defined as

$$E_\gamma = \left\{\theta\in[0,2\pi)\,\middle|\;\; |R(e^{-j\theta})| > \gamma\,|S(e^{-j\theta})|\right\} \tag{5.35}$$

Notice, (5.34) will be maximized when $X^\star$ is colinear with $(|R(-j\omega)| - \gamma|S(-j\omega)|)$; therefore, $X^\star$ has the form

$$X^\star = \begin{cases} 0 & if \quad \omega\in E_\gamma \\ c\left[|R(e^{-j\theta})| - \gamma|S(e^{-j\theta})|\right] & if \quad R(e^{-j\theta}) > \gamma|S(e^{-j\theta})| \\ -c\left[|R(e^{-j\theta})| - \gamma|S(e^{-j\theta})|\right] & if \quad -R(e^{-j\theta}) > \gamma|S(e^{-j\theta})| \end{cases} \tag{5.36}$$

where $c := \|\;|R(e^{-j\theta})| - \gamma|S(e^{-j\theta})|\;\|_2^{-1}$ to make $\|X^\star\|_2 = 1$. Thus, we get

$$\alpha^* = \frac{1}{2\pi}\int_{E_\gamma} c\left(|R(e^{-j\theta})| - \gamma|S(e^{-j\theta})|\right)^2 \tag{5.37}$$

$$= \frac{\int_{E_\gamma}\left[|R(e^{-j\theta})| - \gamma|S(e^{-j\theta})|\right]^2}{\left\{2\pi\int_{E_\gamma}\left[\left(|R(e^{-j\theta})| - \gamma|S(e^{-j\theta})|\right)^*\left(|Re^{-j\theta})| - \gamma|S(e^{-j\theta})|\right)\right]\right\}^{\frac{1}{2}}} \tag{5.38}$$

Equation (5.38) gives a method of determining the optimal two-norm of a mixed control problem for a given γ. However, it does not provide a direct method for determining the optimal controller. If the infimum in (5.13) is achieved for some $Q_0 \in H_\infty$, we can use the alignment condition in Theorem 2.8.2 to determine the unique Q_0. In this case,

$$\langle (R - X_0), X_0^\star \rangle = \|R - X_0\|_2 \|X_0^\star\|_2 \tag{5.39}$$

where $X_0 = SQ_0$. However, from the definition of $X^\star$, it can been seen that the alignment condition will force Q_0 to be a piecewise continuous function. This implies that the controller which minimizes the two-norm of T_{zw} and satisfies the H_∞ constraint will be piecewise continuous and not an $\mathbf{R}H_\infty$ function. However, it will be the limit of a sequence of $\mathbf{R}H_\infty$ functions since H_∞ is the closure of $\mathbf{R}H_\infty$.

The above derivation is based on the assumptions $T_{1_\infty} = 0$ and $T_{2_\infty} T_{3_\infty} = I$. Relaxing these conditions, we return to the original SISO mixed H_2/H_∞ problem, but this problem has yet to be solved using min-norm duality. Megretsky [17] was able to solve this problem (for both continuous and discrete-time systems) by constructing an optimizing sequence of functions, and his results also show the optimal H_2/H_∞ controller has infinite order. Although Megretsky provides a method for constructing an optimizing sequence for the H_2/H_∞ problem, his method is such that it can only be applied (realistically) to small, academic problems. Even for the cases where it can be applied, the resulting solutions will be of such high order that they are only useful as a limit of performance. For this reason, a more practical solution will be sought.

5.2 The Full-Order H_2/H_∞ Control Problem

The previous section has shown that the optimal H_2/H_∞ controller can, in general, be a non-rational function. Although finite order rational approximations to the optimal controller exist, even these may be of such a high order that they cannot be practically implemented in most cases. One approach to the problem involves finding the high-order approximations using a free-order approach, and then performing model order reduction on the controller to obtain an implementable controller. Although this allows a convex

programming approach to the initial optimization problem, there are no guarantees that the reduced order controller will be optimal over other compensators of the same order. Further, the order-reduced controller may no longer be feasible in terms of satisfying the constraints, and it may not even be stabilizing. An alternative approach is to fix the order of the controller at some desired level prior to solving the optimization problem. Although this results in a non-convex problem, there is no further need for model reduction once the compensator has been found.

This section will begin to explore the fixed-order problem by looking at the full-order H_2/H_∞ control problem. By full-order, we are referring to the case whereby the order of the controller is fixed at the order of the H_2 subproblem. Although this problem has yet to be solved analytically, the analytical formulation can be pursued further than most fixed-order problems, and significant insights as to the nature of the solution can be gained without actually solving the problem. This same problem was considered by Ridgely [8] and Walker [9] for continuous-time systems, but only special case problems have been previously considered in discrete-time (see Section 1.2).

5.2.1 State Space Formulation. We will again consider the system shown in Figure 5.1, with the same assumptions regarding the inputs, outputs and states of the system. The transfer function P is formed by augmenting stable weighting transfer functions from an H_2 problem (w to z) and an H_∞ problem (d to e) around the original system $G(z)$, resulting in the state space form

$$P = \left[\begin{array}{c|ccc} \tilde{A} & \tilde{B}_d & \tilde{B}_w & \tilde{B}_u \\ \hline \tilde{C}_e & \tilde{D}_{ed} & \tilde{D}_{ew} & \tilde{D}_{eu} \\ \tilde{C}_z & \tilde{D}_{zd} & \tilde{D}_{zw} & \tilde{D}_{zu} \\ \tilde{C}_y & \tilde{D}_{yd} & \tilde{D}_{yw} & \tilde{D}_{yu} \end{array}\right] \tag{5.40}$$

where $\tilde{(\cdot)}$ are the matrices associated with the system augmented by the H_2 and H_∞ weights. The order of the individual H_2 and H_∞ problems will usually be less than that

of P. An expanded state space realization for the system can be written as

$$\begin{aligned} x_2(k+1) &= A_2 x_2(k) + B_w w(k) + B_{u_2} u(k) \\ z(k) &= C_z x_2(k) + D_{zw} w(k) + D_{zu} u(k) \\ y(k) &= C_{y_2} x_2(k) + D_{yw} w(k) + D_{yu} u(k) \end{aligned} \tag{5.41}$$

$$\begin{aligned} x_\infty(k+1) &= A_\infty x_\infty(k) + B_d d(k) + B_{u_\infty} u(k) \\ e(k) &= C_e x_\infty(k) + D_{ed} d(k) + D_{eu} u(k) \\ y(k) &= C_{y_\infty} x_\infty(k) + D_{yd} d(k) + D_{yu} u(k) \end{aligned} \tag{5.42}$$

where x_2 is the state vector for the underlying H_2 problem, x_∞ is the state vector for the underlying H_∞ problem and n_2 is the dimension of x_2.

The H_2/H_∞ control problem is now that of finding $K(z)$ which satisfies

$$\inf_{K admissible} \|T_{zw}\|_2 \ subject\ to\ \|T_{ed}\|_\infty \leq \gamma$$

where T_{zw} and T_{ed} are the closed-loop transfer functions for the H_2 and H_∞ subproblems, respectively. If we assume a finite, fixed order for the compensator, we can use a state space form of K; namely

$$\begin{aligned} x_c(k+1) &= A_c x_c(k) + B_c y(k) \\ u(k) &= C_c x_c(k) + D_c y(k) \end{aligned} \tag{5.43}$$

This imposes an additional restriction on the problem, because the admissible set of compensators is now restricted to those stabilizing compensators with state dimension equal to that of x_c, defined as n_c. It must be noted that $\underline{\gamma}$ as defined previously may not be achievable by compensators of this order. For this reason, we now redefine $\underline{\gamma}$ as

$$\underline{\gamma} = \inf_{K admissible} \|T_{ed}\|_\infty \tag{5.44}$$

where the admissible set consists of those stabilizing compensators with the specified order. If we assume the H_∞ constraint is non-singular, the infimization problem above becomes a minimization problem due to the finite dimension of the problem.

We will make the following assumptions regarding the H_2 and H_∞ subproblems:

i. (A_2, B_{u_2}) stabilizable, (C_{y_2}, A_2) detectable

ii. $D_{zu}^T D_{zu}$ full rank, $D_{yw} D_{yw}^T$ full rank

iii. $\begin{bmatrix} A_2 - j\omega I & B_{u_2} \\ C_z & D_{zu} \end{bmatrix}$ has full column rank for all ω

iv. $\begin{bmatrix} A_2 - j\omega I & B_w \\ C_{y_2} & D_{yw} \end{bmatrix}$ has full row rank for all ω

v. $D_{yu} = 0$

Assumptions (i)–(iv) assure a non-singular solution to the H_2 subproblem. Assumption (v) is not necessary, but it satisfies the requirement for well-posedness of the problem. As stated earlier, this is usually an easy condition to meet in practice, since any dynamic lag associated with either the sensors or actuators will ensure it is satisfied. The next chapter will specifically address easing assumption (v) for the fixed-order, mixed-norm problem. As in Walker's continuous-time problem, no assumptions are being made regarding regularity of the H_∞ subproblem. Unlike the continuous-time problem, however, it is not necessary to assume $(D_{zw} + D_{zu} D_c D_{yw}) = 0$, since $\|T_{zw}\|_2$ remains finite for non-strictly causal systems. For this reason, we can allow $D_{zw} \neq 0$ and still treat D_c as an independent design variable (see section 3.3 and the reference therein).

Using (5.43), the closed-loop state space equations can be written as

$$\begin{aligned} \mathsf{x}_2(k+1) &= \mathcal{A}_2 \mathsf{x}_2(k) + \mathcal{B}_w w(k) \\ z(k) &= \mathcal{C}_z \mathsf{x}_2(k) + \mathcal{D}_{zw} w(k) \end{aligned} \tag{5.45}$$

$$\begin{aligned} \mathsf{x}_\infty(k+1) &= \mathcal{A}_\infty \mathsf{x}_\infty(k) + \mathcal{B}_d d(k) \\ e(k) &= \mathcal{C}_e \mathsf{x}_\infty(k) + \mathcal{D}_{ed} d(k) \end{aligned} \tag{5.46}$$

where

$$\begin{aligned} \mathsf{x}_2 &= \begin{bmatrix} x_2 \\ x_c \end{bmatrix} \\ \mathsf{x}_\infty &= \begin{bmatrix} x_\infty \\ x_c \end{bmatrix} \end{aligned} \tag{5.47}$$

$$\begin{aligned} \mathcal{A}_2 &= \begin{bmatrix} (A_2 + B_{u_2} D_c C_{y_2}) & B_{u_2} C_c \\ B_c C_{y_2} & A_c \end{bmatrix} \\ \mathcal{A}_\infty &= \begin{bmatrix} (A_\infty + B_{u_\infty} D_c C_{y_\infty}) & B_{u_\infty} C_c \\ B_c C_{y_\infty} & A_c \end{bmatrix} \end{aligned} \tag{5.48}$$

$$\begin{aligned} \mathcal{B}_w &= \begin{bmatrix} (B_w + B_{u_2} D_c D_{yw}) \\ B_c D_{yw} \end{bmatrix} \\ \mathcal{B}_d &= \begin{bmatrix} (B_d + B_{u_\infty} D_c D_{yd}) \\ B_c D_{yd} \end{bmatrix} \end{aligned} \tag{5.49}$$

$$\begin{aligned} \mathcal{C}_z &= \begin{bmatrix} (C_z + D_{zu} D_c C_{y_2}) & D_{zu} C_c \end{bmatrix} \\ \mathcal{C}_e &= \begin{bmatrix} (C_e + D_{eu} D_c C_{y_\infty}) & D_{eu} C_c \end{bmatrix} \end{aligned} \tag{5.50}$$

$$\begin{aligned} \mathcal{D}_{zw} &= \begin{bmatrix} D_{zu} D_c D_{yw} + D_{zw} \end{bmatrix} \\ \mathcal{D}_{ed} &= \begin{bmatrix} D_{eu} D_c D_{yd} + D_{ed} \end{bmatrix} \end{aligned} \tag{5.51}$$

5.2.2 The Lagrangian and Necessary Conditions. The full-order mixed H_2/H_∞ problem is now to determine a $K(z)$ such that:

i. $\mathcal{A}_2$ and $\mathcal{A}_\infty$ are stable

ii. $\|T_{ed}\|_\infty \leq \gamma$ for some given $\gamma > \underline{\gamma}$, ($\gamma \geq \underline{\gamma}$ if the constraint is nonsingular)

iii. $\|T_{zw}\|_2$ is minimized.

The following theorem will help focus the development of the full-order H_2/H_∞ problem.

Theorem 5.2.1 *Let $K = (A_c, B_c, C_c, D_c)$ be given such that $\mathcal{A}_2$ is stable, and assume $(\mathcal{C}_e, \mathcal{A}_\infty)$ has no unobservable modes on the unit circle. Further, assume there exists a*

strong solution $Q_\infty = Q_\infty^T \geq 0$ *to the DARE*

$$\begin{aligned} Q_\infty &= \mathcal{A}_\infty^T Q_\infty \mathcal{A}_\infty + \mathcal{C}_e^T \mathcal{C}_e \\ &\quad - \left(\mathcal{D}_{ed}^T \mathcal{C}_e + \mathcal{B}_d^T Q_\infty \mathcal{A}_\infty\right)^T \left(\gamma^2 I - \mathcal{D}_{ed}^T \mathcal{D}_{ed} - \mathcal{B}_d^T Q_\infty \mathcal{B}_d\right)^{-1} \left(\mathcal{D}_{ed}^T \mathcal{C}_e + \mathcal{B}_d^T Q_\infty \mathcal{A}_\infty\right) \end{aligned} \tag{5.52}$$

such that

$$\left(\gamma^2 I - \mathcal{D}_{ed}^T \mathcal{D}_{ed} - \mathcal{B}_d^T Q_\infty \mathcal{B}_d\right)^{-1} > 0 \tag{5.53}$$

Then the following are true:

i. $\mathcal{A}_\infty$ *is stable and* $\|T_{ed}\|_\infty \leq \gamma$.

ii. $\|T_{zw}\|_2^{\,2} = tr\left[\mathcal{D}_{zw}^T \mathcal{D}_{zw} + \mathcal{C}_z Q_2 \mathcal{C}_z^T\right]$ *where* $Q_2 = Q_2^T \geq 0$ *is the solution to the Lyapunov equation*

$$\mathcal{A}_2 Q_2 \mathcal{A}_2^T + \mathcal{B}_w \mathcal{B}_w^T = Q_2 \tag{5.54}$$

iii. There exists a unique minimal solution to (5.52) in the class of real symmetric solutions.

iv. Q_∞ *is the minimal solution to (5.52) if and only if*

$$\left|\lambda_i\left(\mathcal{A}_\infty + \mathcal{B}_d\left(\gamma^2 I - \mathcal{D}_{ed}^T \mathcal{D}_{ed} - \mathcal{B}_d^T Q_\infty \mathcal{B}_d\right)^{-1}\left(\mathcal{D}_{ed}^T \mathcal{C}_e + \mathcal{B}_d^T Q_\infty \mathcal{A}_\infty\right)\right)\right| \leq 1\,, \quad \forall\, i \tag{5.55}$$

v. $\|T_{ed}\|_\infty < \gamma$ *if and only if*

$$\left|\lambda_i\left(\mathcal{A}_\infty + \mathcal{B}_d\left(\gamma^2 I - \mathcal{D}_{ed}^T \mathcal{D}_{ed} - \mathcal{B}_d^T Q_\infty \mathcal{B}_d\right)^{-1}\left(\mathcal{D}_{ed}^T \mathcal{C}_e + \mathcal{B}_d^T Q_\infty \mathcal{A}_\infty\right)\right)\right| < 1\,, \quad \forall\, i \tag{5.56}$$

Proof: Part (i) follows directly from Theorem 2.6.1, and, since $\mathcal{A}_2$ is stable, part (ii) follows from the discussion on calculating the 2-norm. Parts (iii) and (iv) follow from Theorem 2.5.1, and part (v) is a restatement of Theorem 2.6.2. ■

As in the continuous-time case [9], the key result of the preceding theorem is that, given a stabilizing controller for the H_2 subproblem, we can determine the minimum level of the H_∞ constraint by determining the minimum value of γ for which a positive semi-definite solution to (5.52) exists.

Using Theorem 5.2.1, we can now restate the full-order mixed H_2/H_∞ control problem: Determine $K = (A_c, B_c, C_c, D_c)$ which minimizes

$$J(A_c, B_c, C_c, D_c) = tr\left[\mathcal{D}_{zw}^T \mathcal{D}_{zw} + C_z Q_2 C_z^T\right] \tag{5.57}$$

where $Q_2 = Q_2^T \geq 0$ is the solution to the Lyapunov equation

$$\mathcal{A}_2 Q_2 \mathcal{A}_2^T + \mathcal{B}_w \mathcal{B}_w^T - Q_2 = 0 \tag{5.58}$$

such that there exists a real, positive semi-definite solution to the DARE

$$\begin{aligned} &\mathcal{A}_\infty^T Q_\infty \mathcal{A}_\infty \; - \; Q_\infty \; + \; C_e^T C_e \qquad (5.59) \\ &- \left(\mathcal{D}_{ed}^T C_e + \mathcal{B}_d^T Q_\infty \mathcal{A}_\infty\right)^T \left(\gamma^2 I - \mathcal{D}_{ed}^T \mathcal{D}_{ed} - \mathcal{B}_d^T Q_\infty \mathcal{B}_d\right)^{-1} \left(\mathcal{D}_{ed}^T C_e + \mathcal{B}_d^T Q_\infty \mathcal{A}_\infty\right) = 0 \end{aligned}$$

such that

$$\left(\gamma^2 I - \mathcal{D}_{ed}^T \mathcal{D}_{ed} - \mathcal{B}_d^T Q_\infty \mathcal{B}_d\right)^{-1} > 0 \tag{5.60}$$

This is similar to the continuous-time problem formulated by Ridgely [8], with one significant exception. The final term in (5.60), which must be positive definite, explicitly depends on the solution to (5.59). This prevents us from casting this directly as a Lagrange multiplier problem, as was done by both Ridgely and Walker. The continuous-time problem has an analogous term which must be positive-definite, but it depends only on γ and the fixed plant matrices; the Riccati solution does not appear explicitly in the positive definite constraint for the continuous-time case. Despite these differences, we can show that the same basic necessary conditions hold for both continuous and discrete-time, with one additional constraint for the discrete-time case.

To proceed, we will fix a small $\epsilon > 0$ and positive definite matrix $P \in \mathbf{R}^{n_d \times n_d}$ where n_d is the dimension of input vector for P_{ed}. We will also need to introduce a slack variable β. We can now write the constraint as

$$\gamma^2 I - \epsilon I - \beta^2 P - \mathcal{D}_{ed}^T \mathcal{D}_{ed} - \mathcal{B}_d^T Q_\infty \mathcal{B}_d = 0 \tag{5.61}$$

We can state the Lagrange multiplier problem as follows: Assuming Q_2, Q_∞ are symmetric and positive semi-definite, find a stationary point of the Lagrangian

$$\begin{aligned}
\mathcal{L} &= \mathcal{L}(A_c, B_c, C_c, D_c, Q_2, Q_\infty, \beta, X, Y, Z) \\
&= tr\left[\mathcal{D}_{zw}^T \mathcal{D}_{zw} + \mathcal{C}_z Q_2 \mathcal{C}_z^T\right] + tr\left[\left(\mathcal{A}_2 Q_2 \mathcal{A}_2^T + \mathcal{B}_w \mathcal{B}_w^T - Q_2\right) X\right] \\
&\quad + tr\left[\left(\mathcal{A}_\infty^T Q_\infty \mathcal{A}_\infty - Q_\infty + \mathcal{C}_e^T \mathcal{C}_e\right.\right. \\
&\quad \left.\left. - \left(\mathcal{D}_{ed}^T \mathcal{C}_e + \mathcal{B}_d^T Q_\infty \mathcal{A}_\infty\right)^T \left(\gamma^2 I - \mathcal{D}_{ed}^T \mathcal{D}_{ed} - \mathcal{B}_d^T Q_\infty \mathcal{B}_d\right)^{-1} \left(\mathcal{D}_{ed}^T \mathcal{C}_e + \mathcal{B}_d^T Q_\infty \mathcal{A}_\infty\right)\right) Y\right] \\
&\quad + tr\left[\left(\gamma^2 I - \epsilon I - \beta^2 P - \mathcal{D}_{ed}^T \mathcal{D}_{ed} - \mathcal{B}_d^T Q_\infty \mathcal{B}_d\right) Z\right]
\end{aligned} \tag{5.62}$$

where X, Y and Z are matrix Lagrange multipliers. X, Y, Q_2 and Q_∞ can be partitioned as follows:

$$X = \begin{bmatrix} X_{11} & X_{12} \\ X_{21} & X_{22} \end{bmatrix} \tag{5.63}$$

$$Y = \begin{bmatrix} Y_{11} & Y_{12} \\ Y_{21} & Y_{22} \end{bmatrix} \tag{5.64}$$

$$Q_2 = \begin{bmatrix} Q_{2_{11}} & Q_{2_{12}} \\ Q_{2_{12}}^T & Q_{2_{22}} \end{bmatrix} \tag{5.65}$$

$$Q_\infty = \begin{bmatrix} Q_{\infty_{11}} & Q_{\infty_{12}} \\ Q_{\infty_{12}}^T & Q_{\infty_{22}} \end{bmatrix} \tag{5.66}$$

A partial list of the first order necessary conditions can now be stated as

$$\frac{\partial \mathcal{L}}{\partial X} = \mathcal{A}_2 Q_2 \mathcal{A}_2^T + \mathcal{B}_w \mathcal{B}_w^T - Q_2 = 0 \tag{5.67}$$

$$\frac{\partial \mathcal{L}}{\partial Y} = \mathcal{A}_\infty^T Q_\infty \mathcal{A}_\infty - Q_\infty + \mathcal{C}_e^T \mathcal{C}_e \tag{5.68}$$

$$- \left(\mathcal{D}_{ed}^T \mathcal{C}_e + \mathcal{B}_d^T Q_\infty \mathcal{A}_\infty\right)^T \left(\gamma^2 I - \mathcal{D}_{ed}^T \mathcal{D}_{ed} - \mathcal{B}_d^T Q_\infty \mathcal{B}_d\right)^{-1} \left(\mathcal{D}_{ed}^T \mathcal{C}_e + \mathcal{B}_d^T Q_\infty \mathcal{A}_\infty\right) = 0$$

$$\frac{\partial \mathcal{L}}{\partial Z} = \gamma^2 I - \epsilon I - \beta^2 P - \mathcal{D}_{ed}^T \mathcal{D}_{ed} - \mathcal{B}_d^T Q_\infty \mathcal{B}_d = 0 \tag{5.69}$$

$$\frac{\partial \mathcal{L}}{\partial \beta} = -2\beta P Z = 0 \tag{5.70}$$

$$\frac{\partial \mathcal{L}}{\partial Q_2} = \mathcal{A}_2^T X \mathcal{A}_2 + \mathcal{C}_z^T \mathcal{C}_z - X = 0 \tag{5.71}$$

$$\frac{\partial \mathcal{L}}{\partial Q_\infty} = \hat{\mathcal{A}} Y \hat{\mathcal{A}}^T - \mathcal{B}_d Z \mathcal{B}_d^T - Y = 0 \tag{5.72}$$

where

$$\hat{\mathcal{A}} = \mathcal{A}_\infty + \mathcal{B}_d \left(\gamma^2 I - \mathcal{D}_{ed}^T \mathcal{D}_{ed} - \mathcal{B}_d^T Q_\infty \mathcal{B}_d\right)^{-1} \left(\mathcal{D}_{ed}^T \mathcal{C}_e + \mathcal{B}_d^T Q_\infty \mathcal{A}_\infty\right) \tag{5.73}$$

is the matrix which is stabilized by the solution to the Riccati equation (5.59). Conditions (5.67–5.69) are simply the original constraints which must be satisfied. Condition (5.70) can be written in the form

$$\beta Z = 0 \tag{5.74}$$

since β is a scalar and P is positive definite. In this form, condition (5.70) can now be seen as a statement that either β or Z must be zero. If $\beta = 0$, constraint (5.61) is active which is inadmissible for the real problem ($\epsilon = 0$) we are trying to solve. If this occurs, we need to reduce ϵ and try again. If the constraint remains active ($\beta = 0$) in the limit as $\epsilon \to 0$, then there is no solution to the mixed problem. If, however, for some small $\epsilon > 0$, the solution yields $\beta \neq 0$ and $Z = 0$, then constraint (5.61) is not active. Although this constraint will need to be enforced for a numerical solution to the problem, for the remainder of this discussion we will assume that the strong or stabilizing solution to (5.59) satisfies (5.60).

Condition (5.71) is a Lyapunov equation. Since $\mathcal{A}_2$ must be stable, the solution to (5.71) will be positive semi-definite and symmetric, i.e., $X_{12} = X_{21}^T$, $X_{11} = X_{11}^T$ and $X_{22} = X_{22}^T$. Condition (5.72) is also a Lyapunov equation and, for $Z = 0$ and $\hat{\mathcal{A}}$ strictly

stable, the only solution to (5.72) is $Y = 0$. This is the case when Q_∞ is a stabilizing solution to (5.59), and it indicates that the H_∞ constraint is not active. For this case, the Lagrange multiplier problem can be written as

$$\begin{aligned} \mathcal{L} &= \mathcal{L}(A_c, B_c, C_c, D_c, Q_2, X) \\ &= tr\left[\mathcal{D}_{zw}^T \mathcal{D}_{zw} + \mathcal{C}_z Q_2 \mathcal{C}_z^T\right] + tr\left[\left(\mathcal{A}_2 Q_2 \mathcal{A}_2^T + \mathcal{B}_w \mathcal{B}_w^T - Q_2\right) X\right] \end{aligned} \tag{5.75}$$

which is simply the unconstrained H_2 problem for which there is a unique solution. However, if Q_∞ is a strong solution to (5.59), but not a stabilizing solution, then $\hat{\mathcal{A}}$ will be neutrally stable and there will be a symmetric solution $Y \neq 0$ to (5.72). This indicates the H_∞ constraint is precisely active and $\|T_{ed}\|_\infty = \gamma$. The remainder of the first-order necessary conditions can be derived by taking the partial derivatives of (5.62) with respect to the compensator state-space matrices A_c, B_c, C_c and D_c. These remaining equations provide no further insight into the full-order solution, and since the full set of necessary conditions can not be solved analytically, these remaining equations will not be derived for the full-order H_2/H_∞ problem.

5.2.3 Existence and Uniqueness vs. Compensator Order. Ridgely [8] and Walker [9] have accomplished a considerable amount of work examining existence and uniqueness vs. compensator order for the continuous-time case, and all of their findings will apply in a similar fashion for the discrete-time case. If the order of the solution is fixed to the order of the underlying H_2 problem or greater ($n_c \geq n_2$), the optimal solution to the H_2 subproblem is unique, and the H_∞ subproblem will have $\|T_{ed}\|_\infty = \bar{\gamma}$ for this compensator. With this in mind, if $\gamma \geq \bar{\gamma}$ the optimal controller will exist, and it is in fact the unique $K_{2_{opt}}$. This is the special case discussed at the end of the previous section whereby the Lagrange multiplier Y associated with the H_∞ problem is identically zero. Because this is nothing but the H_2 optimization problem, we can strengthen this to say that no controller of any order exists which can reduce $\|T_{zw}\|_2$ any further. Similarly, if $\gamma < \underline{\gamma}$, there is no compensator of any order which can meet this constraint, implying there is no solution to the mixed H_2/H_∞ problem. This leaves only the region where $\underline{\gamma} \leq \gamma < \bar{\gamma}$.

Consider the case where $\underline{\gamma} < \gamma < \bar{\gamma}$. The necessary condition (5.72), with $Z = 0$, implies that either $\hat{\mathcal{A}}$ is neutrally stable (an active constraint) or $Y = 0$ (an inactive constraint), with the latter condition resulting in the Lagrangian associated with the H_2 optimization problem. We can eliminate this second possibility with the following theorem.

Theorem 5.2.2 *Assume $n_c \geq n_2$ and $\underline{\gamma} < \gamma < \bar{\gamma}$. Then the solution to the mixed H_2/H_∞ problem lies on the boundary of the H_∞ constraint.*

Proof: Assume the solution is off the boundary. This implies $Y = 0$ and the Lagrangian reduces to

$$\begin{aligned} \mathcal{L} &= \mathcal{L}(A_c, B_c, C_c, D_c, Q_2, X) \\ &= tr\left[\mathcal{D}_{zw}^T \mathcal{D}_{zw} + \mathcal{C}_z Q_2 \mathcal{C}_z^T\right] + tr\left[\left(\mathcal{A}_2 Q_2 \mathcal{A}_2^T + \mathcal{B}_w \mathcal{B}_w^T - Q_2\right) X\right] \end{aligned} \tag{5.76}$$

The solution to this optimization problem is the unique $K_{2_{opt}}$, but for the closed-loop system with this controller, $\|T_{ed}\|_\infty = \bar{\gamma} > \gamma$, which is a violation of the constraint. Thus the optimal solution must lie on the boundary of the H_∞ constraint. ∎

For the case where $n_c \geq n_2$ and $\underline{\gamma} < \gamma < \bar{\gamma}$, the solution to (5.59) must be the neutrally stabilizing solution. This is stated formally in the following theorem.

Theorem 5.2.3 *Assume $\mathcal{A}_\infty$ is stable. If there exists $Q_\infty = Q_\infty^T \geq 0$ satisfying (5.59) and (5.60), then the following are equivalent:*

i. $\|T_{ed}\|_\infty = \gamma$

ii. $\hat{\mathcal{A}}$ *is neutrally stable*

Furthermore, in this case Q_∞ is unique.

Proof: This is the discrete equivalent of Theorem 4.2.4 of [8]. ∎

It is now a trivial extension of these results to state that α^* is a monotonically decreasing function of γ, and the proof of this statement will be omitted. For the case where $\gamma = \underline{\gamma}$ and the H_∞ constraint is singular, the solution is not guaranteed to exist since the infimum

$\underline{\gamma}$ may not be achievable. For $\gamma = \underline{\gamma}$ and a nonsingular constraint, we have a minimization problem where the solution exists and the constraint necessarily will be active.

5.3 Summary

In this chapter the mixed H_2/H_∞ optimal control problem was set up and parametrized over a convex set $Q \in H_\infty$. Using this parametrization, we were able to show that the optimal controller for a given γ is unique. The optimal solution was shown to be $K_{2_{opt}}$ if $\gamma \geq \overline{\gamma}$. Furthermore, the optimal solution must satisfy the H_∞ constraint with equality if $\underline{\gamma} < \gamma \leq \overline{\gamma}$. For the SISO mixed problem, the special case $T_{1_\infty} = 0$ and $T_{2_\infty} T_{3_\infty} = I$ was investigated using a minimum-norm duality approach. It was shown that the optimal controller in this case is piecewise continuous and cannot be represented by a rational function. Finally, we investigated the full-order H_2/H_∞ control problem. As in the free-order case, the solution was shown to be $K_{2_{opt}}$ if $\gamma \geq \overline{\gamma}$, and the solution must satisfy the H_∞ constraint with equality if $\underline{\gamma} < \gamma \leq \overline{\gamma}$. Further, we were able to show that the solution to the full-order problem results in a neutrally stabilizing solution to an associated Riccati equation. Although these results have been shown previously for continuous-time systems [8, 9], this chapter showed they apply equally well for discrete-time. Although the optimal (free-order) mixed-norm problem is easily cast as a convex programming problem, it often results in compensators which cannot be implemented. The next chapter will consider a suboptimal fixed-order approach to the general mixed-norm problem. Although the resulting optimization problem will be non-convex, the solutions have a controller order chosen by the designer, thus eliminating the need for order reduction.

VI. The General Fixed-Order, Mixed-Norm Control Problem

6.1 Introduction

Chapters IV and V investigated analytical and/or numerical solutions to various optimal mixed-norm control problems. The results presented so far provide considerable insight as to the nature of the solution to these problems, and, in the case of the free-order numerical solutions, they allow us to find the limits of performance for mixed-norm controllers. The drawback with all the results discussed so far is that, even when a compensator can be found, it is usually of such high order that it cannot be implemented without substantial order reduction. Further, the order reduced compensator is no longer optimal, it may no longer meet the constraints, and there may in fact be compensators of the same order which outperform the order reduced "optimal" compensator in terms of 2-norm performance. An alternative approach is to design directly for a given fixed order, and to iterate for increasing orders. Chapter V discussed the analytical formulation for a full-order H_2/H_∞ problem, but it could not be solved analytically, it does not allow for ℓ_1 constraints, and it does not allow for compensator orders less than that of the H_2 subproblem. Clearly, a more general formulation which overcomes these restrictions would be highly desirable.

Several investigators have looked at direct fixed-order design for mixed-norm control problems. Of these, there are only two known methods which address the general output-feedback problem, allow multiple constraints, and allow the order of the compensator to be specified by the designer. Walker and Ridgely [50] developed algorithms for the continuous-time H_2/H_∞ control problem. Their method used the elements of the compensator state-space as design variables, thus allowing for increased or decreased compensator orders simply by varying the number of design variables. Their method was completely general in that the H_∞ constraints could be singular, and there were no inherent restrictions as to how many constraints could be added to the problem. Walker [9] posed the problem with the addition of an L_1 (continuous-time analog for ℓ_1) constraint, and this problem was then solved numerically (with modifications) by Spillman [51]. Ly and Schomig [16] also developed a general method for the continuous-time H_2/H_∞ problem,

and their method also uses the compensator state-space as design variables. However, Ly and Schomig's method uses symmetric matrix inequalities to represent the H_∞ constraints, and this requires that the solutions to these inequalities be carried as additional design variables. Although it is possible that Ly and Schomig's method is better conditioned than Walker and Ridgely's (neither method results in a convex problem for the general output feedback case), it is likely any perceived benefits will be countered by the increased size and complexity of the problem.

As stated in the introduction to this dissertation, the mixed-norm control problem can be viewed in terms of finding a desired point (or compensator) on a Pareto-optimal surface (or hypersurface), whereby the respective norms of the individual transfer functions define the axes of the space. Viewed in this context, any one of the norms could be used as an objective, with all others applied as constraints. By varying the constraints, the operating location on the surface is changed. For reasons stated in the introduction, this dissertation uses the H_2 norm as the objective function, with the ℓ_1 and H_∞ norms of dissimilar transfer functions being applied as constraints to the problem. This results in a mathematical programming problem for which there is a wide variety of methods available for solving it numerically.

This chapter develops a numerical method for solving the general fixed-order, mixed-norm control problem for discrete-time, linear systems. The method allows the control system designer to combine the H_2 , H_∞ , and ℓ_1 norms of dissimilar transfer functions into a single $H_2/\ell_1/H_\infty$ control problem. It extends the Walker/Ridgely method for H_2/H_∞ optimization in that it applies to discrete-time systems, and it accommodates ℓ_1 norm constraints. As in the work by Walker, the method allows any number of transfer function norms to be minimized or constrained directly, as opposed to limiting conservative upper bounds or approximations to the norms. Further, the constraint transfer functions can be singular, thus allowing the designer to isolate constraints such as sensitivity or control usage. In order to classify the nature of the solution, the theory assumes a unique optimal H_2 solution to the unconstrained problem. This serves to anchor the Pareto-optimal surface, and it also provides a starting point for numerically solving the problem. Although the method will be demonstrated with the compensator order equal to that of the underlying

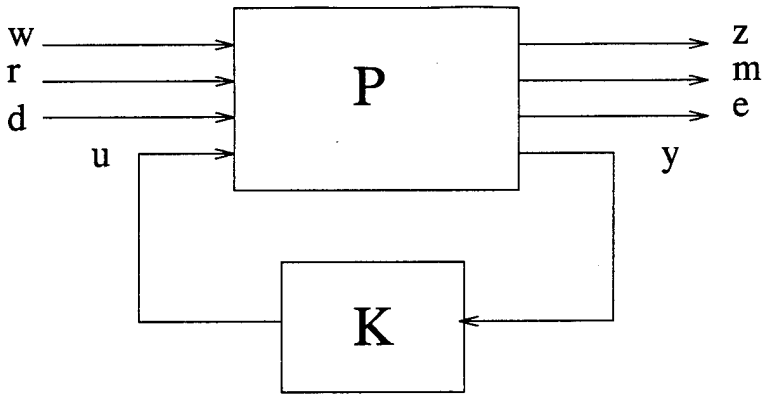

Figure 6.1 General Mixed-Norm Optimization Problem

H_2 problem, the method can be applied without modification to develop either higher or lower order compensators for the same problem. The method carries no claim of uniqueness or global optimality over all compensators; however, it has proven to be effective in balancing performance and robustness design constraints for a wide variety of problems tested to date.

6.2 Problem Setup

The system considered for the general mixed-norm control problem is shown in Figure 6.1. It contains three sets of exogenous inputs and controlled outputs. In general, no relationship is assumed between r, d and w, or m, e and z. The input d is assumed to be a signal of unknown but bounded energy with $\|d\|_2 \leq 1$, and the input r is assumed to be a signal of unknown but bounded magnitude with $\|r\|_\infty \leq 1$. The input w is assumed to be the discrete-time equivalent of zero-mean white Gaussian noise of unit intensity. The state space of P is formed by wrapping the stable weights of an H_2 problem from w to z, the stable weights of an ℓ_1 problem from r to m and the stable weights of an H_∞ problem from d to e around the original plant. The problem setup and weighting strategies will be discussed further in the examples found later in this chapter and in Chapter VII. Once again, the order of the individual problems will in general be less than the order of P. An

expanded state space realization of P can be written as

$$\begin{aligned} x_2(k+1) &= A_2x_2(k) + B_ww(k) + B_{u_2}u(k) \\ z(k) &= C_zx_2(k) + D_{zw}w(k) + D_{zu}u(k) \\ y(k) &= C_{y_2}x_2(k) + D_{yw}w(k) + D_{yu}u(k) \end{aligned} \tag{6.1}$$

$$\begin{aligned} x_1(k+1) &= A_1x_1(k) + B_rr(k) + B_{u_1}u(k) \\ m(k) &= C_mx_1(k) + D_{mr}r(k) + D_{mu}u(k) \\ y(k) &= C_{y_1}x_1(k) + D_{yr}r(k) + D_{yu}u(k) \end{aligned} \tag{6.2}$$

$$\begin{aligned} x_\infty(k+1) &= A_\infty x_\infty(k) + B_dd(k) + B_{u_\infty}u(k) \\ e(k) &= C_ex_\infty(k) + D_{ed}d(k) + D_{eu}u(k) \\ y(k) &= C_{y_\infty}x_\infty(k) + D_{yd}d(k) + D_{yu}u(k) \end{aligned} \tag{6.3}$$

where x_2, x_1 and x_∞ may have some or all states in common.

The objective of mixed $H_2/\ell_1/H_\infty$ control is to minimize the 2-norm of the closed-loop transfer function T_{zw}, while constraining the 1-norm of the transfer function T_{mr} and the ∞-norm of the transfer function T_{ed} to be less than some specified levels. A practical application might be to use the ∞-norm constraint to guarantee a certain level of stability robustness, while acceptable tracking error could be assured by enforcing a 1-norm constraint on the sensitivity, and the 2-norm could be used to optimize noise rejection while still meeting the other constraints. Mathematically, the problem can be stated as follows: For the system shown in Figure 6.1, find an admissible controller $K(z)$ that achieves

$$\inf_{K\,admissible} \|T_{zw}\|_2 \tag{6.4}$$

subject to

$$\|T_{mr}\|_1 \leq \nu$$

$$\|T_{ed}\|_\infty \leq \gamma$$

The following discussion will assume a fixed controller order equal to or greater than the minimal order of the H_2 subproblem; however, extensions of the method for reduced order design will be presented. The following assumptions will be made:

i. (A_2, B_{u_2}) stabilizable, (C_{y_2}, A_2) detectable

ii. (A_1, B_{u_1}) stabilizable, (C_{y_1}, A_1) detectable

iii. (A_∞, B_{u_∞}) stabilizable, (C_{y_∞}, A_∞) detectable

iv. $D_{zu}^T D_{zu}$ full rank, $D_{yw} D_{yw}^T$ full rank

v. $\begin{bmatrix} A_2 - e^{j\theta} I & B_{u_2} \\ C_z & D_{zu} \end{bmatrix}$ full column rank $\forall\ \theta \in [0, 2\pi)$

vi. $\begin{bmatrix} A_2 - e^{j\theta} I & B_w \\ C_{y_2} & D_{yw} \end{bmatrix}$ full row rank $\forall\ \theta \in [0, 2\pi)$

vii. $D_{yu} = 0$

Conditions (i)-(iii) ensure the existence of stabilizing controllers, and if only stable weighting functions are used, the existence of a K which stabilizes the H_2 problem was shown to be necessary and sufficient for K stabilizing the H_∞ and ℓ_1 problems [9]. Conditions (iv)-(vi) ensure that the H_2 problem considered separately has a non-singular solution. A non-singular H_2 subproblem will not be necessary for the numerical solution, but it provides a convenient starting location and an easily defined anchor point for the Pareto-optimal surface. Numerically it will only be necessary that the overall mixed-norm problem be non-singular, so as to avoid solutions which require infinite control power or result in open-loop response characteristics. Condition (vii) is also not necessary, but a strictly causal P_{yu} or K is sufficient for well-posedness of the problem. As stated in previous chapters, a strictly causal P_{yu} is often a mild assumption when actuator dynamics are considered. Further, it frees us from making a similar assumption on the compensator, and it eases the notation required for this development. The relaxation of this final assumption will be discussed at the end of this section.

Under certain conditions, the numerical method presented in this chapter will be applicable to reduced-order control synthesis problems. Specifically, we need to add the as-

sumption that there exist reduced order stabilizing controllers which satisfy the constraints. The difficulty that this presents is that we must be able to find an initial stabilizing controller with the desired order. It should also be noted that the regularity assumptions on the H_2 subproblem are no longer appropriate for reduced order controllers. This second concern is not a problem for the numerical solution because, as stated above, it is only necessary that the overall mixed-norm problem be nonsingular.

The desired compensator (K) can be written in the form

$$\begin{aligned} x_c(k+1) &= A_c x_c(k) + B_c y(k) \\ u(k) &= C_c x_c(k) + D_c y(k) \end{aligned} \tag{6.5}$$

where A_c, B_c, C_c and D_c are to be determined from the optimization problem. Note that for the continuous-time problem, D_c cannot be used as a design variable. This is because it is uniquely determined by

$$D_{zw} + D_{zu} D_c D_{yw} = 0 \tag{6.6}$$

which is necessary in order for $\|T_{zw}\|_2$ to be finite [42]. This is not the case for discrete-time.

Using (6.5), the closed-loop state space equations can be written as

$$\begin{aligned} \mathrm{x}_2(k+1) &= \mathcal{A}_2 \mathrm{x}_2(k) + \mathcal{B}_w w(k) \\ z(k) &= \mathcal{C}_z \mathrm{x}_2(k) + \mathcal{D}_{zw} w(k) \end{aligned} \tag{6.7}$$

$$\begin{aligned} \mathrm{x}_1(k+1) &= \mathcal{A}_1 \mathrm{x}_1(k) + \mathcal{B}_r r(k) \\ m(k) &= \mathcal{C}_m \mathrm{x}_1(k) + \mathcal{D}_{mr} r(k) \end{aligned} \tag{6.8}$$

$$\begin{aligned} \mathrm{x}_\infty(k+1) &= \mathcal{A}_\infty \mathrm{x}_\infty(k) + \mathcal{B}_d d(k) \\ e(k) &= \mathcal{C}_e \mathrm{x}_\infty(k) + \mathcal{D}_{ed} d(k) \end{aligned} \tag{6.9}$$

where

$$\begin{aligned} \mathsf{x}_2 &= \begin{bmatrix} x_2 \\ x_c \end{bmatrix} \\ \mathsf{x}_1 &= \begin{bmatrix} x_1 \\ x_c \end{bmatrix} \\ \mathsf{x}_\infty &= \begin{bmatrix} x_\infty \\ x_c \end{bmatrix} \end{aligned} \tag{6.10}$$

$$\begin{aligned} \mathcal{A}_2 &= \begin{bmatrix} (A_2 + B_{u_2} D_c C_{y_2}) & B_{u_2} C_c \\ B_c C_{y_2} & A_c \end{bmatrix} \\ \mathcal{A}_1 &= \begin{bmatrix} (A_1 + B_{u_1} D_c C_{y_1}) & B_{u_1} C_c \\ B_c C_{y_1} & A_c \end{bmatrix} \\ \mathcal{A}_\infty &= \begin{bmatrix} (A_\infty + B_{u_\infty} D_c C_{y_\infty}) & B_{u_\infty} C_c \\ B_c C_{y_\infty} & A_c \end{bmatrix} \end{aligned} \tag{6.11}$$

$$\begin{aligned} \mathcal{B}_w &= \begin{bmatrix} (B_w + B_{u_2} D_c D_{yw}) \\ B_c D_{yw} \end{bmatrix} \\ \mathcal{B}_r &= \begin{bmatrix} (B_r + B_{u_1} D_c D_{yr}) \\ B_c D_{yr} \end{bmatrix} \\ \mathcal{B}_d &= \begin{bmatrix} (B_d + B_{u_\infty} D_c D_{yd}) \\ B_c D_{yd} \end{bmatrix} \end{aligned} \tag{6.12}$$

$$\begin{aligned} \mathcal{C}_z &= \begin{bmatrix} (C_z + D_{zu} D_c C_{y_2}) & D_{zu} C_c \end{bmatrix} \\ \mathcal{C}_m &= \begin{bmatrix} (C_m + D_{mu} D_c C_{y_1}) & D_{mu} C_c \end{bmatrix} \\ \mathcal{C}_e &= \begin{bmatrix} (C_e + D_{eu} D_c C_{y_\infty}) & D_{eu} C_c \end{bmatrix} \end{aligned} \tag{6.13}$$

$$\begin{aligned} \mathcal{D}_{zw} &= \begin{bmatrix} D_{zu} D_c D_{yw} + D_{zw} \end{bmatrix} \\ \mathcal{D}_{mr} &= \begin{bmatrix} D_{mu} D_c D_{yr} + D_{mr} \end{bmatrix} \\ \mathcal{D}_{ed} &= \begin{bmatrix} D_{eu} D_c D_{yd} + D_{ed} \end{bmatrix} \end{aligned} \tag{6.14}$$

The assumption of $D_{yu} = 0$ can be relaxed via a simple change of variables [52]. Define

$$y' = y - D_{yu}u \;\Rightarrow\; y = y' + D_{yu}u \tag{6.15}$$

Using this substitution, we can obtain an expression for the internal transfer function $P_{y'u}$ which is now strictly causal ($D_{y'u} = 0$). All other portions of the open-loop transfer functions will remain unchanged. We can now find a controller $K' = (A'_c, B'_c, C'_c, D'_c)$ using the modified measurement vector y'. Once this compensator has been found, the initial transformation needs to be absorbed into the final compensator $K = (A_c, B_c, C_c, D_c)$ as follows:

$$A_c = A'_c - B'_c D_{yu} \left(I + D'_c D_{yu}\right)^{-1} C'_c \tag{6.16}$$

$$B_c = B'_c - B'_c D_{yu} \left(I + D'_c D_{yu}\right)^{-1} D'_c \tag{6.17}$$

$$C_c = \left(I + D'_c D_{yu}\right)^{-1} C'_c \tag{6.18}$$

$$D_c = \left(I + D'_c D_{yu}\right)^{-1} D'_c \tag{6.19}$$

The remaining assumption is one of well-posedness, namely $(I + D'_c D_{yu})$ must be invertible. With this relaxation, the only remaining restrictions for numerical solution of the full-order problem will be stabilizability, detectability, well posedness, and an overall mixed-problem which is non-singular. This is a minimal set of assumptions which will be met easily in any meaningful control problem. Note that, if we wish to solve for reduced-order controllers, we must also assume the existence of reduced-order stabilizing controllers. This may turn out to be a difficult assumption to verify.

6.3 The Nature of the Solution

The mixed-norm control problem is now to find a controller $K(z)$ such that:

i. $\mathcal{A}_2$, $\mathcal{A}_1$ and $\mathcal{A}_\infty$ are stable

ii. $\|T_{mr}\|_1 \leq \nu$ for some specified $\nu > 0$

iii. $\|T_{ed}\|_\infty \leq \gamma$ for some specified $\gamma > 0$

iv. The performance index $J = \|T_{zw}\|_2$ is minimized.

In order to discuss the solution, we need to make the following definitions.

$$\underline{\nu} := \inf_{K\text{admissible}} \|T_{mr}\|_1 \tag{6.20}$$

$$\underline{\gamma} := \inf_{K\text{admissible}} \|T_{ed}\|_\infty \tag{6.21}$$

$$\underline{\alpha} := \inf_{K\text{admissible}} \|T_{zw}\|_2 \tag{6.22}$$

$$K_{2_{opt}} := \text{the } K(z) \text{ that makes } \|T_{zw}\|_2 = \underline{\alpha} \tag{6.23}$$

$$\overline{\nu} := \|T_{mr}\|_1 \text{ when } K(z) = K_{2_{opt}} \tag{6.24}$$

$$\overline{\gamma} := \|T_{ed}\|_\infty \text{ when } K(z) = K_{2_{opt}} \tag{6.25}$$

$$K_{mix} := \text{a solution to the mixed-norm problem for some } \gamma, \nu \tag{6.26}$$

$$\nu^* := \|T_{mr}\|_1 \text{ when } K(z) = K_{mix} \tag{6.27}$$

$$\gamma^* := \|T_{ed}\|_\infty \text{ when } K(z) = K_{mix} \tag{6.28}$$

$$\alpha^* := \|T_{zw}\|_2 \text{ when } K(z) = K_{mix} \tag{6.29}$$

If we had not assumed a fixed-order compensator, we could state that, for $\underline{\nu} < \nu \leq \overline{\nu}$ and/or $\underline{\gamma} < \gamma \leq \overline{\gamma}$, if a solution to the $H_2/\ell_1/H_\infty$ control problem exists, it is unique, and lies on the boundary of one or both of the constraints. This follows from the convexity of $\|T_{mr}\|_1$ and $\|T_{ed}\|_\infty$ and the strict convexity of $\|T_{zw}\|_2$ when expressed in terms of the Youla parameter Q. A similar result was shown by Walker for the multiply-constrained H_2/H_∞ problem [9]. Once we fix the order of the compensator, however, we can no longer cast the problem in terms of the Youla parameter. Further, the criteria for admissible controllers now requires that they be of the chosen fixed order. For the constraints, this means that $\underline{\nu}$ will generally be higher than the 1-norm associated with the optimal ℓ_1 compensator, and $\underline{\gamma}$ will generally be higher than the ∞-norm associated with the optimal H_∞ compensator.

Once again, if we restrict ourselves to nonsingular constraints, the infimization problems above become minimization problems due to their finite dimension. We will now examine the existence of fixed-order solutions for given constraint levels.

It was shown in Chapter V that for compensator orders greater than or equal to that of the H_2 plant, the optimal full-order H_2/H_∞ solution will lie on the constraint boundary ($\gamma^* = \gamma$) when $\underline{\gamma} < \gamma \leq \overline{\gamma}$. If $\gamma \geq \overline{\gamma}$, the solution is $K_{2_{opt}}$, and it is unique. For the more general $H_2/\ell_1/H_\infty$ problem, we can characterize the nature of the solution using the Kuhn-Tucker necessary conditions [38]. When a solution exists, assuming linear independence of the active constraint gradients evaluated at the solution, the following conditions must be satisfied:

i. K must be feasible, i.e., it must stabilize the closed loop map from u to y and satisfy the constraints.

ii. $\nabla\|T_{zw}\|_2 + \lambda_1 \nabla\|T_{mr}\|_1 + \lambda_\infty \nabla\|T_{ed}\|_\infty = 0, \;\; \lambda_1 \geq 0, \lambda_\infty \geq 0.$

iii. $\lambda_1 \left(\|T_{mr}\|_1 - \nu\right) = 0, \; \lambda_\infty \left(\|T_{ed}\|_\infty - \gamma\right) = 0, \;\; \lambda_1 \geq 0, \lambda_\infty \geq 0.$

The first condition is merely the feasibility condition, and Walker [9] showed that, if only stable weights were used, stabilizing P_{yu} was sufficient to ensure the stability of T_{zw}, T_{mr}, and T_{zw}. The second condition states that the gradient of the objective function must be balanced by the scaled gradients of the constraints. The third condition provides the most insight into the solution. It states that if either of the constraints is not satisfied with equality, then the Lagrange multiplier (λ-value) associated with that constraint must be equal to zero. This leads us to the conclusion that the optimal fixed-order solution (if it exists) will lie on one or both of the constraints for the case where $\underline{\nu} < \nu \leq \overline{\nu}$ and/or $\underline{\gamma} < \gamma \leq \overline{\gamma}$. Once again, for a full-order solution, if $\nu \geq \overline{\nu}$ and $\gamma \geq \overline{\gamma}$, then the solution to the problem is the unique $K_{2_{opt}}$; a lower-order solution (if it exists) will still be an optimal H_2 solution for this case, but we can no longer claim existence or uniqueness. Cases where either $\nu \geq \overline{\nu}$ or $\gamma \geq \overline{\gamma}$ (but not both) can result in solutions in the interior of the Pareto optimal surface; however, these cases can also result in solutions on the H_2/H_∞ Pareto optimal curve, or the H_2/ℓ_1 Pareto optimal curve, respectively. These curves define part

of the boundary for the overall Pareto optimal surface. The location of solutions on the Pareto optimal surface will be discussed in detail using a specific example in Chapter VII.

6.4 A Numerical Approach to the Solution

The approach taken by Ridgely and Walker [50] to solve the H_2/H_∞ control problem was to define the scalar objective and constraint functions, derive analytic gradients for all functions, and solve the problem numerically using nonlinear programming methods. Early attempts on problems with a single H_∞ constraint forced the constraint to be active by appending it to the scalar cost function using Lagrange multipliers. The resulting minimization problem was then solved using the Davidon-Fletcher-Powell method [38] for unconstrained nonlinear programming. For problems with multiple constraints, it can no longer be assumed that all constraints will be active, thus motivating methods which make it easier to accommodate inequality constraints. Walker et.al. [9, 53, 54] achieved better performance on both single and multiple constraint problems using Sequential Quadratic Programming (SQP) methods [55, 38], which solve the constrained nonlinear programming problem by converting it to, and sequentially solving, a series of Quadratic Programming (QP) problems. Although SQP convergence to a global minimum can be guaranteed only for convex problems, the method performs remarkably well on many non-convex problems, and alternate starting conditions can be used to reduce the likelihood of convergence to local minima that are not global minima. Note that the potential convergence to local minima is due to the non-convexity of the problem, and cannot be avoided by simply changing to a different mathematical-programming technique. The problem of local minima can only be avoided by implementing global search techniques which tend to be very inefficient.

As in Walker's work, constrained nonlinear programming techniques will be used to solve the general $H_2/\ell_1/H_\infty$ control problem. The resulting numerical optimization is cumbersome, but the efficiency of the method is greatly improved by providing relatively clean function and analytic gradient expressions for all aspects of the problem. The objective f

and constraints g are as follows:

$$f(\kappa) := \xi_2 \|T_{zw}\|_2^2 \tag{6.30}$$

$$g_1(\kappa) := \xi_1(\|T_{mr}\|_1 - \nu) \tag{6.31}$$

$$g_\infty(\kappa) := \xi_\infty(\|T_{ed}\|_\infty - \gamma) \tag{6.32}$$

where κ represents a vectorized compensator and the ξ's are scaling parameters. A modal form is assumed for the compensator in order to reduce the number of variables. Although this method does not allow repeated eigenvalues in the compensator, in practice it has shown itself to be sufficient. If it is deemed necessary to allow for repeated eigenvalues, a block-Jordan form or fully populated state-space could be used instead. Finally, because SQP searches over both feasible and infeasible solutions, a stability constraint and exterior penalty function were added to keep the algorithm from getting lost in an unstable region. The stability constraint is stated as

$$g_s(\kappa) = \xi_s(\max_i \left\{|\lambda_i(\mathcal{A}_2)|^2\right\} - 1) \tag{6.33}$$

where $\lambda_i(\mathcal{A}_2)$ denotes the i^{th} eigenvalue of the closed-loop system, and $g_s(X)$ is constrained to be less than zero. The penalty function added to the objective function is simply the square of the stability constraint, thus providing continuous derivatives at the stability boundary.

6.4.1 Computing Gradients of the Two-Norm. We begin by defining n_2 as the number of states, n_w as the number of exogenous inputs, and n_z as the number of controlled outputs of the H_2 subproblem, and n_c as the number of states of the compensator. The square of the 2-norm for stable discrete-time systems can be calculated as

$$\|T_{zw}\|_2^2 = \text{trace}\left[\mathcal{D}_{zw}^T \mathcal{D}_{zw} + \mathcal{C}_z Q_2 \mathcal{C}_z^T\right] \tag{6.34}$$

where Q_2 is a solution to the Lyapunov equation

$$\mathcal{A}_2 Q_2 \mathcal{A}_2^T + \mathcal{B}_w \mathcal{B}_w^T = Q_2 \tag{6.35}$$

Introducing an equivalent expression for the Lyapunov constraint,

$$\mathcal{A}_2 Q_2 \mathcal{A}_2^T + \mathcal{B}_w \mathcal{B}_w^T = Q_2 \iff \text{trace}\left[\left(\mathcal{A}_2 Q_2 \mathcal{A}_2^T + \mathcal{B}_w \mathcal{B}_w^T - Q_2\right) X_2\right] = 0, \ \ \forall\, X_2 \in \mathbf{R}^{2n_2 \times 2n_2} \tag{6.36}$$

we can now define

$$J\left(A_c, B_c, C_c, D_c, Q_2, X_2\right) = \text{trace}\left[\mathcal{D}_{zw}^T \mathcal{D}_{zw} + \mathcal{C}_z Q_2 \mathcal{C}_z^T\right] + \text{trace}\left[\left(\mathcal{A}_2 Q_2 \mathcal{A}_2^T + \mathcal{B}_w \mathcal{B}_w^T - Q_2\right) X_2\right] \tag{6.37}$$

which is equivalent to (6.34) due to (6.36). Further, once the Lyapunov constraint is satisfied, the value of X_2 is arbitrary and does not affect the value of J. In order to obtain gradients of J, define χ as a vector consisting of the components of the matrix X_2. We can define an expression equivalent to (6.37)

$$\mathcal{J}\left(\kappa, \chi\right) = J\left(A_c(\kappa), B_c(\kappa), C_c(\kappa), D_c(\kappa), Q_2(\kappa), X_2(\chi)\right) \tag{6.38}$$

The differential of $\mathcal{J}$ can be written as

$$\delta \mathcal{J} = \delta \mathcal{J}(\kappa, \chi) = \sum_{i=1}^{n_\kappa} \frac{\partial \mathcal{J}}{\partial \kappa_i} \delta \kappa_i + \sum_{i=1}^{n_\chi} \frac{\partial \mathcal{J}}{\partial \chi_i} \delta \chi_i \tag{6.39}$$

However,

$$\frac{\partial J}{\partial X_2} = \mathcal{A}_2 Q_2 {\mathcal{A}_2}^T + \mathcal{B}_w {\mathcal{B}_w}^T - Q_2 = 0 \ \Rightarrow \ \frac{\partial \mathcal{J}}{\partial \chi_i} = 0, \ \ \forall\, i \tag{6.40}$$

Further, we can write

$$\frac{\partial \mathcal{J}}{\partial \kappa_i} = \sum_{p=1}^{n_2+n_c} \sum_{q=1}^{n_2+n_c} \frac{\partial J}{\partial a_{2_{pq}}} \frac{\partial a_{2_{pq}}}{\partial \kappa_i} + \sum_{p=1}^{n_2+n_c} \sum_{q=1}^{n_w} \frac{\partial J}{\partial b_{w_{pq}}} \frac{\partial b_{w_{pq}}}{\partial \kappa_i} \tag{6.41}$$

$$+ \sum_{p=1}^{n_w} \sum_{q=1}^{n_2+n_c} \frac{\partial J}{\partial c_{z_{pq}}} \frac{\partial c_{z_{pq}}}{\partial \kappa_i} + \sum_{p=1}^{n_z} \sum_{q=1}^{n_w} \frac{\partial J}{\partial d_{zw_{pq}}} \frac{\partial d_{zw_{pq}}}{\partial \kappa_i} + \sum_{p=1}^{n_2+n_c} \sum_{q=1}^{n_2+n_c} \frac{\partial J}{\partial q_{2_{pq}}} \frac{\partial q_{2_{pq}}}{\partial \kappa_i}$$

Concentrating on the last term of (6.41), we note

$$\frac{\partial J}{\partial Q_2} = \mathcal{A}_2{}^T X_2 \mathcal{A}_2 + \mathcal{C}_z{}^T \mathcal{C}_z - X_2 \tag{6.42}$$

Since X_2 is arbitrary, we can choose it such that

$$\mathcal{A}_2{}^T X_2 \mathcal{A}_2 + \mathcal{C}_z{}^T \mathcal{C}_z - X_2 = 0 \tag{6.43}$$

With this choice of X_2, the last term of (6.41) is identically zero. Such an X_2 always exists as can be seen by noting that (6.43) is a Lyapunov equation and we are choosing a compensator such that $\mathcal{A}_2$ is stable. Under these conditions, a real, symmetric, positive semi-definite X_2 which solves (6.43) is guaranteed to exist. With this we can define

$$X_2 = \begin{bmatrix} X_{11} & X_{12} \\ X_{12}^T & X_{22} \end{bmatrix}, \quad Q_2 = \begin{bmatrix} Q_{11} & Q_{12} \\ Q_{12}^T & Q_{22} \end{bmatrix} \tag{6.44}$$

The remainder of the gradients can now be expressed as

$$\begin{aligned} \frac{\partial J}{\partial A_c} &= 2\left[X_{12}^T A_2 Q_{12} + X_{12}^T B_{u_2} C_c Q_{22}\right. \\ &\quad \left. + X_{22} B_c C_{y_2} Q_{12} + X_{22} A_c Q_{22} + X_{12}^T B_{u_2} D_c C_{y_2} Q_{12}\right] \end{aligned} \tag{6.45}$$

$$\begin{aligned} \frac{\partial J}{\partial B_c} &= 2\left[X_{12}^T A_2 Q_{11} C_{y_2}^T + X_{12}^T B_{u_2} C_c Q_{12}^T C_{y_2}^T + X_{22} B_c C_{y_2} Q_{11} C_{y_2}^T + X_{22} A_c Q_{12}^T C_{y_2}^T\right. \\ &\quad \left. + X_{12}^T B_w D_{yw}^T + X_{22} B_c D_{yw} D_{yw}^T + X_{12}^T B_{u_2} D_c C_{y_2} Q_{11} C_{y_2}^T + X_{12}^T B_{u_2} D_c D_{yw} D_{yw}^T\right] \end{aligned} \tag{6.46}$$

$$\begin{aligned} \frac{\partial J}{\partial C_c} &= 2\left[D_{zu}^T C_z Q_{12} + D_{zu}^T D_{zu} C_c Q_{22} + B_{u_2}^T X_{11} A_2 Q_{12} + B_{u_2}^T X_{11} B_{u_2} C_c Q_{22}\right. \\ &\quad \left. + B_{u_2}^T X_{12} B_c C_{y_2} Q_{12} + B_{u_2}^T X_{12} A_c Q_{22} + D_{zu}^T D_{zu} D_c C_{y_2} Q_{12} + B_{u_2}^T X_{11} B_{u_2} D_c C_{y_2} Q_{12}\right] \end{aligned} \tag{6.47}$$

$$\frac{\partial J}{\partial D_c} = 2\Big[D_{zu}^T D_{zw} D_{yw}^T + D_{zu}^T D_{zu} D_c D_{yw} D_{yw}^T + D_{zu}^T C_z Q_{11} C_{y_2}^T + D_{zu}^T D_{zu} D_c C_{y_2} Q_{11} C_{y_2}^T$$
$$+D_{zu}^T D_{zu} C_c Q_{12}^T C_{y_2}^T + B_{u_2}^T X_{11} A_2 Q_{11} C_{y_2}^T + B_{u_2}^T X_{11} B_{u_2} D_c C_{y_2} Q_{11} C_{y_2}^T$$
$$+B_{u_2}^T X_{11} B_{u_2} C_c Q_{12}^T C_{y_2}^T + B_{u_2}^T X_{12} B_c C_{y_2} Q_{11} C_{y_2}^T + B_{u_2}^T X_{12} A_c Q_{12}^T C_{y_2}^T$$
$$+B_{u_2}^T X_{11} B_w D_{yw}^T + B_{u_2}^T X_{11} B_{u_2} D_c D_{yw} D_{yw}^T + B_{u_2}^T X_{12} B_c D_{yw} D_{yw}^T\Big] \qquad (6.48)$$

The method for actually computing the gradient $\nabla\|T_{zw}\|_2^2$ at some vectorized compensator κ is as follows:

i. Solve the Lyapunov equations for X_2 and Q_2.

ii. Compute the partials with respect to the compensator state space as shown above.

iii. Compute the gradient with respect to κ as

$$\frac{\partial \mathcal{J}}{\partial \kappa} = \left[\left(\frac{\partial J}{\partial A_c}\right)_{diag}^T \left(\frac{\partial J}{\partial A_c}\right)_{super/subdiag}^T \left(\frac{\partial J}{\partial B_c}\right)_1^T \cdots \left(\frac{\partial J}{\partial B_c}\right)_{n_y}^T \left(\frac{\partial J}{\partial C_c}\right)_1^T \cdots \right.$$
$$\left. \cdots \left(\frac{\partial J}{\partial C_c}\right)_{n_c}^T \left(\frac{\partial J}{\partial D_c}\right)_1^T \cdots \left(\frac{\partial J}{\partial D_c}\right)_{n_y}^T\right]^T \qquad (6.49)$$

where the individual vectors represent the columns (or the diagonals in the case of A_c) of the partial derivative matrices, n_c is the number of compensator states and n_y is the number of measurements. Since we are assuming the subdiagonal of A_c is the negative of the superdiagonal, the elements of the second vector in (6.49) are formed from the difference of the super- and subdiagonal elements.

The penalty function associated with the objective makes it unlikely that a 2-norm gradient calculation for an unstable system will be necessary. However, in the event that it is required, the algorithm detects the unstable closed-loop system and switches to a finite-difference calculation for the gradient of the stable and antistable projections of the objective transfer function.

6.4.2 Computing Gradients of the One-Norm. The state space expression for the 1-norm of a SISO transfer function is

$$\|T_{mr}\|_1 = \sum_{k=0}^{\infty} |\mathcal{C}_m \mathcal{A}_1^k \mathcal{B}_r| + |\mathcal{D}_{mr}| \tag{6.50}$$

The partial derivatives with respect to the closed-loop state space can be expressed as

$$\frac{\partial \|T_{mr}\|_1}{\partial \mathcal{A}_1} = \sum_{k=0}^{\infty} \left[\operatorname{sgn}\left(\mathcal{C}_m \mathcal{A}_1^k \mathcal{B}_r\right) \sum_{l=0}^{k-1} \left[\left(\mathcal{A}_1^T\right)^l \mathcal{C}_m^T \mathcal{B}_r^T \left(\mathcal{A}_1^T\right)^{k-l-1} \right] \right] \tag{6.51}$$

$$\frac{\partial \|T_{mr}\|_1}{\partial \mathcal{B}_r} = \sum_{k=0}^{\infty} \operatorname{sgn}\left(\mathcal{C}_m \mathcal{A}_1^k \mathcal{B}_r\right) \left[\left(\mathcal{A}_1^T\right)^k \mathcal{C}_m^T \right] \tag{6.52}$$

$$\frac{\partial \|T_{mr}\|_1}{\partial \mathcal{C}_m} = \sum_{k=0}^{\infty} \operatorname{sgn}\left(\mathcal{C}_m \mathcal{A}_1^k \mathcal{B}_r\right) \left[\mathcal{B}_r^T \left(\mathcal{A}_1^T\right)^k \right] \tag{6.53}$$

$$\frac{\partial \|T_{mr}\|_1}{\partial \mathcal{D}_{mr}} = \operatorname{sgn}\left(\mathcal{D}_{mr}\right) \tag{6.54}$$

where sgn(·) is 1, -1 or 0 depending on the sign of the argument. From these, we can express the gradients with respect to the compensator state space as

$$\frac{\partial \|T_{mr}\|_1}{\partial A_{c_{i,j}}} = \left[\frac{\partial \|T_{mr}\|_1}{\partial \mathcal{A}_1} \right]_{n_1+i, n_1+j} \tag{6.55}$$

$$\frac{\partial \|T_{mr}\|_1}{\partial B_{c_{i,j}}} = \sum_{p=1}^{n_c} \sum_{q=1}^{n_1} \delta_{p,i} C_{y_{1_{j,q}}} \left[\frac{\partial \|T_{mr}\|_1}{\partial \mathcal{A}_1} \right]_{n_1+p,q} + \sum_{p=1}^{n_c} \sum_{q=1}^{n_r} \delta_{p,i} D_{yr_{j,q}} \left[\frac{\partial \|T_{mr}\|_1}{\partial \mathcal{B}_r} \right]_{n_1+p,q} \tag{6.56}$$

$$\frac{\partial \|T_{mr}\|_1}{\partial C_{c_{i,j}}} = \sum_{p=1}^{n_1} \sum_{q=1}^{n_c} \delta_{j,q} B_{u_{1_{p,i}}} \left[\frac{\partial \|T_{mr}\|_1}{\partial \mathcal{A}_1} \right]_{p,n_1+q} + \sum_{p=1}^{n_m} \sum_{q=1}^{n_c} \delta_{j,q} D_{mu_{p,i}} \left[\frac{\partial \|T_{mr}\|_1}{\partial \mathcal{C}_m} \right]_{p,n_1+q} \tag{6.57}$$

$$\begin{aligned} \frac{\partial \|T_{mr}\|_1}{\partial D_{c_{i,j}}} = & \sum_{p=1}^{n_1} \sum_{q=1}^{n_1} B_{u_{1_{p,i}}} C_{y_{1_{j,q}}} \left[\frac{\partial \|T_{mr}\|_1}{\partial \mathcal{A}_1} \right]_{p,q} + \sum_{p=1}^{n_1} \sum_{q=1}^{n_r} B_{u_{1_{p,i}}} D_{yr_{j,q}} \left[\frac{\partial \|T_{mr}\|_1}{\partial \mathcal{B}_r} \right]_{p,q} \\ & + \sum_{p=1}^{n_m} \sum_{q=1}^{n_1} D_{mu_{p,i}} C_{y_{1_{j,q}}} \left[\frac{\partial \|T_{mr}\|_1}{\partial \mathcal{C}_m} \right]_{p,q} + \sum_{p=1}^{n_m} \sum_{q=1}^{n_r} D_{mu_{p,i}} D_{yr_{j,q}} \left[\frac{\partial \|T_{mr}\|_1}{\partial \mathcal{D}_{mr}} \right]_{p,q} \end{aligned} \tag{6.58}$$

where n_1 is the number of states, n_r is the number of exogenous inputs, and n_m is the number of controlled outputs for the ℓ_1 sub-problem. Naturally, the infinite summations cannot be carried out; the current implementation truncates the summation at some spec-

ified number of time steps. Values for this truncation level vary from 100-500 for systems with closely spaced modes, and 5000-10000 for sytems with widely spaced modes. Once a solution is found for a given truncation level, the tolerance for the 1-norm is checked using either a Hankel singular value method (as defined by Dahleh and Diaz-Bobillo[5]), or by simply recalculating the norm using a significantly higher truncation level. If the error is greater than a specified tolerance, the truncation level is increased and the optimization repeated starting with the last computed compensator.

For MIMO transfer functions, the 1-norm is determined by the maximum row sum of SISO transfer function norms. To implement this, the row where the maximum occurs can be determined first, and SISO norms can be computed for each transfer function in the row. However, the nature of the ℓ_1 optimal solution is such that the max row sum may occur over more than one row, leading to discontinuous derivatives. For this reason, the current implementation is to append each row sum as a separate multi-input single-output transfer function constraint, with the same constraint level used for each row sum. If implemented with an algorithm which uses only active constraints to determine search directions, the inactive row sums will have no effect on the convergence of the problem. The only drawback to this approach is the additional computation time required to compute all the row sums and their gradients. Many optimization subroutines have the capability to limit the gradient calls to active constraints, and this is an application in which that capability would be beneficial. The norms of the inactive rows still need to be checked, but some of the computationally expensive gradient calculations can be eliminated. The active constraint set has not yet been implemented with the current algorithms, but it is recommended as a future enhancement.

The method above works well (albeit slowly) for truncation levels up to approximately 1000, which is often more than sufficient for systems with closely spaced modes and sample rates set at 5-10 times the highest mode. For systems with widely separated poles, it was found that a sampling rate fast enough for the highest mode often resulted in truncation levels of 5,000-10,000 in order to capture the lower modes. These truncation levels resulted in prohibitively high run times and/or numerical instability. For systems such as this, a

modification to the subroutines providing ℓ_1 norm and gradient information was developed by Spillman [51], and is described subsequently.

For now, we limit the discussion to SISO systems. If $\mathcal{A}_1$ is non-defective, and denoting the i^{th} left and right eigenvector as L_i and R_i, respectively, then the partial of ${\mathcal{A}_1}^k$ with respect to any element of $\mathcal{A}_1$ is given by

$$\frac{\partial \mathcal{A}_1^k}{\partial a_{pq}} = \frac{\partial \left[R\Lambda^k R^{-1}\right]}{\partial a_{pq}} = \frac{\partial R}{\partial a_{pq}}\Lambda^k R^{-1} + R\frac{\partial \Lambda^k}{\partial a_{pq}}R^{-1} + R\Lambda^k\frac{\partial R^{-1}}{\partial a_{pq}} \tag{6.59}$$

where Λ is a diagonal matrix of eigenvalues,

$$\frac{\partial R_i}{\partial a_{pq}} = \sum_{j=1, j\neq i}^{n_1} c_{ij}R_j + c_i R_i = V_i + c_i R_i \tag{6.60}$$

$$\frac{\partial R^{-1}}{\partial a_{pq}} = -R^{-1}\frac{\partial R}{\partial a_{pq}}R^{-1} \tag{6.61}$$

$$c_{ij} = \frac{L_j^T\left[R_i\frac{\partial \lambda_i}{\partial a_{pq}} - \frac{\partial \mathcal{A}_1}{\partial a_{pq}}R_i\right]}{\lambda_j - \lambda_i},\quad i \neq j \tag{6.62}$$

$$c_i = -\Re\left(R_i^H M V_i\right) - \frac{1}{2}R_i^H\frac{\partial M}{\partial a_{pq}}R_i \tag{6.63}$$

$$\frac{\partial \Lambda^k}{\partial a_{pq}} = \sum_{i=1}^{n_1}\frac{\partial \Lambda^k}{\partial \lambda_i}\frac{\partial \lambda_i}{\partial a_{pq}} \tag{6.64}$$

$$\frac{\partial \lambda_i}{\partial a_{pq}} = L_i^T\frac{\partial \mathcal{A}_1}{\partial a_{pq}}R_i \tag{6.65}$$

and M is a scaling matrix defined by

$${R_i}^H M R_i = 1 \tag{6.66}$$

Typically the scaling matrix is chosen to be an identity matrix, thus eliminating the partial derivative with respect to M from the gradient expression. Note that the partial of Λ^k with respect to λ_i is an almost trivial calculation due to the diagonal form of Λ. The partial

derivative of the 1-norm with respect to $\mathcal{A}_1$ can now be found element-wise from

$$\frac{\partial \|T_{mr}\|_1}{\partial \mathcal{A}_{1_{pq}}} = \sum_{k=0}^{N} \operatorname{sgn}\left(\mathcal{C}_m \mathcal{A}_1^k \mathcal{B}_r\right) \mathcal{C}_m \frac{\partial \mathcal{A}_1^k}{\partial a_{pq}} \mathcal{B}_r \tag{6.67}$$

The sign of $\mathcal{C}_m \mathcal{A}_1^k \mathcal{B}_r$ can be stored as part of the norm calculation. This eliminates a costly part of the gradient calculation because this factor no longer needs to be recomputed for $k = 0, \ldots, N_{trunc}$. With this, the only remaining part which requires evaluation is the diagonal matrix Λ^k, at each index k, and this only requires the calculation of the diagonal elements. Once these terms have been calculated, the expressions in equations (6.52–6.58) can be quickly evaluated.

One-norm gradients for MIMO systems are caclulated for each output by summing the gradients of the individual SISO transfer functions between each of the outputs and the separate inputs. The same method of defining MIMO constraints using multiple multi-input single-output constraints, as described previously, is then used.

Currently, the new method is limited to non-defective matrices with no repeated eigenvalues in the closed loop $\mathcal{A}_1$ matrix. If the repeated roots stem from weighting functions, it is usually possible to perturb these functions to avoid repeated roots without any adverse affects on the overall design. To a lesser degree, it is also possible to perturb the plant model to avoid having repeated roots. While possible extensions for the case of repeated eigenvalues are currently under investigation, the current method switches to a finite difference calculation in the event they occur. Although this involves a degradation in the efficiency of the gradient algorithm, the accuracy of the finite difference gradient is sufficient to maintain numerical stability and convergence.

6.4.3 Computing Gradients of the Infinity-Norm. The approach for taking gradients of the ∞-norm is based on the singular value sensitivity analysis of Giesy and Lim [56], with some modification required to apply it to a discrete-time problem. If we assume the maximum singular value of T_{ed} evaluated at κ has a single peak for $\theta \in [0, 2\pi)$, the

derivative of $\|T_{ed}\|_\infty$ can be written as

$$\frac{\partial \|T_{ed}\|_\infty}{\partial \kappa_i} = \Re\left[u_1^H \left(\frac{dT_{ed}\left(e^{j\theta_0}\right)}{d\kappa_i}\right)\bigg|_{\kappa_{nom}} v_1\right] \tag{6.68}$$

where u_1 and v_1 are the singular vectors associated with the maximum singular value of T_{ed}, θ_0 is the phase angle where the singular value reaches its maximum, and κ_{nom} is the nominal (vectorized) compensator. The derivative of T_{ed} can be determined from

$$\begin{aligned}\frac{dT_{ed}\left(e^{j\theta_0}\right)}{d\kappa_i}\bigg|_{\kappa_{nom}} &= \left[\frac{d\mathcal{C}_e}{d\kappa_i}\left(e^{j\theta_0}I - \mathcal{A}_\infty\right)^{-1}\mathcal{B}_d + \mathcal{C}_e\left(e^{j\theta_0}I - \mathcal{A}_\infty\right)^{-1}\frac{d\mathcal{B}_d}{d\kappa_i}\right. \\ &+ \left.\mathcal{C}_e\left(e^{j\theta_0}I - \mathcal{A}_\infty\right)^{-1}\frac{d\mathcal{A}_\infty}{d\kappa_i}\left(e^{j\theta_0}I - \mathcal{A}_\infty\right)^{-1}\mathcal{B}_d + \frac{d\mathcal{D}_{ed}}{d\kappa_i}\right]\bigg|_{\kappa_{nom}}\end{aligned} \tag{6.69}$$

The actual implementation of this method uses a banded search to locate any number of singular value peaks. Each peak is then treated as a separate constraint with the same constraint value. Although this may result in carrying inactive constraints in the optimization problem, it avoids the problem of discontinuous derivatives which can occur if gradient information is obtained from a single peak. There are some subtleties associated with the multi-peak method in that a new peak may develop while solving the optimization problem. In this case, the new peak is detected and the problem is restarted with a composite of new and old frequency bands, thus avoiding the problem of bouncing back and forth between two different peaks. A balance between old peak locations and duplication of the frequency bands must be maintained, and this has been implemented using a minimum bandwidth and logic for deciding when a peak has simply moved, as opposed to identifying it as a new peak. The algorithm has proven to be reliable for a wide variety of problems, and it allows for mixed-norm solutions much closer to H_∞ optimal than was possible using either single peak or eigenvalue methods to solve for H_∞ gradients [57].

6.4.4 Computing Stability Gradients. The stability constraint was defined by (6.33). Define

$$\lambda_m = \sigma_m + j\omega_m \equiv \arg\left(\max|\lambda_i(\mathcal{A}_2)|\right)$$

$$|\lambda_m|^2 = \sigma_m^2 + \omega_m^2 \tag{6.70}$$

With this, we can now write the gradient expression as

$$\frac{\partial g_s}{\partial \kappa_i} = 2\xi_s \left(\sigma_m \frac{\partial \sigma_m}{\partial \kappa_i} + \omega_m \frac{\partial \omega_m}{\partial \kappa_i} \right) \tag{6.71}$$

where

$$\begin{aligned} \frac{\partial \sigma_m}{\partial \kappa_i} &= \Re \left(l_m^T \frac{\partial \mathcal{A}_2}{\partial \kappa_i} r_m \right) \\ \frac{\partial \omega_m}{\partial \kappa_i} &= \Im \left(l_m^T \frac{\partial \mathcal{A}_2}{\partial \kappa_i} r_m \right) \end{aligned} \tag{6.72}$$

l_m and r_m denote the left and right eigenvectors, respectively, associated with the maximum eigenvalue, and the partial of $\mathcal{A}_2$ with respect to κ_i can be easily evaluated componentwise.

6.4.5 Implementation Features. The method has been implemented in MATLAB [58] using a modular collection of norm and gradient subroutines for each of the different norms. With this approach, any number or combination of different constraints can be added to the problem without modification to the code. The input to the problem is a stack of transfer functions in state space form, with a second parameter matrix identifying which transfer function should be used as the objective function, and which norm and gradient should be evaluated for each of the different transfer functions. Most of the early example runs were performed using the MATLAB SQP routine (*constr.m*) [59]. The MATLAB routine converges for most of the smaller problems (50-60 design variables or fewer); however, for larger problems *constr.m* has problems maintaining a positive definite approximation to the Lagrangian Hessian. FORTRAN shells have been built to incorporate the ADS [60] collection of optimization subroutines and the IMSL implementation of SQP (DNCONG) [61]. Both the IMSL and ADS subroutines have the ability to call for gradients of only the active constraints, and the ADS collection allows the user to experiment with all the different optimization strategies and line search methods. Of these, the IMSL algorithm seems to be the most efficient, and it has converged successfully for the larger problems (approximately 100 design variables). A limitation of the IMSL subroutine is that the

fixed convergence and line search criteria are so strict that they sometimes fail to solve problems which are solvable using more relaxed criteria. A version of SQP (*sqp.m*) based on Schittkowski's method [55] (essentially what has been coded for IMSL) has recently been coded for MATLAB[62]. This version allows the Hessian to be saved and passed as a variable when sequentially solving for several points on a Pareto optimal curve. This capability results in much greater efficiency on problems in which varying constraint levels must be investigated and has been implemented as the default solver for the mixed-norm algorithm.

One of the more critical decisions associated with the numerical method is that of choosing an initial compensator. The default mode of operation solves the H_2 subproblem for the full-order optimal compensator and uses this as the starting point. This requires that the H_2 subproblem be nonsingular. A singular H_2 subproblem is permissible with the method, but an initial compensator must be provided to start the algorithm, and the overall mixed-norm control problem should be nonsingular. It is important to note that the order of the solution will always be fixed at the order of the initial compensator. Therefore, if a higher or lower order solution is desired, an initial compensator with that order must be provided as the starting point. There are no restrictions as to how these initial compensators may be found. Successful approaches include model order reduction or state augmentation of full-order compensators, and H_2, H_∞, or ℓ_1 synthesis of controllers for reduced or expanded order plants. Once a single stabilizing controller is found with the desired order, successful results from the mixed-norm problem will then provide the necessary compensators for starting the algorithm with new constraint levels.

Although this dissertation deals only with the discrete-time algorithms, the discrete-time algorithms were combined with those for continuous-time [9, 50, 57, 51] to provide a single program capable of solving fixed-order, mixed-norm control problems for both continuous-time and discrete-time systems. A common data structure, naming convention, and calling sequence was developed for all subroutines, and a single shell was created which is capable of running both continuous and discrete-time problems. A more complete description of the Mixed-Norm Toolbox for MATLAB [62] can be found in Appendix C.

6.5 A SISO F-16 Example

Consider a simple longitudinal controller design for a short period approximation of an F-16. The linear, time-invariant, continuous-time model includes second order dynamics with a first order pre-filter to model servo dynamics. The plant states are the angle of attack (α) and pitch rate (q). The control input to the system is a commanded stabilator deflection (δ_e), and the output is a measured normal acceleration (a_z). The plant model is discussed in more detail in Appendix B. The objective is to design a controller which provides good noise rejection as well as acceptable tracking and robust stability. The approach to the problem will be to first investigate the tradeoff between tracking and noise rejection using an H_2/ℓ_1 approach. Once an acceptable level of tracking is found (as defined by a 1-norm constraint level for weighted sensitivity), the stability robustness will be improved by adding an ∞-norm constraint on the complementary sensitivity, resulting in an $H_2/\ell_1/H_\infty$ optimization problem.

The intent of the individual subproblems is to design them for the type of control problem handled best by the particular norm being used. Specifically, while H_2 methods can provide tracking performance, their particular strength seems to be for disturbance and noise rejection (regulator problems). Tracking problems which require fast response often exhibit large overshoot when solved with H_2 methods. The H_∞ method is capable of providing good tracking, but it tends to produce high bandwidth controllers which have poor noise performance. The H_∞ method, however, is very well suited to handling the robust stability problem [4]. The ℓ_1 method, while it is relatively untested as far as applications are concerned, appears to hold great promise for tracking problems. Limited trials with ℓ_1 designs have shown better tracking performance than H_∞ methods, and less of a degradation in terms of noise rejection.

The transfer functions will be provided in continuous-time for ease of interpretation; however, they were discretized using a zero-order hold and sample rate of 20 Hz prior to solving the control problem. The sample rate was chosen to be fast enough to capture the servo dynamics (20 rad/sec), but not so fast as to necessitate large truncation levels for the ℓ_1 subproblem.

6.5.1 H_2 Subproblem. The H_2 problem is to find a stabilizing controller which minimizes the response of the normal acceleration and weighted control due to wind disturbance and measurement noise (a standard steady-state LQG problem). The wind gust is assumed to be white Gaussian noise (WGN) of strength 5×10^{-4} rad^2–sec, and it enters the plant as an angle of attack disturbance. Because we are interested in controlling the g-levels, the state weighting matrix is identical to the system C matrix, and a control weight of 10.0 was chosen (after several interations) to ensure reasonable control usage. The control weighting penalizes the energy of control usage but establishes no explicit constraints on actuator limits or rates. Although it would be possible to constrain specific limits and/or rates using an ℓ_1 constraint [5], this will not be done for this problem. A further check on control usage will be made during the closed loop simulation, and a later example will illustrate the importance of constraining the magnitude of control usage. The measurement noise is modeled as WGN with a strength of 1.6×10^{-6} rad^2–sec. There was no attempt to achieve good reference tracking in the H_2 problem, only noise and disturbance rejection. Tracking considerations will be taken care of by the ℓ_1 constraint. The resulting continuous-time state space matrices for the H_2 sub-problem are

$$
\begin{aligned}
A_2 &= \begin{bmatrix} -1.491 & 0.996 & -0.188 \\ 9.753 & -0.96 & -19.04 \\ 0 & 0 & -20.0 \end{bmatrix}, \quad B_w = \begin{bmatrix} -0.03334 & 0 \\ 0.21808 & 0 \\ 0 & 0 \end{bmatrix}, \quad B_{u_2} = \begin{bmatrix} 0 \\ 0 \\ 20.0 \end{bmatrix} \\
C_z &= \begin{bmatrix} -35.264 & 0.334 & 4.366 \\ 0 & 0 & 0 \end{bmatrix}, \quad D_{zw} = \begin{bmatrix} 0 & 0 \\ 0 & 0 \end{bmatrix}, \quad D_{zu} = \begin{bmatrix} 0 \\ 10.0 \end{bmatrix} \\
C_{y_2} &= \begin{bmatrix} -35.264 & 0.334 & 4.366 \end{bmatrix}, \quad D_{yw} = \begin{bmatrix} 0 & 0.004 \end{bmatrix}, \quad D_{yu} = [0]
\end{aligned}
\tag{6.73}
$$

Figure 6.2 shows the H_2 optimal system response to an initial 5 degree angle of attack disturbance, and Figure 6.3 shows the response to a 1-g step acceleration command. The system does a good job of disturbance rejection, but control usage is relatively high in accomplishing the task. The high control usage is mainly attributed to the impulsive nature in which the disturbance enters the system, which is not entirely realistic. For this reason, and since a control limit of 30 degrees is not exceeded, the control weight will be left as is. As expected, the system has very poor performance in tracking, and this shows up in the high steady-state error to the step command. Once again, the non-zero steady

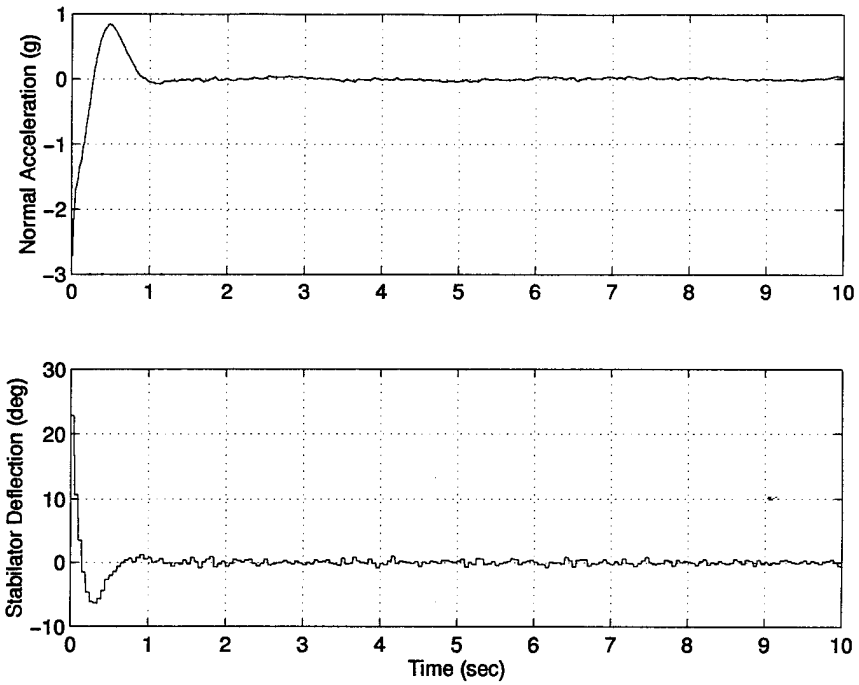

Figure 6.2 Response to initial 5 deg alpha disturbance, H_2 Optimal Design

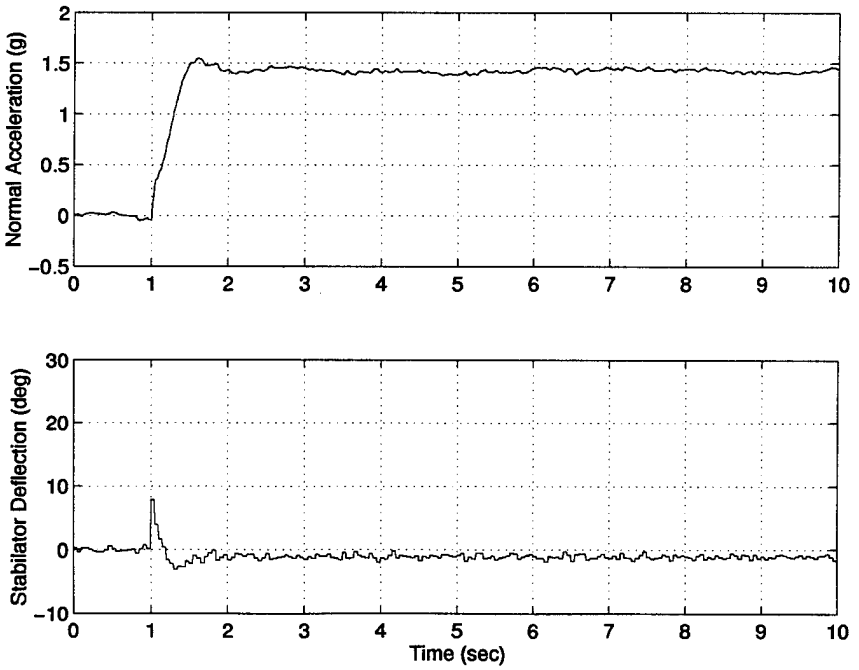

Figure 6.3 Response to 1g Step Command, H_2 Optimal Design

state error is not meant to be indicative of H_2 designs. The H_2 subproblem was designed for disturbance and noise rejection only; the tracking problem will be addressed by the ℓ_1 constraint.

6.5.2 ℓ_1 Subproblem. The ℓ_1 problem is set up to constrain the weighted sensitivity (W_sS) to ensure a certain level of tracking performance. For a SISO problem, the sensitivity minimization problem is equivalent to a reference tracking problem. A frequency-dependent weight will be used to facilitate the tradeoff between low frequency tracking and susceptibility to high frequency measurement noise. Typically, a weight on sensitivity for an H_∞ problem would be the inverse of the desired sensitivity [4]. We want to attenuate system response to sensor noise and unmodeled dynamics at higher frequencies, while maintaining sufficient gain at low frequencies for good tracking and disturbance rejection. This calls for a weight which has high gain at low frequencies and low gain at high frequencies. The ℓ_1 problem doesn't shape singular value plots directly, as in H_∞, but the frequency domain weight works well for this problem due to the low frequency nature of the pilot commands we are interested in tracking. The sensitivity weight used for this example is

$$W_s = \frac{s + 1.0}{s + 0.0001} \tag{6.74}$$

and the resulting continuous-time state space matrices for the ℓ_1 sub-problem are

$$\begin{aligned}
A_1 &= \begin{bmatrix} -1.491 & 0.996 & -0.188 & 0 \\ 9.753 & -0.96 & -19.04 & 0 \\ 0 & 0 & -20.0 & 0 \\ -35.264 & 0.334 & 4.366 & -0.0001 \end{bmatrix}, \quad B_r = \begin{bmatrix} 0 \\ 0 \\ 0 \\ 1.0 \end{bmatrix}, \quad B_{u_1} = \begin{bmatrix} 0 \\ 0 \\ 20.0 \\ 0 \end{bmatrix} \\
C_m &= [-35.264 \quad 0.334 \quad 4.366 \quad 1.0], \quad D_{mr} = [1.0], \quad D_{mu} = [0] \\
C_{y_1} &= [-35.264 \quad 0.334 \quad 4.366 \quad 0], \quad D_{yr} = [1.0], \quad D_{yu} = [0]
\end{aligned} \tag{6.75}$$

The truncation used for the ℓ_1 constraint was 500 time steps (25 seconds), which was sufficient to ensure the finite support length of T_{mr} was captured. The H_2/ℓ_1 cases close to ℓ_1 optimal could be solved using a truncation of 100 time steps, but as the constraint level backed away from ℓ_1 optimal a higher truncation level was necessary. The reason for this

is again the fact that the H_2 subproblem was not set up to track a reference command, thus resulting in a very large value of $\|T_{mr}\|_1$ evaluated using $K_{2_{opt}}$.

6.5.3 H_∞ Subproblem. The H_∞ problem is used to constrain the complementary sensitivity, thus achieving a certain level of stability robustness to unstructured multiplicative uncertainty [4]. Most plant uncertainty effects are at higher frequencies which, for this example, lie beyond the Nyquist frequency. For this reason an unweighted complementary sensitivity was used for the ∞-norm constraint. If more specific structures for the plant uncertainty were available, a less conservative way to handle this constraint would be to apply μ-synthesis [63] to obtain the weighting functions for the H_∞ constraint. An H_2/μ problem such as this was formulated and solved by Walker [64] for a continuous-time example, but it could be applied equally well for discrete-time problems. Since a specific structure for the uncertainty is not known for this problem (or will not be assumed), the unweighted complementary sensitivity will be used to address the robust stability concerns. The continuous-time state space matrices for the H_∞ problem are

$$\begin{aligned} A_\infty &= \begin{bmatrix} -1.491 & 0.996 & -0.188 \\ 9.753 & -0.96 & -19.04 \\ 0 & 0 & -20.0 \end{bmatrix}, \quad B_d = \begin{bmatrix} 0 \\ 0 \\ 20.0 \end{bmatrix}, \quad B_{u_\infty} = \begin{bmatrix} 0 \\ 0 \\ 20.0 \end{bmatrix} \\ C_e &= [0 \;\; 0 \;\; 0], \quad D_{ed} = [0], \quad D_{eu} = [1.0] \\ C_{y_\infty} &= [-35.264 \;\; 0.334 \;\; 4.366], \quad D_{yd} = [0], \quad D_{yu} = [0] \end{aligned} \tag{6.76}$$

6.5.4 The H_2/ℓ_1 Results. Table 6.1 lists the resulting norm values for the H_2/ℓ_1 compensated systems, and Figure 6.4 shows a comparison of the noise-free step responses. Note that, although $\|T_{ed}\|_\infty$ levels appear in Table 6.1, there was no attempt to constrain them for Cases 1-8. The very large value of $\|T_{mr}\|_1$ (unmeasurable for truncation levels up to 50,000) for the H_2 optimal design is indicative of a controller which cannot track a reference with zero steady-state error. With the exception of the H_2 optimal design, all the mixed controllers have zero steady-state error, and the overshoot and settling time decrease with the level of ν. Figure 6.5 shows the singular value plots of the loop transfer function (GK), and Figure 6.6 shows the sensitivity for the H_2 and H_2/ℓ_1 designs. With

the exception of the H_2 optimal design (Case 1), all the mixed controllers give adequate low-frequency response, and the sensitivity improves with decreasing levels of ν. The higher gain for GK at low frequency corresponds to the improved step tracking for these systems.

Table 6.1 Mixed H_2/ℓ_1 Control Results

Case #	$\|T_{zw}\|_2$ α	$\|T_{mr}\|_1$ ν	$\|T_{ed}\|_\infty$ γ
1 (H_2 optimal)	0.171	Very Large	1.43
2	0.176	2.70	1.60
3	0.178	2.60	1.59
4	0.187	2.50	1.51
5	0.240	2.40	1.37
6	0.279	2.30	1.29
7	0.335	2.20	1.20
8 (ℓ_1 optimal)	0.400	2.13	1.16

Figure 6.7 shows the complementary sensitivity plots, which indicate that weighted sensitivity and complementary sensitivity are not actually competing objectives for the controllers shown. Note that the controller which yields the lowest sensitivity (ℓ_1 optimal) also has the lowest complementary sensitivity of all the mixed H_2/ℓ_1 controllers. The low frequency weight is what allows us to have non-competing constraints in this case, but in general sensitivity and complementary sensitivity constraints can compete with each other. An example where they do compete will be shown in the next chapter. Although the complementary nature of the two constraints for this problem would seem to suggest that the ℓ_1 optimal controller is the best choice, Figures 6.8 and 6.9 show that the price of ℓ_1 optimality for this particular plant is poor high frequency noise rejection and high control usage. These properties of the system are clearly improved by blending H_2 features with those of ℓ_1.

6.5.5 The $H_2/\ell_1/H_\infty$ Results. The second part of this example involved improving the complementary sensitivity (as measured by the ∞-norm) for a given level of tracking performance (as measured by the 1-norm on weighted sensitivity). The cases shown in Table 6.2 held a 1-norm constraint level of 2.5, and Figure 6.10 shows the com-

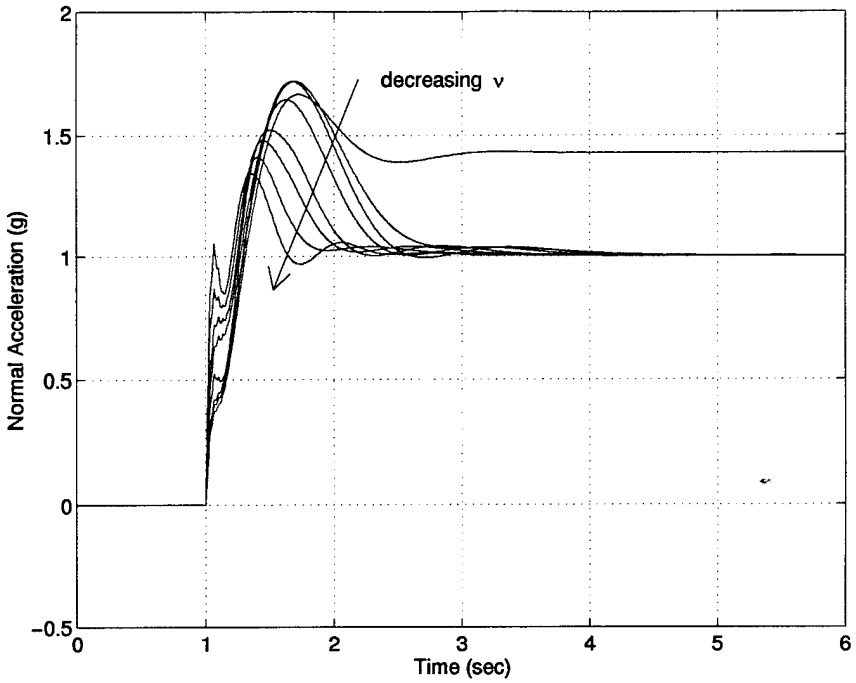

Figure 6.4 Step Response for H_2/ℓ_1 Designs

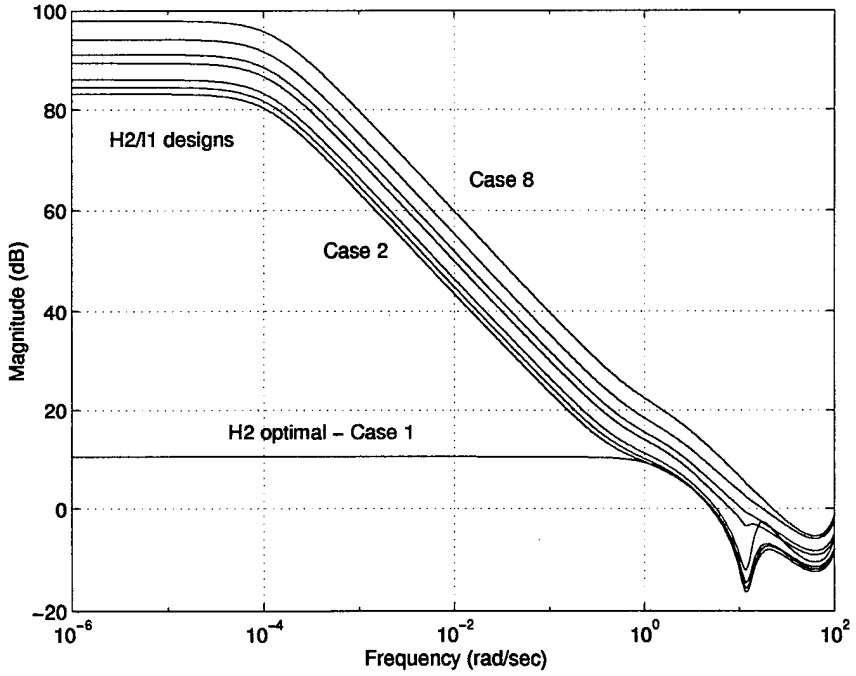

Figure 6.5 Max. Singular Values of GK, H_2/ℓ_1 Designs

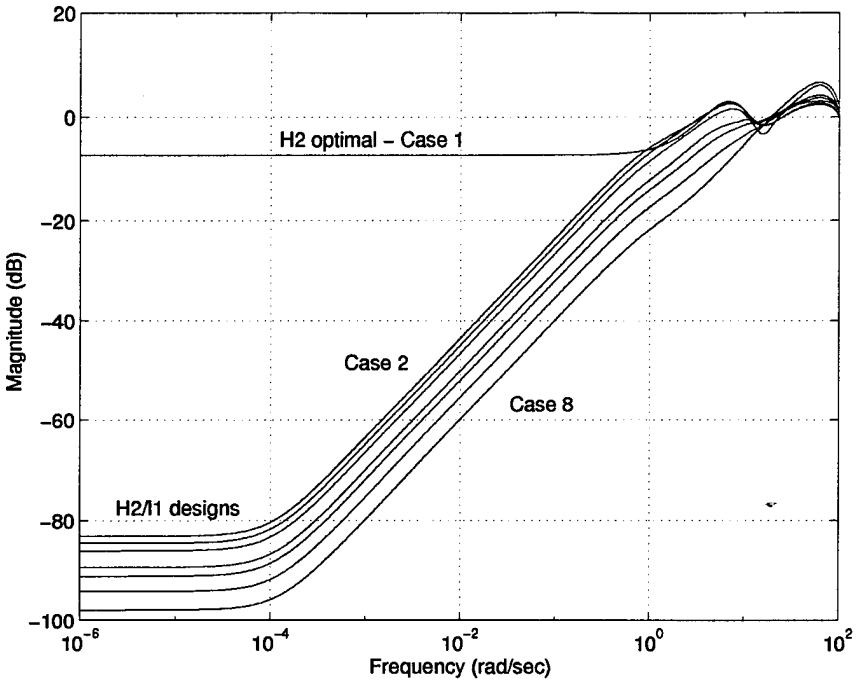

Figure 6.6 Sensitivity, H_2/ℓ_1 Designs

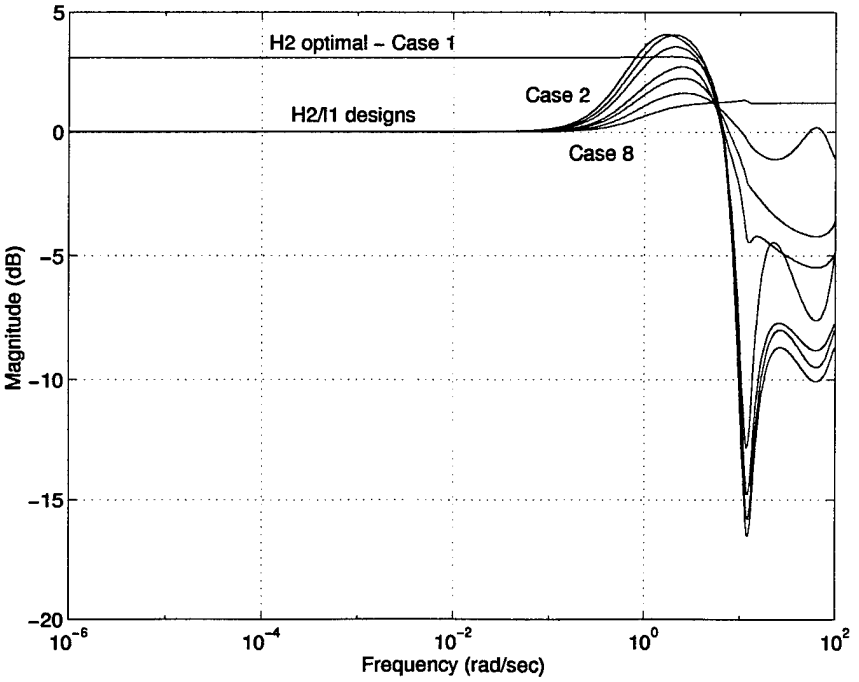

Figure 6.7 Complementary Sensitivity, H_2/ℓ_1 Designs

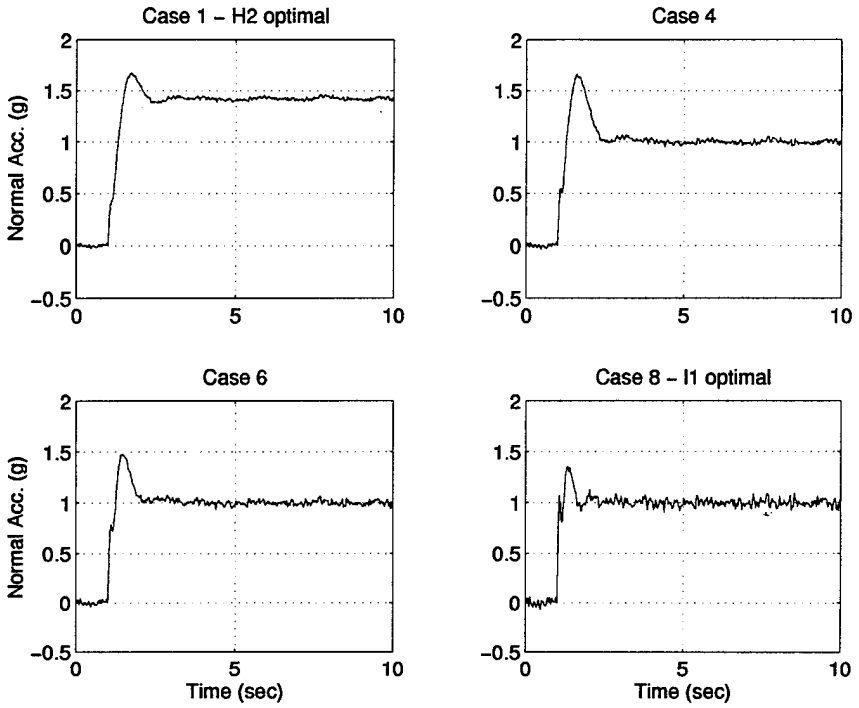

Figure 6.8 Step Response with Noise, H_2/ℓ_1 Designs

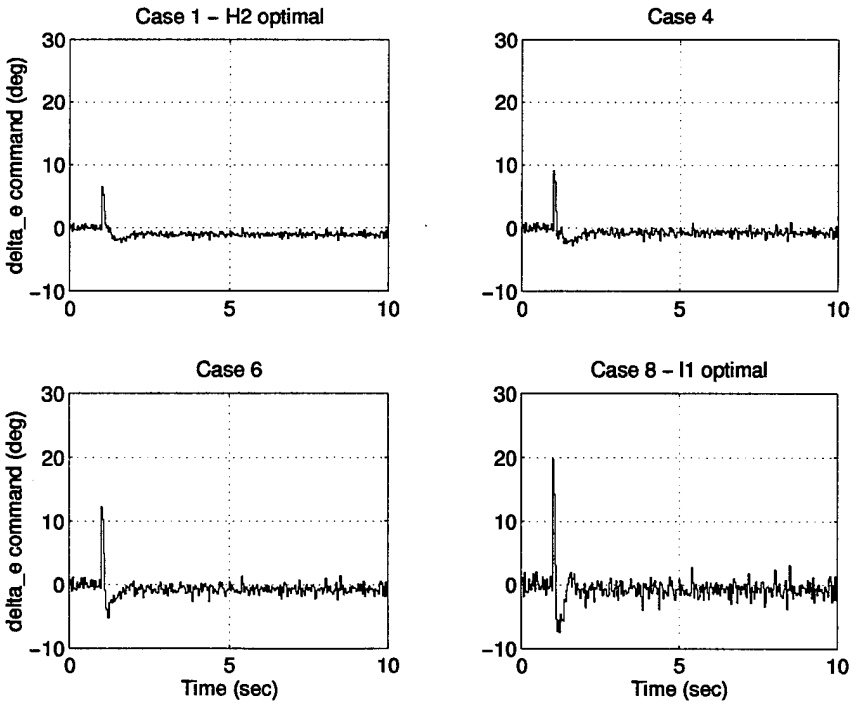

Figure 6.9 Control Usage for Step Response with Noise, H_2/ℓ_1 Designs

plementary sensitivity plots for these cases. As shown in the plots, the method effectively reduced the singular value peak by decreasing γ, while maintaining a desired level of tracking performance. Figure 6.11 shows step responses and control usage for Cases 1, 4 and 13. These particular cases were chosen to make a performance comparison between the H_2 regulator, an H_2/ℓ_1 controller which includes tracking, and an $H_2/\ell_1/H_\infty$ design which includes tracking and improved stability robustness. For this particular problem, the H_∞ constraint imposed on Case 13 actually improved the tracking, but this generally will not be true for more complex MIMO systems. Both Cases 4 and 13 again show that the penalty for improved tracking and robust stability is increased control usage and susceptibility to noise.

Table 6.2 Mixed $H_2/\ell_1/H_\infty$ Control Results

Case #	$\|T_{zw}\|_2$ α	$\|T_{mr}\|_1$ ν	$\|T_{ed}\|_\infty$ γ
9	0.192	2.50	1.45
10	0.202	2.50	1.40
11	0.217	2.50	1.35
12	0.237	2.50	1.30
13	0.259	2.50	1.25
14	0.287	2.50	1.20
15	0.325	2.50	1.15

A final note is in order concerning the F-16 example. This example did not demonstrate a compelling need for a full mixed-norm approach to controller design. Although the H_2/ℓ_1 problem clearly demonstrated the competing objectives of tracking, noise rejection and control usage, the stability margins were good enough that a separate constraint for stability robustness was probably not necessary. As an additional measure of robust stability, the independent gain and phase margins (IGM and IPM, respectively) are shown in Table 6.3. These margins represent the largest independent variation in either gain or phase for which the system remains stable. For a SISO system, the gain margin is the union of the complementary sensitivity gain margin and the sensitivity gain margin. However, for MIMO systems, this is not the case; in general both forms of the gain margins should be considered [65]. As shown, gain margins are $[-10 \quad 6]$ dB or better and phase

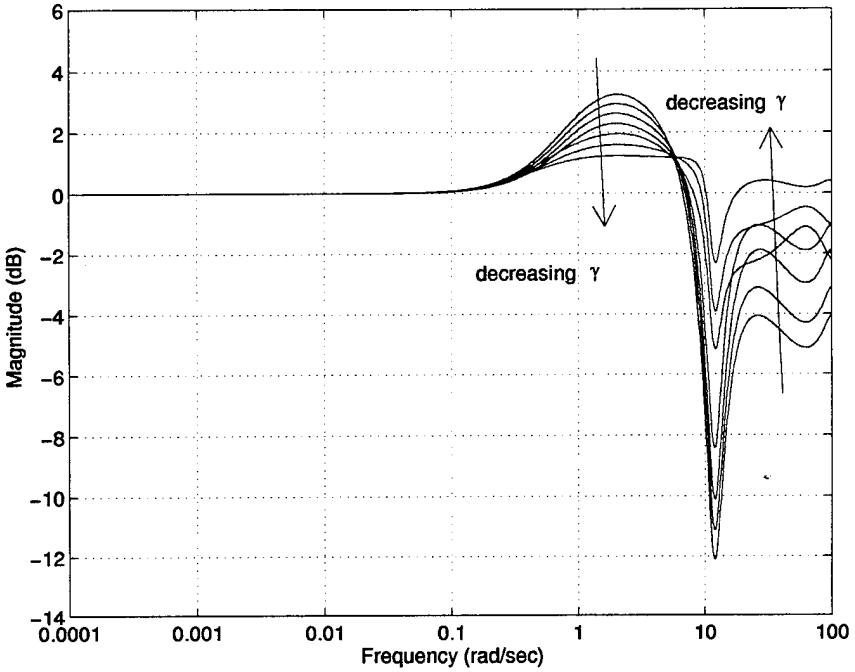

Figure 6.10 Complementary Sensitivity, $H_2/\ell_1/H_\infty$ Designs

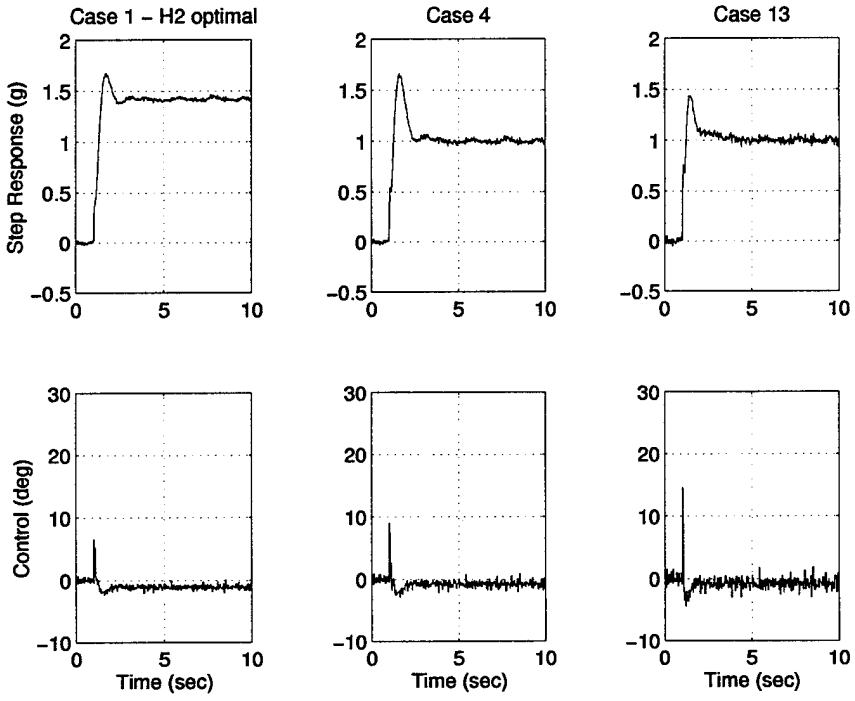

Figure 6.11 Step Response, Design Cases 1, 4 and 13

Table 6.3 Mixed Optimal Independent Gain/Phase Margins

Case #	$\|T_{ed}\|_\infty$	$\|T_{mr}\|_1$	$IGM(dB)$	$IPM(deg)$
1	1.43	Very Large	[−10.38 10.76]	41.6
2	1.60	2.70	[−8.55 10.89]	41.8
3	1.59	2.60	[−8.57 11.49]	43.0
4	1.51	2.50	[−9.48 10.61]	41.3
5	1.37	2.40	[−11.42 9.18]	42.9
6	1.29	2.30	[−12.91 8.39]	45.5
7	1.20	2.20	[−15.47 5.93]	49.1
8	1.16	2.13	[−16.99 5.44]	50.8
9	1.45	2.50	[−10.16 8.96]	40.3
10	1.40	2.50	[−10.88 8.43]	41.8
11	1.35	2.50	[−11.73 7.64]	43.5
12	1.30	2.50	[−12.74 7.02]	45.2
13	1.25	2.50	[−13.98 6.59]	47.2
14	1.20	2.50	[−15.56 6.25]	49.3
15	1.15	2.50	[−17.69 5.93]	51.5

margins are 40 *deg* or better for almost all cases. A worthwhile addition to this problem might be to add ℓ_1 constraints for control usage and/or control rate. As a proof of concept, however, it has been demonstrated that the present method can effectively combine the three different norms in a single constrained optimization problem.

6.6 Convexity vs. Controller Order

Although it is well known that the general output feedback problem is non-convex when the compensator order is fixed, few researchers have explored this potential problem area. In fact, most published results for H_2/H_∞ tend to show smooth convex Pareto curves demonstrating the tradeoffs between the norms. Although a first glance at these results might suggest that the non-convexity of the problem is a theoretical concern only, there are more than enough ill-behaved examples to convince any researcher otherwise. Furthermore, experience with several examples has shown that non-convexity is even more of a problem for H_2/ℓ_1 than it is for H_2/H_∞.

The primary numerical difficulty with non-convex problems is that an optimization algorithm can get stuck at a local minimum which may actually be suboptimal or even infeasible (i.e., it doesn't satisfy the constraints). Further, if the desired result is to define the Pareto curve or surface, a non-convex problem may not allow free movement along the curve or surface, thus requiring the algorithm be reinitialized repeatedly. Curves which appear monotonically decreasing may actually be masking discontinuities in the design space. Figure 6.12 shows the Pareto curve for the SISO F-16 aircraft problem considered in the previous section. The curve clearly shows two distinct segments: one segment is for $\nu \leq 2.43$, and the second segment is for $\nu \geq 2.43$. The two segments actually represent two local "valleys" in the parameter space. Further, it requires a discontinuous jump in the design variables to move from one valley to the next, which is evident in the movement of the compensator eigenvalues (see Figure 6.13). Numerically, this discontinuity makes it necessary to define the two portions of the curve seperately. An unaided optimization algorithm may be unable to transition from one valley to the next when progressing along the curve, making it necessary to restart the optimization algorithm from a new location in the parameter space. Also, the fact that the dicontinuity occurs in the compensator eigenvalues suggests that this problem cannot be avoided simply by choosing a different state space formulation.

Figure 6.14 superimposes the Pareto curves for third, fifth, and tenth order compensators, along with the curve for the optimal compensator. The optimal compensator was found using the free order method from Section 4.6, and it was 106^{th} order without any attempted order reduction. As shown, the apparent non-convexity disappears as the compensator order is increased. This is not surprising, since the free-order problem discussed in Chapter IV was shown to be convex. However, the higher order curves can be deceiving. Despite the convex appearance of the fifth order curve, Figure 6.15 clearly shows that there is still a discontinuity in the movement of the eigenvalues. As in the third order curve, this discontinuity makes it difficult for the unaided algorithm to traverse the entire curve. It becomes necessary to restart the algorithm using a compensator from a different location in the parameter space.

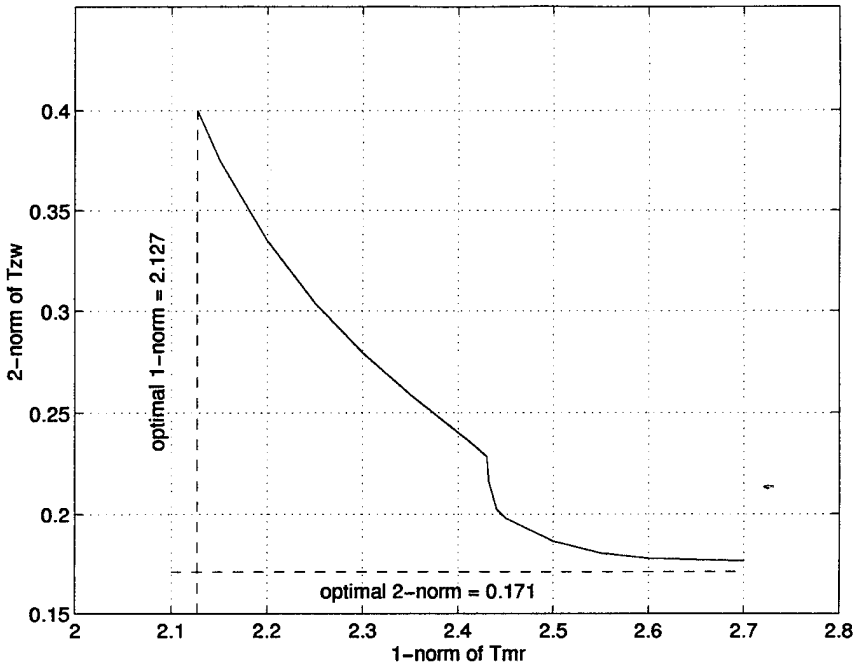

Figure 6.12 H_2/ℓ_1 Results: Compensator order = 3

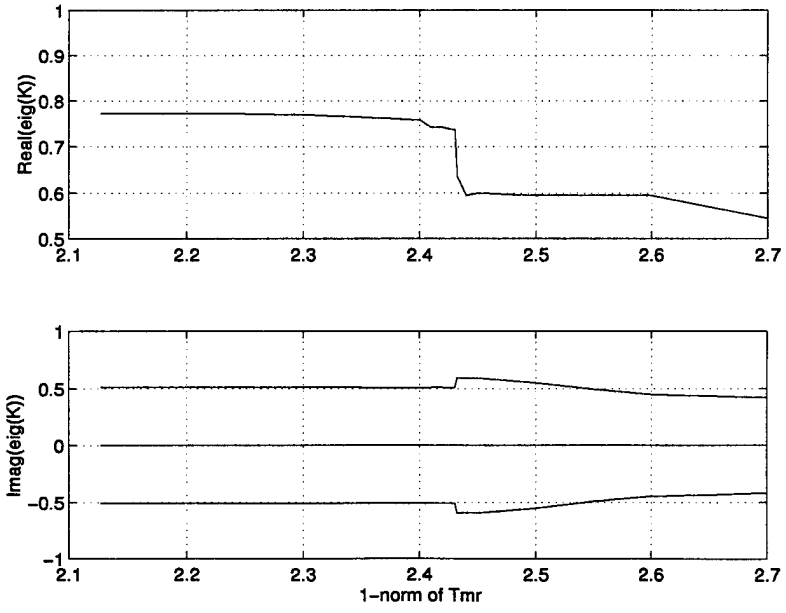

Figure 6.13 Compensator Eigenvalues for Third-order H_2/ℓ_1 Compensators

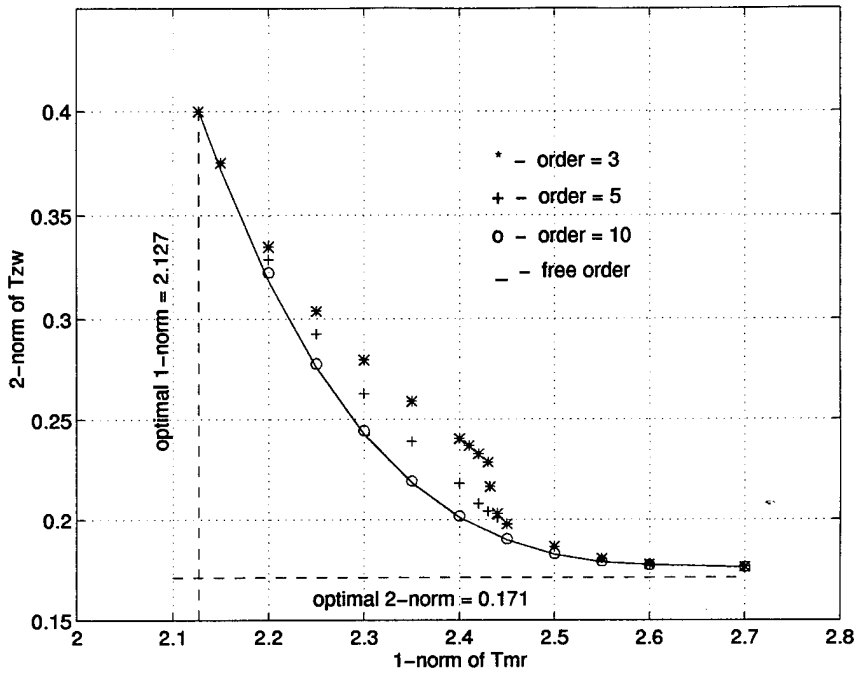

Figure 6.14 H_2/ℓ_1 Results: Fixed vs. Free-Order Compensators

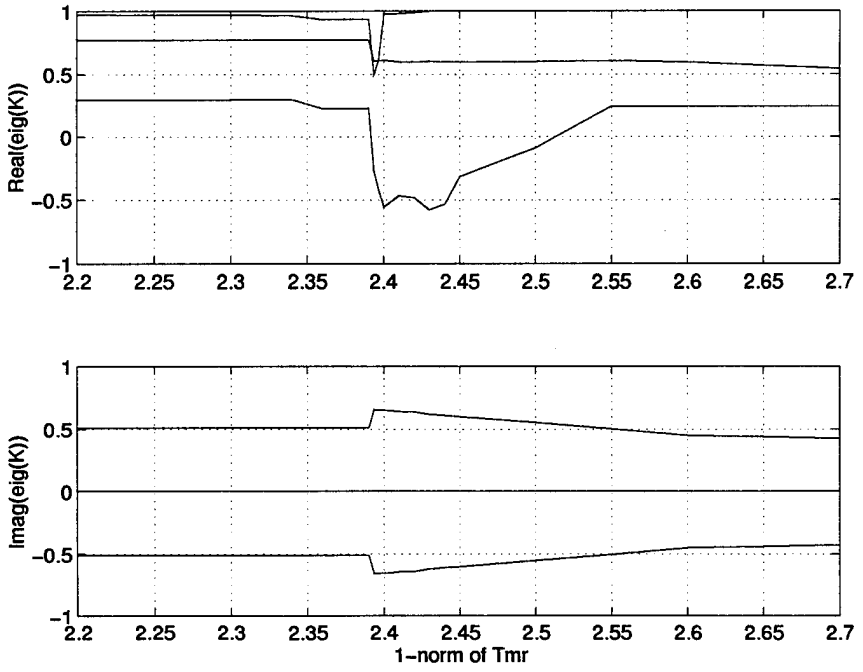

Figure 6.15 Compensator Eigenvalues for Fifth-order H_2/ℓ_1 Compensators

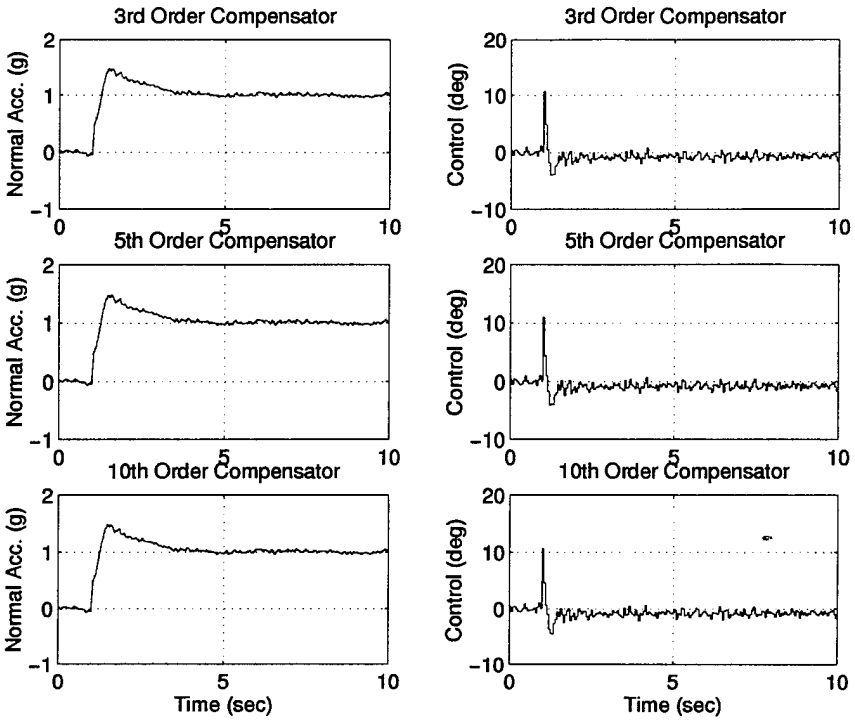

Figure 6.16 Step Responses for Varying Compensator Orders, $\|T_{mr}\|_1 = 2.5$

In addition to demonstrating the non-convexity of the fixed-order problem, Figure 6.14 also highlights an important consideration when choosing a controller order. If, for this problem, a 1-norm constraint level of 2.5 was chosen, very little is sacrificed in terms of 2-norm performance in order to obtain a third-order controller (see Figure 6.16). The curves for third, fifth and tenth-order controllers are almost indistinguishable in terms of step response, noise rejection and control usage. However, a 1-norm constraint level of 2.4 shows a different result (see Figure 6.17). Here we see a slight penalty in terms of control usage for the third-order compensator, and a higher order compensator might be justified by the improvement in performance offered in this case. Issues such as this need to be closely examined prior to selecting an arbitrarily low-order compensator.

A final point should be made regarding the non-convexity of the fixed-order, mixed-norm control synthesis problem. Just as the convexity of the problem may change with controller order, it also changes with the norm used to define the constraint. For example, the F-16 example behaves quite differently when the ∞-norm is used to constrain the weighted sensitivity. (As stated earlier, H_∞ constraints can be used to provide tracking,

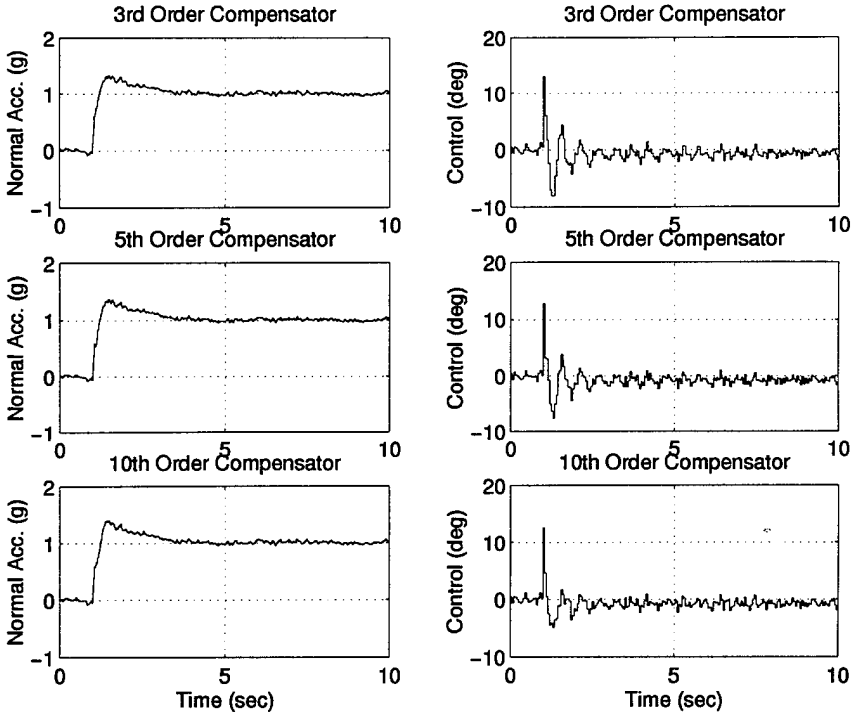

Figure 6.17 Step Responses for Varying Compensator Orders, $\|T_{mr}\|_1 = 2.4$

but they tend to be even more susceptible to high frequency noise than an equivalent ℓ_1 constraint.) Figure 6.18 shows the third order Pareto curve for an H_2/H_∞ problem using the same transfer functions as the H_2/ℓ_1 problem shown earlier. The curve appears convex, and Figure 6.19 reveals no discontinuities in the eigenvalue traces. It is not being suggested that all fixed-order H_2/H_∞ problems will behave like this; indeed, part of this smoothness can be explained by where on the H_2/ℓ_1 curve the H_2/H_∞ results would fall. The value of $\|T_{mr}\|_1$ varies from 3.5 to 3.1 as $\|T_{mr}\|_\infty$ varies from 1.5 to 1.1 for the H_2/H_∞ results. This is well clear of the discontinuity in the H_2/ℓ_1 curve, which occurs around $\|T_{mr}\|_1 = 2.4$. Despite this partial explanation, however, experience with other examples suggests that H_2/ℓ_1 problems are more likely to have problems with local minima and non-convex regions than equivalent H_2/H_∞ problems. This is an area of research which should be pursued further.

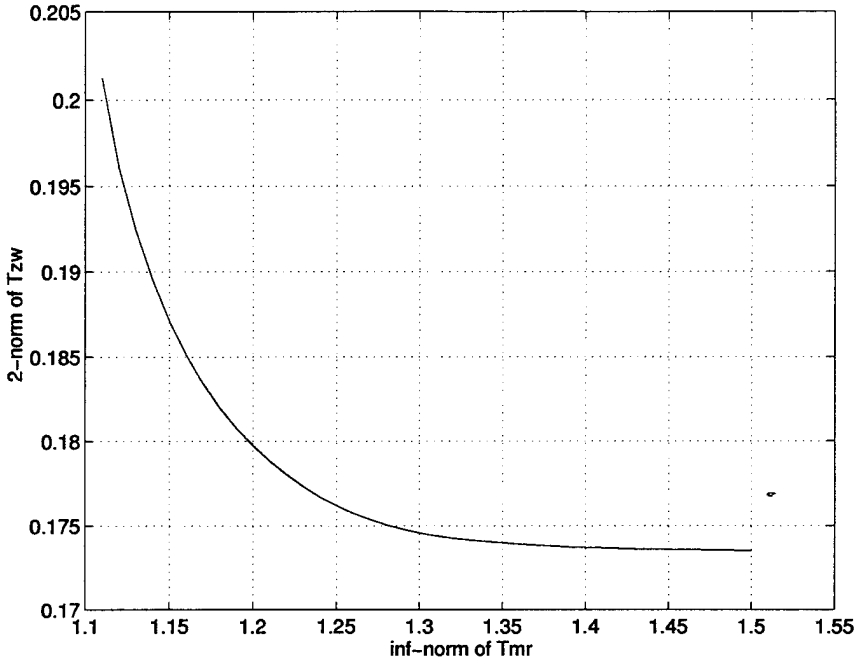

Figure 6.18 H_2/H_∞ Results: Compensator order = 3

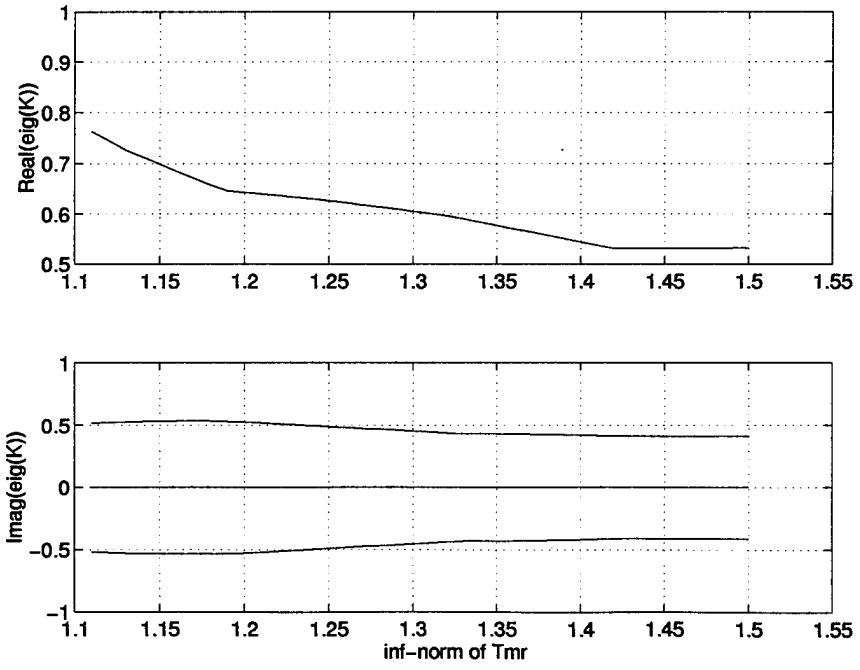

Figure 6.19 Compensator Eigenvalues for Third-order H_2/H_∞ Compensators

6.7 Summary

This chapter developed a numerical method for solving the general fixed-order, mixed-norm control problem for discrete-time linear systems. The method will minimize the 2-norm of a transfer function, while constraining the 1-norms and/or ∞-norms of an arbitrary number of dissimilar but related transfer functions. The method can be used without modification to design controllers of higher or lower order than any of the individual transfer functions. The problem is solved numerically using gradient-based, constrained, nonlinear programming methods. Overall efficiency has been greatly improved by providing analytic gradients for virtually all aspects of the problem, and the discrete-time algorithms have been combined with similar continuous-time algorithms to provide a single Mixed-Norm Toolbox for use with MATLAB. The next chapter will demonstrate two examples of mixed-norm control synthesis, including an example which extends the current method to include the multi-plant problem.

VII. Examples of Fixed-Order, Mixed-Norm Control Synthesis

This chapter provides two examples of fixed-order, mixed-norm control synthesis. The first of these examples is a MIMO longitudinal controller design for an A-4 aircraft in terrain following mode. The purpose of this first example is to explore the application of ℓ_1 constraints for regulating altitude error in terrain following. It has often been postulated that ℓ_1 methods are natural for terrain following due to the need for tight constraints on the absolute magnitude of tracking error. Although this example will demonstrate the benefits of using ℓ_1 constraints for tracking error, it will also show that the actual value of the ℓ_1 norm as a measure of allowable error is too conservative to be used explicitly. This terrain following example also represents one of the most numerically challenging design problems attempted to date using mixed-norm control methods. It is a general multi-block problem, it has widely separated open-loop poles, and the full-order controller design results in a ninth-order compensator with 90 design variables in the optimization problem.

The second example in this chapter extends the fixed-order, mixed-norm method to include multi-plant problems whereby the underlying plant dynamics associated with each of the subproblems are no longer required to be identical. The example chosen to demonstrate this is the 1992 American Control Conference benchmark problem for robust stability [25]. The H_2 and ℓ_1 subproblems will be used to obtain nominal performance for the nominal plant condition, while the H_∞ subproblem will be used to establish robust stability centered about an off-design plant condition. Specifically, the H_2 and ℓ_1 subproblems will be set up to examine root mean square control weighting via an LQG design, versus bounding the worst case magnitude on control usage via an ℓ_1 constraint. This example will highlight the importance of targeting specific constraints, as well as showing an application of the Small Gain Theorem for ensuring robust stability in a mixed-norm design. The H_∞ norm will be used to apply the Small Gain Theorem in this example because it results in a less conservative (less restrictive) constraint on the problem. As a followup to the discussion in the previous chapter concerning the existence of optimal mixed-norm controllers, this example also will be used to define the location of mixed-norm controllers on a Pareto optimal surface of stabilizing controllers.

7.1 MIMO Aircraft Terrain Following Example

7.1.1 Problem Overview. This section will demonstrate $H_2/\ell_1/H_\infty$ control synthesis for a general multi-block plant. The example used will be a longitudinal controller design for a fighter aircraft in a terrain following mode. It has often been speculated that ℓ_1 optimization might be well suited to terrain following applications because of its ability to place upper bounds on the error magnitude for unknown but bounded magnitude inputs; this example will investigate the applicability of ℓ_1 constraints for this purpose.

The objective for this example is to design a controller which has satisfactory performance in the presence of wind gusts and measurement noise, while achieving acceptable error bounds on the magnitude of the altitude error for bounded magnitude command inputs. The aircraft is an A-4 operating at sea level, Mach 0.85 [66]. There are five states in the basic plant: vertical velocity in the aircraft axes (w, meters/sec), altitude perturbation (h, meters), pitch rate (q, radians/sec), pitch angle (θ, radians) and forward velocity perturbation in the aircraft axes (u, meters/sec). The control inputs are elevator deflection (δ_e, radians) and throttle (δ_T). A throttle control was specifically included in this example to help maintain forward velocity during a commanded change in altitude. The throttle repsonse was assumed to be more sluggish than that of the elevator, and this makes it less attractive for controlling the states which vary quickly. However, natural forward velocity variations are mainly due to the slowly varying phugoid mode, and the throttle provides excellent control authority over this state. Measurements are assumed available from a combination of air data and some type of inertial measurement unit, and measurements consist of altitude rate, altitude, normal acceleration felt by the pilot (n_z), pitch angle, and forward velocity perturbation. Commanded inputs will be a combination of flight path angle (or altitude rate) and altitude. Controlled outputs will be various combinations of the measurements. The goal is to enable the aircraft to follow flight path angle and altitude commands quickly and accurately, maintain low overshoot and reasonable settling times, keep control usage and pilot g-levels within reasonable bounds, and have the steady state flight be relatively insensitive to wind gusts and measurement noise. The continuous-time

plant is given by

$$\begin{Bmatrix} \dot{w} \\ \dot{h} \\ \dot{q} \\ \dot{\theta} \\ \dot{u} \end{Bmatrix} = \begin{bmatrix} -2.23 & 0 & 289.13 & 0 & -0.1134 \\ -1 & 0 & 0 & 289.13 & 0 \\ -0.15513 & 0 & -4.1708 & 0 & 0.0041218 \\ 0 & 0 & 1 & 0 & 0 \\ -0.0368 & 0 & 0 & -9.8066 & -0.0308 \end{bmatrix} \begin{Bmatrix} w \\ h \\ q \\ \theta \\ u \end{Bmatrix}$$

$$+ \begin{bmatrix} -57.302 & 0 \\ 0 & 0 \\ -63.754 & .000243 \\ 0 & 0 \\ 0 & .002344 \end{bmatrix} \begin{Bmatrix} \delta_e \\ \delta_T \end{Bmatrix} \tag{7.1}$$

$$\begin{Bmatrix} \dot{h} \\ h \\ n_z \\ \theta \\ u \end{Bmatrix} = \begin{bmatrix} -1 & 0 & 0 & 289.13 & 0 \\ 0 & 1 & 0 & 0 & 0 \\ -0.17918 & 0 & 30.780 & 0 & -.01284 \\ 0 & 0 & 0 & 1 & 0 \\ 0 & 0 & 0 & 0 & 1 \end{bmatrix} \begin{Bmatrix} w \\ h \\ q \\ \theta \\ u \end{Bmatrix} \tag{7.2}$$

Actuator dynamics are assumed for both the elevator and the thrust, and are modelled as follows:

$$\begin{aligned} \delta_e(s) &= \frac{20}{s+20}\delta_{e_c}(s) \\ \delta_T(s) &= \frac{5}{s+5}\delta_{T_c}(s) \end{aligned} \tag{7.3}$$

As mentioned previously, the throttle was assumed to be more sluggish than the elevator in order to discourage its use for controlling the faster varying modes of the system.

The basic plant includes the short period mode ($\omega_{sp} = 7.35$ rad/sec), phugoid mode ($\omega_p = 0.0696$ rad/sec), and an additional pole at the origin resulting from the altitude state. The wide separation in frequency between the modes presents a challenging problem; a sample rate fast enough to accommodate the short period and actuator modes will result in high truncation levels in order to capture the phugoid and integrator state. A sample

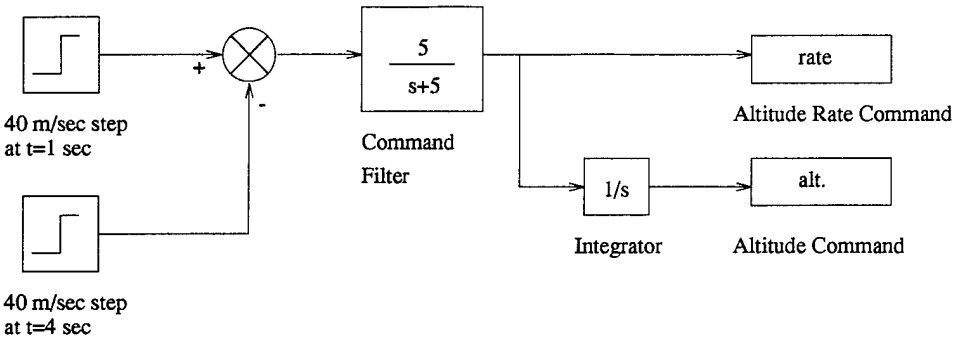

Figure 7.1 Command Generator Used for Simulation

rate of 20 Hz was chosen based on the actuator modes ($6.3 \times \omega_{\delta_e}$), and a zero-order hold was used for discretization of the transfer functions. Simulations of the various closed-loop systems used a continuous-time plant and discrete-time compensators. Further, in order to provide a more realistic reference command (as opposed to a discrete step input) with which to evaluate the controllers, a command generator was used in the closed-loop simulations (see Figure 7.1). The command generator provides a commanded increase in altitude of 120 meters which takes place over 3 seconds. The command filter with $\omega_c = 5$ rad/sec was chosen to model either pilot lag or command smoothing on the part of an automatic terrain following mode. As a pilot model, the command filter represents a "fast" pilot, thus presenting a more challenging design problem.

7.1.2 H_2 Subproblem. The H_2 subproblem is based on a steady state Linear Quadratic Gaussian (LQG) design. A wind disturbance, which enters the plant as an angle of attack disturbance, is modelled as the output of a first-order shaping filter driven by zero-mean white Gaussian noise, and is included in both the design model and the simulation model. Intensity levels and time constants are chosen for sea level flight in cumulus clouds as used for the control designs on the NASA F-8C [67]. The wind gust state and the input vector describing how it enters the plant are as follows:

$$\dot{w}_g = -9.486\, w_g + w \tag{7.4}$$

$$B_{w_g} = [-7.713 \times 10^{-3} \quad 3.459 \times 10^{-3} \quad -5.365 \times 10^{-4} \quad 0 \quad -9.807]^T \tag{7.5}$$

Controlled outputs consist of the measurements with weightings of 10, 1000, 1000, 10 and 1 on $\dot{h}$, h, n_z, θ and u, respectively. To enable non-zero set point tracking, a pseudo-integral state on altitude error was added to the plant as follows:

$$i_h(s) = \frac{1000}{s + 0.001} \; (h(s) \; - \; h_c(s)) \tag{7.6}$$

and a weight of 0.1 was used for the output of the pseudo-integral state. Control weights of 0.1 and 1 were used for δ_e and δ_T, respectively. All of the weights were chosen subjectively and iteratively based on closed-loop simulations, with a goal of maintaining steady forward velocity during a commanded change in altitude, maintaining g-levels below 4 g's for simulated commands, and accurately tracking altitude and altitude rate commands. The most difficult of these design goals was the maintainance of g-levels, but this was partially due to the "fast" pilot model being used for evaluation. Naturally, for any given controller, a slower command will result in a lower g-level and a more sluggish response. The higher weight on δ_T as opposed to that on δ_e is again meant to discourage the use of thrust over elevator commands. Thrust is primarily intended to maintain forward velocity.

The measurements are assumed corrupted by zero-mean, white Gaussian noises with the strength initially set to 10^{-4} rad^2–sec. This noise level was chosen somewhat arbitrarily, but it represents a higher noise level than was used for the F-16 problem in Chapter VI, which used a measurement noise level of 10^{-6} rad^2–sec. After several iterations, the noise strength on the θ measurement was dropped to 10^{-5} to reflect the smaller unit dimensions (radians, as compared to meters, and meters/sec). The H_2 solution was found to be very sensitive to the value of the noise strength placed on the altitude measurements, and this is shown in Figure 7.2 for noise strengths of 10^{-4} and 10^{-5}. As shown, the 10^{-5} setting results in a much quicker response at the expense of higher g-loading (not shown) and much wider fluctuations in pitch response. The final design opted for the quicker tracking associated with a noise strength of 10^{-4} rad^2–sec. It was decided to allow for the high overshoot and large pitch variations in the H_2 portion of the problem in hopes that it could be significantly reduced using an ℓ_1 constraint. Overall, the H_2 subproblem provides quick response to altitude and altitude rate errors, and is generally unaffected by wind

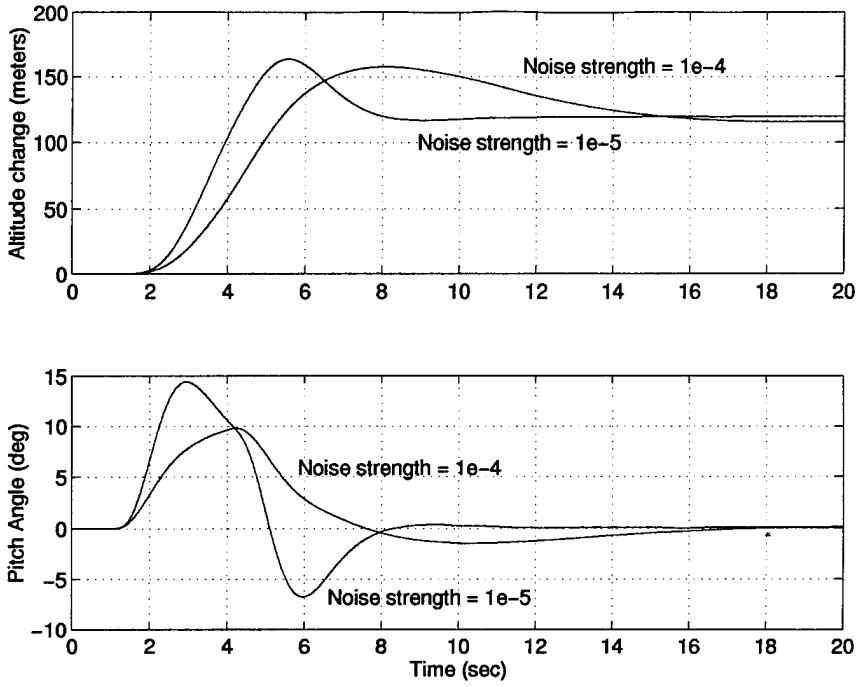

Figure 7.2 Sensitivity of H_2 Performance to Altitude Noise Strength

gusts and measurement noise. The noise levels used for the simulation were generally higher than those used to synthesize the controller. This was done in order to highlight differences between the controllers; the presence of the measurement noise was not always readily apparent in the simulations, with the exception of normal acceleration and control usage.

The final H_2 plant for this example is ninth order, which will also be the order of the H_2 optimal compensator. This example will not attempt to examine reduced-order compensators, so the mixed-norm compensators will also be ninth order. With a ninth-order compensator, the total number of design variables for this example will be 90, of which 45 will be in the compensator B matrix. This represents one of the most challenging examples tried to date (discrete-time or continuous-time) using mixed-norm control synthesis.

7.1.3 ℓ_1 Subproblem. The ℓ_1 subproblem was used to reduce the maximum magnitude of the altitude error, thereby reducing the large overshoot resulting from the H_2 subproblem. The bounded magnitude inputs were taken as the wind gust and commanded

altitude and altitude rate (or flight path angle). We wish to be able to reject the wind gust while tracking the altitude and altitude rate commands. A more general sensitivity constraint could have been used as an alternative, but the H_2 subproblem provided adequate state regulation, and we were exclusively interested in constraining altitude error. The controlled altitude error was band limited in order to reduce the susceptibility to measurement noise,

$$h_o(s) = \frac{4}{s+4} \; (h(s) \; - \; h_c(s)) \tag{7.7}$$

and a weight of 1 was used. The value of the weight for the ℓ_1 constraint is unimportant for this problem because it is a single output constraint. Any scalar weighting factor would simply result in a scaled constraint value with no effect on the solution to the mixed-norm problem. Specifically, a unity weight with a constraint value of ν would be the same as a weight of c and a constraint value of $c\nu$. The bandwidth of the frequency weight was based on the pilot model, and could have been set to 5 rad/sec to coincide with the command filter used for simulation. However, since the ℓ_1 gradient algorithm switches to finite difference methods for the case of repeated roots, the bandwidth was dropped to 4 rad/sec so as not to coincide with the open-loop pole from the throttle dynamics. This still represents relatively fast pilot commands for the design model, and it allows the ℓ_1 gradient algorithm to take advantage of the analytic formulations.

Another consideration in deciding how and when to use ℓ_1 constraints is the high numerical overhead associated with ℓ_1 subproblems. By far, the ℓ_1 function and gradient calculations are the most costly portion of the numerical optimization problem, and each additional ℓ_1 constraint adds to the computational burden. For this reason, it pays to be selective on which outputs ℓ_1 constraints are applied to. The ℓ_1 constraint for this problem had no weights at all on control usage, thus the constraint is singular. Further, no additional ℓ_1 constraints were used to weight either control usage or control rate. The control weights in the H_2 subproblem ensure that the overall synthesis problem will be non-singular, and it will be shown in the next section that the particular flight condition chosen for this example resulted in more than adequate control authority for all of the mixed-norm controllers.

Table 7.1 Mixed H_2/ℓ_1 Control Results

Case #	$\|T_{zw}\|_2$ α	$\|T_{mr}\|_1$ ν
1 (H_2 optimal)	0.15840	3.086
2	0.15840	2.800
3	0.15841	2.600
4	0.15844	2.400
5	0.15851	2.200
6	0.15861	2.000
7	0.15907	1.800
8	0.16164	1.600

7.1.4 H_2/ℓ_1 Results. Table 7.1 shows norm values for several of the H_2/ℓ_1 compensators, and Figure 7.3 shows the corresponding simulation results for a 40 m/sec climb held for 3 sec. As shown, the ℓ_1 constraint can significantly reduce the overshoot without sacrificing rise time and overall speed of response. The large overshoot associated with the higher levels of the 1-norm constraint is especially troublesome, because it represents increased vulnerability of the aircraft. It also represents a potentially hazardous situation for the pilot if a decrease in altitude were commanded in low level flight.

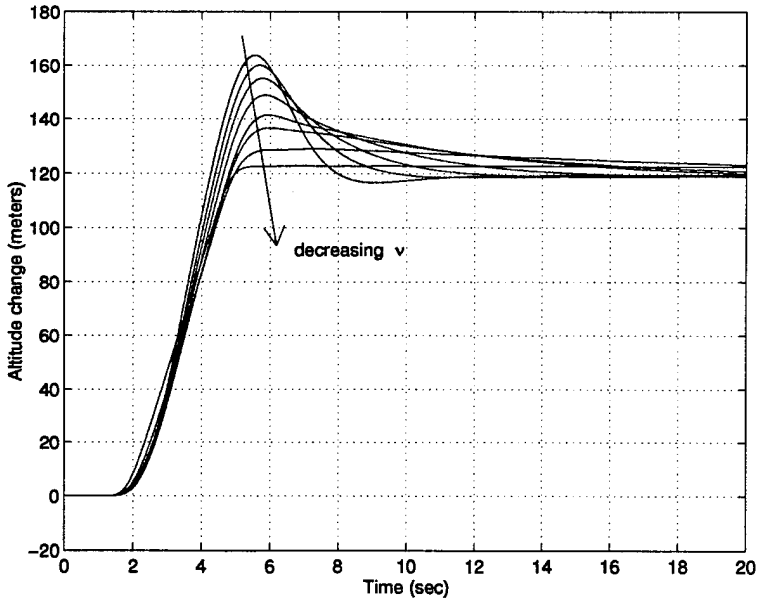

Figure 7.3 Response to Altitude Change for H_2/ℓ_1 Designs, Cases 1-8

The settling time for the H_2/ℓ_1 systems could be improved by using several methods. In addition to the pseudo-integral state added to the H_2 subproblem, a similar weight on altitude error could have been added to the ℓ_1 subproblem. A second method, which would have required only minor modification to the algorithms, would be to add a decaying exponential (time-domain) weight on the ℓ_1 transfer function. For this example, the decision was to leave the ℓ_1 subproblem as is, in order to see if there was any physical significance of the 1-norm value in terms of maximum peak-to-peak gain. As it turned out, the value of $\|T_{mr}\|_1$ is so conservative that the physical significance is almost meaningless. For instance, $\|T_{mr}\|_1 = 2$ indicates that there could be a worst case altitude error of 200 meters resulting from some combination of a 100 m/sec (or less) altitude rate command and 100 m (or less) altitude command. Although this sounds extremely bad, the associated time response for Case 6 shows a relatively good response to a combined altitude and altitude rate command in the presence of wind gusts and measurement noise. For this reason, the actual values of the ℓ_1 norm should probably be used only for comparison purposes in most problems. This has always been the case with the 2-norm and ∞-norm of a transfer function, and it appears to apply to the 1-norm as well.

An additional drawback of the large overshoot associated with the H_2 solution is evident in the pitch angle response shown in Figure 7.4. Neglecting angle of attack, a 40 m/sec climb represents an 8 deg pitch angle. Note that the H_2 solution (Case 1) has a pitch response which peaks at close to 15 deg, while the H_2/ℓ_1 solutions all peak closer to 10 deg. Also, a large negative pitch angle (-7 deg) in Case 1 results from the rapid decrease in altitude as the compensator attempts to damp out the large error associated with the overshoot. The H_2/ℓ_1 systems show negative pitch angles of only -2.5 deg or less for the same commanded inputs. These are clearly desirable features of the H_2/ℓ_1 systems. Drawbacks of the H_2/ℓ_1 systems are increased g-loading on the pilot and greater susceptibility to measurement noise as shown in Figures 7.5 and 7.6. Although all of the systems demonstrate relatively high g levels associated with the command response, the desired g-limit of 4 for the simulated command has been met for $\nu = 2.0$ or higher. Further, a slightly reduced bandwidth on the simulation command filter (down to 2-3 rad/sec) decreases the peak g-level to below 3. Although this results in a slightly more

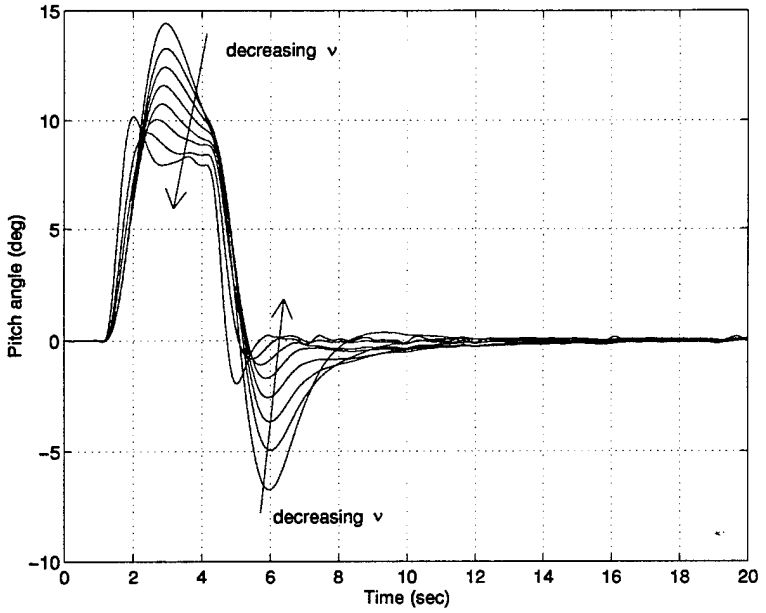

Figure 7.4 Pitch Angle Response for H_2/ℓ_1 Designs, Cases 1-8

sluggish response, 2-3 rad/sec is a more realistic a pilot model. The steady state portion of the responses shown in Figure 7.5 show that the pilot gets an increasingly bumpy ride due to measurement noise as the ℓ_1 constraint level is decreased, and this also shows up in the commanded elevator levels shown in Figure 7.6. Note that the commanded elevator deflection due to the command input is actually lower for the H_2/ℓ_1 systems. It is also apparent that the modelled flight condition results in sufficient actuator authority, with the peak commanded actuator deflection being less than 5 deg for all cases. Actuator rates were not measured, but it is believed that the achieved rates are within allowable levels.

A final observation should be made regarding the 2-norms of the H_2/ℓ_1 compensated systems. Note that a 48% decrease in the value $\|T_{mr}\|_1$ results in only a 2% increase in the value of $\|T_{zw}\|_2$ (Case 1 vs. Case 8), and the two cases represent very different performance on the part of the closed-loop system. This has been found to be somewhat typical of discrete-time systems. The implication of this is that an accurate optimization algorithm, with relatively tight convergence criteria, is necessary in order to stay close to the true optimal H_2/ℓ_1 compensator. If convergence criteria are too loose, the resulting compensator may satisfy the constraints but result in an objective value ($\|T_{zw}\|_2^2$) higher

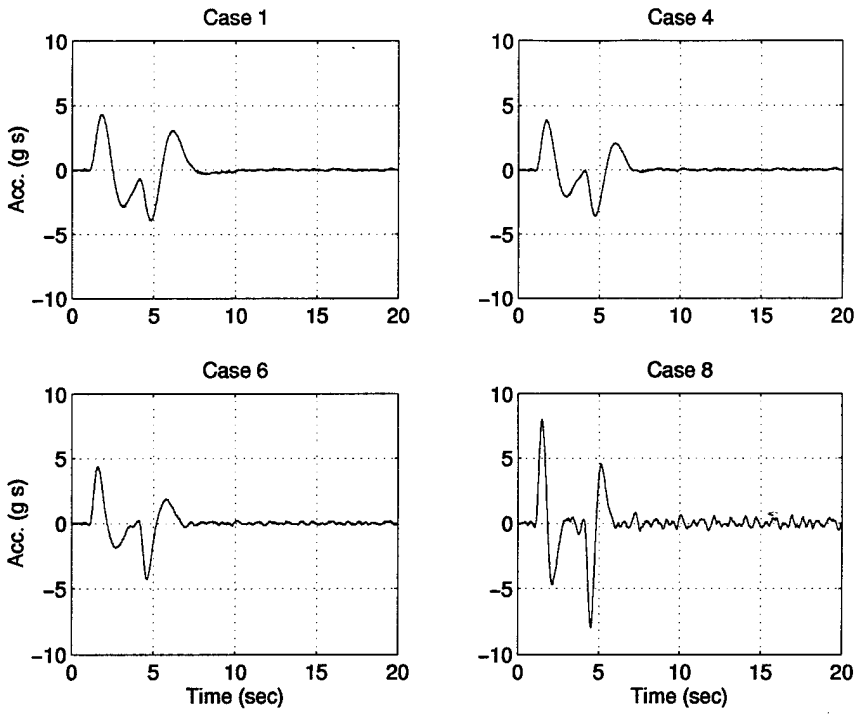

Figure 7.5 Normal Acceleration for H_2/ℓ_1 Designs

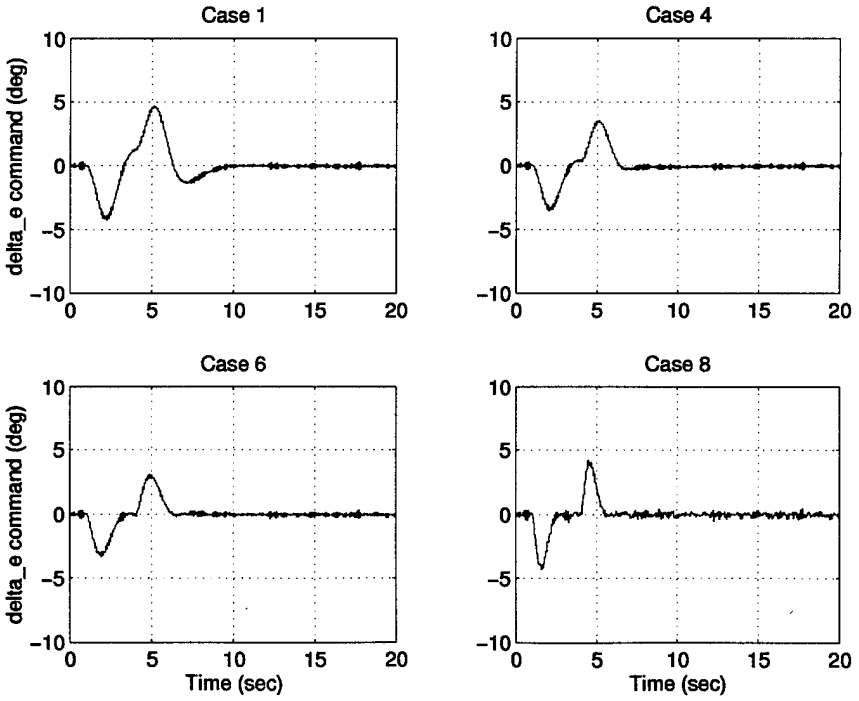

Figure 7.6 Commanded Control for H_2/ℓ_1 Designs

than the minimum attainable for the fixed-order problem. Further, we have shown that even small variations in $\|T_{zw}\|_2$ for this problem can represent significant differences in closed-loop performance.

7.1.5 $H_2/\ell_1/H_\infty$ Results. For the H_2/ℓ_1 cases discussed above, no attempt was made to monitor or improve robust stability levels for the closed-loop system; these concerns were temporarily set aside for the H_∞ subproblem. Figure 7.7 shows the H_2/ℓ_1 Pareto optimal curve and the resulting ∞-norms of the output complementary sensitivity (T_{ed}), used here as a measure of robust stability in the presence of output multiplicative uncertainty [65]. The ∞-norm and 1-norm constraints are not competing until $\|T_{mr}\|_1$ is pushed well below 2.0, after which the value of $\|T_{ed}\|_\infty$ increases significantly. Based on these curves, and the time responses shown previously, a 1-norm constraint level of $\nu = 2.0$ was chosen as the desired level of tracking. Holding this 1-norm constraint level, $\|T_{ed}\|_\infty$ was then reduced using $H_2/\ell_1/H_\infty$ optimization, and the resulting Pareto optimal curve is shown in Figure 7.8. An unweighted complementary sensitivity was used for T_{ed}, since the typical high frequency weight for unmodeled dynamics would take effect beyond the Nyquist sampling frequency for this system. As shown, $\|T_{ed}\|_\infty$ can be reduced further without a significant increase in $\|T_{zw}\|_2$ until γ is pushed below 1.6. The effect of reducing the singular value peaks of T_{ed} can clearly be seen in Figure 7.9, and the appearance of multiple active peaks for the lower γ levels is evident.

As a second measure of robust stability, the independent gain and phase margins are shown in Table 7.2. The gain margins for MIMO systems can not be taken as the union of the sensitivity (IGM_S) and complementary sensitivity (IGM_T) gain margins (as discussed in Section 6.5.5); therefore, both limits are shown. Modest improvements can be made in the gain and phase margins with only slight increases in $\|T_{zw}\|_2$. Acceleration (g) levels and control usage for Cases 9-12 are shown in Figure 7.10 and Figure 7.11, respectively. An unexpected bonus of improving the robust stability for this particular problem is that g-levels and control usage actually decreased. The target level of 4-g's has been met, and elevator commands are very low ($2 - 3deg$) for the simulated commands.

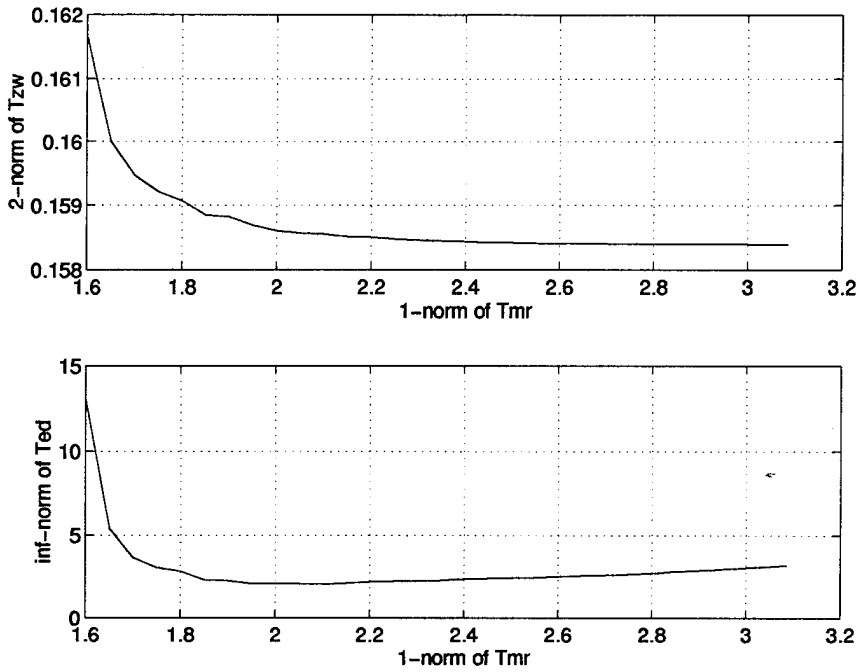

Figure 7.7 Resulting Norm Values for H_2/ℓ_1 Designs

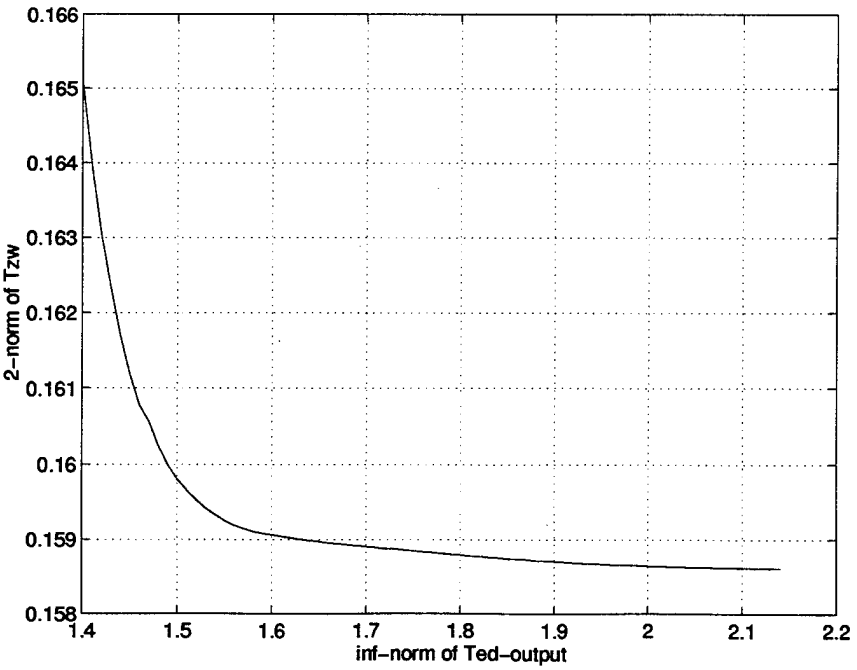

Figure 7.8 Pareto-optimal $H_2/\ell_1/H_\infty$ Curve, $\nu = 2.0$

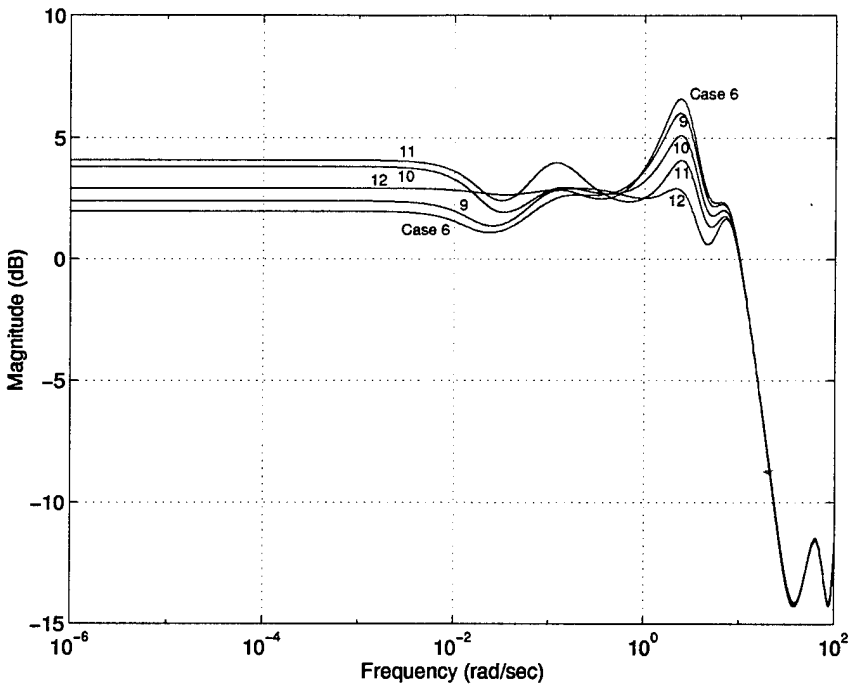

Figure 7.9 Output Complementary Sensitivity for $H_2/\ell_1/H_\infty$ Designs, $\nu = 2.0$

Table 7.2 Mixed Optimal Control Margins

Case #	$\|T_{zw}\|_2$	$\|T_{ed}\|_\infty$	$IGM_S(dB)$	$IGM_T(dB)$	$IPM(deg)$
1	0.15840	3.207	[−2.07 2.74]	[−3.26 2.36]	18.0
2	0.15840	2.741	[−2.31 3.15]	[−3.96 2.71]	21.1
3	0.15841	2.526	[−2.43 3.38]	[−4.39 2.90]	22.9
4	0.15844	2.379	[−2.53 3.58]	[−4.75 3.05]	24.3
5	0.15851	2.224	[−2.64 3.81]	[−5.20 3.23]	26.0
6	0.15861	2.140	[−2.73 4.01]	[−5.49 3.34]	27.1
7	0.15907	2.843	[−2.63 3.79]	[−4.96 3.14]	25.1
8	0.16164	12.942	[−1.67 2.08]	[−2.19 1.75]	12.8
9	0.15864	2.000	[−2.85 4.26]	[−6.04 3.53]	29.0
10	0.15879	1.800	[−3.02 4.68]	[−7.07 3.85]	32.3
11	0.15906	1.600	[−3.23 5.19]	[−8.56 4.23]	36.5
12	0.16507	1.400	[−3.46 5.84]	[−10.96 4.70]	42.0

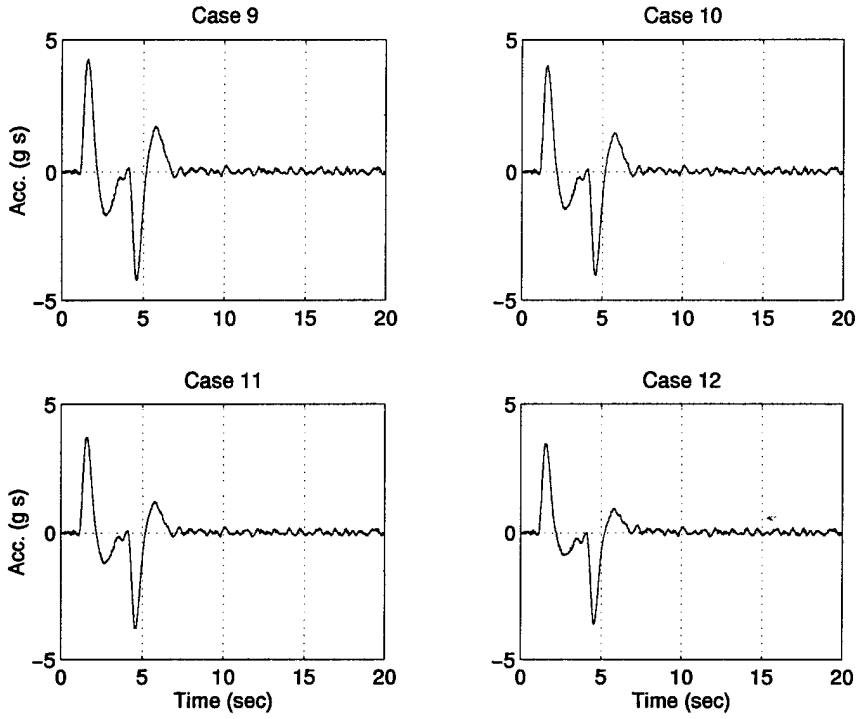

Figure 7.10 Normal Acceleration for $H_2/\ell_1/H_\infty$ Designs

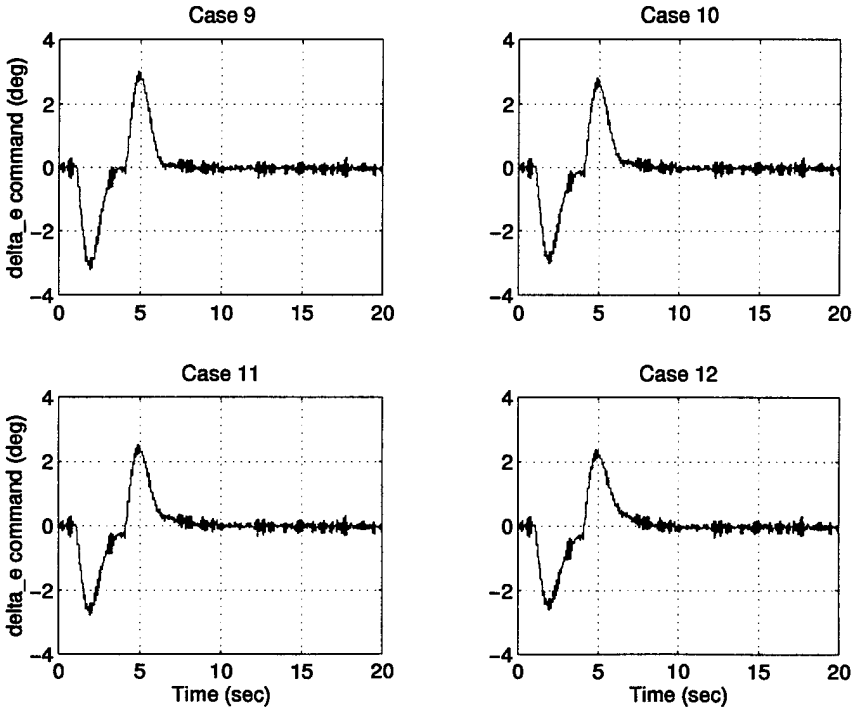

Figure 7.11 Commanded Control for $H_2/\ell_1/H_\infty$ Designs

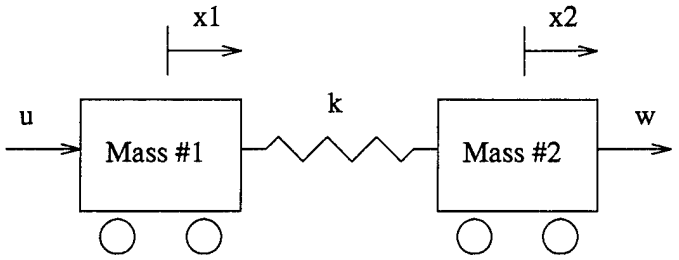

Figure 7.12 ACC Benchmark Problem for Robust Stability

7.2 American Control Conference Benchmark Problem for Robust Stability

7.2.1 Problem Setup. This section will consider the design of a controller to meet nominal performance with robust stability. It will extend the fixed-order method to include slightly different plant dynamics within the individual subproblems, and it will also highlight the importance of targeting specific concerns when choosing the subproblems for the constraints. The example used will be the spring-mass cart example shown in Figure 7.12. This was used as a benchmark problem for robust control at the 1992 American Control Conference [25], and has also appeared in the MATLAB Robust Control Toolbox [68] and a recent paper by Sznaier demonstrating a robust stability problem using a free-order H_2/H_∞ method [18]. The nominal values of the two masses and the spring constant are all assumed equal to 1, but the actual spring constant is treated as uncertain between the limits of 0.5 and 2.0. Measurement feedback is available on the position of Mass #2, and disturbances enter the system as uncertain forces (w) acting at this same point. The objective is to design a controller which achieves some level of nominal performance (to be defined shortly) while assuring the system remains stable for the specified variations in the spring constant. The double-integrator plant (from the undamped spring-mass interaction) and non-collocated sensor and actuator represent a challenging design problem because of the open loop poles at the origin (for continuous-time). Many methods require an initial shift of the stability axis in order to solve the problem; this will not be necessary using the present mixed-norm method.

The continuous-time plant is given by

$$\begin{Bmatrix} \dot{x}_1 \\ \ddot{x}_1 \\ \dot{x}_2 \\ \ddot{x}_2 \end{Bmatrix} = \begin{bmatrix} 0 & 1 & 0 & 0 \\ -k/m_1 & 0 & k/m_1 & 0 \\ 0 & 0 & 0 & 1 \\ k/m_2 & 0 & -k/m_2 & 0 \end{bmatrix} \begin{Bmatrix} x_1 \\ \dot{x}_1 \\ x_2 \\ \dot{x}_2 \end{Bmatrix} + \begin{bmatrix} 0 & 0 \\ 0 & 1/m_1 \\ 0 & 0 \\ 1/m_2 & 0 \end{bmatrix} \begin{Bmatrix} w \\ u \end{Bmatrix} \tag{7.8}$$

$$y = [0 \quad 0 \quad 1 \quad 0] \begin{Bmatrix} x_1 \\ \dot{x}_1 \\ x_2 \\ \dot{x}_2 \end{Bmatrix} \tag{7.9}$$

For a discrete-time implementation, a sample rate of 10 Hz and a zero-order hold will be used for discretization, thus introducing additional phase lag to that already present due to the non-collated sensor and actuator.

A block diagram which incorporates all the inputs and outputs for the system is shown in Figure 7.13. In addition to the force disturbance w acting on Mass #2, we have sensor noise (v), a control weighting (ρ) and an output weighting (ξ) on x_2. The output weighting on x_2 will be used to attain the desired cart position, and the control weight will ensure the compensator does not assume unreasonable control power. The uncertain spring constant has been pulled out as a Δ-uncertainty block in anticipation of using the Small Gain Theorem to pose the robust stability problem. For a nominal spring constant of $k_0 = 1$, the Small Gain Theorem states $\|T_{ed}\|_\infty < 1$ will guarantee the system remains stable for $\|\Delta\|_\infty \leq 1$, which encompasses the possible range of uncertainty ($0.5 \leq k \leq 2.0$). Other researchers [68, 18] have modified the problem by displacing the nominal spring constant to $k_0 = 1.25$, thus establishing a constraint of $\|T_{ed}\|_\infty < 1.33$ whereby the system remains stable for $\|\Delta\|_\infty \leq 0.75$. Although this creates a less stringent ∞-norm constraint, it entails designing the controller for nominal performance and robust stability at an off design condition, possibly sacrificing performance (unnecessarily) under nominal conditions. The approach taken here will be that of a multi-plant design problem [16]. Specifically, the robust stability problem will make use of the shifted spring constant ($k_{0_{rs}} = 1.25$) to create a less stringent ∞-norm constraint, but the nominal performance problem will use

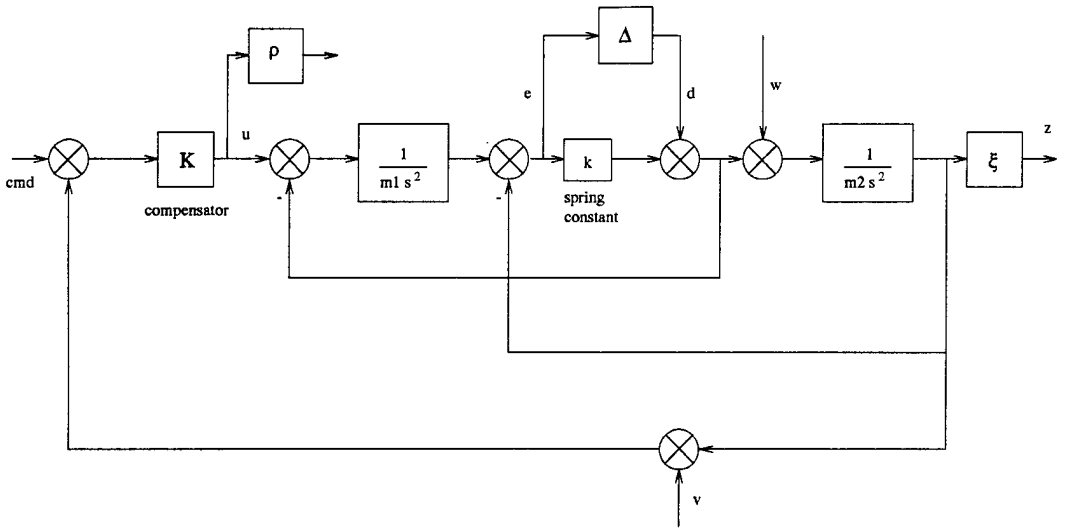

Figure 7.13 Block Diagram for ACC Benchmark Problem

the "true" nominal spring constant of $k_0 = 1$. This requires a slight extension of the problem setup, because we can no longer assume that a controller which stabilizes P_{yu} will stabilize all of the subproblem plants. Because of this, a stability constraint for each different set of plant dynamics is required. With this exception, the fixed-order method described in this dissertation can be used as is for the multi-plant problem. The continuous-time state space matrices for the H_∞ subproblem are as follows:

$$
\begin{aligned}
A_\infty &= \begin{bmatrix} 0 & 1 & 0 & 0 \\ -1.25 & 0 & 1.25 & 0 \\ 0 & 0 & 0 & 1 \\ 1.25 & 0 & -1.25 & 0 \end{bmatrix}, \quad B_d = \begin{bmatrix} 0 \\ -1 \\ 0 \\ 1 \end{bmatrix}, \quad B_{u_\infty} = \begin{bmatrix} 0 \\ 1 \\ 0 \\ 0 \end{bmatrix} \\
C_e &= \begin{bmatrix} 1 & 0 & -1 & 0 \end{bmatrix}, \quad D_{ed} = 0, \quad D_{eu} = 0 \\
C_{y_\infty} &= \begin{bmatrix} 0 & 0 & 1 & 0 \end{bmatrix}, \quad D_{yd} = 0, \quad D_{yu} = 0
\end{aligned}
\tag{7.10}
$$

The nominal performance problem will be addressed by the H_2 and ℓ_1 subproblems. The H_2 subproblem will use static weights on control usage and the position of Mass #2 (x_2), and will assume unit strength, zero-mean white Gaussian noise inputs at w and v. Static weights have been chosen because no assumptions are being made on the frequency content of either the disturbances or the reference commands. A control weight

of $\rho_2 = 0.01$ and output weight of $\xi = 1.0$ were chosen because they result in a reasonable step response and control usage. The ℓ_1 subproblem will weight control magnitude ($\rho_1 = 1.0$) for unknown but bounded magnitude inputs w and v, which will be considered together as the input vector r. This is being done to ensure not only reasonable control power (addressed by the H_2 subproblem), but reasonable magnitudes for control usage in the presence of disturbances and measurement noise. Another important contribution of the ℓ_1 constraint for this example is that it will highlight what can happen when control usage is lumped into a scalar cost functional along with controlled outputs. By maintaining control magnitude as a separate constraint we will be able to see explicitly the effects of the constraint.

The focus of this example will be to show how a robust stability constraint can be met using a multi-plant, mixed-norm approach, and to show how explicit constraints on control usage can affect the final results in a mixed-norm problem. Although the quality of response as measured by rise time, settling time, etc., is important, it is not the focus of this example. As such, the step response for some of the closed-loop systems will be less than enviable.

The continuous-time state space matrices for the H_2 and ℓ_1 subproblems are as follows:

$$\begin{aligned}
A_2 &= \begin{bmatrix} 0 & 1 & 0 & 0 \\ -1 & 0 & 1 & 0 \\ 0 & 0 & 0 & 1 \\ 1 & 0 & -1 & 0 \end{bmatrix}, \quad B_w = \begin{bmatrix} 0 & 0 \\ 0 & 0 \\ 0 & 0 \\ 1 & 0 \end{bmatrix}, \quad B_{u_2} = \begin{bmatrix} 0 \\ 1 \\ 0 \\ 0 \end{bmatrix} \\
C_z &= \begin{bmatrix} 0 & 0 & 1 & 0 \\ 0 & 0 & 0 & 0 \end{bmatrix}, \quad D_{zw} = \begin{bmatrix} 0 & 0 \\ 0 & 0 \end{bmatrix}, \quad D_{zu} = \begin{bmatrix} 0 \\ 0.01 \end{bmatrix} \\
C_{y_2} &= \begin{bmatrix} 0 & 0 & 1 & 0 \end{bmatrix}, \quad D_{yw} = \begin{bmatrix} 0 & 1 \end{bmatrix}, \quad D_{yu} = 0
\end{aligned} \tag{7.11}$$

$$
\begin{aligned}
A_1 &= \begin{bmatrix} 0 & 1 & 0 & 0 \\ -1 & 0 & 1 & 0 \\ 0 & 0 & 0 & 1 \\ 1 & 0 & -1 & 0 \end{bmatrix}, \quad B_r = \begin{bmatrix} 0 & 0 \\ 0 & 0 \\ 0 & 0 \\ 1 & 0 \end{bmatrix}, \quad B_{u_1} = \begin{bmatrix} 0 \\ 1 \\ 0 \\ 0 \end{bmatrix} \\
C_m &= [0 \;\; 0 \;\; 0 \;\; 0], \quad D_{mr} = [0 \;\; 0], \quad D_{mu} = 1 \\
C_{y_1} &= [0 \;\; 0 \;\; 1 \;\; 0], \quad D_{yr} = [0 \;\; 1], \quad D_{yu} = 0
\end{aligned}
\tag{7.12}
$$

7.2.2 Location of Mixed-Norm Controllers on the Pareto Optimal Surface. Figure 7.14 shows the Pareto optimal curve for the H_2/ℓ_1 problem which was used to determine an acceptable constraint level. The value of $\|T_{ed}\|_\infty$ for each of these controllers is computed and plotted versus $\|T_{mr}\|_1$ in Figure 7.15. Unlike the F-16 example from Chapter VI, $\|T_{mr}\|_1$ are $\|T_{ed}\|_\infty$ are directly competing constraints in this example. With the exception of a few bumps (probably due to numerics), we see that $\|T_{ed}\|_\infty$ increases monotonically as $\|T_{mr}\|_1$ decreases for the H_2/ℓ_1 problem. Figure 7.16 shows several Pareto optimal curves for varying levels of $\|T_{mr}\|_1$ ($H_2/\ell_1/H_\infty$ problems), as well as the case where $\|T_{mr}\|_1$ was unconstrained (an H_2/H_∞ problem). The small variation of $\|T_{zw}\|_2$ with $\|T_{mr}\|_1$ can be seen by the close proximity of the $H_2/\ell_1/H_\infty$ curves; however, the offset of the H_2/H_∞ curve from the $H_2/\ell_1/H_\infty$ curves suggests that $\|T_{mr}\|_1$ may take on significantly different values if left unconstrained. This insight is confirmed by Figure 7.17, which shows the unconstrained values of $\|T_{mr}\|_1$ resulting from the H_2/H_∞ control problem. This indicates that, although the H_2 subproblem includes a weight on control for both the H_2/H_∞ and $H_2/\ell_1/H_\infty$ control problems, significantly higher magnitudes of control usage will result unless it is explicitly constrained. This observation will be discussed in more detail later in the example.

If we project the Pareto optimal curves onto the $\nu - \gamma$ plane we can start to get a better picture of where the mixed-norm solutions must lie. Figure 7.18 shows these projections, along with the location of the H_2 optimal controller. Constraint levels of $\gamma \geq \overline{\gamma}$ and $\nu \geq \overline{\nu}$ lie in Region IV, and any problem with constraint levels in this region will have the H_2 optimal controller as its solution. Neither of the constraints will be active for constraint levels in Region IV, except for cases on the boundary of the region. Region III encompasses constraint levels of $\gamma \geq \overline{\gamma}$, and ν between $\overline{\nu}$ and the H_2/ℓ_1 curve for the

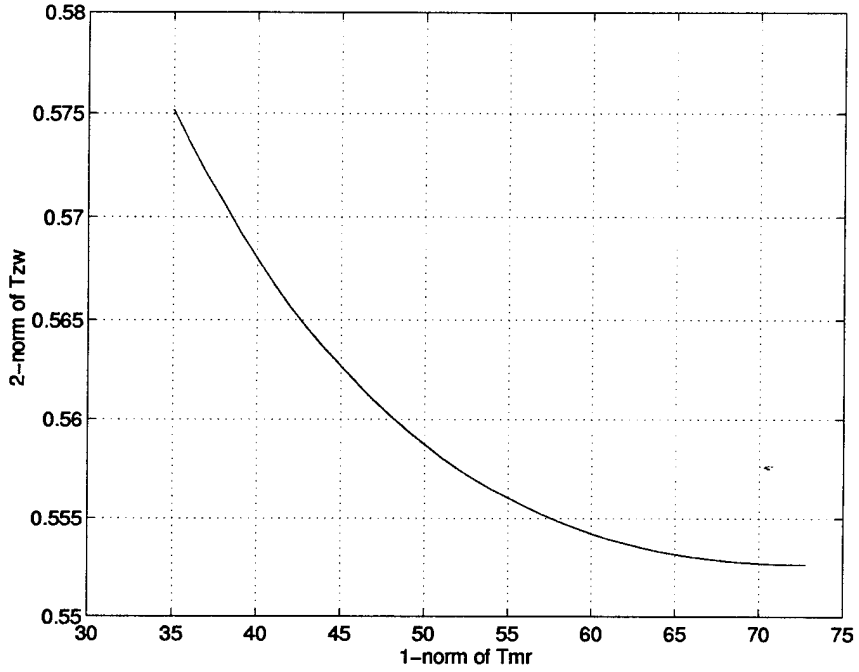

Figure 7.14 Pareto Optimal H_2/ℓ_1 Curve

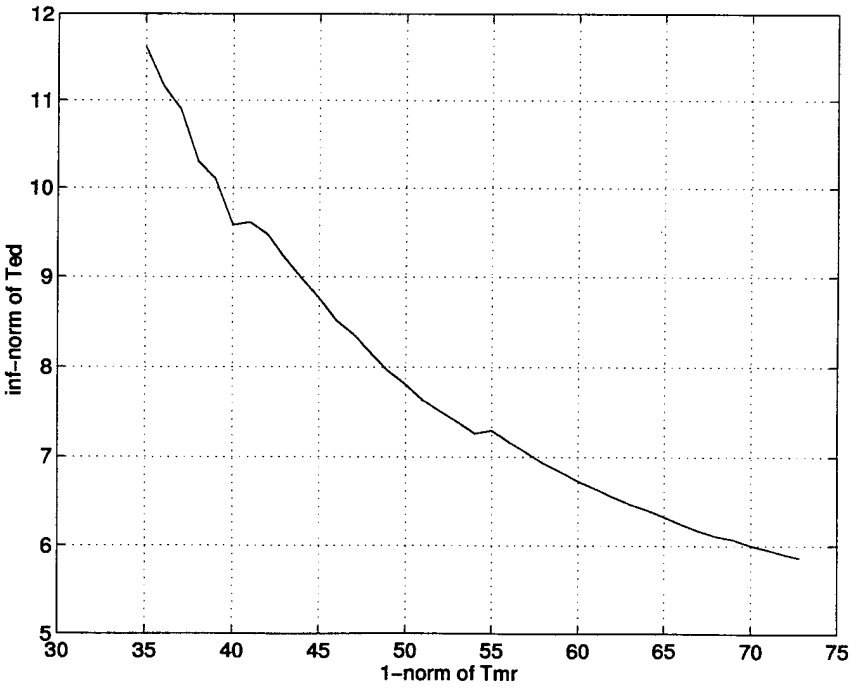

Figure 7.15 γ vs ν for H_2/ℓ_1 Control Problem

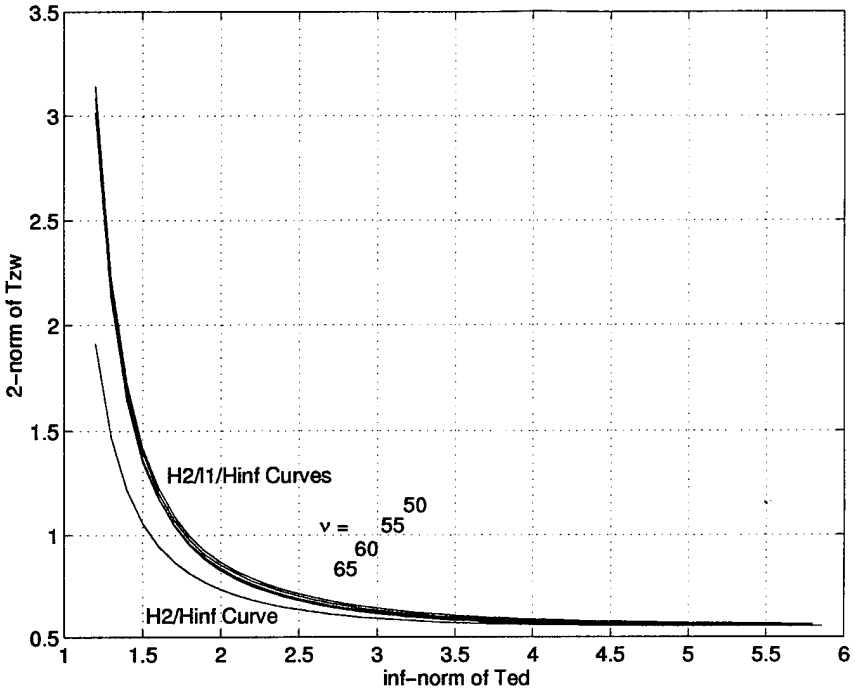

Figure 7.16 α vs γ for H_2/H_∞ and $H_2/\ell_1/H_\infty$ Control Problems

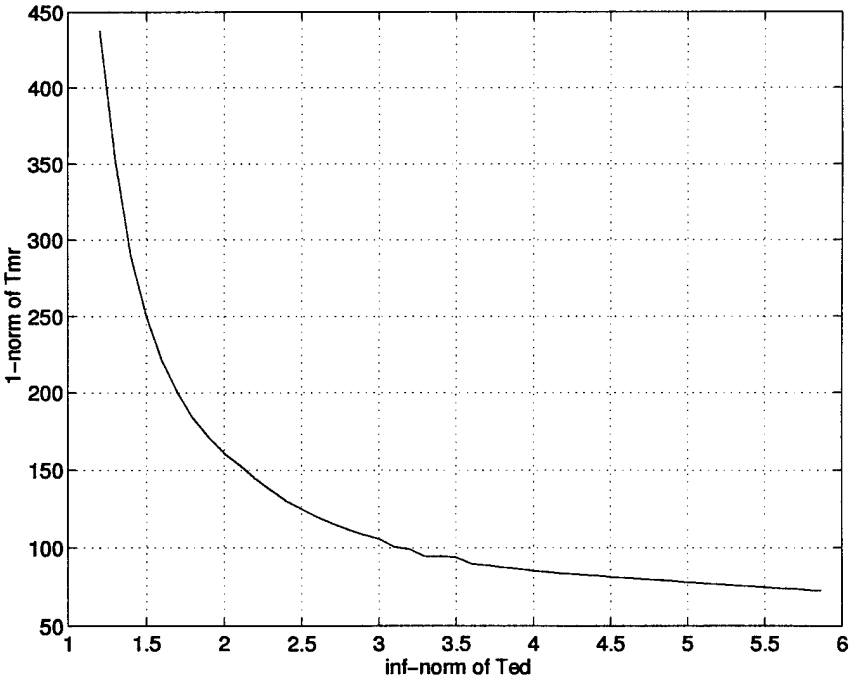

Figure 7.17 ν vs γ for H_2/H_∞ Control Problem

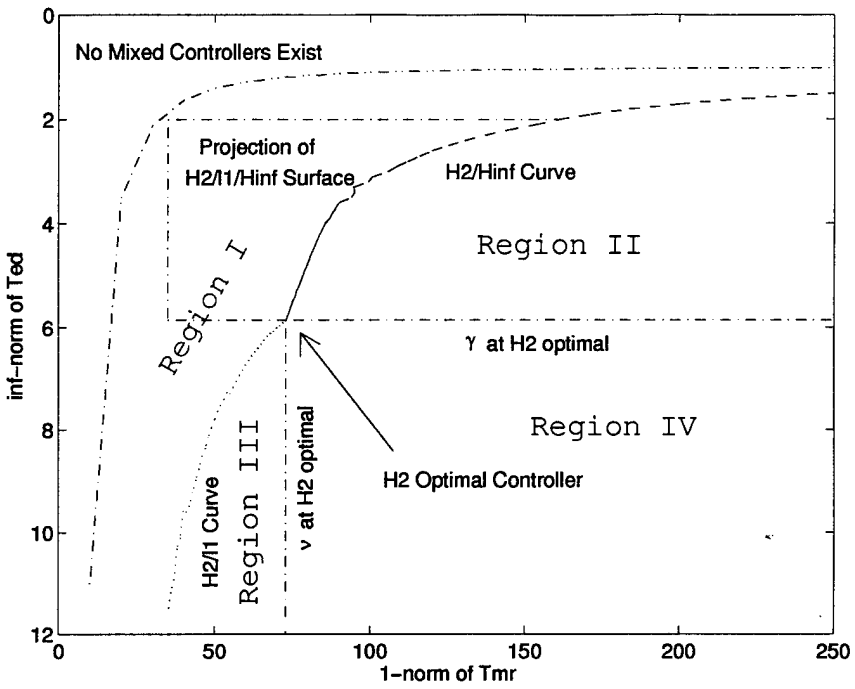

Figure 7.18 Projection of Pareto Optimal Surface onto $\nu - \gamma$ Plane

specified level of γ. Any problem with constraint levels in Region III will have a solution on the H_2/ℓ_1 curve at the specified level of ν. The H_∞ constraint will be inactive for problems in this region. The dual of Region III is Region II, where $\nu \geq \overline{\nu}$ and γ lies between $\overline{\gamma}$ and the H_2/H_∞ curve for the specified level of ν. Problems with constraint levels in Region II will have a solution on the H_2/H_∞ curve at the specified level of γ, and the ℓ_1 constraint will be inactive. An ill-defined region exists whereby one or both of the constraints is so tight that no solutions exist for the mixed-norm problem. The precise boundary of this region usually cannot be defined except for isolated points representing the H_∞ or ℓ_1 optimal controllers.

Region I is the projection of the Pareto optimal surface whereby both constraints will generally be active. A portion of this surface representing $35 \leq \nu \leq 160$ and $2.0 \leq \gamma \leq 5.8$ is shown in Figure 7.19. The surface was generated by plotting the resulting norms from approximately 400 mixed-norm controllers. For constraint levels anywere within these limits, the resulting value of $\|T_{zw}\|_2$ appears as the height (z-axis) of the surface. The lower right edge of the surface is the H_2/H_∞ Pareto optimal curve which defines the

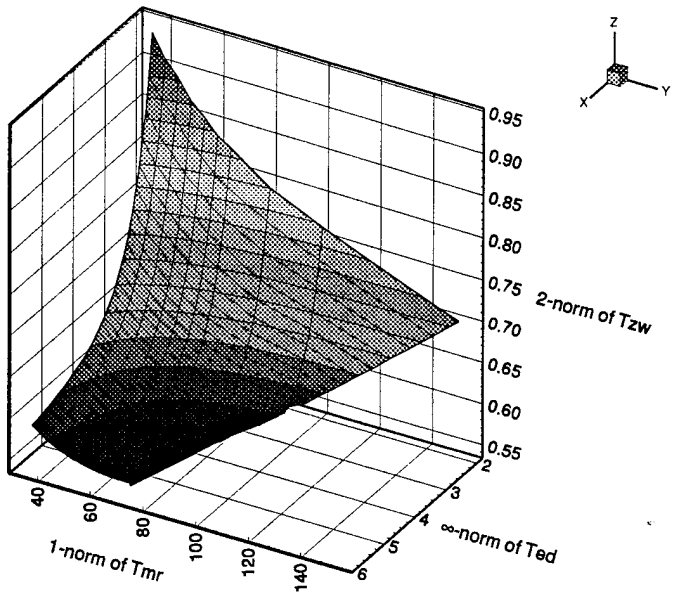

Figure 7.19 Portion of Pareto Optimal Surface for $H_2/\ell_1/H_\infty$ Control Problem

boundary between Regions I and II. Note that, for a 1-norm constraint level of 100, as we increase γ for the ∞-norm constraint, the 1-norm constraint ceases to be active for $\gamma \geq 3.2$. As we further increase γ beyond this level, the solution to the mixed-norm problem will lie on the H_2/H_∞ curve, with $\nu^* < \nu$. Additional controllers could have been found to define larger portions of the Pareto optimal surface, but it was not necessary for purposes of this discussion. As a final note on the Pareto optimal surface, this example showed no evidence of local minima on the surface; however, as discussed in the previous chapter, the existence of local minima cannot be ruled out for the fixed-order, mixed-norm problem.

7.2.3 ACC Benchmark Problem Results. For comparing system performance, 5 controllers were selected from the full range of possible controllers as discussed in the previous section. Table 7.3 shows the resulting norm values for these controllers. Case 1 is the H_2 optimal controller, Case 2 and Case 3 are $H_2/\ell_1/H_\infty$ controllers, and Case 4 and Case 5 are H_2/H_∞ controllers for which $\|T_{mr}\|_1$ was left unconstrained. The choice of $\nu = 50$ for the 1-norm constraint level was arbitrary, since the mass, spring constant, and force values for this example are not tied to any specific units or physical limits. For this reason, the achieved values of $\|T_{zw}\|_2$ and $\|T_{mr}\|_1$ are only important for comparison

Table 7.3 ACC Benchmark Problem $H_2/\ell_1/H_\infty$ Control Results

Case #	$\|T_{zw}\|_2$ α	$\|T_{mr}\|_1$ ν	$\|T_{ed}\|_\infty$ γ
1	0.5527	72.80	5.862
2	0.8664	50.00	2.000
3	2.2218	50.00	1.300
4	0.7309	160.87	2.000
5	1.4714	353.95	1.300

purposes. The same will not be true for $\|T_{ed}\|_\infty$ because it is tied to the specific robust stability constraint via the Small Gain Theorem. Of the five cases, only Case 3 and Case 5 are guaranteed to stabilize the system for the full range of uncertainty in the spring constant, since $\|T_{ed}\|_\infty < 1.33$ insures a stable closed-loop system for $\|\Delta\|_\infty \leq 0.75$.

Figure 7.20 shows a comparison of the unit step response (step applied at t=1 sec) for the first three controllers with a nominal spring constant ($k = 1$). Although the price of robust stability for this example appears to be a decrease in nominal performance, some of this can be attributed to the constraint on the magnitude of control usage (Case 1 had no ℓ_1 constraint, whiles Cases 2 and 3 had a constraint of $\|T_{mr}\|_1 \leq 50$). Both overshoot and settling time increase with decreasing γ levels, and the system demonstrates a non-minimum phase response for Case 3. Figure 7.21 shows Cases 1-3 with disturbances and measurement noise added to the simulation. The control usage for both step response and disturbance rejection is less for the second and third cases, and this is consistent with the lower level of $\|T_{mr}\|_1$. Future work with this example will examine methods for improving performance, and maintaining performance for increased levels of robust stability.

Figures 7.22 and 7.23 show Cases 1-3 for non-nominal spring constants of 1.5 and 0.75, respectively. All cases remain stable for $k = 1.5$, but Case 1 clearly demonstrates a higher level of oscillation not present in Case 2 or Case 3. For $k = 0.75$, the H_2 optimal controller (Case 1) can no longer stabilize the system, and Case 2 also appears to be getting close to the stability boundary. The Small Gain Theorem states that both Case 2 and Case 3 should remain stable for $k = 0.75$, since this represents an uncertainty level of $\|\Delta\|_\infty \leq 0.5$ from $k_{0_{r_s}} = 1.25$. For a spring constant of $k = 0.5$, Case 1 and Case 2 are

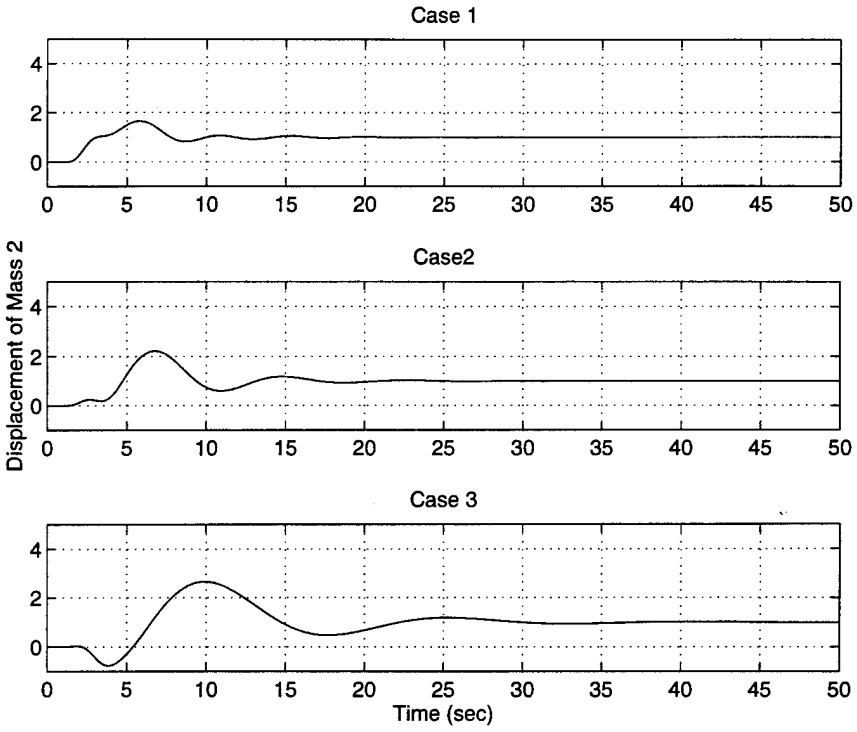

Figure 7.20 Step Responses for Nominal Spring Constant $k_0 = 1$

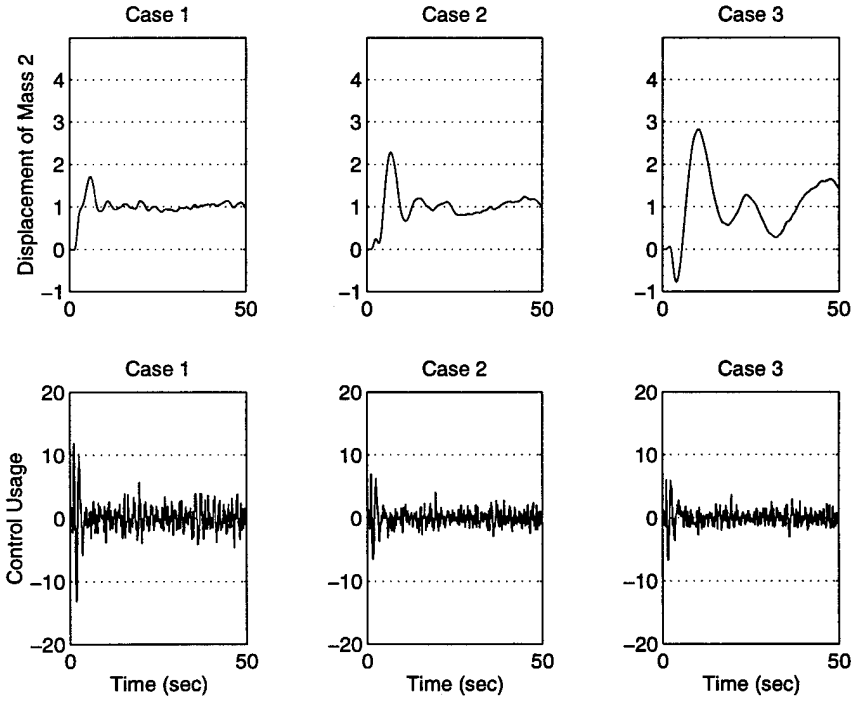

Figure 7.21 Step Responses with Disturbances and Sensor Noise ($k_0 = 1$)

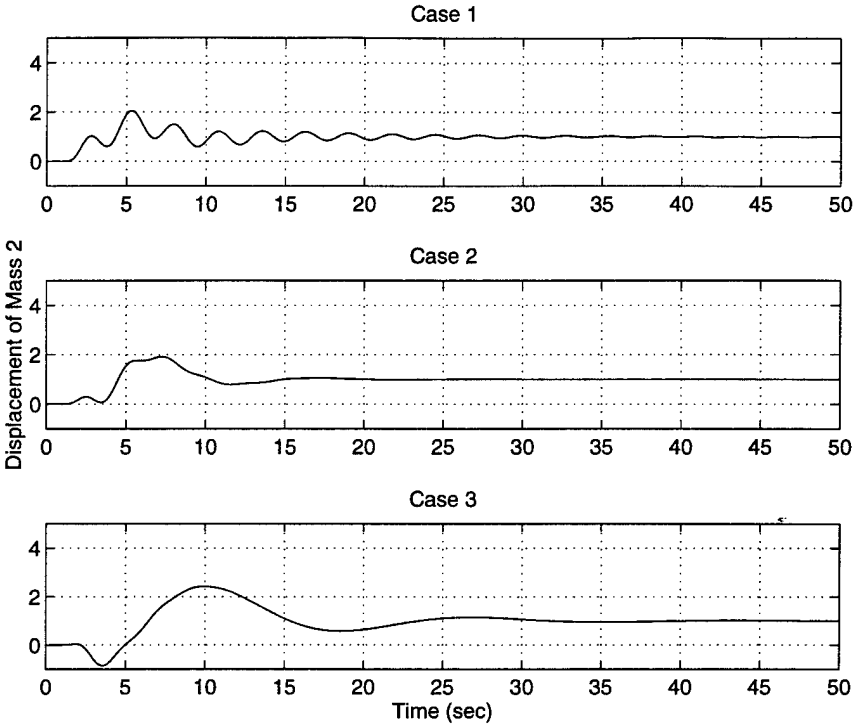

Figure 7.22 Step Responses for Spring Constant $k = 1.5$

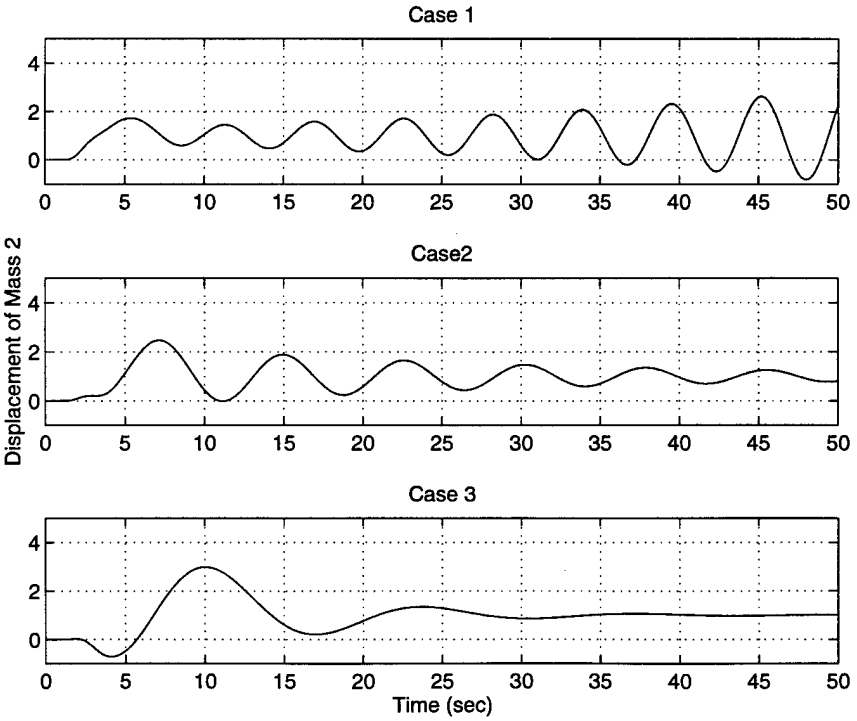

Figure 7.23 Step Responses for Spring Constant $k = 0.75$

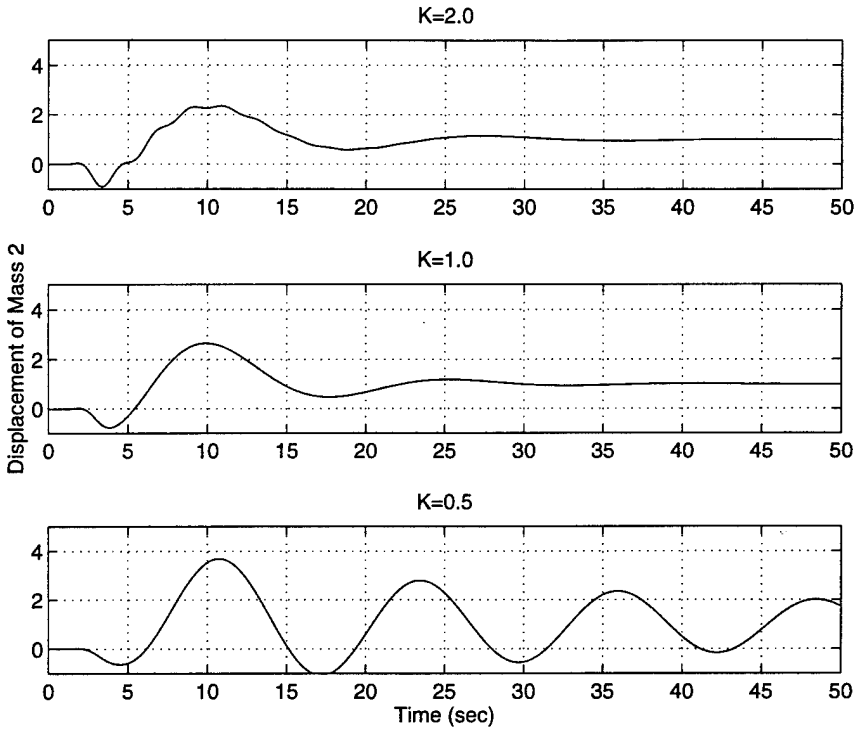

Figure 7.24 Step Responses of Case 3 for Varying Spring Constant

unstable, but Case 3 remains stable as guaranteed by $\|T_{ed}\|_\infty < 1.33$. Figure 7.24 shows the step response of Case 3 for the full uncertainty range of the spring constant. Clearly the system is close to instability for $k = 0.5$, but the robust stability constraint has been met.

For small γ values, an improved response can be obtained by removing the 1-norm constraint on the magnitude of control usage, but not without a dramatic change in control behavior. This can be seen in Figures 7.25 and 7.26 where the off-nominal performance is shown with and without the constraint on $\|T_{mr}\|_1$. Although the systems generally exhibit lower overshoot without the 1-norm constraint, rise time and settling time are not affected significantly. The benefit of the 1-norm constraint is a dramatic reduction in the control usage, especially in the presence of disturbances and sensor noise (see Figure 7.27). Bear in mind that all of these systems had the same penalty on control energy in the H_2 subproblem, but Case 2 and Case 3 constrained the worst case magnitude of control usage. An apparent contradiction is that Case 5, despite its very high control usage in the presence of noise, has a lower value of $\|T_{zw}\|_2$ than that of Case 3. The explanation for this is that,

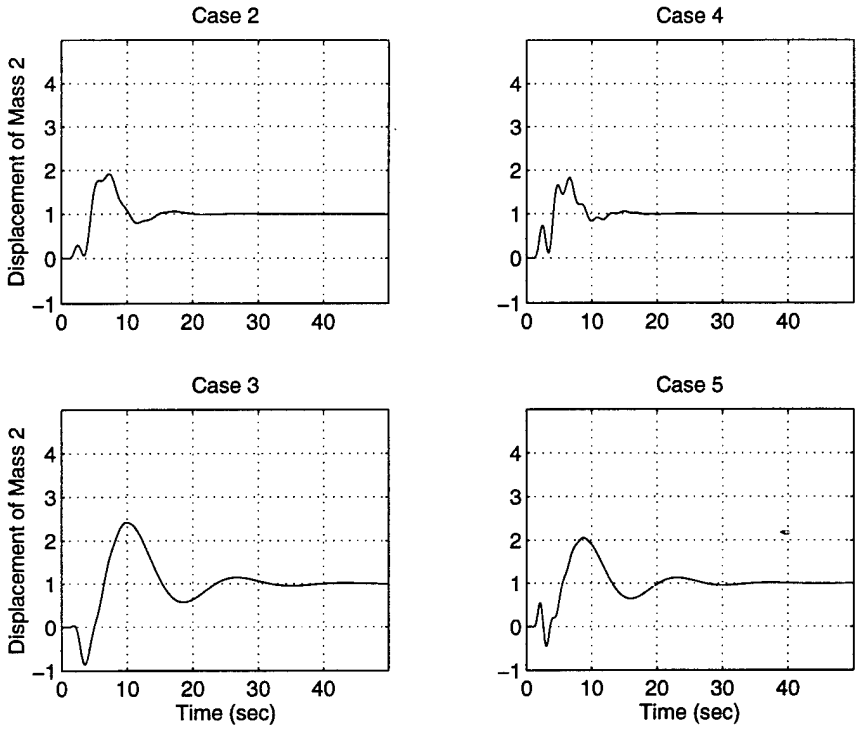

Figure 7.25 Step Responses With and Without ℓ_1 Constraint, $k = 1.5$

despite the identical 2-norm cost functional for the two cases, the contribution toward this cost from control usage is minor compared to state deviations for Case 3 (and Case 2), and the opposite is true for Case 5 (and Case 4). This demonstrates how scalar functionals can mask the contributions of the individual components. For problems such as this, a mixed-norm approach can be used to establish more specific constraints which highlight the tradeoffs between the individual features of the problems. The mixed-norm approach by itself does not guarantee that these tradeoffs will become evident, because each of the constraints is a scalar functional in itself which can hide the individual components within it. The key appears to be in using the mixed-norm approach to constrain specific attributes which are important to the final design. The investigation of implementation strategies such as this is seen as a very fruitful area for future research.

7.3 Summary

This chapter demonstated several applications for mixed-norm control synthesis. The first example represented a challenging multi-block MIMO design problem for an aircraft

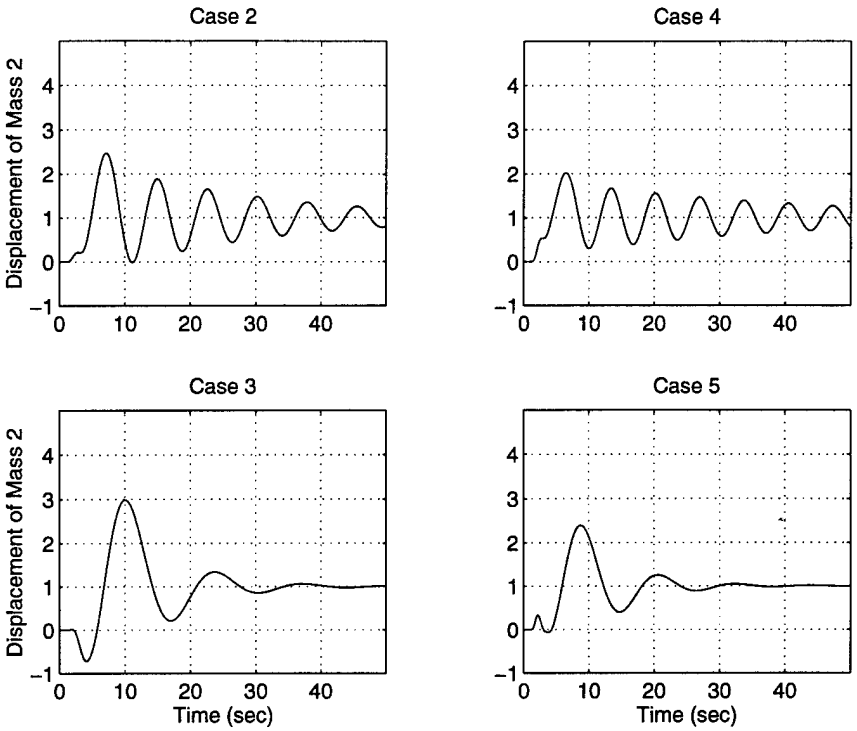

Figure 7.26 Step Responses With and Without ℓ_1 Constraint, $k = 0.75$

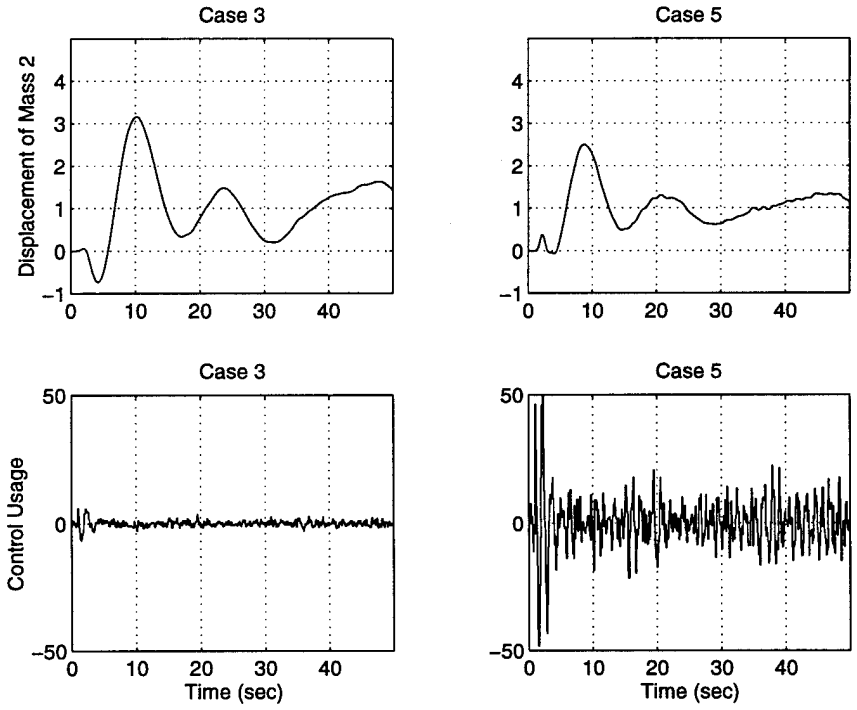

Figure 7.27 Step Response and Control Usage for Case 3 vs Case 5, $k = 0.75$

terrain following controller. Using an ℓ_1 norm constraint for altitude error shows great promise, as it significantly reduces the overshoot in the response to altitude commands. However, it should also be noted that the actual value of the 1-norm can be so conservative that its physical significance becomes meaningless. This is important because ℓ_1 optimization has often been mentioned as a method to put absolute bounds on errors, control usage, and control rates. While ℓ_1 does an excellent job of limiting the magnitude of controlled outputs, the achieved values of the outputs for actual inputs are usually far less than might be indicated by the value of the norm. The second example of this chapter extended the fixed-order, mixed-norm method to the multi-plant problem. The ACC benchmark problem was solved using an ∞-norm constraint on an off-design plant condition to guarantee stability for a specified range of uncertainty. Finally, this second example demonstrated the benefits of explicit constraints in understanding the tradeoffs between competing performance features.

VIII. Conclusions and Recommendations

8.1 Summary

This dissertation has investigated the general mixed-norm control problem for discrete-time, linear systems. The particular approach taken was to minimize the 2-norm of a specified transfer function, subject to constraints on the 1-norm and/or ∞-norm of dissimilar but related transfer functions. This was used to define Pareto optimal curves or surfaces of mixed-norm controllers. Several different problems were posed and solved using this same approach. The first problem was a free-order approach to H_2/ℓ_1 using the Youla parametrization of all stabilizing controllers. The problem was shown to be convex with a unique solution. It was conjectured, with supporting evidence, that the optimal solution to the SISO and one-block MIMO H_2/ℓ_1 control problem will result in a FIR constraint transfer function, but generally non-FIR objective transfer function. Based on this conjecture, a numerical method was developed which is capable of solving exactly the H_2/ℓ_1 control problem for SISO and one-block MIMO problems. The resulting compensator is usually of such high order that it is impractical, at best, for implementation, but it provides an important limit of performance for the H_2/ℓ_1 control problem. Various methods for approximating the optimal solution were also explored, and it was shown how these methods could significantly reduce the size of the resulting optimization problem. A second free-order numerical method for the H_2/ℓ_1 control problem was developed, and this method was shown to be capable of approaching the optimal solution to within arbitrary precision using a radius constraint on the closed-loop poles. The important aspect of this second method is that it is readily extendable to general multi-block problems. Further, this second method can accommodate an H_∞ constraint for a full free-order $H_2/\ell_1/H_\infty$ control problem.

A special case of the SISO H_2/H_∞ optimal control problem was solved using minimum-norm duality, and it was shown that the optimal controller is non-rational or infinite-order. This was not a surprising result since it was the same special case considered by Walker [9] for continuous-time systems, but it had not been previously shown for discrete-time. Similarly, the analytical development of the full-order, discrete-time, H_2/H_∞ control problem

was shown to have all the same features as the continuous-time problem investigated by Ridgely [8] and Walker [9]. The nature of the optimal full-order solution was characterized based on the desired level of the H_∞ constraint, and the solution was shown to depend on the neutrally stabilizing solution to an associated Riccati equation.

Analytical development is important for characterizing the nature of the solution, and numerical methods for finding the true optimal compensator are important for providing limits of performance. However, if a synthesis method is to have practical applications, it must provide easily implementable controllers. Along these lines, a general fixed-order, discrete-time method was developed. This method minimizes the 2-norm of an objective transfer function, subject to an arbitrary combination of 1-norms and/or ∞-norms of dissimilar (but related) transfer functions. Further, the method can be used iteratively at increasing compensator orders to approach the same limits of performance that free-order methods provide. Using the elements of the compensator state-space as design variables, the method is capable of solving directly the reduced or expanded order mixed-norm control problem. Further, existing algorithms for continuous-time systems were incorporated into the program structure to provide a single MATLAB toolbox for mixed-norm control synthesis (see Appendix C), and the toolbox is being made publicly available throughout the controls community.

Fixing the order of the compensator results in a non-convex program for the general output feedack problem, but it can be solved efficiently using gradient based nonlinear programming methods. The method was first demonstrated using a longitudinal controller design for a SISO model of an F-16 aircraft. An H_2/ℓ_1 control problem demonstrated the tradeoffs between noise and disturbance rejection (the H_2 subproblem) and tracking (the ℓ_1 subproblem). An $H_2/\ell_1/H_\infty$ problem was then formulated to improve the robust stability as measured by the ∞-norm on complementary sensitivity. For this example, specific non-convex areas of the design space were highlighted. It was shown that these areas resulted in discontinuous jumps in the compensator eigenvalues as the Pareto optimal curve was traversed. Convexity improved as controller order was increased, which is to be expected based on the convex free-order problem.

Besides the F-16 problem, two other design problems were used to demonstrate the new numerical method. The first of these was a terrain following controller for a MIMO longitudinal model of an A-4 aircraft. This was a challenging design problem due to widely separated poles from the short period and phugoid modes, and a high number of design variables (90). The H_2 subproblem was again used to provide noise and disturbance rejection while regulating control usage. The ℓ_1 subproblem was used to limit the absolute magnitude of the altitude tracking error. While it was shown that the ℓ_1 constraint did a good job of reducing the magnitude of the tracking error, it was also shown that the actual value of the norm was much too conservative to be used for specific error limits. An H_∞ constraint was again added to the problem to improve robust stability, while maintaining tracking and noise/disturbance rejection.

The final example was the 1992 American Control Conference benchmark problem for robust stability. This was used to extend the fixed-order numerical method to the multi-plant problem, whereby the underlying dynamics associated with each of the subproblems are no longer required to be identical. The H_∞ subproblem was based on an off-design plant condition, and specific constraint levels were established for the ∞-norm in order to guarantee stability for the full range of plant uncertainty. The H_2 problem was set up as a regulator on states and control usage, and the ℓ_1 subproblem was used to bound the magnitude of control usage. In addition to demonstrating the multi-plant approach to robust stability, this example demonstrated how the mixed-norm approach could be used to isolate specific constraints which are determined to be important to the design problem. Once isolated, the varying constraint level can be used to show design tradeoffs between specific features of the problem.

8.2 Recommendations for Future Research

While there is always more that can be done to develop the theory for the mixed-norm control problem, the theory has already far out-paced the ability of the controls engineer to implement it. For this reason, the recommendation for future research is to concentrate on the more practical aspects of the mixed-norm control problem. First, and foremost, determine when it makes sense to employ mixed-norm synthesis methods, and

what is the best way to formulate these problems. The limited results to date suggest that the synthesis problem is further complicated by mixed-norm methods, because each subproblem must be as well conceived as if it were the full problem. Although the shaping filters and weighting matrices from H_2 and H_∞ synthesis methods are available for the subproblems, the question remains as to whether or not this is the best way to weight the subproblems within the mixed-norm context. The ℓ_1 synthesis method is open to both frequency and time-domain weighting functions, and these also need to be explored further within the mixed-norm context. The best results for the ℓ_1 subproblems seem to occur when specific features of the problem are targeted for magnitude constraints. Certainly tracking error and control usage fit into this class of features, but control rates and robust stability for bounded magnitude disturbances are candidate features which have yet to be tried in a mixed-norm setting. The recommendation here is simple: examples, good examples, and more examples!

The method, as is, is capable of solving the reduced-order design problem, but few examples have demonstrated this capability. The reduced-order problem adds another question to those above; namely, is it better to reduce the size of the weights, or to use higher-order weights (which more accurately describe either the uncertainty or the desired range for the controlled outputs) with a reduced-order compensator? An example of the latter is the mixed H_2/μ problem formulated and solved by Walker [9]. However, the H_2/μ problem is one in which the high order weights are on the constraint transfer function. Examples should be tried where the weighted objective transfer function is of significantly higher order than the desired compensator. In order to simplify the process of starting a reduced-order design problem, the process of finding an initial stabilizing controller should be automated to whatever degree is possible for the reduced-order controller. Presently, the person operating the code must come up with an initial stabilizing controller (with the desired controller order) through whatever *ad hoc* means are available. Any automation added to this process would go a long way towards making the reduced-order synthesis problem much more palatable. Tangled up in this problem is the question of minimum order for a given system, but this remains a wide open theoretical problem in the controls community.

The non-convex nature of the design space for the general fixed-order problem is not a new finding, but this dissertation demonstrated that these non-convex regions actually represent discontinuous "valleys" in the design space. Further, the fact that the discontinuity occurs in the compensator eigenvalues indicates that the discontinuity can not be avoided by using a different form of the compensator. The problem of convexity vs. compensator order needs to be explored further, and it should be tied together with the free-order limits of performance. For the Mixed-Norm Toolbox, methods of traversing the discontinuities should be examined. Along these lines, the possibility of wrapping a globally convergent method around the present nonlinear programming problem should be considered. The extra run times associated with globally convergent methods may not be warranted for many problems, but for cases where local minima are troublesome it would be useful.

The Mixed-Norm Toolbox is relatively "canned" for combinations of transfer function norms. Although this covers a wide variety of problems with generally uncertain inputs, there are many problems of interest whereby the response to known inputs is very important. For these problems, the Mixed-Norm Toolbox could be extended to incorporate both output norm constraints (ℓ_∞ for example) and specific time domain constraints such as rise time, settling time and overshoot. A finite horizon approach would be necessary to enforce these constraints, but it should be relatively straightforward to accommodate them within the existing structure of the algorithms.

A final recommendation is that the Mixed-Norm Toolbox be maintained by AFIT and distributed throughout the controls community. By allowing many diverse organizations to try (and sometimes break) the code, we will learn what it does best, where it falls short, and how it can be improved. Further, the many different examples and design approaches of other researchers will greatly aid in our understanding of how best to apply mixed-norm control methods.

Appendix A. Proof of Claim from Chapter IV

This appendix contains the remainder of the proof of the claim in Chapter IV, Section 4.5.

Claim $\alpha(x^\star) \leq \|x'\|_2$

Proof: We will consider separately the cases where $|x^\star(N)| = \|\overline{P}_c x^\star\|_\infty$ occurs for $N = 0, 1, 2$, and $N \geq 3$.

Case 0. $(N = 0)$

$$\alpha(x^\star) = \left[\sum_{k=0}^{\infty} r(k)x^\star(k) - \|\overline{P}_c x^\star\|_\infty\right] \tag{A.1}$$

$$= x^\star(0) + \frac{x^\star(1)}{2} + \frac{x^\star(2)}{3} + \sum_{k=3}^{\infty} \frac{x^\star(k)}{k+1} - |x^\star(0)| \tag{A.2}$$

$$\leq \frac{x^\star(1)}{2} + \frac{x^\star(2)}{3} + \sum_{k=3}^{\infty} \frac{x^\star(k)}{k+1} \tag{A.3}$$

$$= \overline{x}\,(x'(0) + x'(1) + x'(2)) + \sum_{k=3}^{\infty} x^\star(k)x'(k) \tag{A.4}$$

$$= \langle x', g\rangle \tag{A.5}$$

$$\leq \|x'\|_2 \|g\|_2 \tag{A.6}$$

$$= \|x'\|_2 \left(\sqrt{3\overline{x}^2 + \sum_{k=3}^{\infty} x^\star(k)^2}\right) \tag{A.7}$$

where

$$\overline{x} = \frac{3x^\star(1)}{5} + \frac{2x^\star(2)}{5} \tag{A.8}$$

$$g = \{\overline{x}, \overline{x}, \overline{x}, x^\star(3), x^\star(4), x^\star(5), \ldots\} \tag{A.9}$$

To show that

$$3\overline{x}^2 \leq x^\star(0)^2 + x^\star(1)^2 + x^\star(2)^2 \tag{A.10}$$

will be sufficient to prove Case 0, since $\|x^\star\|_2 \leq 1$ has been assumed. Expanding the expression for $3\overline{x}^2$,

$$3\overline{x}^2 = x^\star(1)^2 + x^\star(2)^2 + \frac{2x^\star(1)^2}{25} - \frac{13x^\star(2)^2}{25} + x^\star(1)x^\star(2) + \frac{11x^\star(1)x^\star(2)}{25} \tag{A.11}$$

Suppose $|x^\star(2)| \geq |x^\star(1)|$.

$$\begin{aligned} 3\overline{x}^2 &\leq x^\star(1)^2 + x^\star(2)^2 + \frac{2}{25}|x^\star(1)x^\star(2)| \\ &\quad -\frac{13}{25}|x^\star(1)x^\star(2)| + |x^\star(1)x^\star(2)| + \frac{11}{25}|x^\star(1)x^\star(2)| && \text{(A.12)} \\ &= x^\star(1)^2 + x^\star(2)^2 + |x^\star(1)x^\star(2)| && \text{(A.13)} \\ &\leq x^\star(0)^2 + x^\star(1)^2 + x^\star(2)^2 && \text{(A.14)} \end{aligned}$$

Now suppose $|x^\star(1)| \geq |x^\star(2)|$.

$$\begin{aligned} 3\overline{x}^2 &= x^\star(1)^2 + x^\star(2)^2 + \frac{1}{25}\left(2x^\star(1)^2 + 36x^\star(1)x^\star(2) - 13x^\star(2)^2\right) && \text{(A.15)} \\ &\leq x^\star(0)^2 + x^\star(2)^2 + \frac{1}{25}\left(2x^\star(1)^2 + 36x^\star(1)x^\star(2) - 13x^\star(2)^2\right) && \text{(A.16)} \end{aligned}$$

We need to show that the last term in (A.16) is less than or equal to $x^\star(1)^2$. Define

$$\begin{aligned} f(r = x^\star(2)/x^\star(1)) &:= \frac{1}{25}\left(2x^\star(1)^2 + 36x^\star(1)x^\star(2) - 13x^\star(2)^2\right) \\ &\quad -x^\star(1)^2 && \text{(A.17)} \\ &= -\frac{x^\star(1)^2}{25}\left(13r^2 - 36r + 23\right) && \text{(A.18)} \end{aligned}$$

Examining (A.18), we see that $f(r) \leq 0 \; \forall \; r \in [-1, 1]$, which is equivalent to all $|x^\star(1)| \geq |x^\star(2)|$. Thus, we have (A.10) for the case where $N = 0$.

Case 1. $(N = 1)$

$$\alpha(x^\star) = x^\star(0) + \frac{x^\star(1)}{2} + \frac{x^\star(2)}{3} + \sum_{k=3}^{\infty} \frac{x^\star(k)}{k+1} - |x^\star(1)| \tag{A.19}$$

$$\leq x^\star(0) - \frac{|x^\star(1)|}{2} + \frac{x^\star(2)}{3} + \sum_{k=3}^{\infty} \frac{x^\star(k)}{k+1} \tag{A.20}$$

$$\leq \frac{x^\star(0)}{2} + \frac{x^\star(2)}{3} + \sum_{k=3}^{\infty} \frac{x^\star(k)}{k+1} \tag{A.21}$$

$$= \overline{x}\,(x'(0) + x'(1) + x'(2)) + \sum_{k=3}^{\infty} x^\star(k)x'(k) \tag{A.22}$$

$$= \langle x', g \rangle \tag{A.23}$$

$$\leq \|x'\|_2 \|g\|_2 \tag{A.24}$$

$$= \|x'\|_2 \left(\sqrt{3\overline{x}^2 + \sum_{k=3}^{\infty} x^\star(k)^2} \right) \tag{A.25}$$

where we now define $\overline{x}$ as

$$\overline{x} = \frac{3x^\star(0)}{5} + \frac{2x^\star(2)}{5} \tag{A.26}$$

As in Case 1, to show that

$$3\overline{x}^2 \leq x^\star(0)^2 + x^\star(1)^2 + x^\star(2)^2 \tag{A.27}$$

will be sufficient to prove Case 1. This proof follows directly from that of Case 0 by switching the roles of $x^\star(0)$ and $x^\star(1)$.

Case 2. $(N = 2)$

$$\alpha(x^\star) = x^\star(0) + \frac{x^\star(1)}{2} + \frac{x^\star(2)}{3} + \sum_{k=3}^{\infty} \frac{x^\star(k)}{k+1} - |x^\star(2)| \tag{A.28}$$

$$\leq x^\star(0) + \frac{x^\star(1)}{2} - \frac{2|x^\star(2)|}{3} + \sum_{k=3}^{\infty} \frac{x^\star(k)}{k+1} \tag{A.29}$$

$$\leq \frac{x^\star(1)}{2} + \frac{x^\star(0)}{3} + \sum_{k=3}^{\infty} \frac{x^\star(k)}{k+1} \tag{A.30}$$

$$= \overline{x}\,(x'(0) + x'(1) + x'(2)) + \sum_{k=3}^{\infty} x^\star(k)x'(k) \tag{A.31}$$

$$= \langle x', g \rangle \tag{A.32}$$

$$\leq \|x'\|_2 \|g\|_2 \tag{A.33}$$

$$= \|x'\|_2 \left(\sqrt{3\overline{x}^2 + \sum_{k=3}^{\infty} x^\star(k)^2} \right) \tag{A.34}$$

where we now define $\overline{x}$ as

$$\overline{x} = \frac{3x^\star(1)}{5} + \frac{2x^\star(0)}{5} \tag{A.35}$$

This is easily seen to be equivalent to Case 0 by switching the roles of $x^\star(0)$ and $x^\star(2)$.

Case 3. $(N \geq 3)$

Assume

$$|x^\star(0)| = \max\{|x^\star(0)|, |x^\star(1)|, |x^\star(2)|\} \leq |x^\star(N)| \tag{A.36}$$

Then

$$\alpha(x^\star) = x^\star(0) + \frac{x^\star(1)}{2} + \frac{x^\star(2)}{3} + \sum_{k=3}^{\infty} \frac{x^\star(k)}{k+1} - |x^\star(N)| \tag{A.37}$$

$$\leq \frac{x^\star(1)}{2} + \frac{x^\star(2)}{3} + \sum_{k=3}^{\infty} \frac{x^\star(k)}{k+1} \tag{A.38}$$

$$= \overline{x}\,(x'(0) + x'(1) + x'(2)) + \sum_{k=3}^{\infty} x^\star(k) x'(k) \tag{A.39}$$

$$= \langle x', g \rangle \tag{A.40}$$

$$\leq \|x'\|_2 \|g\|_2 \tag{A.41}$$

$$= \|x'\|_2 \left(\sqrt{3\overline{x}^2 + \sum_{k=3}^{\infty} x^\star(k)^2} \right) \tag{A.42}$$

where

$$\overline{x} = \frac{3x^\star(1)}{5} + \frac{2x^\star(2)}{5} \tag{A.43}$$

The results of Case 0 apply directly. Similarly, if we assume

$$|x^\star(1)| = \max\{|x^\star(0)|, |x^\star(1)|, |x^\star(2)|\} \leq |x^\star(N)| \tag{A.44}$$

the results of Case 1 apply directly, and if we assume

$$|x^*(2)| = \max\{|x^*(0)|, |x^*(1)|, |x^*(2)|\} \leq |x^*(N)| \tag{A.45}$$

the results of Case 2 apply directly. Thus, we have shown that $\alpha(x^*) \leq \|x'\|_2$ for all $\|x^*\|_2 \leq 1$. ■

Appendix B. SISO F-16 Short Period Model

This appendix describes the evaluation model for the SISO F-16 problem used in this dissertation. It is the same model that was used by Walker [9], and this appendix itself was taken, with one modification, from Walker's dissertation. The only modification was to remove the Padé approximation of the sampling time delay. This was not necessary since the discrete-time controllers were implemented using a sample and hold arrangement.

The F-16 normal acceleration command control system is modeled by a continuous, time-invariant linear system shown in Figure B.1. The system consists of a two-state short period approximation of the normal acceleration command system augmented with a pre-filter for the servo dynamics and a post-filter to model the control delay. The plant states are the angle of attack (α) and the pitch rate (q). The input is the stabilator deflection (δ_e) and the output is normal acceleration (a_z). The unweighted plant (W_p) is given by

$$\begin{aligned} \begin{bmatrix} \dot{\alpha} \\ \dot{q} \end{bmatrix} &= \begin{bmatrix} -1.491 & 0.996 \\ 9.753 & -0.96 \end{bmatrix} \begin{bmatrix} \alpha \\ q \end{bmatrix} + \begin{bmatrix} -0.188 \\ -19.04 \end{bmatrix} \begin{bmatrix} \delta_e \end{bmatrix} \\ \begin{bmatrix} a_z \end{bmatrix} &= \begin{bmatrix} 35.264 & -0.334 \end{bmatrix} \begin{bmatrix} \alpha \\ q \end{bmatrix} + \begin{bmatrix} -4.367 \end{bmatrix} \begin{bmatrix} \delta_e \end{bmatrix} \end{aligned} \tag{B.1}$$

The actuator dynamics (W_s) are modeled as a first order relation between the commanded stabilator deflection ($\delta_{e_{com}}$) and the actual deflection given by

$$\dot{\delta}_e = -20.0\delta_e + 20.0\delta_{e_{com}} \tag{B.2}$$

A wind disturbance is modeled as an angle of attack perturbation by a zero-mean white Gaussian noise with a strength of 5.0×10^{-4} rad^2-sec. The measurement is corrupted by zero-mean, white Gaussian noise of strength 1.6×10^{-5} g^2-sec. The strength of the noises were determined by tuning a linear quadratic estimator. The truth model for the tuning and analysis includes a first order Von Karman wind model (W_w) for the low frequency process noise ξ, which enters the plant as an angle of attack perturbation (Γ), and a high-

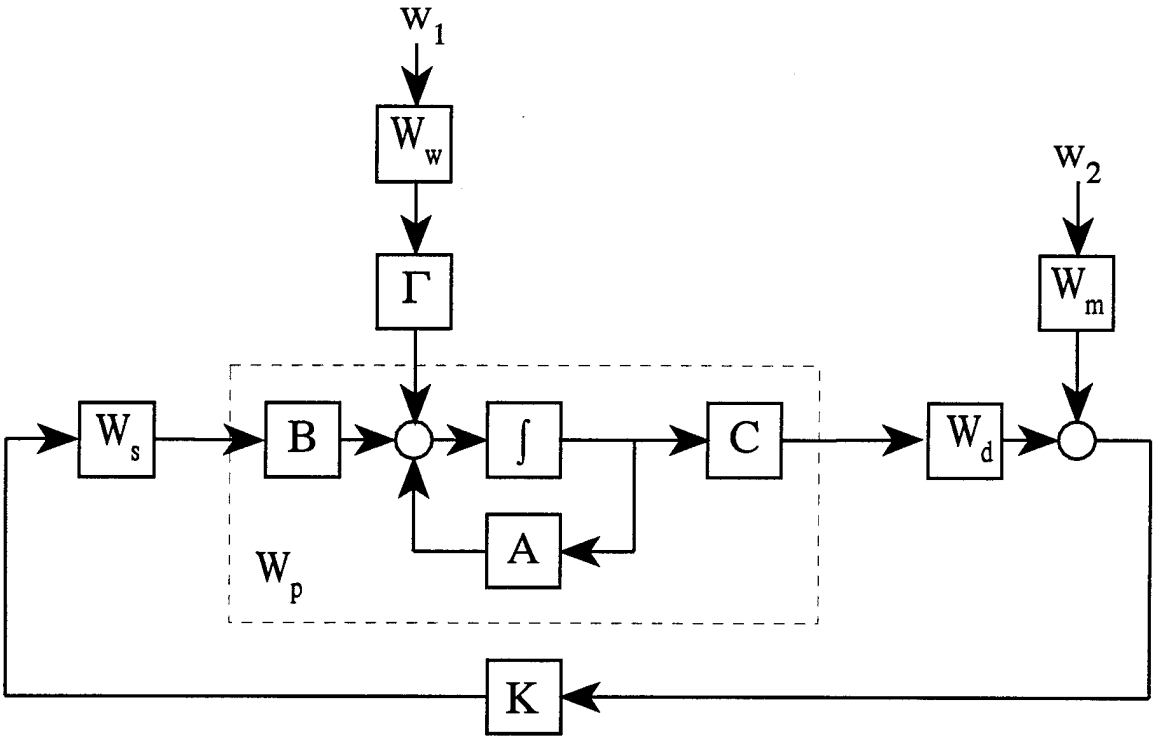

Figure B.1 F-16 model block diagram

pass filter (W_m) to model the measurement noise η. These models are given, respectively, as

$$\dot{x_w} = -6.7x_w + 0.0187w_1 \tag{B.3}$$

$$\xi = x_w \tag{B.4}$$

$$\dot{x_m} = -10x_m + 0.004w_2 \tag{B.5}$$

$$\eta = 1.0x_m + 0.004w_2 \tag{B.6}$$

where w_1 and w_2 are unit strength white-Gaussian noises, x_w is the wind state, x_m is the measurement noise state, ξ is the process noise, and η is the measurement noise. Γ is the

first column of the plant A matrix given in (B.1). W_s is a control weighting function which was set to unity for the examples in this dissertation.

Appendix C. The Mixed-Norm Toolbox for MATLAB

C.1 Overview

The Mixed-Norm Toolbox (MXTOOLS) for MATLAB solves the general fixed-order, mixed-norm control problem for both discrete-time and continuous-time linear systems. Specifically, it minimizes the H_2 norm of a transfer function subject to constraints on the ℓ_1 (L_1 for continuous-time) and/or H_∞ constraints on dissimilar transfer functions associated with the same underlying plant dynamics. Structured singular value (μ) constraints can be accommodated as a special case of H_∞ constraints [64]. Further, an arbitrary number and variety of constraints can be added to the problem without modification to the code. The resulting non-convex optimization problem is solved numerically using gradient-based, nonlinear programming methods.

C.2 Mixed-Norm Toolbox Structure

The Mixed-Norm Toolobox is made up of a modular collection of norm and gradient subroutines, bound together with calling shells and utility routines to facilitate easy problem setup (see Figure C.1). With this approach, any number or combination of different constraints can be added to the problem without modification to the code. The overall structure is identical for both the continuous-time and discrete-time portions of the toolbox, with a "cc" or "c" prefix referring to a continuous-time routine, and a "dd" or "d" prefix referring to a discrete-time routine. Ordinarily, the user only needs to interact with the main shells (*ccmxopt.m* or *ddmxopt.m*). These shells determine which of the various subroutines need to be called, and they store this information in a parameter matrix which is passed to the appropriate subshells via the optimization solver. Besides the basic MATLAB [58] package, the Mixed-Norm Toolbox requires the *μ-Analysis and Synthesis Toolbox* [63] and the *Optimization Toolbox* [59]. Specifically, the transfer function storage scheme and star product subroutine are used from the *μ-Toolbox*, and several of the optimization routines from the *Optimization Toolbox* are used.

The first of the inputs to the main shell consists of a stack of transfer functions, each of which is in the *μ-Toolbox* system matrix form. The objective function will be the 2-norm

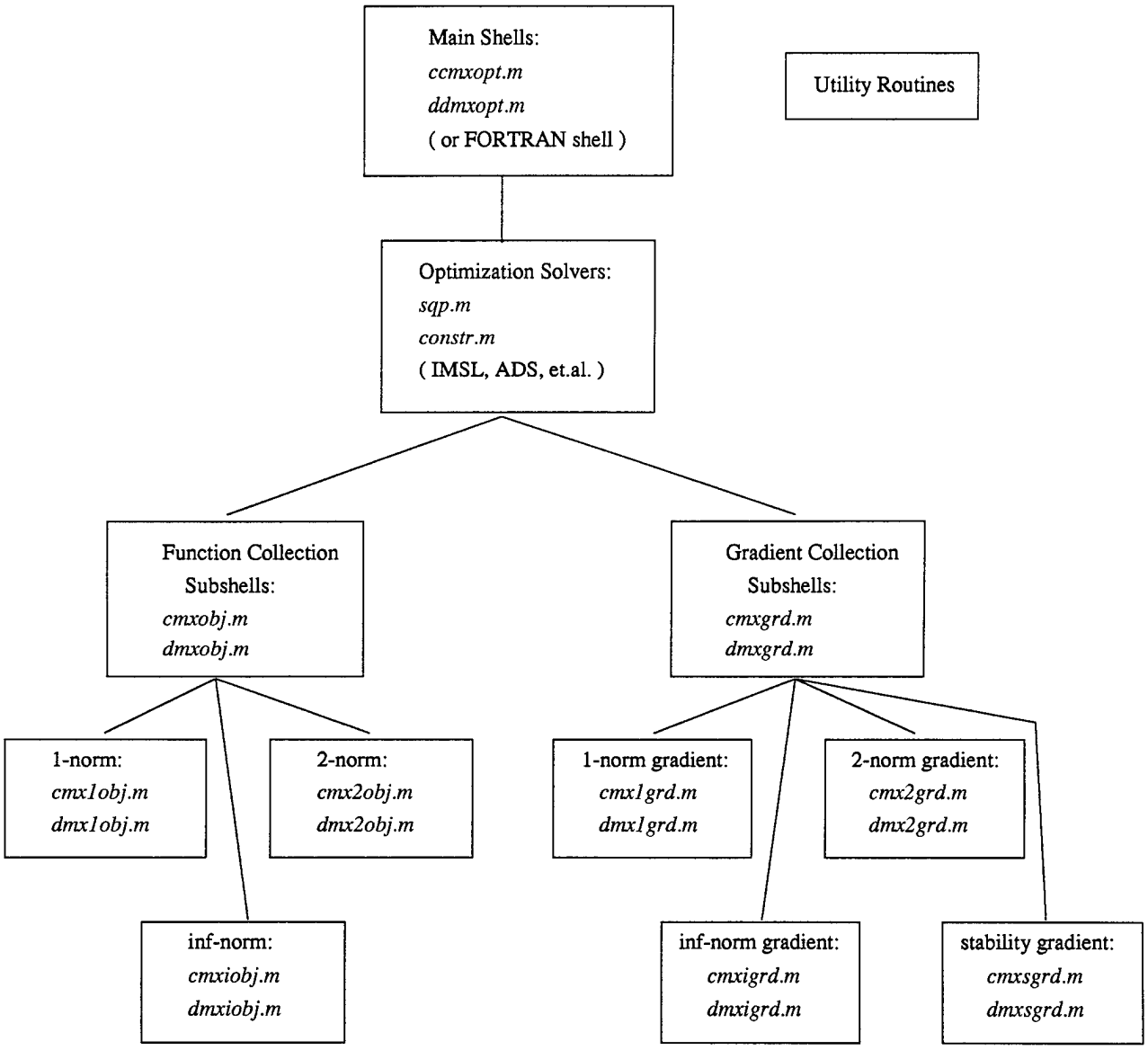

Figure C.1 Mixed-Norm Toolbox Structure

of the first transfer function in the stack. The second input is the parameter matrix which identifies the number of exogenous inputs and outputs for each of the transfer functions in the stack, and which norm (1, 2, or ∞) is being constrained for each of the transfer functions. The third input is simply the name of the output file where the results will be written. The fourth (optional) input is an initial compensator used as a starting point. If the fourth input is not present, the objective transfer function must be non-singular so that the H_2 optimal compensator can be computed as the starting point. Any or all of the constraint transfer functions may be singular. The order of the resulting compensator will be the same order as the starting compensator; therefore, if a compensator of higher or lower order than the objective transfer function is desired, an initial stabilizing compensator with the desired order must be provided as the third input. Although the data input format is documented within the routines, an interactive shell to format the inputs has been constructed (*loader.m*), and a brief user's manual will be provided as part of the Mixed-Norm Toolbox. The outputs of the main shell are the mixed-norm compensator and a matrix of transfer function norms which compare the specified constraint levels with the final achieved norms for the various transfer functions. The help file for the main shells list the complete set of inputs and outputs, and the help file for the discrete-time shell (*ddmxopt.m*) is listed here:

```
DDMXOPT  Finds optimal mixed-norm solution using numerical optimization
         techniques.

[Komp,normvec,xvecsave,H]=ddmxopt(TF,params,outfile,Kinit,H,options)

This is a numerical optimization approach to finding the fixed order (nsk),
compensator which minimizes the 2-norm subject to infinity, 1-norm, or
2-norm constraints for a continuous linear system.

INPUTS:

TF      = [P1;P2;P3;...;Pn] where each Pi is in packed (musyn) format
params  = [nin_obj   nout_obj       2      opt         objexp        0
```

```
            nin_con1  nout_con1  type_con1  start_con1  end_con1  step_con1
            nin_con2  nout_con2  type_con2  start_con2  end_con2  step_con2
              ...       ...        ...        ...         ...       ...
            nin_conn  nout_conn  type_conn  start_conn  end_conn  step_conn
            Ntrunc    tol        fsamp          0           0         0    ]
```

nin = # exogenous inputs for each of the transfer functions

nout = # controlled outputs for each of the transfer functions

type = either 1, 2, or 3 for 1-norm, 2-norm, or inf-norm
Note: OBJECTIVE MUST BE AN H2 PROBLEM

start = starting constraint level

end = ending constraint level

step = step size between the starting con level and ending con level
Note: Each constraint interval is nested inside the next one
(i.e. constraint 1 is nested inside constraint 2, etc.).
To set a constant constraint, set start=end and step=0.

opt = Indicator for Optimization Algorithm
0 - Will use sqp.m (default)
1 - Will use constr.m (an SQP routine from Opt. Toolbox)

objexp = Scaling exponent for objective fcn. Scale=10^(-objexp)
Default = 0

Ntrunc = truncation for 1-norm problems

tol = tolerance for 1-norm problems

fsamp = sampling frequency at which plants were discretized

outfile = (optional) string name of outfile, must be in single quotes.
normvec and xvecsave (see below) are saved in this file.

Kinit = (optional) initial controller. Must be put into packed, modal form (i.e. use canon then pck). Default=H2 optimal controller.
Note: MUST REPRESENT A STABILIZING CONTROLLER.

H = (optional) intial positive definite approximation of the Hessian

options = (optional) allows a vector of optimization parameters to be defined. For more information type HELP FOPTIONS.

Note: to skip an optional input set it equal to [].

```
OUTPUTS:

Komp    = optimal compensator in packed, modal form
normvec = [nrm1 nrm2 con2 nrm3 con3 ... ... nrmn conn]
xvecsave= [xvec1 xvec2 xvec3 ...], xvec is the vectorized compensator
          which corresponds to the points described in each row of normvec.
          dkvec2ss can be used to transform each vectorized compensator
          to musyn format.
H       = final positive definite approximation of the Hessian

Note: n, above, is currently restricted to be <=10

   Created by:    Capt. Dave Jacques
                  AFIT/ENY
                  Created:       4/94
                  Last modified: 3/29/95
```

In addition to the inputs and outputs, there are several features of the main shell with which the user should be familiar. Since the ∞-norm subproblem constrains only the singular value peaks, it is possible that additional peaks will appear as the algorithm pushes down on the initial peaks. If this occurs, the new peak(s) will be detected, and the constrained optimization will be repeated with a new set of frequency bands. This ensures that the specified H_∞ constraint has been met. Similarly, the 1-norm subroutines depend on a specified truncation level to approximate the norm expressions. Following convergence, the truncation level is increased and the error between the two approximations is compared to a specified threshold. If the threshold is exceeded, the constrained optimization is repeated with the higher truncation level. Default truncation levels and thresholds are provided in the main setup routine (*loader.m*). In addition to setting the default parameters, *loader.m* can be used to stack the transfer functions, establish the parameters input matrix and run the main shells using default values. If default values require modification prior to running the main shell, *loader.m* can be exited prior to en-

tering the optimization problem, and the appropriate elements of the parameters matrix can be modified at that time.

A complete listing of the functions in MXTOOLS can be obtained from within MATLAB by typing

```
help mxtools
```

at the system prompt (>>). The main help help file for MXTOOLS is repeated here:

```
Mixed-Norm Toolbox
Version: Beta 0.91  3/95

   The Mixed-Norm Toolbox contains routines for the synthesis of
   fixed-order, mixed-norm compensators.  The problem it seeks to solve
   is that of minimizing the 2-norm of a closed-loop transfer function,
   subject to constraints on the 1-norm, 2-norm, or infinity-norm of
   related, but generally different transfer functions.  It attempts
   to do this using a gradient-based constrained numerical optimization.

   CONTROL SYNTHESIS ROUTINES

     loader    An interactive script for running either ccmxopt or ddmxopt
     ccmxopt   Main shell for continuous-time mixed-norm control synthesis
     ddmxopt   Main shell for discrete-time mixed-norm control synthesis
     ddh2      Discrete-time H2 solver - strictly causal compensator
     ddh2nc    Discrete-time H2 solver - not strictly causal compensator
     ddlqr     Discrete-time LQR solver

   SUBSHELLS

     cmxobj    Function collection subshell for ccmxopt
     cmxgrd    Gradient collection subshell for ccmxopt
     dmxobj    Function collection subshell for ddmxopt
     dmxgrd    Gradient collection subshell for ddmxopt
```

FUNCTION EVALUATION ROUTINES

cmx1obj	Continuous-time 1-norm for cmxobj
cmx2obj	Continuous-time 2-norm for cmxobj
cmxiobj	Continuous-time inf-norm for cmxobj
dmx1obj	Discrete-time 1-norm for dmxobj
dmx2obj	Discrete-time 2-norm for dmxobj
dmxiobj	Discrete-time inf-norm for dmxobj

GRADIENT EVALUATION ROUTINES

cmx1grd	Gradients of the continuous-time 1-norm for cmxgrd
cmx2grd	Gradients of the continuous-time 2-norm for cmxgrd
cmxigrd	Gradients of the continuous-time inf-norm for cmxgrd
cmxsgrd	Continuous-time stability gradients for cmxgrd
dmx1grd	Gradients of the discrete-time 1-norm for dmxgrd
dmx2grd	Gradients of the discrete-time 2-norm for dmxgrd
dmxigrd	Gradients of the discrete-time inf-norm for dmxgrd
dmxsgrd	Discrete-time stability gradients for dmxgrd

TRANSFER FUNCTION NORM ROUTINES

cc1norm	1-norm of a continuous-time system
ccinorm	inf-norm of a continuous-time system using sv-search
dd1norm	1-norm of a discrete-time system
dd2norm	2-norm of a discrete-time system
ddinorm	inf-norm of a discrete-time system using sv-search

UTILITY ROUTINES

care	Solves continuous algebraic Riccati equation (A.J. Laub)
dare	Solves discrete algebraic Riccati equation (A.J. Laub)
qzexch	Performs unitary equivalence for care and dare (A.J. Laub)
sqp	Sequential quadratic programming algorithm

```
   merit      Evaluates merit function for sqp
   cpkfind    Finds singular value peaks for cmxigrd
   cbands     Establishes frequency bands around singular value peaks
   maxcsv     Used 1-D optimization to find location of sv peaks
   dpkfind    Finds singular value peaks for dmxigrd
   dbands     Establishes frequency bands around singular value peaks
   maxdsv     Used 1-D optimization to find location of sv peaks
   ckvec2ss   Converts vectorized compensator to musyn form (cont-time)
   ckss2vec   Converts musyn compensator to vectorized form (cont-time)
   dkvec2ss   Converts vectorized compensator to musyn form (disc-time)
   dkss2vec   Converts musyn compensator to vectorized form (disc-time)
   ftime      Evaluates final time for cc1norm
   blkrsch2
   dstabprj

 EXAMPLES

   rundbr     A simple continuous-time H2/Hinf example
   runf16     A SISO H2/l1/Hinf longitudinal controller
                for F16 aircraft using a discrete-time design

The Mixed-Norm Toolbox is the result of work by several researchers
     at the Air Force Institute of Technology.

The contributors are:

     Capt Dave Jacques
     Capt Mark Spillman
     Dr D. Brett Ridgely
     Maj Bob Canfield
     LtCol Dave Walker
     Capt Linda Smith

The Mixed-Norm Toolbox is not copyrighted, and we encourage
```

```
users to freely distribute it.  However, we request that it
be distributed intact, and we also (humbly) request that this
contents file and all acknowledgement banners be left as is.
We encourage feedback from all who might come across this toolbox.
Feedback is best directed to:

                Dr D. Brett Ridgely
                AFIT/ENY
                2950 P Street
                Wright Patterson AFB, OH  45433-7765

                e-mail: dridgely@afit.af.mil
```

C.3 Optimization Solvers

The Mixed-Norm Toolbox has been designed to work with a variety of math programming algorithms. In fact, although main shells are provided for several specific solvers, it is relatively easy to adapt these main shells to almost any math programming algorithm capable of solving nonlinear constrained optimization problems. The experience of the AFIT research team has been that Sequential Quadratic Programming (SQP) methods provide the best overall performance in terms of efficiency and ability to handle a wide variety of problems. The *Optimization Toolbox* contains an SQP algorithm (*constr.m*) which has been used successfully, primarily for smaller problems (less than 40-50 design variables). For larger problems, *constr.m* has problems maintaining a positive definite approximation to the Lagrangian Hessian, and other solvers should be considered. For larger problems (presently as many as 100 design variables), the IMSL set of FORTRAN subroutines [61] contains an excellent SQP routine (*DNCONG*). Use of the IMSL routine requires a FORTRAN shell (provided as part of the toolbox) that calls the MATLAB computational engine (*libmat.a*) for function and gradient evaluations. A limitation of the IMSL subroutine is that the fixed convergence and line search criteria are so strict that they sometimes fail to solve problems which are solvable using more relaxed criteria. A

new addition to the Mixed-Norm Toolbox is a MATLAB SQP routine (*sqp.m*) based on the work of Schittkowski [55]. Preliminary trials with this routine show performance on a par with the IMSL routine, and this routine is now the default solver for MXTOOLS. A very useful feature of *sqp.m* is that it allows the user to reuse the approximation to the Hessian, thus greatly improving the efficiency of the algorithm when moving between successive points on the Pareto optimal curve.

In addition to SQP algorithms, the Method of Feasible Directions [10] has been successfully used for some problems, and FORTRAN shells have been constructed to interface the toolbox with the entire ADS [60] collection of optimization subroutines. Although performance is not necessarily improved with the ADS subroutines, they allow experimentation with a wide variety of optimization strategies and line search methods. As a side note, many of the optimization routines listed above use an active set method whereby only the active (or nearly active) constraints need to be calculated. Although not currently implemented, the capability to accommodate solvers using active set methods is being added to the code, and its use will be recommended for problems where all of the constraints are not expected to remain active.

As with any non-convex optimization problem, convergence to the global minimum for any given set of constraint levels cannot be guaranteed with the Mixed-Norm Toolbox. Having said this, a standard set of guidelines for working with the toolbox should be considered. First, convergence criteria will most likely require adjustment in order to trade off accuracy of the solution with time to achieve convergence. Second, since global convergence cannot be guaranteed, it is sometimes necessary to use several different starting controllers. This technique often can be used to provide evidence of (or avoid) local minima which may be present. H_∞ and/or ℓ_1 solvers can be very useful for providing compensators at different locations on the Pareto surface. Third, small steps between successive constraint levels should be used when attempting to define a Pareto curve or surface, especially in regions of steep tradeoff between the objective and constraint(s). Along these lines, the algorithms seem to converge more quickly if only one constraint level is varied from one point to the next. Fourth, although reduced-order controllers may be more susceptible

to local minima, the reduced number of design variables may produce an overall problem which is numerically easier to solve than the full-order design.

Bibliography

1. D. C. Youla, H. A. Jabr, and J. J. Bongiorno. Modern Wiener-Hopf design of optimal controllers, Part II: The multivariable case. *IEEE Trans. Auto. Control*, AC-21:319–338, 1976.
2. H. Kwakernaak and R. Sivan. *Linear Optimal Control Systems.* Wiley Interscience, NY, 1972.
3. P. S. Maybeck. *Stochastic Models, Estimation, and Control, Volume 3.* Mathematics in Science and Engineering, Vol 141-3. Academic Press, San Diego, CA, 1982.
4. J. C. Doyle, B. A. Francis, and A. R. Tannenbaum. *Feedback Control Theory.* Macmillan, NY, 1992.
5. M. A. Dahleh and I. J. Diaz-Bobillo. *Control of Uncertain Systems: A Linear Programming Approach.* Prentice-Hall, 1994.
6. J. C. Doyle and G. Stein. Multivariable feedback design: Concepts for a classical/modern synthesis. *IEEE Trans. on Auto. Control*, AC-26(1):4–16, Feb 1981.
7. G. Zames. On the input–output stability of time–varying nonlinear feedback systems, Part I: Conditions derived using concepts of loop gain, conicity, and positivity. *IEEE Trans. Auto. Control*, AC-11:228–238, April 1966.
8. D. B. Ridgely. *A Nonconservative Solution to the General Mixed H_2/H_∞ Optimization Problem.* PhD thesis, Massachusetts Institute of Technology, Cambridge, MA, 1992.
9. D. E. Walker. *H_2 Optimal Control with H_∞, μ, and L_1 Constraints.* PhD thesis, Air Force Institute of Technology, WPAFB, OH, June 1994.
10. G.N. Vanderplaats. *Numerical Optimization Techniques for Engineering Design: with Applications.* McGraw Hill, NY, 1984.
11. P. A. Iglesias and K. Glover. State-space approach to discrete-time H_∞ control. *International Journal of Control*, 54(5):1031–1073, 1991.
12. D. S. Bernstein W. M. Haddad and D. Mustafa. Mixed-norm H_2/H_∞ regulation and estimation: The discrete-time case. *Systems and Control Letters*, 16:235–247, 1991.
13. P. P. Khargonekar I. Kaminer and M. A. Rotea. Mixed H_2/H_∞ control for discrete-time systems. *Automatica*, 29(1):57–70, 1992.
14. D. Mustafa P. A. Iglesias and K. Glover. Discrete-time H_∞ controllers satisfying a minimum entropy criterion. *Systems and Control Letters*, 14:275–286, 1990.
15. P. A. Iglesias and D. Mustafa. State space solution of the discrete-time minimum entropy control problem via separation. *IEEE Trans. Auto. Control*, AC-38(10):1525–1530, Oct 1993.
16. U. L. Ly and E. Schomig. A new approach to mixed H_2/H_∞ controller synthesis using gradient based parameter optimization methods. University of Washington, Final Technical Report under NASA grant contract NAG-2-629, 1993.

17. A. Megretski. On the Order of optimal controllers in the mixed H_2/H_∞ control. In *Proceedings of the 33rd Conference on Decision and Control*, pages 3173–3174, Lake Buena Vista FL, December 1994.

18. M. Sznaier. An Exact solution to general siso mixed H_2/H_∞ problems via convex optimization. In *Proceedings of the American Control Conference*, pages 250–254, San Francisco CA, June 1993.

19. M. Sznaier and H. Rotstein. An Exact solution to general 4-blocks discrete-time mixed H_2/H_∞ problems via convex optimization. In *Proceedings of the American Control Conference*, pages 2251–2256, Baltimore MD, June 1994.

20. J. W. Helton and A. Sideris. Frequency response algorithms for H_∞ optimization with time domain constraints. *IEEE Trans. Auto. Control*, AC-34(4):427–434, Apr 1989.

21. A. Sideris and H. Rotstein. H_∞ optimization with time domain constraints over a finite horizon. In *Proceedings of the 29th Conference on Decision and Control*, pages 1802–1807, Honolulu HI, December 1990.

22. A. Sideris and H. Rotstein. Single-input single-output H_∞ control with time domain constraints. *Automatica*, 29(3):969–983, 1993.

23. M. Sznaier. A Mixed ℓ_∞/H_∞ optimization approach to robust controller design. In *Proceedings of the American Control Conference*, pages 727–732, Chicago IL, June 1992.

24. P. Voulgaris. Optimal h_2/ℓ_1 control: The siso case. In *Proceedings of the 33rd Conference on Decision and Control*, pages 3181–3186, Lake Buena Vista FL, December 1994.

25. B. Wie and D. Bernstein. Benchmark problems for robust control design (1992 ACC version). In *Proceedings of the American Control Conference*, Chicago, IL, June 1992.

26. J. M. Maciejowski. *Multivariable Feedback Design.* Addison-Wesley Publishing Company. Inc., 1989.

27. B. A. Francis. *A Course in H_∞ Control Theory.* Lecture Notes in Control and Information Sciences. Springer-Verlag, Berlin, 1987.

28. V. Kucera. *Analysis and Design of Discrete Linear Control Systems.* Prentice-Hall, Englewood Cliffs, NJ, 1991.

29. A. C. M. Ran and R. Vreugdenhil. Existence and comparison theorems for algebraic Riccati equations for continuous and discrete-time systems. *Linear Algebra and its Applications*, 99:63–83, 1988.

30. B. P. Molinari. The stabilizing solution of the discrete algebraic Riccati equation. *IEEE Trans. Auto. Control*, AC-20:396–399, Jun 1975.

31. T. Pappas, A. J. Laub, and N. R. Sandell. On the numerical solution of the discrete-time algebraic Riccati equation. *IEEE Trans. Auto. Control*, AC-25(4):631–641, Aug 1980.

32. S. Bittanti, A. J. Laub, and J. C. Willems, editors. *The Riccati Equation.* Springer-Verlag, Berlin, 1991.

33. V. Ionescu and M. Weiss. Two Riccati formula for the discrete-time H_∞ control problem. *International Journal of Control*, 57(1):141–195, 1993.

34. C. E. de Souza and L. Xie. On the discrete-time bounded real lemma with application in the characterization of static state feedback H_∞ controllers. *Systems and Control Letters*, 18:61–72, 1992.

35. A. V. Balakrishnan. *Applied Functional Analysis.* Applications of Mathematics. Springer-Verlag, Berlin, 1981.

36. S. P. Boyd and C. H. Barratt. *Linear Controller Design: Limits of Performance.* Prentice-Hall, Englewood Cliffs, NJ, 1991.

37. Ivar Ekeland. *Convex Analysis and Variational Problems.* North-Holland, 1976.

38. R. Fletcher. *Practical Methods of Optimization, Volume 2: Constrained Optimization.* John Wiley & Sons. Ltd., NY, 1981.

39. D. G. Luenberger. *Optimization by Vector Space Methods.* John Wiley & Sons, Inc, NY, 1969.

40. A. L. Peressini, F. E. Sullivan, and Jr. J. J. Uhl. *The Mathematics of Nonlinear Programming.* Undergraduate Texts in Mathematics. Springer-Verlag, 1988.

41. P. S. Maybeck. *Stochastic Models, Estimation, and Control, Volume 1.* Mathematics in Science and Engineering, Vol 141-1. Academic Press, San Diego, CA, 1979.

42. D. B. Ridgely and D. Walker. The general mixed H_2/H_∞ control problem. *Submitted to Automatica*, 1995.

43. M. Vidyasagar. Optimal rejection of persistent bounded disturbances. *IEEE Trans. Auto. Control*, AC-31(6):527–534, Jun 1986.

44. M. A. Dahleh and J. B. Pearson. ℓ_1 optimal feedback controllers for MIMO discrete-time systems. *IEEE Trans. Auto. Control*, Apr 1987.

45. M. A. Dahleh and J. B. Pearson. Optimal rejection of persistent disturbances, robust stability and mixed sensitivity minimization. *IEEE Trans. Auto. Control*, AC-33, Aug 1988.

46. I. J. Diaz-Bobillo and M. A. Dahleh. Minimization of the maximum peak-to-peak gain: The general multiblock problem. *IEEE Trans. Auto. Control*, AC-38(10):1459–1482, Oct 1993.

47. T. Kailath. *Linear Systems.* Prentice-Hall, Englewood Cliffs, NJ, 1980.

48. M. Vidyasagar. Further results on the optimal rejection of persistent bounded disturbances. *IEEE Trans. Auto. Control*, AC-36(6):642–652, Jun 1991.

49. M. Salapaka, M. Dahleh, and P. Voulgaris. MIMO optimal control design: Interplay of the H_2 and the ℓ_1 norms. Submitted to the *1995 IEEE Conference on Decision and Control*, 1995.

50. D. E. Walker and D. B. Ridgely. A new numerical method for the general mixed H_2/H_∞ optimal control problem. In *Preprint*, 1994.

51. M. Spillman. Applications of ℓ_1 and mixed H_2/ℓ_1 optimization. Master's thesis, Air Force Institute of Technology, WPAFB, OH, December 1994.

52. M. G. Safonov, D. J. N. Limebeer, and R. Y. Chiang. Simplifying the H_∞ theory via loop-shifting, matrix-pencils and descriptor concepts. *International Journal of Control*, 50(6):2467–2488, 1989.

53. J. Ullauri, D. E. Walker, and D. B. Ridgely. Reduced order mixed H_2/H_∞ optimization with multiple H_∞ constraints. In *AIAA Guidance, Navigation, and Control Conference*, pages 1051–1060, Scottsdale, AZ, August 1994.

54. J. C. Luke, D. B. Ridgely, and D. E. Walker. Flight controller design using mixed H_2/H_∞ optimization with a singular H_∞ constraint. In *Proceedings of the AIAA Guidance, Navigation, and Control Conference*, pages 1061–1071, Scottsdale AZ, August 1994.

55. K. Schittkowski. NLPQP: A Fortran subroutine solving constrained nonlinear programming problems. In *Annals of Operation Research*, pages 485–500. J. C. Baltzer A. G., Scientific Publishing Company, 1985/6.

56. D. P. Giesy and K. B. Lim. H_∞ norm sensitivity formula with control system design applications. *Journal of Guidance, Control, and Dynamics*, 16(6):1138–1145, November-December 1993.

57. L. D. Smith. Improved numerical solution of mixed H_2/H_∞ with applications. Master's thesis, Air Force Institute of Technology, WPAFB, OH, December 1994.

58. MATLAB: High performance numeric computation and visualization software. The Math Works, Inc., Natick MA, 1994.

59. A. Grace. *Optimization Toolbox.* The Mathworks. Inc., Natick, MA, 1992.

60. G.N. Vanderplaats. ADS: A FORTRAN program for automated design synthesis. Engineering Design Optimization, Inc., Santa Barbara CA, 1985.

61. MATH/LIBRARY: FORTRAN subroutines for mathematical applications. IMSL, Houston TX, 1991.

62. D. R. Jacques, D. B. Ridgely, R. A. Canfield, and M. A. Spillman. A MATLAB toolbox for fixed-order, mixed-norm control synthesis. Submitted to *1995 IEEE Conference on Control Applications*, 1995.

63. G. J. Balas, J. C. Doyle, K. Glover, A. Packard, and R. Smith. *μ-Analysis and Synthesis Toolbox.* The Mathworks. Inc., Natick, MA, 1991.

64. D. E. Walker and D. B. Ridgely. Mixed H_2/μ optimization. In *13th IFAC Symposium on Automatic Control in Aerospace*, San Jose CA, September 1994.

65. D. B. Ridgely and S. S. Banda. *Introduction to Robust Multivariable Control.* AFWAL-TR-85-3102. USAF, 1986.

66. I. Ashkenas D. McRuer and D. Graham. *Aircraft Dynamics and Automatic Control.* Princeton University Press, Princeton, NJ, 1973.

67. M. Athans et al. The Stochastic control of the F-8C aircraft using a multiple model adaptive control (MMAC) method - Part 1: Equilibrium flight. *IEEE Trans. on Auto. Control*, AC-22(5):768–780, October 1977.

68. R. Y. Chiang and M. G. Safonov. *Robust Control Toolbox.* The Mathworks. Inc., Natick, MA, 1992.

Vita

Captain David R. Jacques was born on 13 April 1960, in Beverly, Massachusetts. He graduated from Liberty High School, Bethlehem, Pennsylvania, in 1978, and attended Lehigh University, also in Bethlehem. He completed a Bachelor of Science in Mechanical Engineering and was commissioned a Second Lieutenant in June, 1983. Captain Jacques began active duty in the USAF in October, 1983 as an armament systems analyst for the Foreign Technology Division (FTD), Wright Patterson AFB, Ohio. While at FTD, Capt Jacques authored numerous studies and tech reports for the Defense Intelligence Agency (DIA) and HQ/USAF describing the capabilities and limitations of foreign air-to-air missile systems. In May, 1988, Captain Jacques entered a masters degree program at the Air Force Institute of Technology (AFIT) where he majored in structural dynamics and automatic control. He completed an experimental thesis investigating vibration control for large space structures and graduated in December, 1989. Following AFIT, Captain Jacques was assigned to the 6595th Test and Evaluation Group, Vandenberg AFB, California. While assigned to the 6595th, he resolved safety issues and coordinated tri-service range support for the Small ICBM, Peacekeeper, and Peacekeeper Rail Garrison flight test programs. Captain Jacques served as the Mission Controller for the first successful flight of the Small ICBM in April, 1991. In June of 1992, Captain Jacques returned to the AFIT Graduate School of Engineering for doctoral studies. Captain Jacques is married to Lynette (Virgallito) of Beavercreek, Ohio, and they have a daughter, Nicole.

Permanent address: 1740 Chelsea Avenue
Bethlehem, PA 18017

REPORT DOCUMENTATION PAGE

Form Approved
OMB No. 0704-0188

1. AGENCY USE ONLY (Leave blank)	2. REPORT DATE	3. REPORT TYPE AND DATES COVERED
	June 1995	Doctoral Dissertation

4. TITLE AND SUBTITLE
Optimal Mixed-Norm Control Synthesis for Discrete-Time Linear Systems

5. FUNDING NUMBERS

6. AUTHOR(S)
David R. Jacques, Capt, USAF

7. PERFORMING ORGANIZATION NAME(S) AND ADDRESS(ES)
Air Force Institute of Technology, WPAFB OH 45433-6583

8. PERFORMING ORGANIZATION REPORT NUMBER
AFIT/DS/ENY/95-2

9. SPONSORING / MONITORING AGENCY NAME(S) AND ADDRESS(ES)
Dr Marc Jacobs
AFOSR/NM
110 Duncan Ave, Suite B115
Bolling AFB DC 20332-0001

10. SPONSORING / MONITORING AGENCY REPORT NUMBER

11. SUPPLEMENTARY NOTES

12a. DISTRIBUTION / AVAILABILITY STATEMENT
Approved For Public Release;
Distribution Unlimited

12b. DISTRIBUTION CODE

13. ABSTRACT *(Maximum 200 words)*

A mixed-norm approach to control synthesis for discrete-time linear systems is developed. Specifically, the problem of minimizing the H_2 norm of a transfer function, subject to a combination of ℓ_1 and/or H_∞ norm constraints on dissimilar but related transfer functions is considered. The uniqueness of the optimal solution is shown, and numerical methods for approximating the optimal solution to within arbitrary accuracy are developed. These methods generally result in high order compensators which can not be implemented in most practical applications. In response to this, a numerical method is developed which solves for suboptimal solutions of a fixed, specifiable order. The method is packaged as a toolbox for the popular MATLAB software program. Several examples are developed which demonstrate potential applications for the mixed-norm method.

14. SUBJECT TERMS
Control Theory, Mathematical Programming, Discrete-time control, H2 Optimization, H-inf Optimization, l1 Optimization, Multiobjective Optimal Control

15. NUMBER OF PAGES
233

16. PRICE CODE

17. SECURITY CLASSIFICATION OF REPORT	18. SECURITY CLASSIFICATION OF THIS PAGE	19. SECURITY CLASSIFICATION OF ABSTRACT	20. LIMITATION OF ABSTRACT
UNCLASSIFIED	UNCLASSIFIED	UNCLASSIFIED	UL